THE DEVELOPMENTAL ORIGINS OF MAMMOGRAPHIC DENSITY AND BREAST CANCER RISK

Amita Gautam Ghadge

Discipline of Surgery, Adelaide Medical School

Faculty of Health Sciences

The University of Adelaide

September 2021

A thesis submitted to The University of Adelaide in fulfilment of the requirements for the admission to the degree Doctor of Philosophy

Table of contents

List of Figures.....i

List of Tables.....v

Abstract.....vi

Declaration.....viii

Acknowledgements.....ix

Publications arising from this thesis.....x

Abstracts arising from this thesis.....xi

Awards and honours.....xiii

Abbreviations.....xiv

Chapter One.....1

1.1 Introduction.....2

1.2 Mammographic density is a breast cancer risk factor.....3

1.3 Pubertal breast development.....6

1.4 Adiposity, mammographic density, and breast cancer risk.....6

1.5 Timing of puberty onset affects adult mammographic density.....12

1.6 Endocrine regulators of pubertal breast development and mammographic density.....16

1.6.1 Sex hormones.....16

1.6.2 Growth hormone and insulin-like growth factor 1.....17

1.6.3 Endocrine function of adipose tissue.....19

1.7 Paracrine regulators of pubertal breast development and mammographic density.....20

1.7.1 Stromal fibroblasts and extracellular matrix.....20

1.7.2 Immune cells and signalling molecules.....21

1.8 Molecular determinants of pubertal mammary gland development and mammographic density.....22

1.8.1 Heritability and genetics.....22

1.8.2 Epigenetic basis.....23

1.9 Current controversies, conclusions and outlook.....25

1.10 Hypothesis and aims.....28

Chapter Two.....29

2.1 Animals and general procedures.....30

2.1.1 Mice strains 30
2.1.2 General animal procedures 31
2.2 Histology and Immunohistochemistry 38
2.2.1 Carmine alum staining 38
2.2.2 Tissue embedding and sectioning 39
2.2.3 Haematoxylin and eosin staining 39
2.2.4 BrdU staining 40
2.2.5 F4/80 staining of paraffin embedded tissues 41
2.2.6 Masson's trichrome staining 41
2.3 Real time PCR analysis 42
2.3.1 RNA extraction 42
2.3.2 RNA storage by precipitation 43
2.3.3 Complementary DNA (cDNA) preparation 43
2.3.4 Quantitative real-time PCR 43
2.4 Cytokine analysis 44
2.5 Statistical analyses 44

Chapter Three 47

3.1 Introduction 48
3.2 Results 49
3.2.1 Female *bbb/bbb* mice exhibit increased mammary gland adiposity during puberty 49
3.2.2 Increased development of mammary gland terminal end buds in pubertal *bbb/bbb* mice 54
3.2.3 No change in mammary gland fibroglandular density in pubertal *bbb/bbb* mice 57
3.2.4 Increased abundance of mammary gland macrophages in pubertal *bbb/bbb* mice 57
3.2.5 Altered abundance of adipokines and proinflammatory cytokines in pubertal *bbb/bbb* mice 67
3.3 Discussion 73
3.3.1 Increased mammary gland adiposity in *bbb/bbb* mice 73
3.3.2 Effect of increased mammary gland adiposity on mammary gland development during puberty 74
3.3.3 Effect of increased mammary gland adiposity on the mammary gland microenvironment 76

3.3.4 Limitations and future directions 77
3.4 Conclusion 78

Chapter Four 79

4.1 Introduction 80
4.2 Results 83
4.2.1 Selection of 7 weeks as the end of pubertal mammary gland growth period 83
4.2.2 Estrous cycling in control and *bbb/bbb* mice during adulthood 83
4.2.3 Female *bbb/bbb* mice exhibit increased adiposity during adulthood 84
4.2.4 Increased development of mammary gland ducts in adult *bbb/bbb* mice 89
4.2.5 Decrease in mammary gland fibroglandular density in adult *bbb/bbb* mice 93
4.2.6 Altered abundance of mammary gland macrophages in adult *bbb/bbb* mice 93
4.2.7 Altered abundance of adipokines and proinflammatory cytokines in adult *bbb/bbb* mice 104
4.3 Discussion 119
4.3.1 Increased mammary gland adiposity in adult *bbb/bbb* mice 119
4.3.2 Effect of increased mammary gland adiposity on mammary gland density during adulthood 119
4.3.3 Effect of increased mammary gland adiposity on the mammary gland microenvironment 120
4.3.4 Effect of increased adiposity on the visceral adipose tissue microenvironment 123
4.3.5 Limitations and future directions 125
4.4 Conclusion 125

Chapter Five 126

5.1 Introduction 127
5.2 Results 130
5.2.1 Female matched PyMT-*bbb/bbb* mice exhibit greater tumour latency in adulthood 130
5.2.2 Matched PyMT-*bbb/bbb* mice exhibit decreased mammary cancer development in adulthood 130
5.2.3 No difference in the tumour progression in PyMT-*bbb/bbb* mice 134
5.2.4 Altered abundance of adipokines and proinflammatory cytokines in PyMT-*bbb/bbb* mice 139
5.3 Discussion 144

5.3.1 Effect of increased pubertal adiposity on mammary cancer development during adulthood....144
5.3.2 Effect of increased pubertal adiposity on the mammary tumour microenvironment....144
5.3.3 Limitations and future directions....146
5.4 Conclusion....146

Chapter Six....148

6.1 Introduction....149
6.2 Pubertal adiposity alters adult mammary gland density....149
6.3 Pubertal adiposity is causative in mammary cancer development....150
6.4 Proposed mechanism....151
6.5 Developmental origins of breast cancer risk....152
6.6 What is optimal adolescent growth for long-term breast health?....158
6.7 Future studies....159
6.8 Conclusions....160

Chapter Seven....161

Appendix A: Pubertal mammary gland development is a key determinant of adult mammographic density....162
Appendix B: Copyright licence agreement with Wolters Kluwer Health, Inc....179
Appendix C: Copyright licence agreement with Wolters Kluwer Health, Inc....185

References....191

List of Figures

Figure 1.1. Mammographic density refers to the radiological appearance of the breast and reflects the relative proportion of fibroglandular and adipose tissue**……5**

Figure 1.2. Development of epithelial, stromal, and adipose tissue in the breasts occurs during puberty**……7**

Figure 1.3. Puberty is a key developmental stage in the establishment of adult mammographic density**……14**

Figure 1.4. Schematic diagram of the factors that initiate pubertal mammary gland development in girls**……18**

Figure 1.5. Schematic diagram of endocrine, paracrine, and molecular regulators of pubertal mammary gland development that may affect adult mammographic density**……27**

Figure 2.1. Genotyping of *Alms1 bbb/bbb* by PsiI restriction digestion**……33**

Figure 2.2. Genotyping MMTV transgene by PCR**……35**

Figure 2.3. Determination of estrous cycle stages by vaginal cytology**……36**

Figure 3.1. Relative weights of female control and *bbb/bbb* mice at puberty**……51**

Figure 3.2. Mammary gland adiposity in control and *bbb/bbb* mice at puberty**……52**

Figure 3.3. Deposition of visceral adipose tissue in control and *bbb/bbb* mice at puberty**……53**

Figure 3.4. Whole-mount analysis of developing mammary glands in control and *bbb/bbb* mice at puberty**……55**

Figure 3.5. Proliferation of epithelial cells in mammary gland terminal end buds in control and *bbb/bbb* mice at puberty**……56**

Figure 3.6. Percent mammary gland fibroglandular density in control and *bbb/bbb* mice at puberty**……58**

Figure 3.7. Collagen deposition around the mammary gland ducts in control and *bbb/bbb* mice at puberty**……59**

Figure 3.8. F4/80-positive macrophages around mammary gland terminal end buds in control and *bbb/bbb* mice at puberty**……60**

Figure 3.9. Abundance of macrophages around mammary gland terminal end buds in control and *bbb/bbb* mice at puberty**……61**

Figure 3.10. F4/80-positive macrophages in the mammary gland adipose tissue of control and *bbb/bbb* mice at puberty**……..….63**

Figure 3.11. Abundance of macrophages in the mammary gland adipose tissue in control and *bbb/bbb* mice at puberty**……..….64**

Figure 3.12. F4/80-positive macrophages in the visceral adipose tissue in control and *bbb/bbb* mice at puberty**…….……...….65**

Figure 3.13. Abundance of macrophages in the visceral adipose tissue in control and *bbb/bbb* mice at puberty**…….66**

Figure 3.14. Protein abundance of adipokines and proinflammatory cytokines in the mammary glands in control and *bbb/bbb* mice at puberty**…….……68**

Figure 3.15. Gene expression profile of adipokines and proinflammatory cytokines in the mammary glands in control and *bbb/bbb* mice at puberty**…….……69**

Figure 3.16. Gene expression profile of adipokines and proinflammatory cytokines in the visceral adipose tissue in control and *bbb/bbb* mice at puberty**……71**

Figure 4.1. Illustration of experimental design to study the impact of pubertal adiposity on mammary gland development and density in adulthood**…….……82**

Figure 4.2. Estrous cycle length in female controls, matched *bbb/bbb*, and ad lib *bbb/bbb* mice at adulthood**…….…….85**

Figure 4.3. Relative weights of female controls, matched *bbb/bbb*, and ad lib *bbb/bbb* mice at adulthood**…….…..…….86**

Figure 4.4. Mammary gland adiposity in controls, matched *bbb/bbb*, and ad lib *bbb/bbb* mice at adulthood**…….…..…….87**

Figure 4.5. Deposition of visceral adipose tissue in controls, matched *bbb/bbb*, and ad lib *bbb/bbb* mice at adulthood**…….…..….90**

Figure 4.6. Whole-mount analysis of developing mammary glands in controls, matched *bbb/bbb*, and ad lib *bbb/bbb* mice at adulthood**…….……....92**

Figure 4.7. Percent mammary gland fibroglandular density in controls, matched *bbb/bbb*, and ad lib *bbb/bbb* mice at adulthood**……94**

Figure 4.8. Collagen deposition around the mammary gland ducts in controls, matched *bbb/bbb*, and ad lib *bbb/bbb* mice at adulthood**…….96**

Figure 4.9. F4/80-positive macrophages around mammary gland ducts in controls, matched *bbb/bbb*, and ad lib *bbb/bbb* mice at adulthood**……97**

Figure 4.10. Abundance of macrophages around mammary gland ducts in controls, matched *bbb/bbb*, and ad lib *bbb/bbb* mice at adulthood**……98**

Figure 4.11. F4/80-positive macrophages in the mammary gland adipose tissue in controls, matched *bbb/bbb*, and ad lib *bbb/bbb* mice at adulthood**……100**

Figure 4.12. Abundance of macrophages in the mammary gland adipose tissue in controls, matched *bbb/bbb*, and ad lib *bbb/bbb* mice at adulthood**……101**

Figure 4.13. F4/80-positive macrophages in the visceral adipose tissue in controls, matched *bbb/bbb*, and ad lib *bbb/bbb* mice at adulthood**……...102**

Figure 4.14. Abundance of macrophages in the visceral adipose tissue in controls, matched *bbb/bbb*, and ad lib *bbb/bbb* mice at adulthood**……103**

Figure 4.15. Serum concentration of adipokines and proinflammatory cytokines in controls, matched *bbb/bbb*, and ad lib *bbb/bbb* mice at adulthood**……...…105**

Figure 4.16. Protein abundance of adipokines and proinflammatory cytokines in the mammary glands in controls, matched *bbb/bbb*, and ad lib *bbb/bbb* mice at adulthood**……107**

Figure 4.17. Gene expression profile of adipokines and proinflammatory cytokines in the mammary glands in controls, matched *bbb/bbb*, and ad lib *bbb/bbb* mice at adulthood**…….110**

Figure 4.18. Gene expression profile of adipokines and proinflammatory cytokines in the mammary glands in controls, matched *bbb/bbb*, and ad lib *bbb/bbb* mice at adulthood**……112**

Figure 4.19. Gene expression profile of adipokines and proinflammatory cytokines in the visceral adipose tissue in controls, matched *bbb/bbb*, and ad lib *bbb/bbb* mice at adulthood**…115**

Figure 4.20. Gene expression profile of adipokines and proinflammatory cytokines in the visceral adipose tissue in controls, matched *bbb/bbb*, and ad lib *bbb/bbb* mice at adulthood**…117**

Figure 5.1. Illustration of experimental design to study the impact of pubertal adiposity on mammary cancer development in adulthood**……...…129**

Figure 5.2. Body and adipose tissue weights of female PyMT-control, matched PyMT-*bbb/bbb*, and ad lib PyMT-*bbb/bbb* mice at adulthood**……...…131**

Figure 5.3. Tumour latency in PyMT-control, matched PyMT-*bbb/bbb*, and ad lib PyMT-*bbb/bbb* female mice at adulthood**……...…….132**

Figure 5.4. Tumour development in PyMT-control, matched PyMT-*bbb/bbb*, and ad lib PyMT-*bbb/bbb* female mice at adulthood**……..……...…133**

Figure 5.5. Tumour development in PyMT-control, matched PyMT-*bbb/bbb*, and ad lib PyMT-*bbb/bbb* female mice at adulthood**……..……...…135**

Figure 5.6. Histopathological stage of mammary tumours in PyMT-control, matched PyMT-*bbb/bbb*, and ad lib PyMT-*bbb/bbb* female mice at adulthood**……136**

Figure 5.7. Presence of cytological atypia in mammary tumours in PyMT-control, matched PyMT-*bbb/bbb*, and ad lib PyMT-*bbb/bbb* female mice at adulthood**……...…137**

Figure 5.8. Presence of necrosis in mammary tumours in PyMT-control, matched PyMT-*bbb/bbb*, and ad lib PyMT-*bbb/bbb* female mice at adulthood**……..…138**

Figure 5.9. Gene expression profile of adipokines and proinflammatory cytokines in the mammary tumours of PyMT-control, matched PyMT-*bbb/bbb*, and ad lib PyMT-*bbb/bbb* female mice at adulthood**……...……140**

Figure 5.10. Gene expression profile of adipokines and proinflammatory cytokines in the mammary tumours of PyMT-control, matched PyMT-*bbb/bbb*, and ad lib PyMT-*bbb/bbb* female mice at adulthood**……...……142**

Figure 6.1. Schematic illustration of proposed mechanism linking pubertal adiposity to mammary gland density and mammary cancer development in adulthood**……154**

Figure 6.2. Life course model for breast cancer risk**……..…157**

List of Tables

Table 1.1. Summary of studies reporting association of early life growth measures with mammographic density**……...…….10**

Table 1.2. Summary of studies reporting association of timing of puberty onset with mammographic density**……...…….15**

Table 2.1. Composition of buffers and solutions used for animal experiments**……32**

Table 2.2. Classification of estrous cycle stages by cellular components in vaginal smears**….37**

Table 2.3. Real-time PCR primer pairs specific to mouse genes used to quantify gene expression in mammary glands and mammary tumours in mice**…….46**

Abstract

Mammographic density is one of the most significant risk factors for breast cancer. Breast tissue with high mammographic density is characterised by increased abundance of fibroglandular tissue and reduced abundance of adipose tissue compared to breasts of low density. Mammographic density is a consequence of cellular and molecular events that occur during adolescent breast development. Epidemiological studies show that increased body mass index in adolescence is associated with low mammographic density as an adult and reduced lifetime risk of breast cancer. This suggests that adiposity during pubertal development could be a significant, and modifiable factor that affects adult breast health. However, the causal relationships are yet to be investigated. The studies described in this thesis investigated whether increased pubertal adiposity is causal in mammary gland density and cancer development in adulthood in a mouse model.

Alms1 bbb/bbb mice exhibit hyperphagia, resulting in increased adiposity and body weight relative to wildtype (+/+) and heterozygous (*bbb/+*) littermates when fed a normal mouse chow diet. To investigate the impact of increased adiposity on mammary gland development during puberty, mammary glands were dissected from controls (*bbb/+* or +/+) and *bbb/bbb* female mice during puberty (6 weeks; n=10/gp). At puberty, the adipocyte size in the mammary adipose tissue was significantly increased in *bbb/bbb* mice compared to controls ($p<0.001$). Further, *bbb/bbb* mice exhibited increased number of terminal end buds ($p=0.003$), increased number of proliferating epithelial cells ($p=0.002$), and increased abundance of macrophages around terminal end buds ($p=0.008$) and in the mammary adipose tissue ($p<0.001$), compared to controls.

To investigate the impact of increased pubertal adiposity on mammary gland development and density in adulthood, *bbb/bbb* mice were calorie-matched with controls from 7 weeks of age, such that weight of adult *bbb/bbb* mice was comparable to that of wildtype. Mammary glands were dissected from calorie-restricted *bbb/bbb* mice (and controls) at adulthood (12 weeks; n=10/gp). At adulthood, the adipocyte size in the mammary adipose tissue was significantly increased in matched *bbb/bbb* mice compared to controls ($p<0.01$). Interestingly, matched *bbb/bbb* mice exhibited significantly reduced percent fibroglandular density ($p<0.001$), reduced stroma/epithelium ratio ($p=0.003$), and reduced collagen deposition around ducts ($p<0.001$), compared to controls. Further, mammary glands of matched *bbb/bbb* mice demonstrated increased expression of mRNA encoding adiponectin ($p<0.01$), TGFB1 ($p=0.044$), CSF1 ($p=0.033$), IGF1 ($p=0.007$), and STAT3 ($p=0.033$), compared to controls.

To determine the impact of increased pubertal adiposity on mammary cancer development, the MMTV-PyMT tumour model was crossed with *Alms1 bbb/+* mice to generate female PyMT-control and PyMT-*bbb/bbb* mice. At 18 weeks, PyMT-*bbb/bbb* mice exhibited significant increase in tumour free survival (LogRank $p=0.002$), greater tumour latency ($p<0.01$) and reduced number of tumours ($p=0.006$), compared to PyMT-control mice. Interestingly, matched PyMT-*bbb/bbb* mice exhibited significantly increased expression of mRNA encoding TGFB1, compared to PyMT-control mice ($p=0.037$).

This research in mice provides the first evidence that increased pubertal adiposity might be causative in affecting mammographic density and breast cancer risk in adulthood. Together with epidemiological studies, this research provides the foundation for a new paradigm for the origins of mammographic density and breast cancer risk during pubertal breast development.

Declaration

I certify that this work contains no material which has been accepted for the award of any other degree or diploma in my name, in any university or other tertiary institution and, to the best of my knowledge and belief, contains no material previously published or written by another person, except where due reference has been made in the text. In addition, I certify that no part of this work will, in the future, be used in a submission in my name, for any other degree or diploma in any university or other tertiary institution without the prior approval of the University of Adelaide and where applicable, any partner institution responsible for the joint award of this degree.

I give permission for the digital version of my thesis to be made available on the web, via the University's digital research repository, the Library Search and also through web search engines, unless permission has been granted by the University to restrict access for a period of time.

…….

Amita Gautam Ghadge

September 2021

Acknowledgements

Foremost, I would like to thank my principal supervisor, Associate Professor Wendy Ingman, for her immense support, advice, and guidance throughout the years. I consider myself very fortunate to have the opportunity to study under her supervision. I am very grateful for her constant encouragement and patience she has shown through these years, and this has helped me to achieve the most of my potential.

I am grateful to my co-supervisor Dr Pallave Dasari for her mentorship and sincere advice at both academic and personal level during my candidature. Her guidance helped me to expand my communication and networking skills. I am thankful to my co-supervisor Professor Rebecca Robker for her invaluable insights and advice in my PhD studies. My sincere thanks to Haley Sheree Connaughton and Dr David Sharkey for their time and help associated with this project. I would like to thank Suzanne Edwards for her help in statistical analysis of data in my studies. I am also thankful to Dr Lucy Woolford for pathological assessment of tissue samples in my studies.

I am truly grateful to all members of Breast Biology and Cancer Unit past and present for creating positive and friendly work environment. Many thanks to everyone at the Basil Hetzel Institute and The Hospital Research Foundation for their support during my candidature. I am grateful to the University of Adelaide for the opportunity, and to receive the International Wildcard Scholarship to support me financially during my PhD studies.

To my friends here in Adelaide, Claire, Tharu, Dayan, Matt, and Max, thank you for your friendship and constant support throughout the years. I am glad to have shared this journey with you all; celebrating our successes together and supporting each other through the difficult times. I consider myself very fortunate to be friends with you all.

To my loving parents, thank you so much for supporting me in all my adventures. I dedicate this whole journey to you both. I am extremely blessed to have parents who believe in me and my life decisions. I am grateful for your patience, guidance, and multiple reassurances in the moments of crisis. Thank you for being by my side in all my successes and failures. I cannot imagine having completed my PhD studies without your unconditional love and encouragement.

Publications arising from this thesis

Journal articles

Ghadge AG, Dasari P, Stone J, Thompson EW, Robker RL and Ingman WV (2021). Pubertal mammary gland development is a key determinant of adult mammographic density. Semin Cell Dev Biol. 114:143-158. doi.org/10.1016/j.semcdb.2020.11.011.

(Appendix A)

Abstracts arising from this thesis

2021

Ghadge AG, Dasari P, Sharkey DJ, Robker RL, Ingman WV. "The developmental origins of mammographic density and breast cancer risk". Australian Society for Medical Research. Adelaide, Australia. Oral Presentation.

2020

Ghadge AG, Dasari P, Sharkey DJ, Robker RL, Ingman WV. "Deposition of adipose tissue during puberty alter mammary cancer risk in adulthood". Australian Society for Medical Research. Adelaide, Australia. Oral Presentation.

Ghadge AG, Dasari P, Sharkey DJ, Robker RL, Ingman WV. "The impact of pubertal adipose tissue deposition on mammary cancer development during adulthood". The Joint Annual Scientific Meetings of the Endocrine Society of Australia and the Society for Reproductive Biology. Adelaide, Australia. Oral Presentation.

Ghadge AG, Dasari P, Sharkey DJ, Robker RL, Ingman WV. "Deposition of adipose tissue during puberty affects mammary gland density and cancer development during adulthood". Robinson Research Institute Symposium. Adelaide, Australia. Poster Presentation.

Ghadge AG, Dasari P, Sharkey DJ, Robker RL, Ingman WV. "Deposition of adipose tissue during puberty affects mammary gland density and cancer development during adulthood". The Queen Elizabeth Hospital Research Expo. Adelaide, Australia. Oral Presentation.

2019

Ghadge AG, Dasari P, Robker RL, Ingman WV. "The impact of pubertal adiposity on breast development, breast density, and breast cancer risk". European Molecular Biology Laboratory (EMBL) Australia. Melbourne, Australia. Poster Presentation.

Ghadge AG, Dasari P, Sharkey DJ, Robker RL, Ingman WV. "The impact of pubertal adiposity on breast development and breast cancer risk". Australian and New Zealand Society for Immunology. Adelaide, Australia. Oral Presentation.

Ghadge AG, Dasari P, Robker RL, Ingman WV. “Impact of pubertal adiposity on breast development, breast density, and breast cancer risk”. Florey Postgraduate Research Conference. Adelaide, Australia. Poster Presentation.

Ghadge AG, Dasari P, Robker RL, Ingman WV. “Impact of pubertal adiposity on breast development, breast density, and breast cancer risk”. Robinson Research Institute Symposium. Adelaide, Australia. Poster Presentation.

Ghadge AG, Dasari P, Robker RL, Ingman WV. “Impact of pubertal adiposity on breast development, breast density, and breast cancer risk”. The Queen Elizabeth Hospital Research Expo. Adelaide, Australia. Oral Presentation.

2018

Ghadge AG, Dasari P, Robker RL, Ingman WV. “Impact of pubertal fatness on breast development, breast density, and breast cancer risk”. The Queen Elizabeth Hospital Research Expo. Adelaide, Australia. Poster Presentation.

Awards and honours

2021

- Ross Wishart Memorial Award, Australian Society for Medical Research

2020

- Best Student Oral presentation Award, Australian Society for Medical Research

2019

- Best Student Oral presentation Award, The Queen Elizabeth Hospital Research Expo
- Science in Public Media & Communications Workshop Award, The Hospital Research Foundation and The Basil Hetzel Institute
- European Molecular Biology Laboratory (EMBL) Australia Postgraduate Symposium Travel Award
- Industry Mentoring Network in STEM (IMNIS) Program Award, The University of Adelaide

Abbreviations

ACTH: Adrenocorticotropic hormone

ACTB: Beta-actin

ALMS1: Alstrom syndrome protein 1

BI-RADS: Breast Imaging Reporting and Data System

BMI: Body mass index

COX2: Cyclooxygenase 2

CSF1: Colony stimulating factor 1

CCL2: C-C motif chemokine ligand 2

DHEA: Dehydroepiandrosterone

DHEAS: Dehydroepiandrosterone sulfate

DAB: 3,3 diaminobenzidine

ECM: Extracellular matrix

ESR1: gene encoding estrogen receptor alpha

ENU: N-ethyl-N-nitrosourea

FSH: Follicle-stimulating hormone

GAPDH: Glyceraldehyde 3-phosphate dehydrogenase

GnRH: Gonadotropin releasing hormone

GHRH: Growth hormone-releasing hormone

GH: Growth hormone

HER2: Human epidermal growth factor receptor 2

HPG axis: Hypothalamic-pituitary-gonadal axis

HMD: High mammographic density

HRT: Hormone replacement therapy

IGF1: Insulin-like growth factor 1

IL4: Interleukin 4

IL6: Interleukin 6

LMD: Low mammographic density

LH: Luteinizing hormone

MRI: Magnetic resonance imaging

MMTV: Mouse mammary tumour virus

MMPs: Matrix metalloproteinases

PAI1: Plasminogen activator inhibitor 1

PyMT: Polyomavirus middle T-antigen

SHBG: Sex hormone binding globulin

STAT3: Signal transducer and activator of transcription 3

TNFA: Tumour necrosis factor alpha

TIMPs: Tissue inhibitors of metalloproteinases

TEBs: Terminal end buds

TGFB1: Transforming growth factor beta 1

CHAPTER ONE
Literature review and aims

1.1 Introduction

Mammographic density (also known as breast density) is an important risk factor for breast cancer (1, 2). It refers to the proportion of radiologically dense fibroglandular tissue present in the breast in comparison to radiologically non-dense adipose tissue, when observed on a mammogram. At the cellular level, epithelial and stromal cells are the predominant cell types in white dense regions and adipocytes are the predominant cell type in dark non-dense regions (3). Forty years of epidemiological research has demonstrated that women with 'extremely dense' breasts have a 4-6-fold increased risk of breast cancer in comparison to women with 'mostly fatty' breasts, when adjusted for age and body mass index (BMI) (2-6). Although the association between mammographic density and breast cancer risk is well-established, the molecular and cellular events that lead to the development of mammographic density, and why this is associated with an increased risk of cancer are yet to be elucidated.

Puberty is a critical time for breast development. Endocrine and paracrine signalling drive development of epithelial, stromal, and adipose tissue in the breast (7-12). As the relative abundance of these cell types determines the radiological appearance of the adult breast, puberty should be considered as a key developmental stage in the establishment of mammographic density. This important stage of growth and development has a significant impact on both adult mammographic density and breast cancer risk. Epidemiological studies have consistently shown an inverse association between pubertal adiposity measures such as weight, BMI and body shape with percent mammographic density (13-20) as well as adult breast cancer risk (21-26). Commencement of menstrual cycling - known as menarche, and timing of appearance of breast buds - known as thelarche, also impact adult mammographic density. Later onset of menarche and regular menstrual cycles is associated with increased mammographic density and earlier age at thelarche is associated with lower adult mammographic density (27).

Although these epidemiological studies point to significant associations between pubertal adiposity, adult mammographic density, and breast cancer risk, causal relationships are yet to be established. If it could be shown that adult mammographic density is modifiable during the pubertal growth period, there could be opportunities to intervene during adolescence to reduce lifetime mammographic density-associated breast cancer risk. Therefore, understanding biological mechanisms active during puberty that might drive high mammographic density hold great potential in breast cancer prevention. Here we discuss potential roles of endocrine and paracrine signalling during puberty as well as genetic and epigenetic factors that affect adult mammographic density.

1.2 Mammographic density is a breast cancer risk factor

The Breast Imaging Reporting and Data System (BI-RADS) developed by the American College of Radiology describes four categories of mammographic density: (a) 'mostly fatty'; (b) 'scattered density'; (c) 'heterogeneously dense'; and (d) 'extremely dense' (28) (Figure 1.1.A). Approximately 8% of women aged 40-74 have breasts classified as 'extremely dense' and around 35% have breasts classified as 'heterogeneously dense' (29). Combined, these two categories of density are often termed "high mammographic density" and define what it means for a woman to have "dense breasts". The cellular components of mammographic density can be identified through image-guided biopsies of x-rayed breast tissue samples (Figure 1.1.B; (30)). Breast tissue regions with low mammographic density exhibit increased abundance of adipocytes and reduced abundance of epithelium and stroma (Figure 1.1.C). Conversely, high mammographic density is characterised by abundant stromal and epithelial cells and fewer adipocytes (Figure 1.1.D).

Thirty nine percent of premenopausal and 26% of postmenopausal breast cancers are attributed to high mammographic density (2). Mammographic density also masks cancer on a mammogram; dense fibroglandular tissue and breast cancers both appear white on the mammogram, therefore increased mammographic density can reduce the sensitivity of mammography to detect breast cancer (1, 31-33). Early research suggested that the increased risk of breast cancer associated with high mammographic density was the consequence of the masking effect of density (34). However, the masking effect of mammographic density is only partly responsible for the association of mammographic density with breast cancer risk. A landmark meta-analysis in 2006 demonstrated that women with increased mammographic density, assessed at least 5 years earlier, had a 3.25-fold increased breast cancer risk, in comparison to women of similar age with low mammographic density (4). In another study, the association between high mammographic density and breast cancer risk remained intact for an average of 7 years after mammographic screening (35).

High mammographic density appears to be associated with an increased risk of all breast cancer subtypes although there are still mixed findings in the literature (comprehensively reviewed by (36)). Breast cancer is 5 times more likely to develop in dense breast tissue regions compared to non-dense regions (37). An autopsy study of women without clinically detectable breast cancer demonstrated that precancerous microscopic columnar cell lesions are found in 1 of 4 women with dense breasts (38). This suggests that the cellular and molecular components that comprise high mammographic density could be associated with a pro-tumorigenic microenvironment that increases the susceptibility of the breast to all cancer subtypes (3, 39).

The breast is a highly heterogeneous tissue containing 3 distinct tissue compartments: (1) epithelium (containing epithelial cells), (2) stroma (containing a combination of fibroblasts, immune cells, and extracellular matrix), and (3) adipose tissue (containing adipocytes and immune cells). All of these cell types, as well as the extracellular matrix, contribute to the mammographic density of the breast, and could also affect breast cancer risk. However, the molecular and cellular mechanisms that link high mammographic density with increased breast cancer risk are yet to be elucidated.

The prevalence of high mammographic density in the population is greatest in younger women and gradually decreases with increasing age (29). Studies have shown that percent mammographic density decreases an average of 1% per year (40, 41) and more (~5%) over menopause (41). High mammographic density is associated with increased breast cancer risk across all age groups, with the strongest association in premenopausal women and women receiving postmenopausal hormone therapy (42). Although mammographic density declines as women age, young women with high density tend to have high density throughout life relative to their peers (43, 44). Therefore, mammographic density tends to be at its highest in young women following breast development during puberty, and this sets the trajectory for mammographic density over the life course.

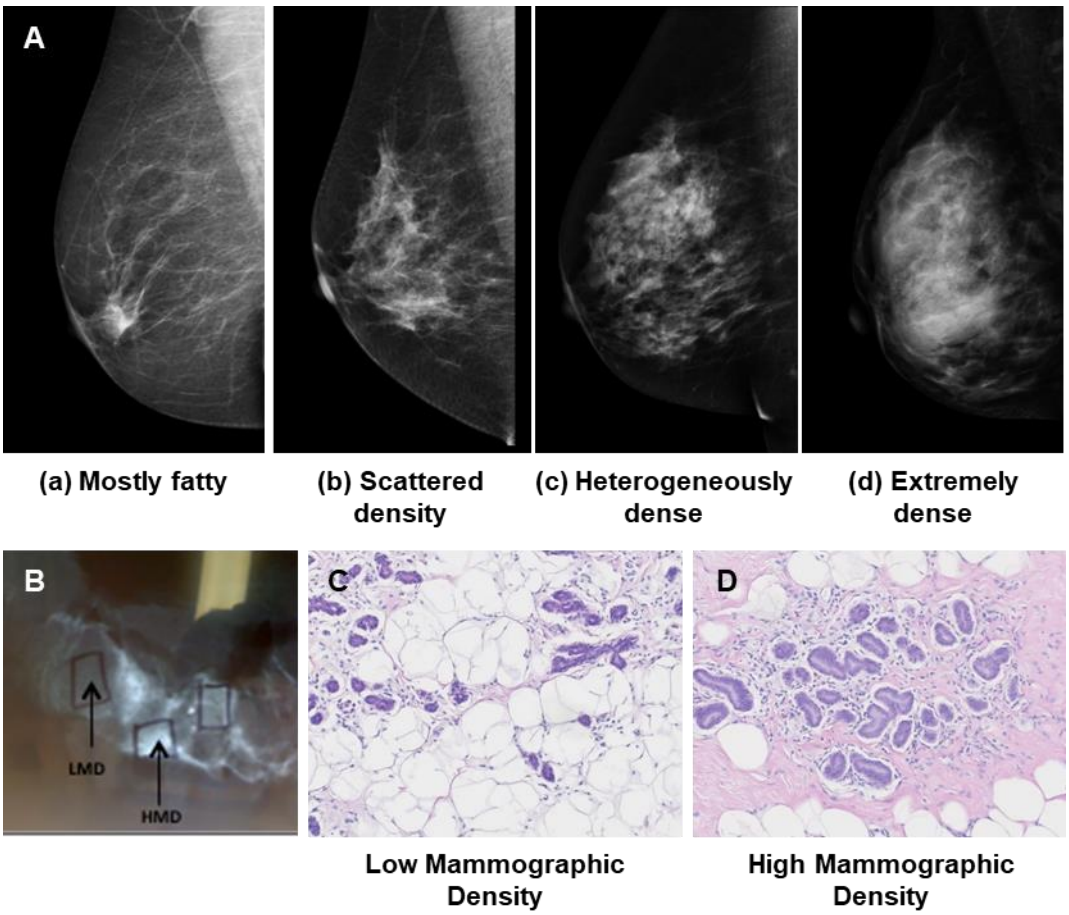

Figure 1.1. Mammographic density refers to the radiological appearance of the breast and reflects the relative proportion of fibroglandular and adipose tissue. (A) Four categories of mammographic density are described by the American College of Radiology; (a) mostly fatty, (b) scattered density, (c) heterogeneously dense, and (d) extremely dense, images are reproduced from InforMD (www.informd.org.au). (B) In order to explore the cellular structures associated with high and low mammographic density (HMD and LMD respectively), surgically-excised breast tissue is X-rayed and the image used to guide biopsies of high and low density regions for further analysis. (C, D) Hematoxylin and eosin stained sections of low and high mammographic density respectively from a 35-year old woman undergoing breast reduction surgery. Regions of low mammographic density consist predominantly of adipocytes (large white cells), and regions of high mammographic density consist predominantly of epithelial cells (purple-stained cells) and stroma (pink-stained regions).

1.3 Pubertal breast development

Puberty is a critical time for breast development when endocrine and paracrine factors drive development of epithelial, stromal, and adipose tissue in the breast (7-12, 45) (Figure 1.2). Prior to puberty, the mammary gland consists of a rudimentary framework, with ductal elongation occurring at a rate proportional to general growth of the body (46). At this stage, the epithelium is two-layered, and the dense supporting stroma can be distinguished from the less dense periductal connective tissue, with these different tissue compartments having been established around the age of 8 months (47). Thelarche occurs prior to menarche. During puberty, with activation of the hypothalamus and pituitary gland leading to increased secretion of ovarian, adrenal, and somatotropic hormones, the rudimentary mammary gland begins to show active responses and there are changes in both the epithelium and the stroma (48). Solid epithelial buds form along the already laid ducts, which with the progression of development become canalised (46). The growth and branching of the solid epithelial buds are supported by proliferation of connective tissue that replaces the fatty tissue (47). This results in the formation of groups of small ductules surrounded by loose connective tissue, which finally form typical terminal duct lobular structures seen by the end of puberty. After the completion of puberty, there is minimal development in the epithelium and stromal components of the adult breast until the first pregnancy (48). The adult breast is thus comprised of three broad tissue compartments: epithelium, stroma and adipose tissue. As the relative abundance of these cell types determines the radiological appearance of the adult breast, puberty therefore can be considered as a key developmental stage in the establishment of mammographic density.

1.4 Adiposity, mammographic density, and breast cancer risk

There is compelling evidence of associations between measures of adiposity over the life course with adult mammographic density and breast cancer risk. However, the relationships are complex; increased adiposity at different developmental stages affects breast cancer risk differently. Adiposity is often expressed in terms of BMI, and calculated as the ratio of weight (in kilograms) to square of height (in meters). In the literature linking pubertal growth measures with adult mammographic density, weight and recalled body shape or somatotype are also used as measures of adiposity. The association between BMI and mammographic density is dependent on how mammographic density is expressed (percent or absolute) and measured (area or volume). Increased BMI often increases breast size (49-51) and the relative abundance of non-dense adipose breast tissue compared to dense fibroglandular tissue influences percent mammographic density simply by its calculation.

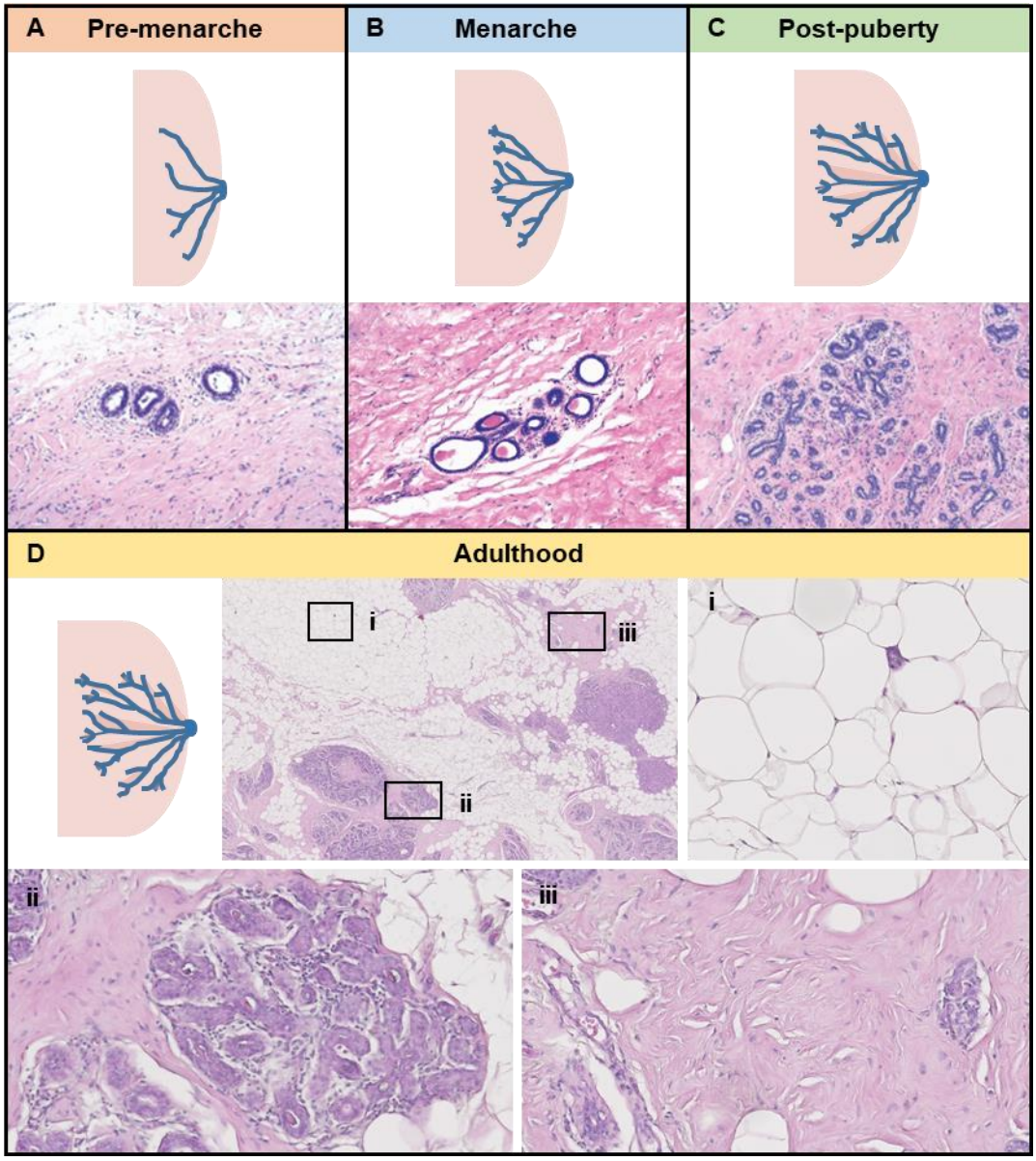

Figure 1.2. Development of epithelial, stromal, and adipose tissue in the breasts occurs during puberty. (A-D) Schematic diagrams and hematoxylin and eosin (H&E)-stained sections of ductal morphology in the breast in the pre-menarche, menarche, post-puberty stages, and adult stages respectively. (A) H&E-stained section is breast tissue of an 11-year old pre-menarcheal girl with no lobular differentiation; (B) H&E-stained section is breast tissue showing initiation of lobular differentiation and development of intralobular stroma in an 11-year old girl at menarche; (C) H&E-stained section is breast tissue showing lobular structures observed in the follicular phase of the menstrual cycle in a 15-year old girl; and (D) H&E-stained sections are of breast tissue from a 27-year old woman undergoing mastectomy for inherited high breast cancer risk of unknown genetic origin, boxes show magnified regions predominantly containing (i) adipocytes, (ii) epithelial cells, and (iii) stroma. H&E-stained sections in A and C are reproduced from Hoda *et al*., Rosen's Breast Pathology 3rd edition, Wolters Kluwer Health Inc, 2008 (Copyright licence in Appendix B); H&E-stained section in B is reproduced from Hoda *et al*., Rosen's Diagnosis of Breast Pathology by Needle Core Biopsy 3rd edition, Wolters Kluwer Health Inc, 2010 (Copyright licence in Appendix C).

BMI has been shown to be inversely associated with absolute dense area, which is the two-dimensional dense tissue area projected on the mammogram, but positively associated with dense volume, which takes into account the thickness of dense tissue (52-55). This highlights the importance of adjusting for confounding adiposity measures when investigating associations between mammographic density and breast cancer risk.

Adult BMI affects breast cancer risk, however the direction of this relationship varies by menopausal status. Premenopausal women with high BMI have lower risk of breast cancer, but postmenopausal women with high BMI have increased risk (56, 57). In obese premenopausal women, increased frequency of anovulatory menstrual cycles results in reduced exposure to ovarian hormones, which may contribute to the reduced risk of breast cancer (57). On the other hand, there can be an increased concentration of estrogen in obese postmenopausal women due to increased aromatisation of adrenal androgens in adipose tissue, which increases breast cancer risk (58). Obesity also increases inflammatory markers in adipose tissue which could drive increased breast cancer risk (59-64).

Several studies have shown an inverse association of pubertal body adiposity with breast cancer risk (21-26), however, there are other studies that do not support this association (65-67). Prospective data from a British birth cohort (68, 69) showed that women diagnosed with breast cancer had been consistently thinner during childhood than women without breast cancer (70). Interestingly, a post-hoc analysis within the earlier Nurses' Health Study showed that gain in body adiposity between ages 5-10 years was associated with lower postmenopausal breast cancer risk, but gain in body adiposity between ages 10-20 years was associated with greater risk (71). Epidemiological studies show that excess body adiposity or abnormal leanness in adolescents, both associated with decreased risk of breast cancer, also have an association with ovulatory dysfunction (72-77). With abnormal leanness, child gymnasts, athletes, and ballet dancers who commonly experience delayed menarche and irregular menstrual cycles, have reduced breast cancer risk (78). Although the biological basis of the association between childhood and pubertal adiposity and adult breast cancer risk is not clearly understood, it may be mediated through mammographic density (20, 79, 80).

There is a growing body of evidence for a relationship between pubertal growth measures and adult mammographic density (Table 1.1). A number of studies show consistent inverse associations between pubertal adiposity using measures such as BMI, weight and recalled body shape, and percent mammographic density in adult women when adjusted for adult BMI (13, 14, 16-19), while there are few studies that oppose this association (81, 82). One study demonstrated that mammographic density mediates the association of childhood BMI with

breast cancer risk in premenopausal women (83). In a register-based cohort study, the significant inverse association of BMI at age 13 with breast cancer risk was weakened when adjusted for mammographic density (19), which further supports the notion that mammographic density could mediate the association between pubertal BMI and breast cancer risk. Other studies have suggested the mediating effect of mammographic density on the association of pubertal adiposity with breast cancer risk is weak (15). However, these studies have examined mammographic density in older, predominantly postmenopausal women where the impact of pubertal growth could be mitigated by other factors during adulthood.

Mammographic density in girls and younger women has not been well characterised because routine radiographic screening is not implemented until age 40 or older. When mammographic density is measured by magnetic resonance imaging (MRI) in women aged less than 30, it is found to be inversely associated with childhood body size (84, 85). A limitation in some studies investigating relationships between pubertal BMI and adult mammographic density is that the pubertal BMI is self-reported, however, the accuracy of this is thought to be reasonably good (86). A further degree of caution is needed when assessing pubertal body adiposity using the adult BMI scale. Weight and height can change in adolescents as part of normal pubertal growth and development. Therefore, it is important to use a BMI scale that is age appropriate, such as BMI-percentiles (87). Compared to the median BMI-percentile (20.7 kg/m^2), a BMI over 22.3 kg/m^2 (75th BMI-percentile) at age 18 is associated with a 45% decrease in adult mammographic density, adjusted for adult BMI and timing of menarche (88). Higher BMI percentile in adolescence is also associated with reduced risk of breast cancer (71, 89, 90). Overall, these studies demonstrate that increased pubertal body adiposity is associated with reduced mammographic density and breast cancer risk in adult women.

Table 1.1. Summary of studies reporting association of early life growth measures with mammographic density. Somatotype assessment is based on 9-level figure pictogram, participants recall the figure that best represented their body shape at a particular age (1 represented extremely lean and 9 represented extremely obese). The correlation of recalled somatotype and BMI measured at approximately same ages range from 0.60 to 0.75 (91). BMI Z-scores are BMI expressed as a Z-score relative to Centres for Disease Control and Prevention (CDC) 2000 growth charts (92). Breast water is the water content of the breast measured by magnetic resonance imaging, provides measurement of amount of fibroglandular breast tissue, without exposure of young women to radiation (93). Breast water is strongly correlated to mammographic density (94). MRI: Magnetic resonance imaging; DXA: Dual energy X-ray absorptiometry.

Reference	Number of participants	Growth measure	Age at growth measure	Mammographic density measure	Menopausal status at mammographic density assessment	Association of adiposity with mammographic density
Samimi et al. [13]	1398	Recalled somatotype	5, 10 years	Percent mammographic density	Pre-, Post-	Inverse association
Sellers et al. [14]	1893	Recalled somatotype	12 years	Percent mammographic density	Pre-, Post-	Inverse association
Jeffreys et al. [16]	608	BMI	Young adult at University	Percent mammographic density	Pre-, Post-	Inverse association
Lope et al. [17]	3557	Self reported relative weight	Before menarche	Percent mammographic density	Pre-, Post-	Inverse association
McCormack et al. [18]	1298	BMI	2-53 years	Wolfe grade	Peri-	Inverse association
Andersen et al. [19]	13572	BMI	7-13 years	Mixed/dense or fatty	Post-	Inverse association
Yochum et al. [81]	Review of 9 epidemiologic studies	Direct measurement or self-reported BMI, recalled somatotype relative to peers	≤18 years	Percent mammographic density	Pre-	No association
Rice et al. [82]	1531	Recalled somatotype	Before menarche, two years after menarche, 18-20 years	Percent mammographic density	Pre-, Post-	No association
Bertrand et al. [84]	182	Age-specific BMI Z-scores	8-10 years	Percent mammographic density (MRI)	Pre-	Inverse association
Boyd et al. [85]	400	Measured weight	15-30 years	Percent breast water (MRI)	Pre-	Inverse association
Alexeeff et al. [88]	24840	BMI-percentile	18 years	Percent mammographic density	Pre-, Post-	Inverse association
Novotny et al. [98]	113	BMI	10-16 years	Percent fibroglandular volume (DXA)	Adolescence	Inverse association

1.5 Timing of puberty onset affects adult mammographic density

In humans, puberty is marked by maturation of reproductive organs, linear growth acceleration, development of secondary sex characteristics, and, in females, the occurrence of menarche. The transition into puberty is driven by two physiological processes: gonadarche and adrenarche. In females, gonadarche is the growth and maturation of the ovary with secretion of estrogen and progesterone, initiation of ovulation, and menarche. Adrenarche, which typically precedes gonadarche, is associated with increased secretion of adrenal androgens, such as dehydroepiandrosterone (DHEA), dehydroepiandrosterone sulfate (DHEAS), and androstenedione (95). In females, increased secretion of ovarian and adrenal hormones cause thelarche and menarche. The age at onset of puberty and the time interval between thelarche and menarche, known as pubertal tempo, are dependent on many factors and highly varied between individuals.

Onset of pubertal breast development, onset of menstrual cycling, and pubertal tempo, all impact adult mammographic density (Table 1.2). Most studies analysing the association of age at puberty onset with adult mammographic density have utilized age at menarche (17, 18, 96-101). A recent study (27) found that later onset of menarche and later onset of regular cycles are associated with increased mammographic density. Most studies show a positive association between age at menarche with mammographic density (17, 18, 27, 96, 97, 99, 100, 102), but not all (98, 99, 101). Similarly, age at thelarche and pubertal tempo are also found to be associated with adult mammographic density. Early age at thelarche has been shown to be associated with lower adult mammographic density (27). Women who experienced a longer interval between thelarche and menarche (i.e., tempo), and between thelarche and regular menstrual cycles, have increased dense breast area, independent of age at onset of menarche (27). Women whose pubertal tempo was 2.9 years or longer, had 40% higher percent dense breast volume than women whose pubertal tempo was less than 1.6 years (103).

Childhood weight is likely to be an important factor in the association between puberty onset and adult mammographic density (18, 27, 102). Multiple longitudinal and cross-sectional studies demonstrate that girls with higher body adiposity during childhood, undergo earlier pubertal development (104-108). A recent pooled analysis of five cohort studies (104, 106, 109-111) indicated that the proportion of obese girls with early puberty was significantly greater than girls with average weight (112). A number of studies add support to the notion that increased adiposity may be a significant driving factor for early onset of puberty in girls (113-115). However, the relationship between excess adiposity and early menarche is not universal. A meta-analysis based on two cohorts (116, 117) indicated no statistical difference in the age

of menarche between obese and normal-weight girls. Another study reported no correlation between age at menarche and pubertal BMI (118). Like menarche, onset of thelarche is also dependent on body adiposity during puberty. Studies have shown that girls with thelarche exhibit greater body adiposity compared to age-matched girls without thelarche (106, 108), and similarly, that girls with excessive adiposity more commonly have earlier thelarche compared to girls with normal BMI (119). However, more accurate assessment of breast development in obese girls is needed, as excessive subcutaneous adiposity in the breasts can be mistaken for breast development and thus, errors can occur in estimating the onset of puberty (120).

Despite some minor controversy around the relationship between obesity and early menarche, it is clear that a certain amount and distribution of adipose tissue is necessary for the onset of menarche (121) and increased body adiposity is associated with earlier pubertal development (104-108). Body adiposity is thought to increase in mammalian females during puberty as it guarantees a healthy future pregnancy and maternal survival (117). Interestingly, adipose tissue localised to the gluteofemoral depots is associated with onset of menarche, and this specific fat deposit appears to be more closely associated with puberty initiation than the amount of total body fat (122-124). Thus, adiposity is a significant regulator of puberty onset in healthy children affecting the timing of thelarche and menarche (Figure 1.3). In turn, these key pubertal milestones, and the time interval between them, appear to affect the relative abundance of fibroglandular and adipose tissue within the breast. Pubertal changes in mammary gland development may persist into adulthood where they are observed on a mammogram as altered mammographic density.

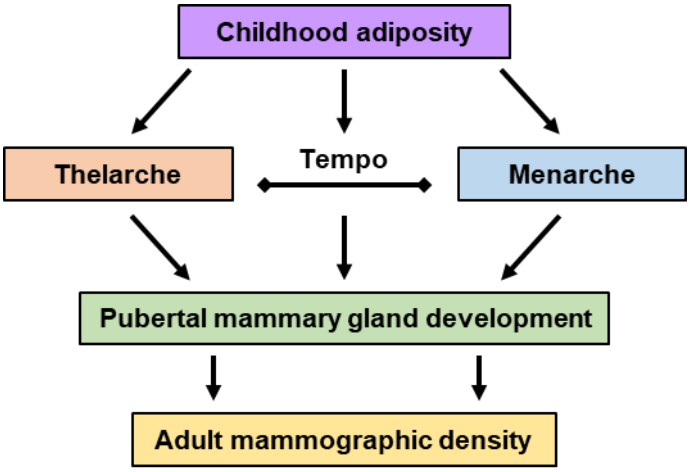

Figure 1.3. Puberty is a key developmental stage in the establishment of adult mammographic density. Adiposity during childhood affects the timing of thelarche, menarche, and the time interval between these developmental stages (tempo). These factors collectively affect pubertal mammary gland development, which in turn affects the establishment of adult mammographic density.

Table 1.2. Summary of studies reporting association of timing of puberty onset with mammographic density. DXA: Dual energy X-ray absorptiometry.

Reference	Number of participants	Timing of puberty onset	Mammographic density measure	Association of pubertal stages with mammographic density
Lope et al. [17]	3557	Menarche	Percent mammographic density	Positive association
McCormack et al. [18]	1298	Menarche	Wolfe grade	Positive association
Schoemaker et al. [27]	1105	Menarche	Percent mammographic density, absolute dense area	Positive association
		Thelarche	Percent mammographic density	
		Pubertal tempo	Absolute dense area	
Butler et al. [92]	801	Menarche	Percent mammographic density	Positive association
Dite et al. [93]	571 monozygotic, 380 dizygotic	Menarche	Dense area	Positive association
Dorgan et al. [94]	176	Menarche	Percent dense breast volume	No association
Heng et al. [95]	803	Menarche	Percent mammographic density	No association
Titus-Ernstoff et al. [96]	144018	Menarche	Dichotomized as dense versus not dense	Positive association
Tehranifar et al. [97]	191	Menarche	Dense area	Inverse association
Novotny et al. [98]	113	Menarche	Adolescent percent fibroglandular volume (DXA)	Positive association
Houghton et al. [99]	182	Pubertal tempo	Percent dense breast volume	Positive association

1.6 Endocrine regulators of pubertal breast development and mammographic density

The onset of puberty and mammary gland development is a consequence of activation of the hypothalamic-pituitary axes, with the timing influenced by nutrition and genetic factors that affect adipose tissue deposition (Figure 1.4). The hypothalamus is activated by the production of kisspeptin resulting in the release of gonadotropin releasing hormone (GnRH) and growth hormone-releasing hormone (GHRH). In females, the anterior pituitary secretes growth hormone (GH) that acts on the liver to form the hypothalamic-pituitary-somatotropic axis; and adrenocorticotropic hormone (ACTH) that stimulates the adrenal gland to form the hypothalamic-pituitary-adrenal axis. In addition, luteinizing hormone (LH) and follicle-stimulating hormone (FSH) act on the ovaries to form the hypothalamic-pituitary-gondal (HPG) axis. FSH promotes ovarian biosynthesis of estrogen and LH induces ovulation (125, 126). Rising estrogen acts on the hypothalamus creating a negative feedback loop in this cycle (127). Breast development typically starts around 9 years of age and is well-progressed by the time of menarche (128-131). Thus, breast tissue in pre-pubertal and early pubertal girls is exposed to relatively lower levels of estradiol (132). However, increased body adiposity is shown to affect the abundance of sex hormones in girls. Increased total and free testosterone, in association with lower concentration of sex hormone binding globulin (SHBG), and higher fasting insulin, have been reported in peripubertal obese girls (133). In addition, around the time of thelarche, girls with higher BMI had lower circulating concentration of estradiol (128).

1.6.1 Sex hormones

Few studies have investigated the role of peripubertal hormones on determination of adult mammographic density. Irrespective of menarche status, estrogens (85, 134-138), progesterone (85, 134, 136, 138), testosterone (85, 135, 137-145) and androstenedione (135, 139, 142, 145, 146) measured during puberty were found to be non-significantly associated with mammographic density in adult women. In contrast, elevated premenarcheal concentration of circulating dehydroepiandrosterone sulfate (DHEAS) is associated with increased breast dense area during adulthood (147). DHEAS is also found to be positively associated with growth factors during puberty (148), which can have substantial impact on pubertal breast development (149-151). DHEAS can have estradiol-like proliferative effects in an environment of low estrogen (152), which is typical during early puberty in girls (132). In pre-pubertal girls, prior to the activation of the HPG axis, DHEAS can be metabolised to estrogens in adipose tissue (128). This could explain the early breast development, mediated independent of ovarian hormones, in girls with excess adiposity (129, 153).

Premenarcheal SHBG is also shown to be positively associated with adult percent dense breast volume in premenopausal (134, 135, 137, 147, 154) and postmenopausal women (134, 146, 155), although other studies do not support this association (139-142, 145, 156). Further, cell surface SHBG receptors and intracellular SHBG are detected in the breasts, which further suggest that SHBG could influence mammographic density via other mechanisms (157) besides controlling steroid hormone bioavailability. Hence, both SHBG and DHEAS could be potential candidates to mediate the effect of pubertal adiposity on development of adult breasts with low mammographic density.

1.6.2 Growth hormone and insulin-like growth factor 1

Growth hormone (GH) acts on both the stromal and epithelial cell components of the mammary gland to promote the formation of terminal end buds and ductal elongation (151, 158-160). In addition to pituitary secretion, GH is also produced locally in the mammary gland (161, 162). In mice, expression of GH mRNA and protein is detected in mammary gland epithelium, with maximum expression observed during puberty (160). Over-expression of GH in a transgenic mouse model results in precocious mammary gland development (163), while deficiency of functional GH leads to severe impairment of mammary gland development (164). In humans, autocrine GH and GH receptor mRNA and protein expression are primarily observed in the luminal epithelial and myoepithelial ductal cells (161, 162, 165, 166).

Insulin-like growth factor 1 (IGF1) is believed to be a key mediator of GH signalling in mammary gland development (151, 158-160). This is demonstrated by the inability of GH to have any effect on mammary gland development in animals unable to produce IGF1 (167). Rodent studies have demonstrated that locally derived IGF1 promotes pubertal mammary gland development (168-170). Further, the expression of GH receptor is also observed in the stroma (171) and it is hypothesised that the presence of GH activates the GH receptor within the stromal cells leading to the expression of IGF1, which further activates IGF1 receptors in the epithelium (172). Lower circulating concentrations of both GH and IGF1 are observed in pubertal girls with excess adiposity (173), however this may not reflect levels within the breast tissue.

In adult women, case-control and cohort studies have demonstrated a positive association between elevated circulating concentration of IGF1 with breast cancer risk (174-179), however other studies have found no association (180, 181). The GH/IGF1 axis is also shown to be associated with mammographic density. IGF1 and GH are positively associated with percent mammographic density in both premenopausal and postmenopausal women, without adjustment for other risk factors (182).

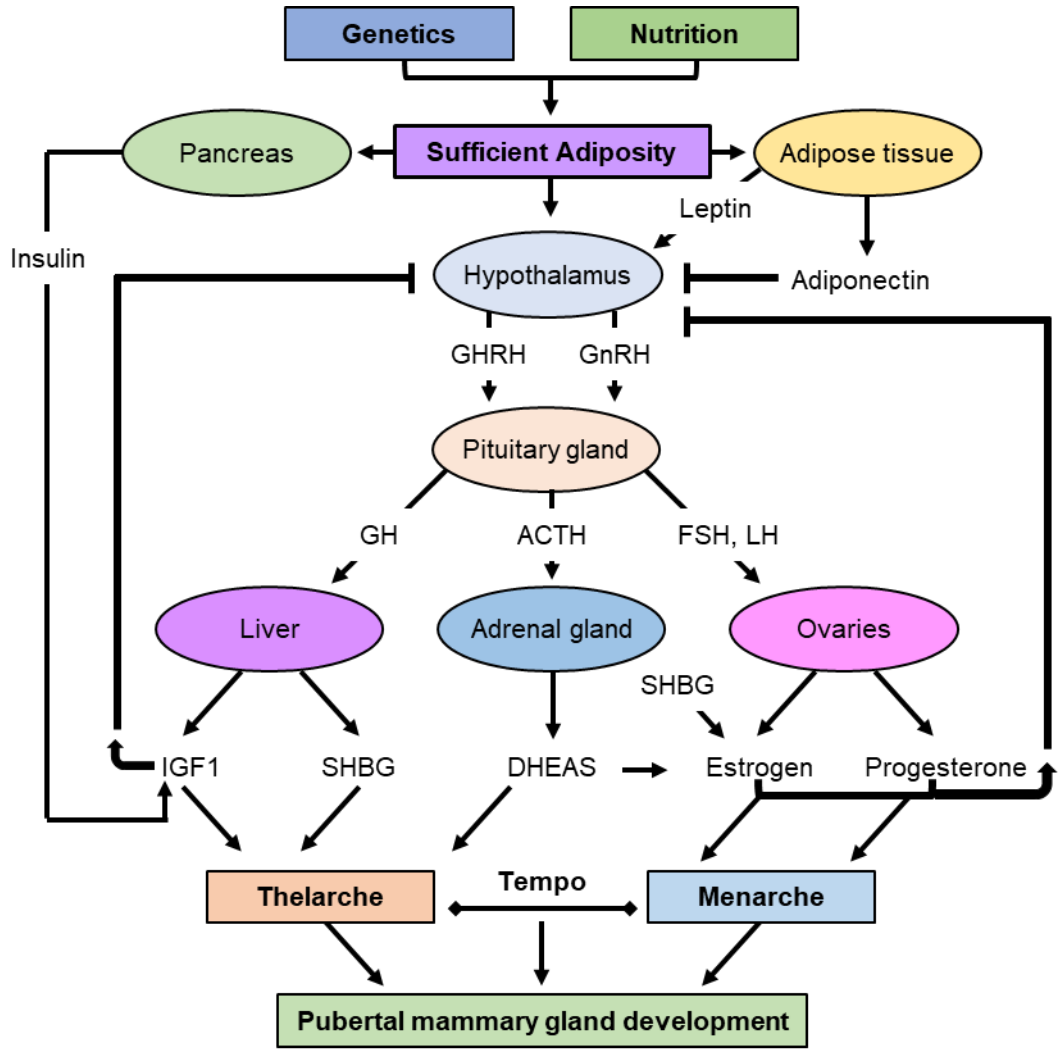

Figure 1.4. Schematic diagram of the factors that initiate pubertal mammary gland development in girls. Nutrition and inherited genetic factors regulate the abundance of childhood adipose tissue and govern secretion of insulin by the pancreas, secretion of leptin, and adiponectin by adipose tissue, and activation of hypothalamic-pituitary axes. Activation of the hypothalamic-pituitary-somatotropic axis results in secretion of growth hormone-releasing hormone (GHRH) from the hypothalamus, followed by release of growth hormone (GH) from the anterior pituitary gland. The secretion of insulin-like growth factor 1 (IGF1) from the liver then creates a negative feedback loop in this cycle. Activation of the hypothalamic-pituitary-adrenal axis results in secretion of adrenocorticotropic hormone (ACTH) from the anterior pituitary gland and dehydroepiandrosterone sulfate (DHEAS) from the adrenal gland. Activation of hypothalamic-pituitary-ovarian axis results in secretion of gonadotropin-releasing hormone (GnRH) from the hypothalamus, followed by release of luteinizing hormone (LH) and follicle-stimulating hormone (FSH) from the anterior pituitary gland. The secretion of sex hormones, estrogen and progesterone, then create a negative feedback loop in this cycle. Secretion of sex hormone-binding globulin (SHBG) from the liver and DHEAS from the adrenal gland regulates the activity of estrogen. This whole process, starting from the activated hypothalamus and pituitary gland, results in thelarche, menarche, and pubertal mammary gland development.

However, another study adjusted for waist circumference and only IGF1 remained significantly associated with percent mammographic density, and only in premenopausal women (134), supporting other findings that circulating concentration of IGF1 is positively correlated with percent mammographic density in premenopausal women, but not in postmenopausal women (183). Within breast tissue, IGF1 is elevated in tissue of high density compared to low density, with greater differences observed in women under the age of 50 compared to older women (184).

1.6.3 Endocrine function of adipose tissue

Adipose tissue is an active endocrine organ that secretes adipokines including leptin, adiponectin, tumour necrosis factor alpha (TNFA) and interleukin 6 (IL6). The abundance of adipose tissue can affect the circulating concentration of these adipokines and thus influence tissue development and homeostasis. Circulating leptin concentration is strongly correlated with abundance of gluteofemoral fat depots in human females (123), can stimulate the secretion of kisspeptin, and subsequently activate the HPG axis (121). On the other hand, obese individuals exhibit low circulating concentration of adiponectin (185, 186), an insulin-sensitising adipokine, which affects the HPG axis via adiponectin receptors present in the hypothalamus, pituitary gland, and gonads (186, 187). Adiponectin acts as a negative regulator of puberty onset through inhibition of kisspeptin and GnRH secretion in the hypothalamus and inhibition of GH and LH in the pituitary gland (186-189). These findings suggest that adipose tissue-derived leptin and adiponectin affect initiation of puberty (121).

Studies in animal models suggest leptin may regulate mammary gland development and function through direct effects on the mammary gland and also indirectly through inhibition of IGF1. Leptin inhibits IGF1-mediated proliferation in a bovine mammary epithelial cell line (190) as well as in the bovine mammary gland (191). Heavier girls have elevated circulating leptin (192) and lower IGF1 (193, 194), and these factors in adulthood are shown to be associated with lower mammographic density (134, 183, 195-197). In addition, leptin might act directly on mammary fibroblasts (198), thereby altering the stromal compartment of the breast and mammographic density (199).

Excess adiposity is also known to establish a state of chronic low-grade inflammation characterised by increased inflammatory cytokines such as TNFA and IL6 (200) as well as other adipokines, including omentin, visfatin, resistin, and chemerin (201-204). These factors affect ovarian function with downstream consequences for pubertal mammary gland development and

potentially mammographic density. In addition, immune signalling cytokines can act as paracrine regulators of pubertal mammary gland development and mammographic density.

1.7 Paracrine regulators of pubertal breast development and mammographic density

1.7.1 Stromal fibroblasts and extracellular matrix

Fibroblasts are one of the main cell types in the mammary stroma and significantly contribute to the fibroglandular tissue compartment that comprises high mammographic density. During puberty, mammary fibroblasts around the terminal end buds become activated by estrogen and growth hormones and interact with epithelial cells to promote mammary gland morphogenesis (205). These fibroblasts actively produce factors such as TGFB, IGF1, and hepatocyte growth factor (HGF), which regulate epithelial cell proliferation (206-212). TGFB also regulates the growth and activity of fibroblasts, modulating expression of tissue remodelling factors including extracellular matrix (ECM) proteins, proteases, and angiogenic factors (213, 214).

In situ, fibroblasts proliferate slowly and synthesise low levels of ECM proteins, matrix metalloproteinases (MMPs) that degrade ECM, and tissue inhibitor of metalloproteinases (TIMPs) that inhibit MMP-mediated degradation to maintain breast tissue integrity (205). Mammographic density is positively associated with extracellular matrix proteins produced by fibroblasts such as collagen, lumican, decorin, and syndecan-1 (184, 199, 215, 216). ECM proteins can be active players in promotion of tumorigenesis and metastasis, for example, a highly dense collagen matrix promotes tumour formation and progression in a mouse model associated with increased neutrophils and inflammatory COX2 (217-219). High mammographic density tissue is associated with increased TIMP3, compared to low mammographic density tissue in adult women (184), although this association was not found in another study (220). TIMP3 is expressed in the mammary stroma and acts on epithelial cells to promote cancer onset in mouse models (221). Further, a study in mice xenografted with human breast tissue (222) found that high mammographic density breast tissue significantly increased tumour weight, had greater proportions of high grade DCIS and metastasis of DCIS.com cells compared to the low mammographic density breast tissue from the same woman, suggesting that high mammographic density promotes tumour development and progression.

Using in vitro and in vivo screening of human and murine mammary tissue samples, gene expression profiling of fibroblasts associated with high and low mammographic density tissue revealed that CD36 expression was reduced in high mammographic density-associated

fibroblasts (223). CD36, also known as fatty acid translocase, is involved in adipocyte differentiation, immune signalling, TGFB activation, and cell–ECM interactions (224, 225). CD36 knockout in mice caused decrease in fat accumulation and increase matrix accumulation (223). Taken together, these studies suggest that fibroblast-associated CD36 may be actively involved in regulating the abundance of adipocytes versus abundance of stromal ECM that determines mammographic density.

1.7.2 Immune cells and signalling molecules

Immune system cells and signalling molecules are essential components of the mammary gland, with macrophages, eosinophils, neutrophils, mast cells, and lymphocytes (T and B cells) all contributing to mammary gland development and function (205, 226-228). Of particular significance in pubertal mammary gland development, macrophages promote collagen fibrillogenesis, which supports the development of terminal end buds and ductal elongation (229). Colony stimulating factor 1 (CSF1) is a key factor responsible for the proliferation and survival of macrophages (230). The mammary glands of mice homozygous for a null mutation in Csf1 exhibit reduced number of macrophages, lower numbers of terminal end buds as well as reduced ductal branching and elongation (227). C-C motif chemokine ligand 2 (CCL2) is an inflammatory cytokine known to be a chemoattractant for monocytes and macrophages to the sites of inflammation (231, 232). In CCL2-overexpressing mice, the mammary gland exhibits increased abundance of macrophages, elevated deposition of stroma and collagen, and increased susceptibility to carcinogen-induced mammary cancer (233). Human and murine studies reported that increased abundance of inflammatory CCL2, cyclooxygenase 2 (COX2), IL4, and IL6, as well as macrophages, dendritic cells, and B cells are all observed in high mammographic density breast tissue, in comparison to tissue with low mammographic density, suggestive of a protumour inflammatory microenvironment (39, 215, 233-235).

Eosinophils are detected around the developing terminal end buds (TEBs) in pubertal mouse mammary glands, where they promote ductal elongation and branching (227). Similarly, IL5, a key cytokine that promotes eosinophil differentiation and survival, is also required for ductal elongation (235). However, overabundance of eosinophils due to transgenic expression of IL5 results in delayed onset of ovarian cycling accompanied by perturbed pubertal mammary gland development (236). Therefore, the abundance and activity of mammary gland eosinophils during puberty appear to be critical for appropriate development. Eosinophils secrete eosinophil peroxidase, an enzyme that promotes fibroblast recruitment and establishment of collagen-rich ECM (237). While the role of eosinophils in establishment of mammographic density is yet to

be explored, eosinophil peroxidase promotes breast cancer progression in a mouse model, associated with increased collagen deposition and elevated COX2 (238).

Excess adiposity enhances bioavailability of transforming growth factor beta (TGFB) (239, 240), an anti-inflammatory cytokine with diverse roles in pubertal mammary gland development in mice. Epithelial cell-derived TGFB limits both proliferation and cell death of mammary epithelium as well as regulating local immune cell populations (241). The mammary glands of mice heterozygous for a null mutation in *Tgfb1* exhibit increased ductal invasion, with increased epithelial cell proliferation during puberty (212). Stromal- or endocrine-derived TGFB promotes mammary gland development possibly through regulation of the HPG axis or through regulation of macrophage function (211, 242). TGFB signalling is reduced in breast tissue with high mammographic density in adult women (243, 244).

1.8 Molecular determinants of pubertal mammary gland development and mammographic density

1.8.1 Heritability and genetics

Twin studies have provided strong evidence that percent mammographic density is partially heritable (245-247) and that a large proportion of variation in absolute dense area and absolute non-dense area is also attributed to genetic factors (248). A study comparing 571 pairs of monozygotic twins to 380 pairs of dizygotic twins from Australia and North America suggests that genetics accounts for 60-67% of the variability in all three of the mammographic density measures (percent, absolute dense and absolute non-dense area) when adjusted for other major breast cancer risk factors (245). The overlap between genetic determinants of both breast cancer risk and mammographic density measures is estimated to be around 14-18% (249, 250). Twin studies have also shown that the circulating concentration of IGF1 is strongly heritable (251, 252). Excess pubertal adiposity is associated with lower IGF1 and lower mammographic density (173), suggesting this may be one role of genetic factors in regulation of pubertal adipose tissue deposition and development of mammographic density. A number of common genetic variants are associated with mammographic density including rs3817198, which is a polymorphism of the gene encoding lymphocyte-specific protein 1, and rs2241716, a polymorphism of the gene encoding TGFB1 (250, 253-256).

Surprisingly, elevated concentration of androgens have been observed in girls with breast cancer family history in comparison to girls without breast cancer family history (257). This suggests that elevated concentration of hormones during puberty may be an important factor explaining the familial clustering of breast cancer (258). Hence, it has been postulated that

association of elevated androgen concentrations and increased breast cancer risk is established during puberty and modified by breast cancer family history (258), which indicates that both pubertal development and genetic factors play a crucial role in breast cancer risk. However, the interaction between genetic factors and environmental factors in pubertal development that could determine adult mammographic density is still not known and will surely be multi-factorial.

1.8.2 Epigenetic basis

DNA methylation can modulate gene expression without altering the DNA sequence and is believed to play a role in regulating homeostasis and risk of disease. Peripheral blood DNA hypermethylation in breast cancer susceptibility genes, such as BRCA1 and ATM is shown to be associated with increased breast cancer risk (259-261). Several genome-wide DNA methylation studies have suggested that peripheral blood DNA methylation, at both global and site-specific levels, is associated with breast cancer risk (262-265). An analysis of the association of genome-wide average methylation and epigenetic age acceleration within participants of the Australian Mammographic Density Twins and Sisters Study (253) found that genome-wide average methylation was associated with hormone-related risk factors (number of live births and age at first live birth), while epigenetic age acceleration was associated with lifestyle risk factors (BMI, smoking, and alcohol intake) and hormone-related risk factors (age at menarche and age at first live birth) (266).

The association between lifestyle risk factors and epigenetic age acceleration points to the proposition that an unhealthy lifestyle can impact epigenetic ageing to modify breast cancer risk (266). Although there appears to be no association between blood DNA methylation and mammographic density in adult women (267), peripheral blood DNA methylation at several genomic locations show association with current BMI, BMI at ages 18-21 years, and BMI change, suggesting adiposity through the life course can impact on future breast cancer risk through epigenetic modifications (268). Environmental factors such as exposure to synthetic estrogens may also be responsible for these DNA modifications (269, 270). Twin pair correlations in genome-wide average DNA methylation at birth, decrease with age during adolescence, suggesting individual environmental exposures during early life can affect DNA methylation (271). Use of oral contraceptives during puberty (98, 272) or before pregnancy (273) is associated with increased rates of breast tissue proliferation (273), increased dense breast volume (98), and higher breast cancer risk (272). Thus, environmental and lifestyle factors, as well as endogenous and exogenous sex hormone exposure during puberty, possess the potential to induce epigenetic changes to modify the composition of breast tissue.

Epigenetic age acceleration is also postulated to predict onset of puberty. Increased epigenetic age acceleration was observed to be strongly associated with decreased pubertal tempo and earlier menarche (274). Previous studies have shown the association of timing of puberty and pubertal tempo with pubertal percent fibroglandular volume (102). Another study, however, observed that epigenetic age acceleration was positively associated with pubertal percent fibroglandular volume in adjusted models, but was weakened after adjusting for cellular heterogeneity (274). Through the existing literature, the role of epigenetic age acceleration in determining pubertal mammographic density is still not clear and thus needs further investigation.

Estrogen receptor alpha (ERA) is a crucial transcriptional regulator that mediates the action of estrogen in regulating mammary gland development and function (275, 276). Variants in the gene encoding ERA (ESR1) are associated with increased percent fibroglandular volume in both premenopausal and postmenopausal women (277-279). A recent study observed that average ESR1 DNA methylation pattern at Tanner stage B4 is inversely associated with total breast volume and fibroglandular volume measured at Tanner stage B4, after adjustment of breast fat percentage, ESR1 DNA methylation pattern at Tanner stage B2, and cellular heterogeneity (280). It is hypothesised that ESR1 downregulation might increase expression of inhibitory factors, such as TGFB, to cause cell cycle arrest and this may result in reduced mammary epithelial proliferation in the later stages of breast maturation (281-283).

Recently, a study identified that breast tissue in healthy women ages faster than blood, as measured by DNA methylation (284). Further, women with luminal breast cancer were observed to have significant epigenetic age acceleration in normal adjacent breast tissue, in comparison to healthy women (285). These studies suggest that breast tissue age is determined by exposure to endogenous and exogenous factors during a women's lifetime. Taken together, the limited studies available do not provide enough evidence to support an epigenetic basis of mammographic density during puberty. However, if we could understand the impact of pubertal body adiposity on epigenetic ageing of breast tissue, epigenetic age of the breast tissue during puberty could be used to understand the changing internal milieu of the breasts and establishment of mammographic density during puberty.

1.9 Current controversies, conclusions and outlook

Adolescence is a time of developmental plasticity (286, 287), and as breast tissue develops there is the potential for environmental and lifestyle exposures to have a significant influence on future breast cancer risk. Pubertal adiposity, timing of menarche, and timing of thelarche are all demonstrated to affect mammographic density, an important risk factor for breast cancer. Activation of hypothalamic-pituitary axes during puberty, genetic and epigenetic molecular determinants, together with stromal fibroblasts, extracellular matrix, and immune signalling factors in the mammary gland are likely to act in concert to drive breast development and ultimately the histological structure of the adult breast (Figure 1.5).

The interaction between established risk factors for breast cancer and mammographic density is currently somewhat paradoxical, and further research is required to address these complexities. For example, epidemiological studies suggest that earlier menarche, which is an established breast cancer risk factor, is associated with reduced mammographic density, which is protective against breast cancer. This complicated relationship between age at onset of menarche, mammographic density, and breast cancer risk has not been sufficiently explored in the published literature. However, it is possible that age at menstrual onset affects breast development and establishment of mammographic density via the simultaneous increase in adiposity, while independently increasing breast cancer risk through longer term exposure to ovarian hormones estrogen and progesterone with menstrual cycling.

Another paradox lies in the relationship between adipose tissue at different stages of the life course and breast cancer risk. Obesity is a risk factor for breast cancer in postmenopausal women, but might be protective during adolescence. A key uncertainty resides in the assessment of pubertal body size and shape, making it difficult to discriminate between healthy adolescent weight gain and excessive weight gain. Whilst adipose tissue deposition is a key driver of puberty onset, it can be difficult to distinguish healthy pubertal weight gain from overweight/obesity in the published literature. For instance, the mass component of BMI reflects the accumulation of adipose tissue, but does not distinguish between localised deposition in gluteofemoral or breast depots, which is indicative of healthy pubertal weight gain, versus abdominal and subcutaneous depots, which characterise obesity. Thus, varied study approaches using different growth measures remain a barrier in synthesising a clear understanding of the relationship between adipose tissue deposition and mammographic density. Further research that specifically investigates the association between pubertal adipose tissue deposition at localised depots and adult mammographic density is required to address this uncertainty.

Beyond these complexities, a critical research question yet to be addressed is whether interventions that modify body adiposity during puberty alter adult breast cancer risk. Given the limitations of human studies, controlled animal experiments can provide clues regarding possible biological mechanisms through which pubertal development might affect adult mammographic density and long-term changes in risk of breast cancer. Future research in understanding how pubertal mammary gland development might determine adult breast composition and mammographic density could be a new key to reducing the incidence of breast cancer.

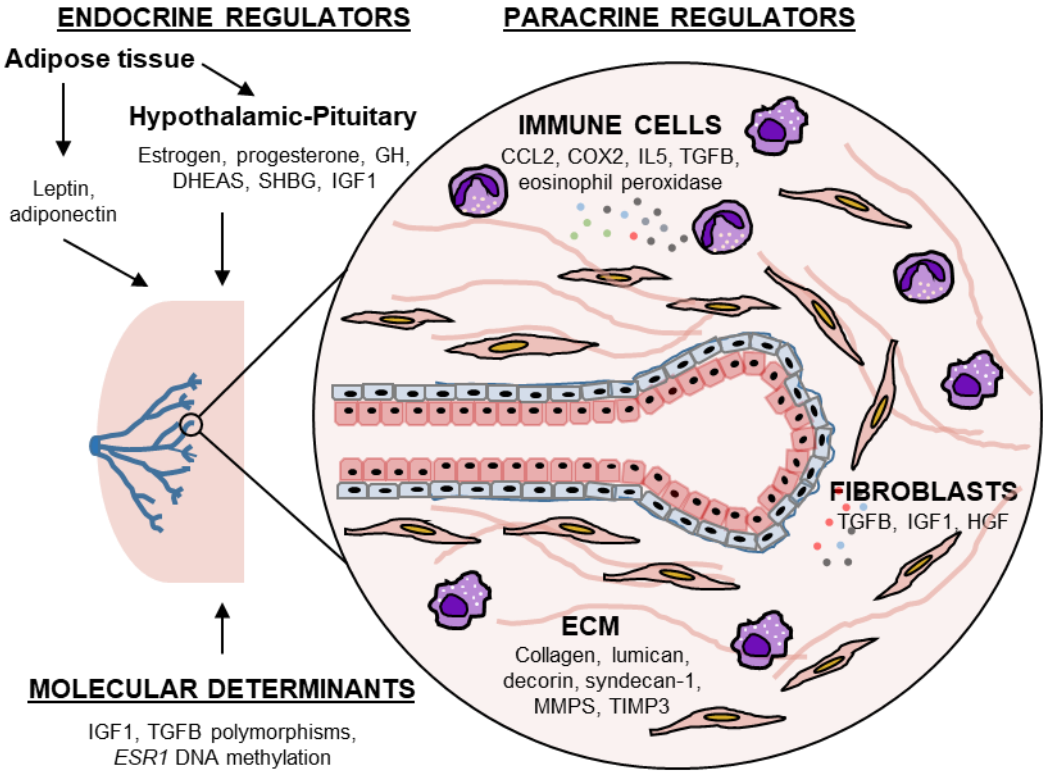

Figure 1.5. Schematic diagram of endocrine, paracrine, and molecular regulators of pubertal mammary gland development that may affect adult mammographic density. Endocrine hormones from adipose tissue and hypothalamic-pituitary axes, combined with genetic and epigenetic determinants, regulate pubertal mammary gland development and may affect adult mammographic density. Within the pubertal mammary gland, paracrine regulators associated with immune cells, stromal fibroblasts and the extracellular matrix direct the development of the epithelial, stromal and adipose tissue compartments that determine adult mammographic density.

1.10 Hypothesis and aims

Mammographic density is one of the most significant risk factors for breast cancer. High mammographic density attributes to 29% of all breast cancer diagnoses. Breast tissue with high mammographic density is characterised by increased abundance of fibroglandular tissue and reduced abundance of adipose tissue compared to breasts of low density. Mammographic density is a consequence of cellular and molecular events that occur during adolescent breast development. Epidemiological studies show that increased BMI in adolescence is associated with low mammographic density as an adult and reduced lifetime risk of breast cancer. This suggests that adiposity during pubertal development could be a significant, and modifiable factor that affects adult breast health. However, the research to date has demonstrated epidemiological associations; causal relationships between pubertal adiposity with adult mammographic density and breast cancer risk have not been investigated.

The studies described in this thesis aim to address the following hypothesis:

Increased adiposity during puberty is causal in mammary gland density and cancer development in adulthood.

The validity of this hypothesis was investigated by addressing the following aims:

(1) To explore the impact of increased adiposity on mammary gland development and function during puberty in a mouse model.

(2) To investigate the impact of increased pubertal adiposity on mammary gland development and density during adulthood in a mouse model.

(3) To explore the effect of increased pubertal adiposity on mammary cancer development in adulthood in a mouse model.

CHAPTER TWO
Materials and methods

2.1 Animals and general procedures

2.1.1 Mice strains

All animal experiments were approved by the University of Adelaide Animal Ethics Committee (Approval number: M-2018-045) and conducted in accordance with the Australian Code of Practice for the Care and use of Animals for Scientific Purposes (8th edition, 2004) (288). All mice were maintained in specific pathogen-free conditions with controlled 12:12 hour light-dark cycles, and temperature at the Laboratory Animal Services Helen Mayo Animal Facility and The Queen Elizabeth Hospital animal facility.

2.1.1.1 Alms1 bbb/bbb mice

Transgenic C57BL/6JSfdAnu-Alms1^{bbb}/Apb (*bbb/bbb*) mice have an ENU-induced T to A mutation at position 6507 (exon 10) on the *Alms1* gene, which results in a truncated Alms1 protein (289). These mice exhibit hyperphagia and increased weight gain by 5 weeks of age when fed normal mouse diet (290). These mice were used to model the impact of increased adipose tissue deposition on mammary gland development at 6 weeks (puberty) and 12 weeks (adulthood) of age.

2.1.1.2 MMTV-PyMT transgenic mice

MMTV-PyMT transgenic mice harbour the polyomavirus middle T-antigen oncogene (PyMT), which is driven by the mammary gland specific mouse mammary tumour virus promoter (MMTV) (291). Female MMTV-PyMT$^{+/-}$ mice on a FVB background spontaneously develop mammary tumours with 100% penetrance and an average latency of 6 weeks. Male MMTV-PyMT mice were used for mating.

2.1.1.3 PyMT-bbb/bbb mice

Male MMTV-PyMT mice were mated with female *bbb/+* mice. Male PyMT-*bbb/+* offspring were mated with female *bbb/+* mice to generate female PyMT-control (PyMT-*bbb/+* or PyMT-+/+) and PyMT-*bbb/bbb* mice. Female offspring that are PyMT-*bbb/bbb* spontaneously develop mammary tumours and gain weight as they age. These mice were used to model the effect of increased pubertal adiposity on mammary cancer development in adulthood. PyMT-control mice were littermate controls that did not gain excess weight.

2.1.2 General animal procedures

2.1.2.1 Genotyping mice

2.1.2.1.1 Tail tip digestion

Tail tips were collected from weaned 3 week old mice in sterile 1.5 mL Eppendorf tubes. The tissue was digested in 250µL of digestion buffer (Table 2.1) with 0.1mg proteinase K (Sigma-Aldrich, Cat No. P2308) added, at 55°C for 4 hours. Proteins and cellular debris were precipitated by adding 4M ammonium acetate (Merck; Cat No. A1542), followed by incubation at room temperature for 25 minutes and centrifugation at 14,000*g* for 10 minutes. The aqueous layer was transferred to a new Eppendorf tube, and DNA was precipitated by adding 2x sample volumes of 100% ethanol (Sigma-Aldrich, Cat No. E7023). DNA was pelleted by centrifugation at 14,000g for 10 minutes, followed by rinsing the pellet with 70% ethanol. The pellet was air-dried and resuspended in 250µL of PCR-grade water (ThermoFisher Scientific, Cat No. 10977015). Extracted genomic DNA was stored at -20°C.

2.1.2.1.2 Genotyping conditions for Alms1 transgene

To screen for the *Alms1* gene mutation, the extracted genomic DNA was first PCR amplified using mutation-specific primers (forward: 5'AAAGCCCCACATGTAGATCG 3', reverse: 5' TGAGGTATATGCTGAACCTCATAT 3') by PCR kit (Invitrogen; Cat No. 10342-053). The PCR reaction contained 1x DNA polymerase reaction buffer, 2mM $MgCl_2$, 100µM dNTPs (Invitrogen, Cat No. R0192), 5µM each forward and reverse primers (Integrated DNA technologies), 1.5U Taq polymerase, and 9.7µL extracted DNA in a final reaction volume of 50µL. PCR conditions were 94°C for 2 minutes, followed by 38 cycles of 94°C for 30 seconds, 59°C for 1 minute, 72°C for 2 minutes; and 72°C for 5 minutes.

PCR products were then digested using PsiI restriction digestion kit (New England Biolabs, Cat No. R0744S). The restriction digestion reaction containing 1x Cut Smart buffer, 8U PsiI restriction enzyme, and 2µL PCR product in a final reaction volume of 20µL was incubated at 37°C for 3 hours.

The digested products were detected by gel electrophoresis. Digested products containing 1x loading buffer (New England Biolabs, Cat No. R0744S) were run on 4% agarose gel with GelRed (Gene target solutions, Cat No. 41003) in TAE (Tris-acetate EDTA) buffer (Table 2.1) at 100V for 2 hours. The size of the digested products was estimated on the gel by using a DNA ladder (Invitrogen, Cat No. 15628019). The gels were visualised under UV light using Gel DocTM EZ Imager (BioRad). Wildtype control mice DNA produced a single 190bp band,

heterozygous *bbb/+* produced 190 and 200bp bands, and homozygous *bbb/bbb* produced a single 200bp band (Figure 2.1).

Table 2.1. Composition of buffers and solutions used for animal experiments.

Digestion buffer	50mM Tris (Sigma-Aldrich; T1378), 20mM EDTA (Sigma-Aldrich; Cat No. E6758), 120mM NaCl (Sigma-Aldrich; Cat No. S9888), and 1% (w/v) SDS (Sigma-Aldrich; Cat No. L3771) dissolved and made up to a volume of 1L with H2O at pH = 8. Stored at room temperature.
10x TAE buffer	48.4g Tris base (Sigma-Aldrich, T1378), 20mL 0.5M EDTA (Sigma-Aldrich, Cat No. E6758), 11.42mL glacial acetic acid (Merck, CAS No. 64-19-7) dissolved and made up to a volume of 1L with H2O. For 1x stock, diluted 1:10 with H2O. Stored at room temperature.
Avertin	Dissolved 1g 2,2,2-tribromomethanol (Sigma-Aldrich, Cat No. T48402) in 1mL 2-methyl-2-butanol (Sigma-Aldrich, Cat No. 152463), then volume made up to 50mL with H2O. Aliquots stored at -20°C.

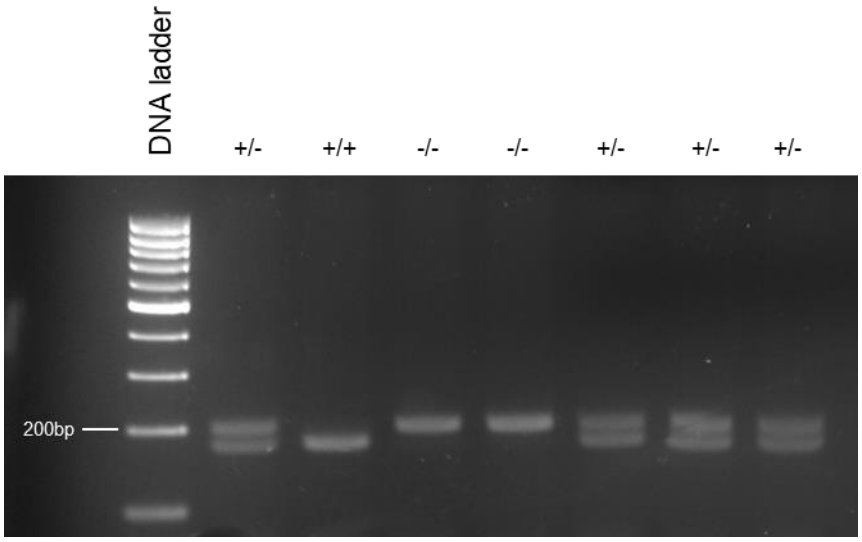

Figure 2.1. Genotyping of *Alms1 bbb/bbb* by PsiI restriction digestion. Genomic DNA of control and *bbb/bbb* mice was first amplified using *Alms1* gene-specific primers by PCR, and then digested by PsiI restriction enzyme. Wildtype control mice (+/+) DNA produced a single 190bp band, heterozygous *bbb/+* (+/-) produced 190 and 200bp bands, and homozygous *bbb/bbb* (-/-) produced a single 200bp band.

2.1.2.1.3 Genotyping conditions for MMTV transgene

Presence of the MMTV-PyMT allele was detected by PCR amplification using allele-specific primers. The extracted genomic DNA was PCR amplified using primers (MMTV-490 forward: 5' CGTCCAGAAAACCACAGTCA 3', MMTV-685 reverse: 5' CCGCTCGTCACTTATCCTTC 3') by PCR kit (Invitrogen; Cat No. 10342-053). The PCR reaction contained 1x DNA polymerase reaction buffer, 2.5mM $MgCl_2$, 100µM dNTPs (Invitrogen, Cat No. R0192), 5µM each forward and reverse primers (Integrated DNA technologies), 0.55U Taq polymerase, and 5µL extracted DNA in a final reaction volume of 25µL. PCR conditions were 94°C for 5 minutes, followed by 35 cycles of 94°C for 30 seconds, 55°C for 30 seconds, 72°C for 1 minute; and 72°C for 7 minutes.

PCR products were detected by gel electrophoresis. PCR products containing 1x loading buffer (ThermoFisher Scientific, Cat No. R0611) were run on 4% agarose gel with GelRed (Gene target solutions, Cat No. 41003) in TAE buffer at 100V for 1 hour. The size of PCR products was estimated on the gel by using a DNA ladder (Invitrogen, Cat No. 15628019). The gels were visualised under UV light using Gel DocTM EZ Imager (BioRad). Mice with MMTV transgene were confirmed by the presence of a 195bp product (Figure 2.2).

2.1.2.2 Estrous cycle tracking

The estrous cycles in adult control and *bbb/bbb* mice were tracked by vaginal cytology, as described previously (292). In brief, the vagina was flushed with 20µL of sterile phosphate buffered solution (PBS) (Sigma-Aldrich; Cat No. P3813) and the recovered fluid was then pipetted on a glass slide and coverslipped. The cellular components of the collected smears were examined under a phase contrast microscope, and the relative proportion of cell types determined the estrous cycle stage for each mouse (Figure 2.3, Table 2.2). Vaginal smears were collected from mice daily from 8 to 12 weeks of age. Mice were euthanized at the estrus phase of the estrous cycle, and tissues were collected.

2.1.2.3 Bromodeoxyuridine (BrdU) administration

Pubertal *bbb/bbb* and control mice were intraperitoneally injected with 1mg of BrdU solution (Sigma-Aldrich, Cat No. B5002) 1 hour prior to sacrifice and tissue collection. The BrdU In-situ Detection kit (BD Pharmingen, Cat No. 550803) containing a specific biotinylated anti-BrdU antibody was used to detect proliferating epithelial cells in tissue sections, according to the manufacturer's instructions (see section 2.2.4).

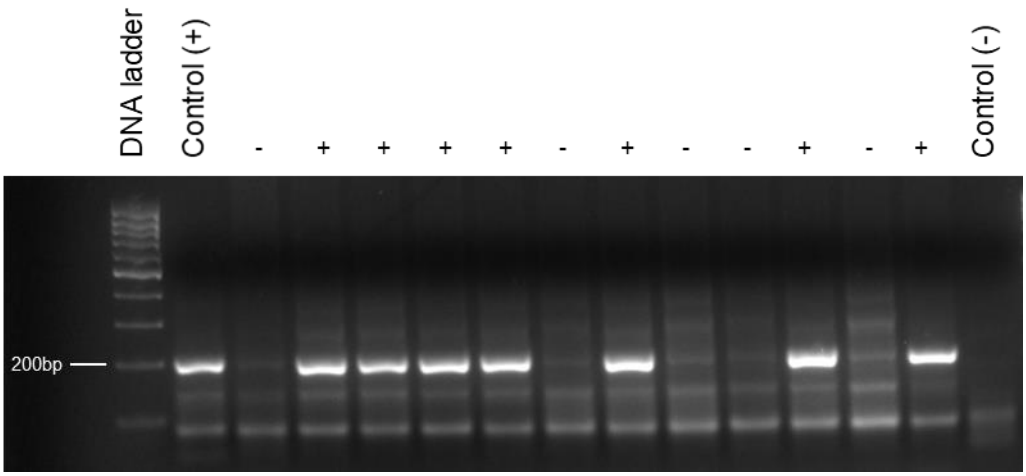

Figure 2.2. Genotyping MMTV transgene by PCR. Genomic DNA of PyMT-control and PyMT-*bbb/bbb* mice was amplified using MMTV specific primers by PCR, and presence of a 195bp product confirmed the mice carrying the MMTV-PyMT transgene. Control (+) is the DNA of pre-confirmed MMTV-positive mice that produced a single 195bp band and control (-) is the no template control.

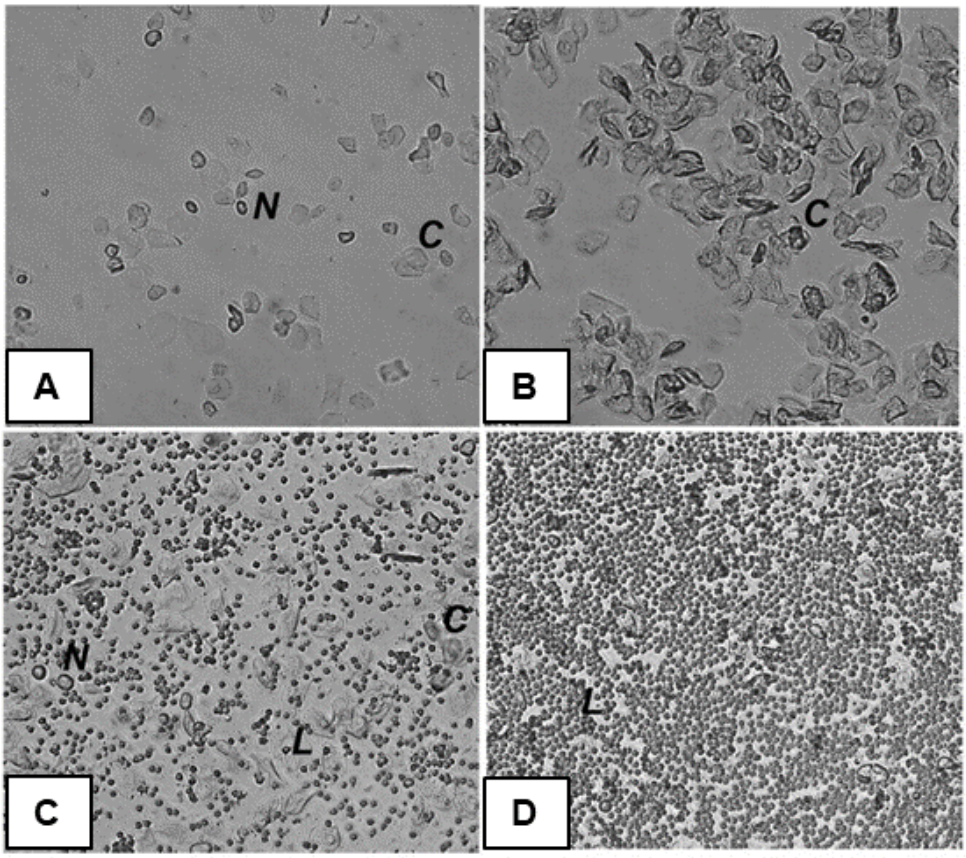

Figure 2.3. Determination of estrous cycle stages by vaginal cytology. Representative images of vaginal cytology at (A) proestrus; (B) estrus; (C) metestrus; and (D) diestrus stages of the mouse estrous cycle. N: nucleated epithelial cells, L: leukocytes, and C: cornified cells. Image adapted from (293).

Table 2.2. Classification of estrous cycle stages by cellular components in vaginal smears.

	Cell type		
Estrous cycle stage	Epithelial cells	Cornified epithelial cells	Leukocytes
Proestrus	+ to ++	0 to +	0
Estrus	0 to +	++ to +++	0
Metestrus	0 to +	Clumps + to ++	++ to +++
Diestrus	0	- -	- -

Cell density: 0 = none; + = few; ++ = moderate; +++ = heavy; - - = low number of cells

2.1.2.4 Tumour detection and monitoring

PyMT-control and PyMT-*bbb/bbb* mice were monitored twice a week for tumour development by palpation. In brief, mice were gently restrained by grasping the scruff of the neck between the thumb and the forefinger, and the base of the tail with the little finger. To identify any tumour, mice were palpated from first mammary gland to the tenth mammary gland. After the identification of the first mammary tumour, the tumour growth was monitored by measuring the length and width of the tumour. Tumour volumes were calculated as:

Tumour volume (mm^3) = (*length x width x width x* π)/6

Mice were sacrificed at 18 weeks of age unless the tumour volume exceeded 2000mm^3, in that case mice were euthanised before 18 weeks of age.

2.1.2.5 Blood collection

Prior to humane killing, blood was collected from mice under deep anaesthesia by cardiac puncture. Firstly, mice were injected intraperitoneally with 0.5 mL of 2% Avertin (Table 2.1). After confirming lack of reflex by toe pinch, up to 500µl to 1mL of blood was collected directly from the heart. Blood was centrifuged at 10,000*g* for 10 minutes. Serum was collected in a new sterile Eppendorf tube and stored at -80°C.

2.2 Histology and Immunohistochemistry

2.2.1 Carmine alum staining

From the same mouse, fourth pair mammary glands were used for histology and immunohistochemistry analysis, and third pair mammary glands were used for real-time PCR analysis (section 2.3). Fourth pair mammary glands were collected from *bbb/bbb* and control mice aged 6 weeks and 12 weeks. The mammary glands were spread onto a glass slide and fixed in Carnoy's fixative (60% ethanol, 30% chloroform (ChemSupply, Cat No. CA038) and 10% glacial acetic acid (ChemSupply, Cat No. AA009)) overnight. The slides were then washed with 70% ethanol and rinsed with MilliQ water for 5 minutes. The slides were stained with 2% carmine alum (Sigma-Aldrich, Cat No. C6152) overnight. Stained whole-mounts were washed with 70% ethanol for 15 minutes, twice with 100% ethanol (ChemSupply, Cat No. EA043) for 15 minutes each. Slides were cleared in xylene and mounted with Entellan mounting media (Proscitech, Cat No. IM0225).

The mammary gland whole-mounts were imaged using an Olympus SZ61 stereo microscope. Ductal invasion area, ductal length, branching, and number of terminal end buds were measured

using ImageJ software. Ductal invasion area was calculated by measuring the area invaded by the ducts into the mammary adipose tissue from the lymph node. Ductal length was calculated as the length from the nipple to the furthest duct. Branching was calculated as the number of branch points per millimetres of duct. Only terminal end bud structures of size greater than 100µm were included in quantification (294).

2.2.2 Tissue embedding and sectioning

Tissues collected for histology were fixed in neutral buffered formalin (Australian Biostain; Product code: ANBFC). Tissues were then washed in 1X phosphate buffered saline (Sigma-Aldrich; Cat No. P3813) overnight before storing in 70% ethanol until tissue processing. Tissue was processed using the Excelsior AS Tissue Processor (ThermoFischer Scientific) with the following protocol: 60 minutes in 70% ethanol, 60 minutes in 85% ethanol, 60 minutes in 90% ethanol, 60 minutes in 90% ethanol, 2 x 60 minutes in 100% ethanol, 2 x 60 minutes in xylene (ChemSupply; Cat No. 158775000) and held in paraffin wax at 62°C under vacuum conditions until embedding. Tissues were embedded into the paraffin wax blocks and cut into 5µm thick sections using a microtome (Leica Biosystems). Tissue sections were allowed to bond onto the glass slides on a 37°C heating block for 30 minutes and then stored at room temperature.

2.2.3 Haematoxylin and eosin staining

Paraffin-embedded tissue sections cut at 5µm thickness using a microtome were stained with haematoxylin and eosin for histological analysis. Briefly, tissue sections were dewaxed in xylene, and rehydrated subsequently through 100%, 90%, 70% and 50% ethanol. Slides were stained with haematoxylin (Gills No.2, Sigma-Aldrich; Cat No. GHS232) and counterstained with eosin (Sigma-Aldrich; Cat No. HT110132). Sections were dehydrated subsequently through 90% and 100% ethanol, and cleared in xylene, before mounting with Entellan mounting media. Stained slides were imaged using Nanozoomer 1.0 (Hamamatsu, Shizouka, Japan) at zoom magnification of 40X.

2.2.3.1 Adiposity assessment

Images of haematoxylin and eosin-stained mammary gland and visceral adipose tissue sections of pubertal and adult mice were used to measure adiposity. Average area of adipocytes, number of adipocytes per area, and frequency of adipocyte size were manually quantified using NanoZoomer Digital Pathology Image (ndpi) software (Hamamatsu, Shizouka, Japan). Four random areas in a tissue section from each mouse were selected for quantification. Area of three hundred adipocytes in mammary gland tissue sections and area of two hundred adipocytes in visceral adipose tissue sections was quantified to determine the average area of adipocytes in

mammary gland and visceral adipose tissue respectively, for each mouse. The adipocyte size cut-off point is defined by approximately 10th percentile of frequency distribution of adipocyte area in controls (*bbb/+* or *+/+*), which was ≤1000μm^2 for small adipocytes and >1000μm^2 for large adipocytes (295). Frequency of adipocytes was estimated for adipocyte area of ≤1000μm^2 versus >1000μm^2.

2.2.3.2 Pathological assessment of tumours

Haematoxylin and eosin-stained mammary tumours from PyMT-control and PyMT-*bbb/bbb* mice were assessed by a veterinary pathologist (Dr Lucy Woolford) blinded to mouse genotype. The primary mammary tumours were assessed for tumour grade, cytological atypia, and tumour necrosis.

2.2.4 BrdU staining

The BrdU In-situ Detection kit (BD Pharmingen, Cat No. 550803) containing a specific biotinylated anti-BrdU antibody was used to detect proliferating epithelial cells, according to the manufacturer's instructions. BrdU staining to detect BrdU-positive proliferating epithelial cells in terminal end buds was performed on tissue sections of mammary glands of pubertal *bbb/bbb* and control mice. Tissue sections were dewaxed in xylene, and rehydrated subsequently through 100%, 90%, 70% and 50% ethanol. Endogenous peroxidase activity was blocked by incubating the slides in 3% hydrogen peroxide (ChemSupply; Cat No. HA154) in PBS. After rinsing the slides in PBS, slides were incubated with antigen retrieval solution from the kit. The biotinylated anti-BrdU antibody was used at 1:10 dilution and incubation for 1 hour in a humidified chamber. Slides were washed thrice with PBS and Streptavidin-HRP solution was applied on the sections for 30 minutes at room temperature. Antibody binding was detected using 3,3'-diaminobenzidine substrate solution (Dako, Cat No. K3467) according to the manufacturer's instructions. Sections were counterstained with haematoxylin and dehydrated subsequently through 90% and 100% ethanol, cleared in xylene, and mounted with Entellan mounting media (Proscitech; IM0225). Negative controls were the adjacent serial tissue section stained with only secondary antibody. Stained slides were imaged using a Nanozoomer 1.0 (Hamamatsu, Shizouka, Japan) at zoom magnification of 40x.

To quantitate BrdU-positive proliferating cells, three random terminal end buds were selected in a tissue section from each mouse. The number of BrdU-positive cells was manually counted. All quantification was conducted by an assessor blinded to the mouse genotype.

2.2.5 F4/80 staining of paraffin embedded tissues

Mammary glands and visceral adipose tissue were collected from *bbb/bbb* and control mice at puberty and adulthood. F4/80 staining to detect F4/80-positive macrophages was performed on 5µm sections mounted on glass slides. Tissue sections were dewaxed in xylene, and rehydrated subsequently through 100%, 90%, 70% and 50% ethanol. Sections were incubated with a quenching solution (50% (v/v) methanol (ChemSupply; Cat No. MA004-2) and 5% (v/v) hydrogen peroxide (ChemSupply; Cat No. HA154) in water) to inactivate endogenous peroxidase activity. Tissue sections were then incubated with 15% normal rabbit serum (Sigma-Aldrich; Cat No. R9133) in PBS at 37°C for 30 minutes to block non-specific antibody binding. The primary antibody (rat anti-mouse F4/80 (Ebioscience; Cat No. 14480182)) was used at a dilution of 1:50 in 1.5% normal rabbit serum and incubated at 4°C overnight. After washing the slides with PBS, sections were incubated with secondary antibody (biotinylated rabbit anti-rat IgG antibody (Vector Laboratories; Cat No. BA4000)) at a dilution of 1:200 dilution for 1 hour at room temperature. Antibody binding was detected using Vectastain ABC Elite kit (Vector Laboratories; Cat No. VEPK6100) and 3,3'-diaminobenzidine (Dako; Cat No. K3467) according to the manufacturer's instructions. Sections counterstained with haematoxylin and dehydrated subsequently through 90% and 100% ethanol, and then xylene, were mounted with Entellan mounting media (Proscitech; Cat No. IM0225). Negative controls were included; and were the adjacent serial tissue sections stained with only secondary antibody. Stained slides were imaged using a Nanozoomer 1.0 (Hamamatsu, Shizouka, Japan) at zoom magnification of 40x.

To assess the number of F4/80-positive macrophages around terminal end buds in pubertal mice and in stroma around ducts in adult mice, three random terminal end buds and three random ducts were selected for quantification respectively. To quantify F4/80-positive macrophages in the mammary gland adipose tissue and visceral adipose tissue sections, four random areas containing F4/80-positive staining were measured across the entire tissue section. The number of positively stained cells was manually counted. All quantification was conducted by an assessor blinded to mouse genotype.

2.2.6 Masson's trichrome staining

Paraffin-embedded tissue sections were stained with Masson's trichrome stain to detect collagen deposition. The Masson's trichrome staining kit (Australian Biostain; Product code: AMT.K) was used to detect collagen deposition in the mammary gland tissue sections, according to the manufacturer's instructions. Tissue sections were dewaxed in xylene, and rehydrated subsequently through 100%, 90%, 70% and 50% ethanol. Slides were then fixed in

Bouin's fluid from the kit for 1 hour. After washing the slides with running water, sections were stained with Weigert's haematoxylin solution for 10 minutes. Slides were rinsed with 80% ethanol and immersed in Biebrich Scarlet solution for 2 minutes, followed by washing with water. Mammary gland tissue sections of pubertal *bbb/bbb* (and wildtypes) were stained with Light Green stain and sections of adult *bbb/bbb* (and controls) were stained with Aniline blue stain, according to the manufacturer's instructions. Excess staining was cleared in 1% glacial acetic acid. Sections dehydrated subsequently through 90% and 100% ethanol, and then xylene, were mounted with Entellan mounting media (Proscitech; Cat No. IM0225). Stained slides were imaged using a Nanozoomer 1.0 (Hamamatsu, Shizouka, Japan) at zoom magnification of 40x. The images were analysed using NanoZoomer Digital Pathology Image (ndpi) software (Hamamatsu, Shizouka, Japan) to estimate thickness of collagen (µm) deposited around three random ducts in a mammary gland tissue section for each mouse. Quantification was conducted by an assessor blinded to mouse genotype.

2.3 Real time PCR analysis

2.3.1 RNA extraction

Total RNA was extracted from mammary gland and mammary tumours using TRIzol (Invitrogen; Cat No. 15596026). Briefly, tissue was transferred into a new sterile Eppendorf tube containing 0.6g of 1.4mm ceramic beads (Qiagen; Cat No. 13113-50) and 1mL TRIzol and were homogenised using a Powerlyser 24 homogeniser (MoBio, USA) at 30Hertz for 5 minutes. Samples were incubated on ice before adding 200µL chloroform (Sigma-Aldrich; Cat No. 288306). Samples were vigorously mixed by manual shaking and incubated on ice for 15 minutes. Samples were centrifuged at 11,000*g* at 4°C for 15 minutes, and the top aqueous layer containing RNA was transferred to a new sterile Eppendorf tube. Approximately equal sample volumes of isopropanol (Sigma-Aldrich; Cat No. I9516) was added and incubated overnight at -20°C. Samples were then centrifuged at 11,000*g* at 4°C for 30 minutes. The recovered RNA pellet was washed twice with ice cold 70% ethanol, and centrifuged at 11,000*g* at 4°C for 10 minutes each. The RNA pellet was air-dried for 30 minutes and resuspended in 50µL of RNase-free water (ThermoFisher Scientific; Cat No. 10977015).

To eliminate DNA contamination, samples were treated with DNase using a TURBO DNA-free kit (Life Technologies; AM1906) according to the manufacturer's instructions. In brief, 5µL of 10x TURBO DNase buffer and 1µL of TURBO DNase was added to the RNA sample and incubated at 37°C for 30 minutes. To inactivate the DNase enzyme, 5µL of DNase Inactivation Reagent was added, and samples were incubated at room temperature for 5 minutes

with occasional mixing. The samples were then centrifuged at 10,000*g* at 4°C for 1.5 minutes, and RNA solution was transferred to a new sterile Eppendorf tube.

The extracted RNA was quantified using Nanodrop Spectrophotometer 2000. The purity of the RNA samples was confirmed by absorbance ratios at 260/280. All extracted RNA samples were deemed pure (ie with absorbance ratios of ~2.0) and included in downstream analyses.

2.3.2 RNA storage by precipitation

For long-term storage of samples, RNA was precipitated with 2.5x sample volumes of 100% ethanol and 0.1x sample volume of 3M sodium acetate (ThermoFisher Scientific; Cat No. AM9740). The tube contents were mixed and stored at -20°C. To recover RNA, samples were centrifuged at 11,000*g* at 4°C for 20 minutes. The RNA pellet was washed twice with ice cold 70% ethanol, and centrifuged at 11,000*g* at 4°C for 10 minutes each. The RNA pellet was air-dried for 30 minutes and resuspended in 50µL of RNase-free water.

2.3.3 Complementary DNA (cDNA) preparation

For mammary gland and mammary tumours, cDNA was reverse transcribed from 750ng of RNA using iScript cDNA synthesis kit (Bio-Rad; Cat No. 1708891) according to the manufacturer's instructions. The reaction contained 1x iScript reaction mix and 1µL of iScript reverse transcriptase in a 20µL final reaction volume. Reactions were then incubated at 25°C for 5 minutes, 42°C for 25 minutes, and 85°C for 5 minutes. The cDNA was then diluted 1:10 in RNase-free water and stored at -20°C.

2.3.4 Quantitative real-time PCR

Real-time PCR amplification was performed on a Bio-Rad CFX96 using SYBR Green PCR Master Mix (Bio-Rad; Cat No. 1725271). Sequences of the primer pairs (Integrated DNA Technologies) specific to mouse genes used in this study are listed in Table 2.3. The reactions contained 1x SYBR green master mix, 4µM each forward and reverse primers, and 2µL cDNA template in a final reaction volume of 10µL. PCR conditions were 95°C for 10 minutes, then 44 cycles of 95°C for 15 seconds, 60°C for 15 seconds, 72°C for 30 seconds.

The gene expression for each sample was measured in triplicate and defined as the average of number of cycles required to reach threshold (Ct). Normalised gene expression was then calculated by 2^(-ΔΔCt) method, relative to the expression of a housekeeping gene, *Rpl13a*. Three housekeeping genes, *Rpl13a, Gapdh, and Actb* were assessed to determine a suitable endogenous reference gene for these studies. The expression of *Gapdh* and *Actb* was found to be highly altered within genotype groups. Therefore, *Gapdh* and *Actb* were not used as the

endogenous reference gene for normalization of real-time PCR data. The housekeeping gene *Rpl13a* had an invariable expression within the genotype groups, thus, it was used as the endogenous reference gene for these studies.

2.4 Cytokine analysis

Cytokine concentrations in serum collected from adult *bbb/bbb* and control mice were quantified by multiplex assay. In addition, protein was extracted from whole mammary glands of *bbb/bbb* and control mice at puberty and adulthood for cytokine detection and measurement. Tissue was homogenised in protein extraction buffer containing 500mM Tris-HCl (Sigma-Aldrich; Cat No. T1378), 200mM NaCl (Sigma-Aldrich; Cat No. S9888), and 10mM $CaCl_2$ (Sigma-Aldrich; C1016), with one tablet of EDTA-free protease inhibitor (Roche Diagnostics; Cat No. 11836153001). The homogenised tissue was centrifuged at 14,000*g* at 4°C for 20 minutes. The top fat layer was discarded, and the aqueous layer was collected in a new Eppendorf tube. The aqueous solution was homogenised again after adding 10% Triton X-100 (Bio-Rad; Cat No. T8787). Samples were centrifuged at 14,000*g* at 4°C for 20 minutes, and the aqueous layer was collected in a new Eppendorf tube after discarding the top fat layer. This process was repeated until the top fat layer was completely depleted from the samples. Protein concentration was estimated using Bradford reagent assay (Bio-Rad; Cat No. 5000006), according to the manufacturer's instructions. The protein extracts were stored at -80°C until use.

The concentration of the respective cytokines in the mammary gland protein extracts and serum was quantified using Milliplex® MAP mouse adipocyte magnetic bead assay (Millipore; Cat No. MADCYMAG-72K), as per the manufacturer's instructions. The cytokines detected in the extracts are as follows: adiponectin, leptin, IL6, CCL2, PAI1 (plasminogen activator inhibitor 1), resistin and TNFA. All sample measurements were performed in a single assay. The inter-assay coefficients of variation were lower than 15%. The minimum detection limits of the assay were 1.9 pg/mL adiponectin, 2.8 pg/mL IL6, 2.2 pg/mL leptin, 4.0 pg/mL CCL2, 2.3 pg/mL PAI1, 2.9 pg/mL resistin, and 6.3 pg/mL TNFA. The measured cytokine concentrations are presented as picograms per milligram of protein (pg/mg).

2.5 Statistical analyses

All statistical analyses were performed using SPSS Statistics version 24 software (IBM Corporation, USA) with consultation from a statistician (Ms Suzanne Edwards, Adelaide Health Technology Assessment, University of Adelaide). Results were considered statistically

significant at $p<0.05$. An asterisk (*) identified that data measures were significantly different between two groups.

Data are presented as mean+SEM (standard error of mean) and analysed using a linear regression model to account for within group variability. All molecular experimental data such as Luminex assay and RT-PCR analysis data are presented as box-plots with median in between the first quartile and third quartile and analysed using a linear regression model to account for within group variability and skewness of the data.

Kaplan Meier's survival analyses were performed to investigate the difference in survival with time of detection of first palpable tumour in *Alms* mice crossed with the *MMTV-PyMT* tumour mouse model. LogRank test was performed to compare the survival curves of each group.

Table 2.3. Real-time PCR primer pairs specific to mouse genes used to quantify gene expression in mammary glands and mammary tumours in mice. *Rpl13a* is the 'housekeeping' reference gene highlighted in bold.

Gene	Primer sequence
Leptin	Forward – 5' GCTGGAGACCCCTGTGTCGGT 3'
	Reverse – 5' GCCAGTGACCCTCTGCTTGGC 3'
Adiponectin	Forward – 5' GTCAGTGGATCTGACGACACCAA 3'
	Reverse – 5' ATGCCTGCCATCCAACCTG 3'
Il4	Forward – 5' ATCCTGCTCTTCTTTCTCGAATGT 3'
	Reverse – 5' GCCGATGATCTCTCTCAAGTGATT 3'
Il6	Forward – 5' ACAACCACGGCCTTCCCTAC 3'
	Reverse – 5' TCCACGATTTCCCAGAGAACA 3'
Tnfa	Forward – 5' GGCAGGTTCTGTCCCTTTCAC 3'
	Reverse – 5' TTCTGTGCTCATGGTGTCTTTTCT 3'
Tgfb1	Forward – 5' GAGAAGAACTGCTGTGTGCG 3'
	Reverse – 5' GTGTCCAGGCTCCAAATATAGG 3'
Ccl2	Forward – 5' CCAGCAAGATGATCCCAATGA 3'
	Reverse – 5' TCTCTTGAGCTTGGTGACAAAAAC 3'
Csf1	Forward – 5' CGGGCATCATCCTAGTCTTGCTGACTGT 3'
	Reverse – 5' ATAGTGGCAGTATGTGGGGGGCATCCTC 3'
Igf1	Forward – 5' CTGAGCTGGTGGATGCTCT 3'
	Reverse – 5' CACTCATCCACAATGCCTGT 3'
Stat3	Forward – 5' GCACCTTGGATTGAGAGTCA 3'
	Reverse – 5' CCCAAGAGATTATGAAACACCA 3'
Cox2	Forward – 5' AACCGCATTGCCTCTGAAT 3'
	Reverse – 5' CATGTTCCAGGAGGATGGAG 3'
Rpl13a	Forward – 5' GAGGTCGGGTGGAAGTACCA 3'
	Reverse – 5' TGCATCTTGGCCTTTTCCTT 3'

CHAPTER THREE

Impact of increased pubertal adiposity on mammary gland development

3.1 Introduction

Puberty is a critical developmental stage in girls that can affect the chances of developing breast cancer in adulthood. Epidemiological studies have consistently demonstrated an inverse association of body adiposity during puberty with adult breast cancer risk (21-26). Compared to the median BMI-percentile (20.7 kg/m²), a BMI over 22.3 kg/m² (75th BMI-percentile) at age 18 is associated with reduced lifetime risk of breast cancer, adjusted for adult BMI (71, 90, 296). BMI-percentiles are an age-appropriate BMI scale that is used for adolescents to compensate for the changes in weight and height that occur as part of normal pubertal growth and development. The association between pubertal adiposity and adult breast cancer risk may be mediated through mammographic density (20, 79, 80).

Mammographic density is a well-established risk factor for breast cancer. Thirty nine percent of premenopausal and 26% of postmenopausal breast cancers are attributed to high mammographic density (297). Puberty is a key developmental stage in the establishment of adult mammographic density. Endocrine and paracrine signalling that occurs during puberty drive the development of epithelial, stromal, and adipose tissue in the breast (7-12). The relative proportion of these tissue compartments determines the radiological appearance of the adult breast and thus mammographic density.

A number of studies have shown an inverse association between pubertal adiposity and adult mammographic density (13, 14, 16-19). For example, high BMI at ages 7-13 years is inversely associated with adult mammographic density (19). Compared to the median BMI-percentile (20.7 kg/m²), a BMI over 22.3 kg/m² (75th BMI-percentile) at age 18 is associated with a 45% decrease in adult mammographic density, adjusted for adult BMI and timing of menarche (88). Overall, the above studies demonstrate that increased pubertal body adiposity is associated with reduced mammographic density and breast cancer risk in adult women.

Although these epidemiological studies demonstrate significant associations between pubertal adiposity, adult mammographic density, and breast cancer risk, causal relationships are yet to be established. Currently, it remains unclear whether pubertal adiposity is causal in adult mammographic density and breast cancer risk. To begin to address this question, we investigated the impact of increased adiposity on mammary gland development and function during puberty in a mouse model. We used the *Alms1 bbb/bbb* mouse model to address this question. Female *bbb/bbb* mice exhibit hyperphagia, resulting in increased body weight relative to wildtype (+/+) and heterozygous (*bbb/*+) littermates from 5 weeks of age leading to obesity, hyperinsulinemia, and dyslipidemia at 14 weeks of age (290). The mice progressively gain more

adipose tissue when fed a normal chow diet; they do not require a high-fat diet for them to gain weight. Hence, *bbb/bbb* mice are an ideal mouse model to study the impact of healthy weight gain and adiposity during puberty.

We hypothesised that *bbb/bbb* female mice will exhibit increased adiposity during puberty compared to controls (*bbb/+* or +/+), and this will impact mammary gland development. In this chapter, we investigated the impact of increased adiposity on development of terminal end buds and abundance of macrophages in the mammary gland. Further, to understand the effect of increased pubertal adiposity on the mammary gland microenvironment, we assessed protein and gene expression of cytokines including leptin, IL6, TNFA, and CCL2 in the mammary glands. Results from this chapter demonstrate that increased adiposity in *bbb/bbb* mice promotes mammary gland development, resulting in increased number of terminal end buds, number of proliferating epithelial cells, and abundance of macrophages, compared to controls.

3.2 Results

3.2.1 Female *bbb/bbb* mice exhibit increased mammary gland adiposity during puberty

To investigate the impact of increased adiposity during puberty on mammary gland development, controls (*bbb/+* or +/+) and *bbb/bbb* mice were fed a normal mouse diet ad libitum until 6 weeks of age. Mice were euthanised and then weighed and dissected. Mammary glands and visceral adipose tissue were collected from these mice. At puberty i.e., 6 weeks, *bbb/bbb* mice did not exhibit a statistically significant gain in body weight, compared to controls ($p=0.32$) (Figure 3.1.A). Weight of visceral adipose tissue ($p=0.27$) (Figure 3.1.B) and total weight of fourth pair mammary glands ($p=0.47$) (Figure 3.1.C) was not significantly different between the two genotypes.

To determine whether controls and *bbb/bbb* mice exhibit differences in adiposity, we characterised hematoxylin-eosin stained fourth pair mammary gland adipose tissue and visceral adipose tissue. The adipocyte size in the mammary adipose tissue was significantly increased in *bbb/bbb* mice compared to controls ($p<0.001$) (Figure 3.2.A, B). Consistent with adipocyte size, number of adipocytes per area was significantly reduced in *bbb/bbb* mice compared to controls ($p=0.017$) (Figure 3.2.C). Further, percent frequency of smaller adipocytes (≤1000 μm^2) versus larger adipocytes (>1000 μm^2) were estimated in the mammary gland adipose tissue of both genotypes. The mammary gland adipose tissue of *bbb/bbb* mice was predominantly occupied by larger adipocytes compared to controls ($p<0.001$) (Figure 3.2.D). On the other hand, the mammary gland adipose tissue of controls had relatively smaller

adipocytes population than *bbb/bbb* mice ($p<0.001$) (Figure 3.2.D). These results demonstrate that *bbb/bbb* mice exhibit increased mammary gland adiposity during puberty.

In contrast to mammary gland adipose tissue, the adipocyte size in visceral adipose tissue was similar in controls and *bbb/bbb* mice ($p=0.952$) (Figure 3.3.A, B). No statistically significant difference was observed in the number of adipocytes per area in *bbb/bbb* mice compared to controls ($p=0.788$) (Figure 3.3.C). This result was also reflected in analysis of percent frequency. Percent frequency of either smaller adipocytes ($p=0.943$) or larger adipocytes ($p=0.943$) was not significantly different between both genotypes (Figure 3.3.D).

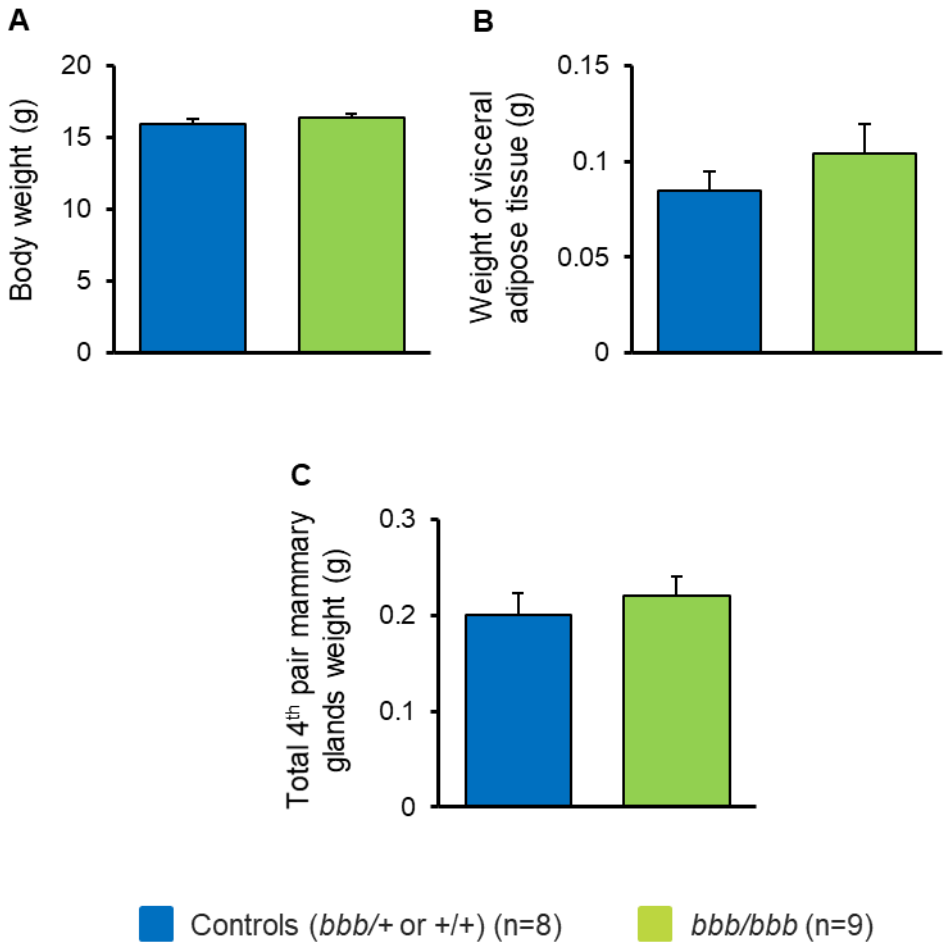

Figure 3.1. Relative weights of female control and *bbb/bbb* mice at puberty. Mice were fed normal mouse diet ad libitum till 6 weeks of age, euthanised, and then weighed and dissected to collect visceral adipose tissue and fourth pair mammary glands. (A) Total body weight. (B) Weight of visceral adipose tissue. (C) Total fourth pair mammary glands weight. Total fourth pair mammary glands weight is the combined weight of left and right fourth pair mammary glands. Colour code - Blue: Controls (*bbb/+* or +/+) (n=8) and Green: *bbb/bbb* (n=9). Data are presented as mean+SEM and analysed using linear regression model with statistical significance at $p<0.05$.

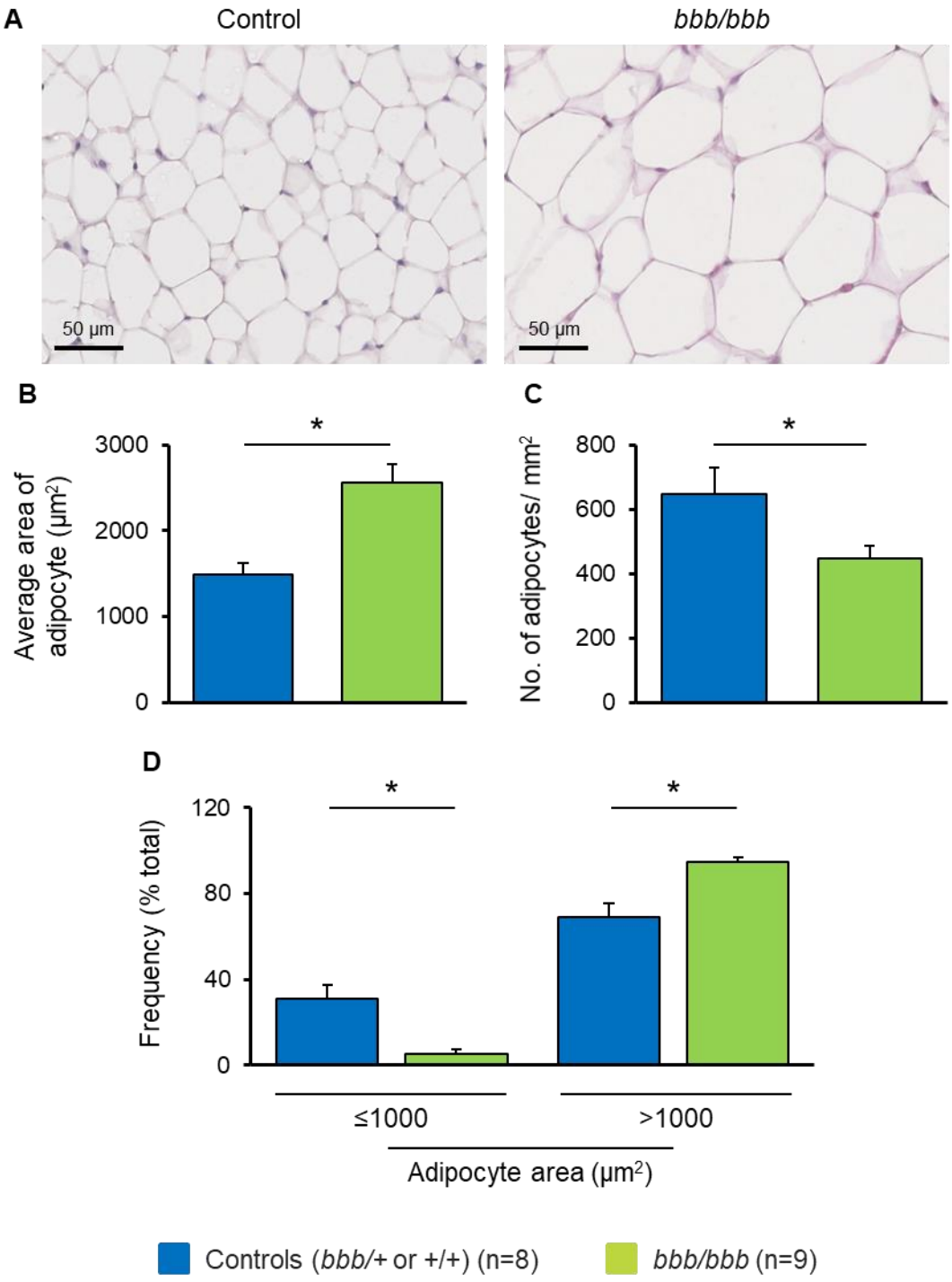

Figure 3.2. Mammary gland adiposity in control and *bbb/bbb* mice at puberty. (A) Representative images of hematoxylin-eosin stained mammary gland adipose tissue of fourth pair mammary glands of controls and *bbb/bbb* mice. Scale bars: 50 µm. (B) Average adipocyte area. (C) Number of adipocytes per area. (D) Frequency of smaller adipocytes (≤1000 µm^2) versus larger adipocytes (>1000 µm^2). Colour code - Blue: Controls (*bbb/+* or +/+) (n=8) and Green: *bbb/bbb* (n=9). Data are presented as mean+SEM and analysed using linear regression model. * indicates statistical significance at $p<0.05$.

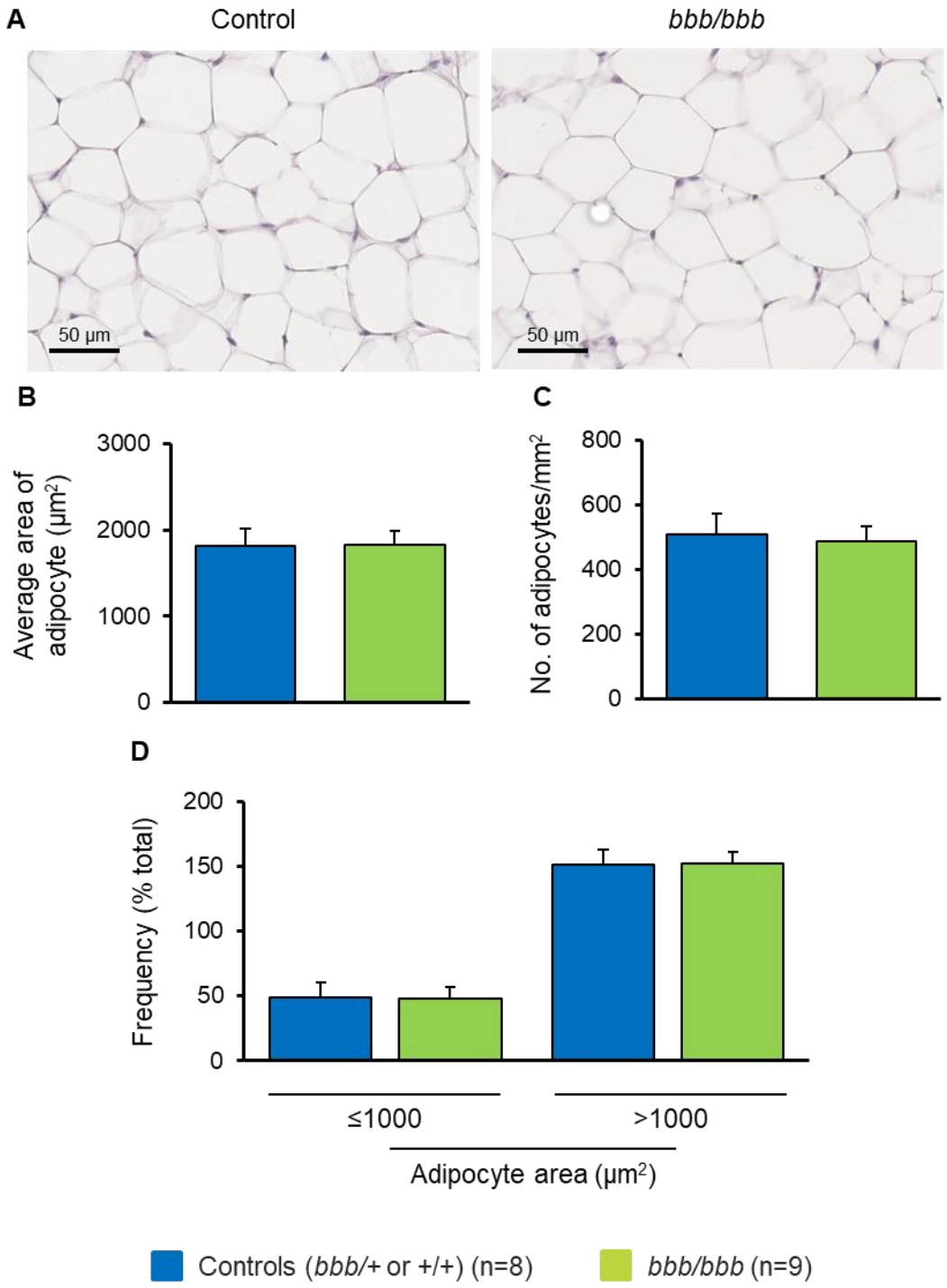

Figure 3.3. Deposition of visceral adipose tissue in control and *bbb/bbb* mice at puberty. (A) Representative images of hematoxylin-eosin stained visceral adipose tissue collected from the abdominal cavity of controls and *bbb/bbb* mice. Scale bars: 50 µm. (B) Average adipocyte area. (C) Number of adipocytes per area. (D) Frequency of smaller adipocytes (≤1000 µm^2) versus larger adipocytes (>1000 µm^2). Colour code - Blue: Controls (*bbb/+* or +/+) (n=8) and Green: *bbb/bbb* (n=9). Data are presented as mean+SEM and analysed using linear regression model with statistical significance at $p<0.05$.

3.2.2 Increased development of mammary gland terminal end buds in pubertal *bbb/bbb* mice

To investigate the impact of the *bbb/bbb* mutation on mammary gland development, mammary gland whole-mounts were stained with carmine alum and analysed (Figure 3.4.A). Ductal invasion area was determined by how far the ducts had grown into the mammary gland adipose tissue. No significant difference was observed in ductal invasion area between controls and *bbb/bbb* mice (p=0.067) (Figure 3.4.B).

Ductal elongation was assessed by measuring the length between the nipple to the furthest end of the duct. The mammary glands of controls and *bbb/bbb* mice exhibited similar ductal elongation (p=0.161) (Figure 3.4.C). Ductal branching analysis demonstrated that there was no significant difference in the degree of branching between the two genotypes (p=0.385) (Figure 3.4.D).

Terminal end buds (TEBs) are specialised structures that drive mammary gland development during puberty by growing through the mammary adipose tissue. Interestingly, the number of TEBs was significantly increased in *bbb/bbb* mice compared to controls (p=0.003) (Figure 3.4.E).

Following this, epithelial cell proliferation was quantified by BrdU incorporation in TEBs. BrdU-positive cells (Figure 3.5.A, B, arrows indicated) represented the proliferating epithelial cells in the TEBs of controls and *bbb/bbb* mice. The negative control showed no BrdU-positive staining (Figure 3.5.C). The number of proliferating epithelial cells in TEBs was significantly increased in *bbb/bbb* mice in comparison to controls (p=0.002) (Figure 3.5.D). These results suggest that increased mammary adiposity promotes mammary gland development during puberty.

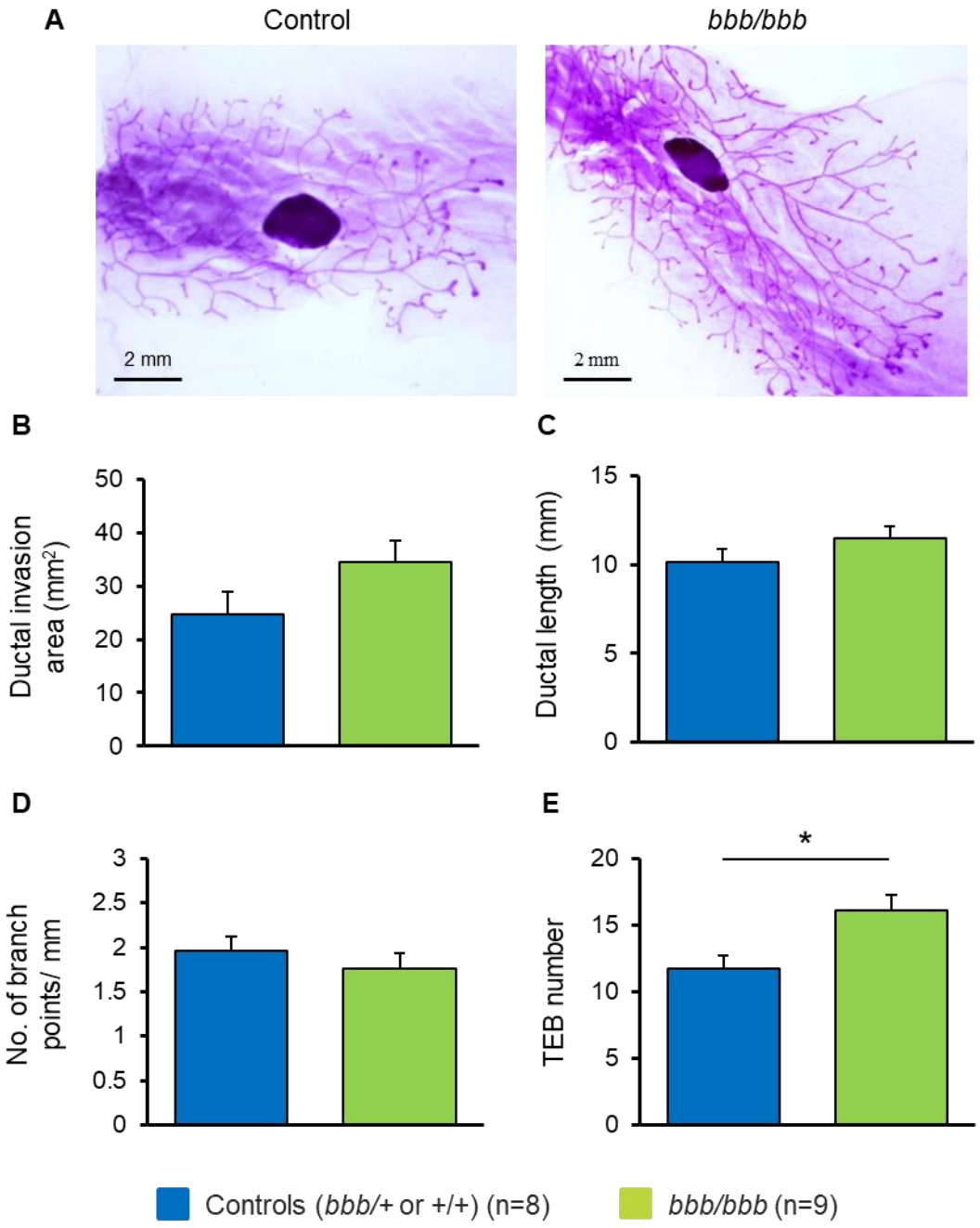

Figure 3.4. Whole-mount analysis of developing mammary glands in control and *bbb/bbb* mice at puberty. (A) Representative images of alum-carmine stained whole-mounts of fourth pair mammary glands of controls and *bbb/bbb* mice. Scale bars: 2 mm. (B) Ductal invasion area. It is estimated by calculating the area covered by ducts from the lymph node. (C) Ductal length. It is calculated as the length from the nipple to the furthest duct. (D) Branching. It is calculated as the number of branch points per millimetres. (E) Terminal end buds number. Only terminal end buds of size greater than 100 µm are considered for calculation. Colour code - Blue: Controls (*bbb/+* or *+/+*) (n=8) and Green: *bbb/bbb* (n=9). Data are presented as mean+SEM and analysed using linear regression model. * indicates statistical significance at $p<0.05$.

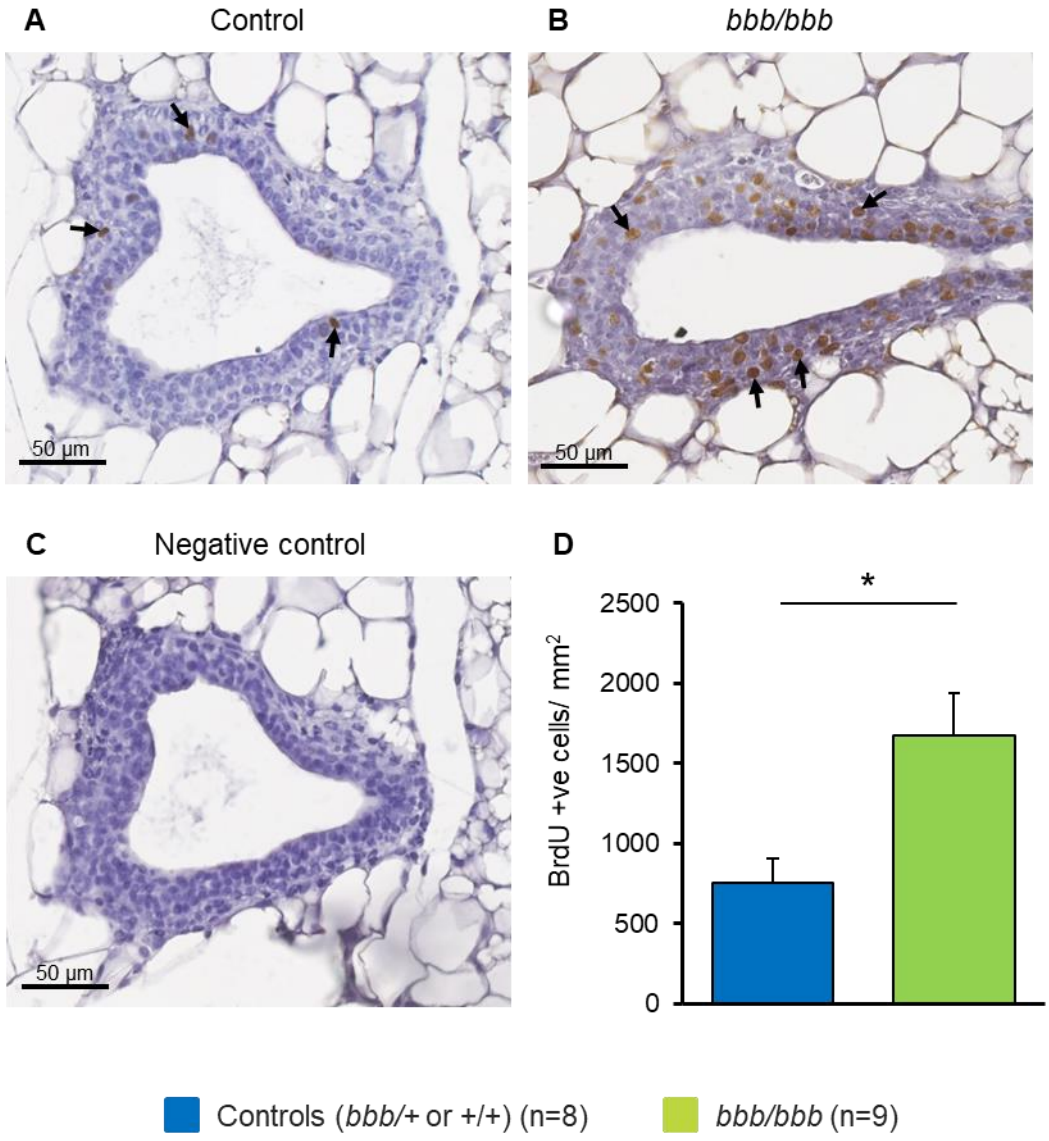

Figure 3.5. Proliferation of epithelial cells in mammary gland terminal end buds in control and *bbb/bbb* mice at puberty. Immunostaining of mammary gland sections from 6-week-old controls and *bbb/bbb* mice with BrdU-antibody. Representative images of BrdU-positive cells (arrows indicated) are the proliferating epithelial cells in the terminal end buds from (A) controls and (B) *bbb/bbb* mice. (C) Negative control without primary antibody shows no BrdU-positive staining. Original magnification 40X. Scale bars: 50 µm. (D) Quantification of number of BrdU-positive cells per area. Colour code - Blue: Controls (*bbb/+* or +/+) (n=8) and Green: *bbb/bbb* (n=9). Data are presented as mean+SEM and analysed using linear regression model. * indicates statistical significance at $p<0.05$.

3.2.3 No change in mammary gland fibroglandular density in pubertal *bbb/bbb* mice

To investigate the impact of the *bbb/bbb* mutation on mammary gland density, percent fibroglandular density was calculated in hematoxylin-eosin stained mammary glands. It is measured as the percentage of fibroglandular tissue present per area in the mammary gland. Both genotypes exhibited similar percent fibroglandular density (p=0.846) (Figure 3.6). Further, Masson's trichrome-stained mammary glands were assessed to analyse collagen deposition around the ducts of mammary glands in these mice. No significant difference was observed in the collagen deposition around the ducts in controls and *bbb/bbb* mice (p=0.352) (Figure 3.7).

3.2.4 Increased abundance of mammary gland macrophages in pubertal *bbb/bbb* mice

Macrophages are key immune cells in mammary gland development during puberty. As TEBs grow through mammary adipose tissue, macrophages reside in the stroma along the neck of TEBs to support ductal elongation (298). To investigate the impact of the *bbb/bbb* mutation on abundance of macrophages around TEBs, F4/80-antibody immunostaining of the mammary glands was performed. F4/80-positive cells (Figure 3.8.A, B, arrows indicated) represented the F4/80-positive macrophages around TEBs of controls and *bbb/bbb* mice. Negative control showed no F4/80-positive staining (Figure 3.8.C). Increased abundance of F4/80-positive macrophages around TEBs was evident in *bbb/bbb* mice compared to controls (p=0.008) (Figure 3.9).

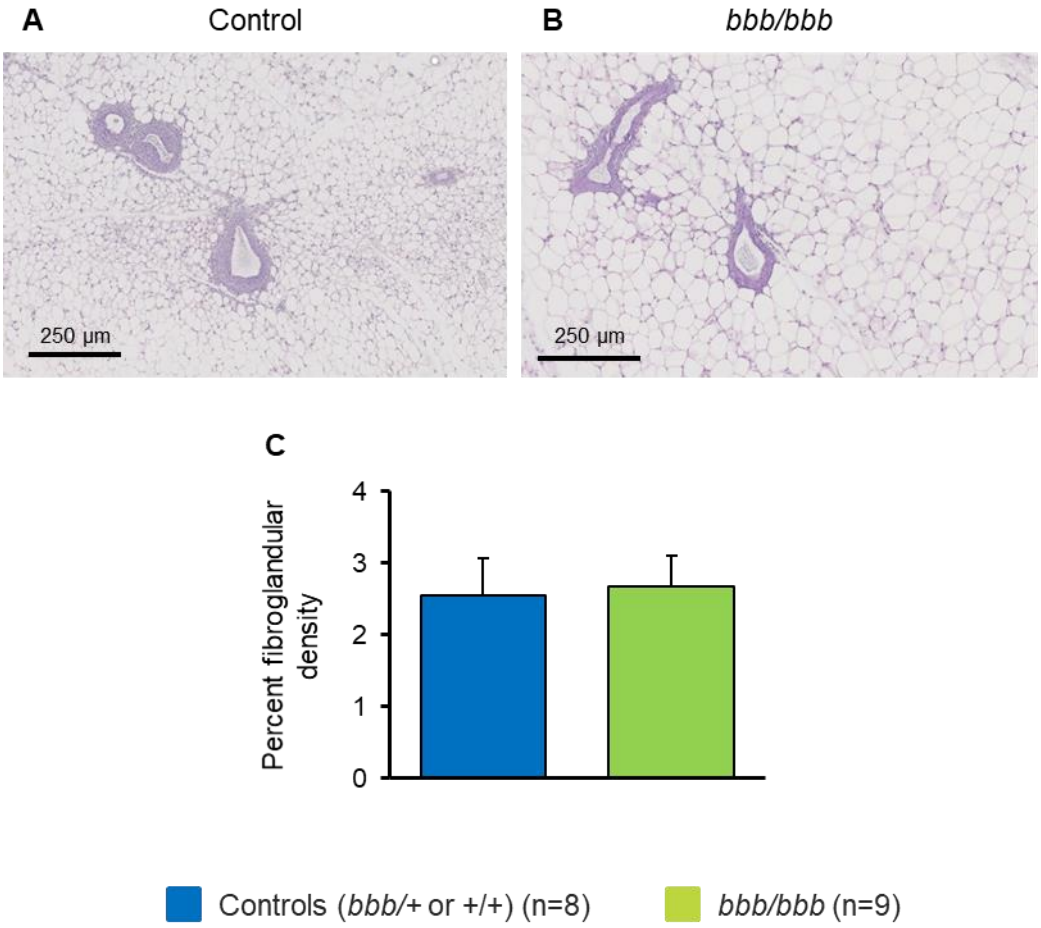

Figure 3.6. Percent mammary gland fibroglandular density in control and *bbb/bbb* mice at puberty. Representative images of hematoxylin-eosin stained mammary gland sections of (A) controls and (B) *bbb/bbb* mice. Scale bars: 250 µm. (C) Quantification of percent fibroglandular density. It is calculated by the percentage of fibroglandular tissue present per area in the mammary gland. Colour code - Blue: Controls (*bbb/+* or *+/+*) (n=8) and Green: *bbb/bbb* (n=9). Data are presented as mean+SEM and analysed using linear regression model. * indicates statistical significance at $p<0.05$.

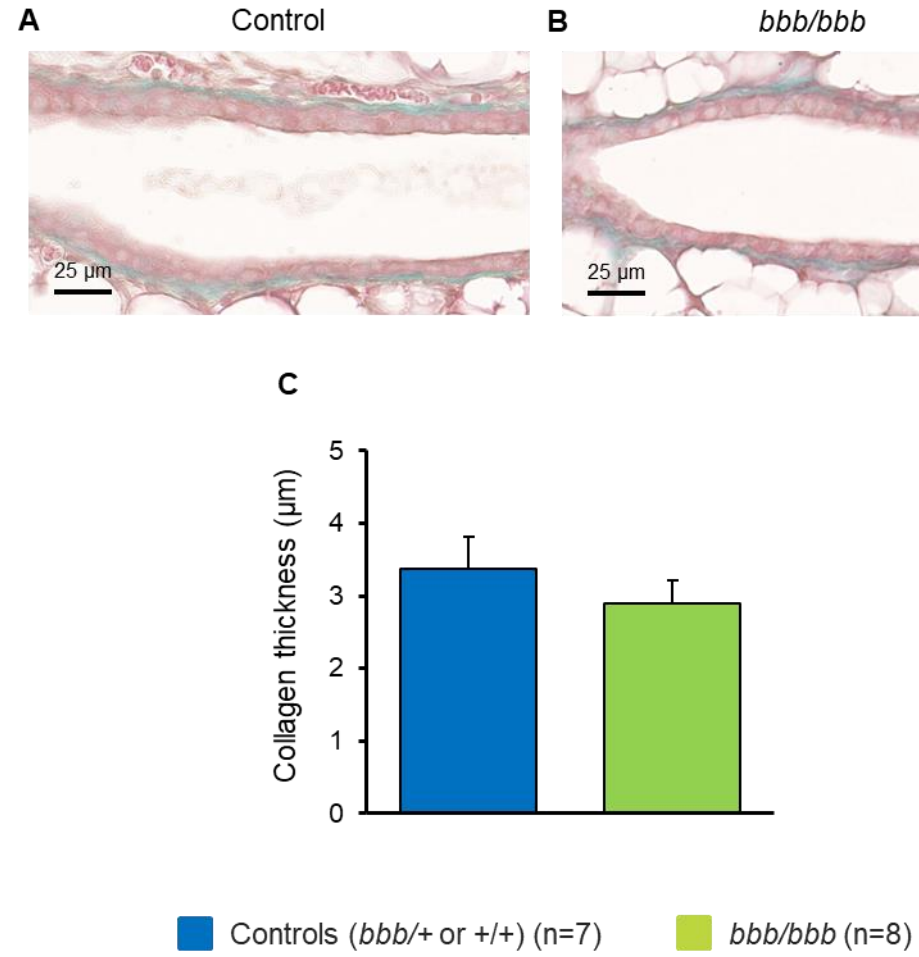

Figure 3.7. Collagen deposition around the mammary gland ducts in control and *bbb/bbb* mice at puberty. Representative images of Masson's trichrome-stained mammary gland sections of (A) controls and (B) *bbb/bbb* mice. Scale bars: 25 µm. (C) Quantification of collagen (green stain) deposition around ducts. It is measured as the thickness of collagen deposited surround the ducts. Colour code - Blue: Controls (*bbb*/+ or +/+) (n=7) and Green: *bbb/bbb* (n=8). Data are presented as mean+SEM and analysed using linear regression model. * indicates statistical significance at $p<0.05$.

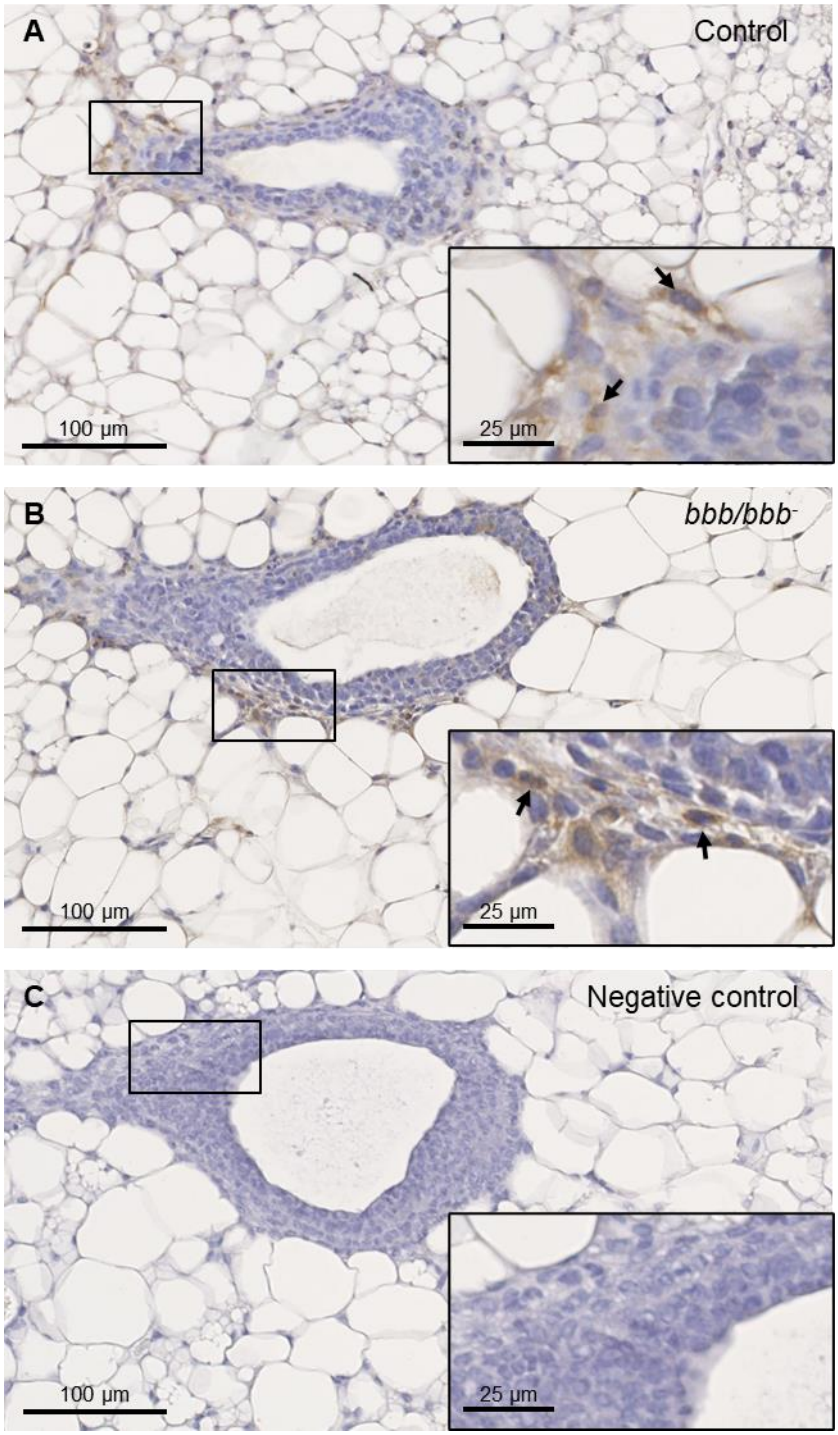

Figure 3.8. F4/80-positive macrophages around mammary gland terminal end buds in control and *bbb/bbb* mice at puberty. Representative images of F4/80-positive cells (arrows indicated) are the F4/80-positive macrophages around terminal end buds from (A) controls and (B) *bbb/bbb* mice. (C) Negative control without primary antibody showed no F4/80-positive staining. Images at original magnification of 40X and scale bars: 100 µm, with inset images at original magnification of 80X and scale bars: 25 µm.

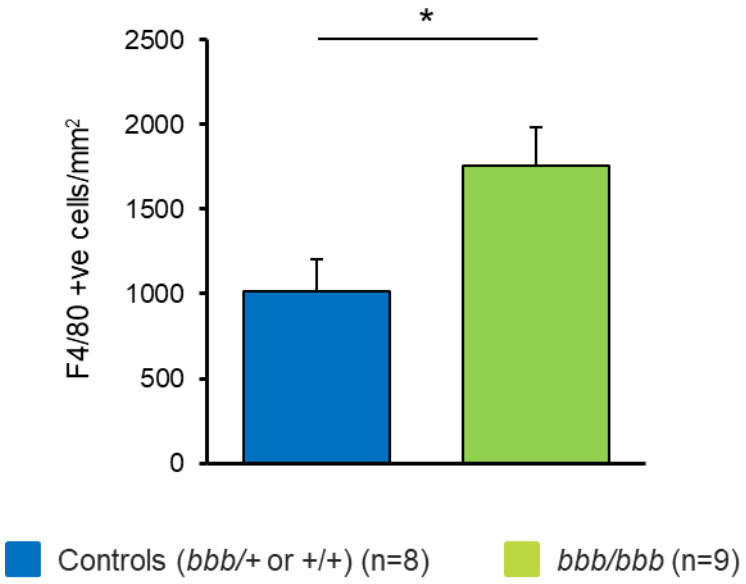

Figure 3.9. Abundance of macrophages around mammary gland terminal end buds in control and *bbb/bbb* mice at puberty. Quantification of F4/80-positive macrophages per area around terminal end buds of 6-week-old controls and *bbb/bbb* mice. Colour code - Blue: Controls (*bbb*/+ or +/+) (n=8) and Green: *bbb/bbb* (n=9). Data are presented as mean+SEM and analysed using linear regression model. * indicates statistical significance at $p<0.05$.

Macrophages within mammary adipose tissue stroma are important for mammary gland development and tissue homeostasis (299). To examine the effect of the *bbb/bbb* mutation on abundance of macrophages residing in adipose tissue, F4/80-antibody immunostaining of the mammary gland adipose tissue and visceral adipose tissue was performed. F4/80-positive cells (Figure 3.10.A, B, arrows indicated) represented the F4/80-positive macrophages in mammary gland adipose tissue of controls and *bbb/bbb* mice. Negative control showed no F4/80-positive staining (Figure 3.10.C). Interestingly, statistically significant increase in the number of F4/80-positive macrophages per area was exhibited in the mammary gland adipose tissue of *bbb/bbb* mice, in comparison to controls ($p<0.001$) (Figure 3.11.A).

As previously mentioned, there was a significant difference in the number of adipocytes per area in both genotypes, it is logical to also quantitate the number of macrophages to the number of adipocytes in an area of adipose tissue in each genotype group. We quantitated the number of macrophages in an area consisting of 100 adipocytes and presented data as the number of macrophages per 100 adipocytes. Consistent with the previous result, *bbb/bbb* mice exhibited significantly increased abundance of macrophages per 100 adipocytes than controls ($p<0.001$) (Figure 3.11.B).

Further, we quantitated abundance of macrophages in the visceral adipose tissue of these mice. F4/80-positive cells (Figure 3.12.A, B, arrows indicated) represented the F4/80-positive macrophages in visceral adipose tissue of controls and *bbb/bbb* mice. Negative control showed no F4/80-positive staining (Figure 3.12.C). No difference was demonstrated in the number of F4/80-posive macrophages between these mice ($p=0.167$) (Figure 3.13.A). Consistently, no significant difference in abundance of F4/80-positive macrophages per 100 adipocytes between both genotypes ($p=0.296$) was observed (Figure 3.13.B).

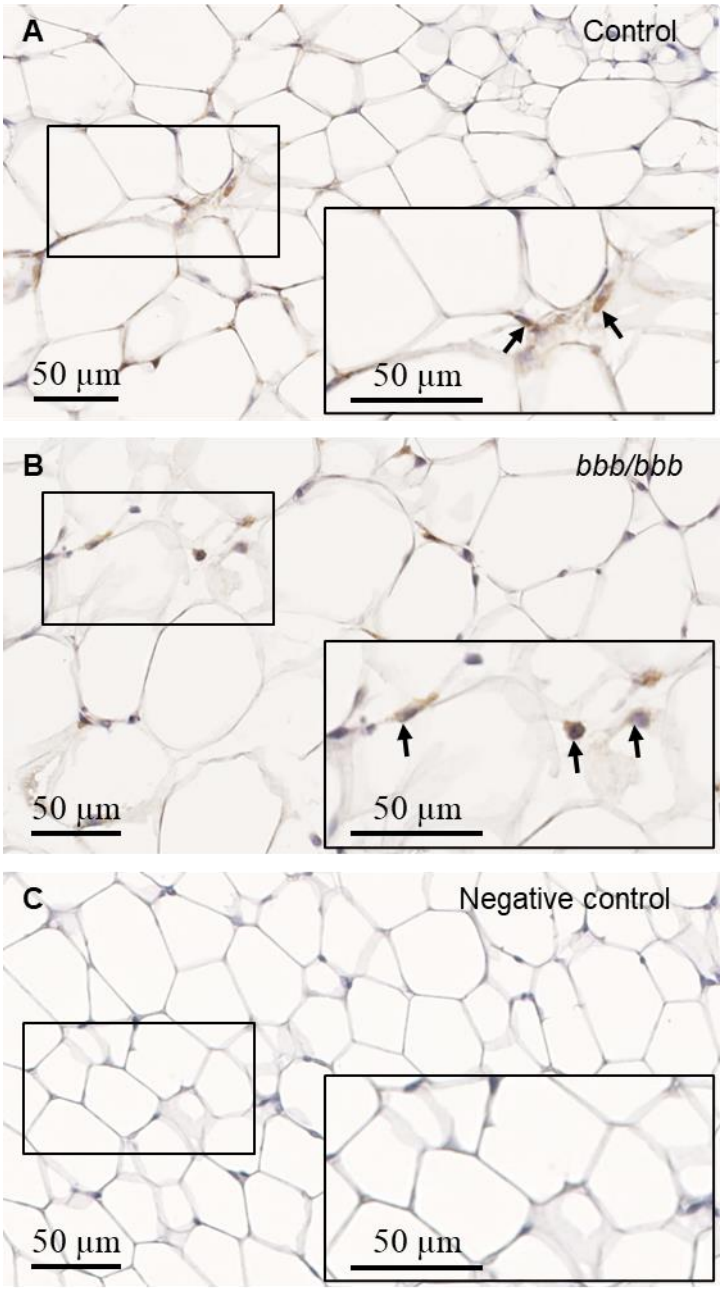

Figure 3.10. F4/80-positive macrophages in the mammary gland adipose tissue of control and *bbb/bbb* mice at puberty. Representative images of F4/80-positive cells (arrows indicated) are the F4/80-positive macrophages in the mammary adipose tissue from (A) controls and (B) *bbb/bbb* mice. (C) Negative control without primary antibody shows no F4/80-positive staining. Original magnification 40X. Scale bars: 50 µm.

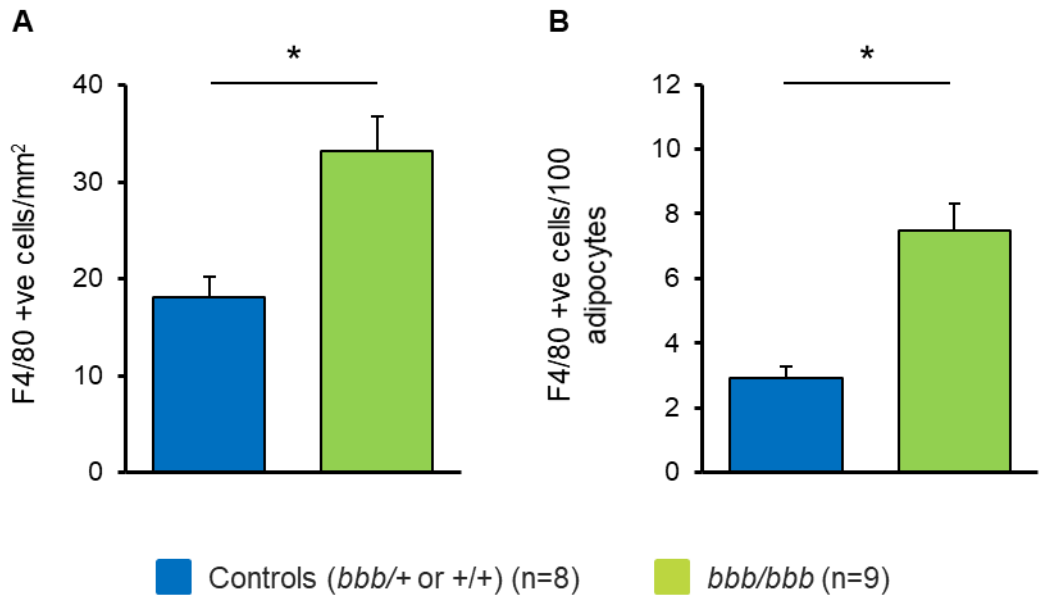

Figure 3.11. Abundance of macrophages in the mammary gland adipose tissue in control and *bbb/bbb* mice at puberty. Quantification of F4/80-positive macrophages (A) per area and (B) per 100 adipocytes in the mammary gland adipose tissue of 6-week-old controls and *bbb/bbb* mice. Colour code - Blue: Controls (*bbb/+* or *+/+*) (n=8) and Green: *bbb/bbb* (n=9). Data are presented as mean+SEM and analysed using linear regression model. * indicates statistical significance at $p<0.05$.

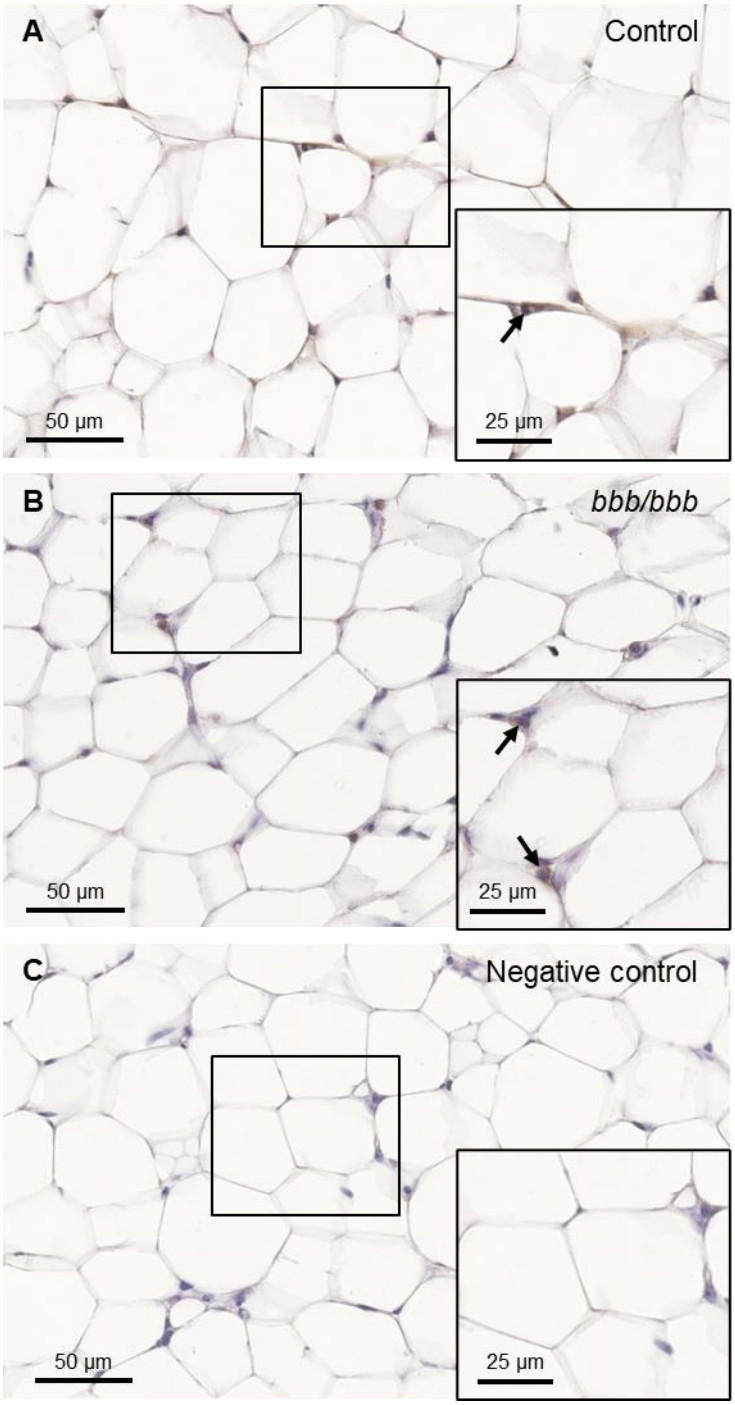

Figure 3.12. F4/80-positive macrophages in the visceral adipose tissue in control and *bbb/bbb* mice at puberty. Representative images of F4/80-positive cells (arrows indicated) are the F4/80-positive macrophages in visceral adipose tissue from (A) controls and (B) *bbb/bbb* mice. (C) Negative control shows no F4/80-positive staining. Images at original magnification of 40X and scale bars: 50 µm, with inset images at original magnification of 80X and scale bars: 25 µm.

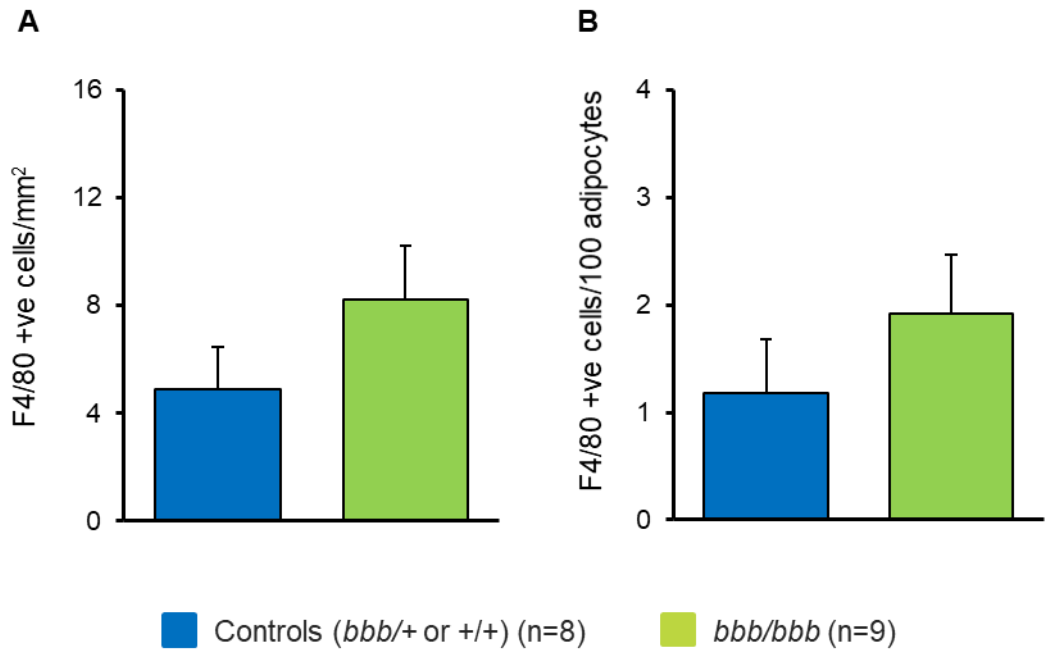

Figure 3.13. Abundance of macrophages in the visceral adipose tissue in control and *bbb/bbb* mice at puberty. Quantification of F4/80-positive macrophages (A) per area and (B) per 100 adipocytes in visceral adipose tissue of 6-week-old controls and *bbb/bbb* mice. Colour code - Blue: Controls (*bbb*/+ or +/+) (n=8) and Green: *bbb/bbb* (n=9). Data are presented as mean+SEM and analysed using linear regression model with significance at $p<0.05$.

3.2.5 Altered abundance of adipokines and proinflammatory cytokines in pubertal *bbb/bbb* mice

To investigate the impact of the *bbb/bbb* mutation on mammary gland microenvironment, we assessed the concentrations of the most well characterised markers of obesity and tumour development in the mammary glands. Luminex assay was performed to estimate the protein levels of IL6, CCL2, leptin, TNFA, PAI1 and resistin in the mammary glands. No significant difference was observed in the levels of IL6 (p=0.549), CCL2 (p=0.150), leptin (p=0.569), TNFA (p=0.821) and PAI1 (p=0.478) between the two genotypes (Figure 3.14). However, protein levels of resistin was significantly decreased in *bbb/bbb* mice compared to controls (p=0.029) (Figure 3.14.F).

To investigate the impact of the *bbb/bbb* mutation on gene expression of adipokines and proinflammatory cytokines, RT-PCR analysis was performed to estimate the gene expression of *leptin*, *adiponectin*, *Il4*, *Il6*, *Tnfa*, *Tgfb1*, *Ccl2*, *Csf1*, *Igf1*, *Stat3*, and *Cox2*. Data was plotted as box plots to account for a high degree of variability with genotype groups and skewness of the data set. No significant difference was observed in the expression of *leptin* (p=0.668), *adiponectin* (p=0.602), *Il4* (p=0.177), *Il6* (p=0.412), *Tnfa* (p=0.373), *Tgfb1* (p=0.878), *Ccl2* (p=0.481), *Csf1* (p=0.779), *Igf1* (p=0.650), *Stat3* (p=0.697), and *Cox2* (p=0.161) in the mammary glands (Figure 3.15).

Similarly, expression of the above-mentioned genes was analysed in visceral adipose tissue. Likewise, no significant difference with high degree of variability was observed in the expression of *leptin* (p=0.526), *adiponectin* (p=0.575), *Il4* (p=0.563), *Il6* (p=0.783), *Tnfa* (p=0.297), *Tgfb1* (p=0.723), *Ccl2* (p=0.676), *Csf1* (p=0.509), *Igf1* (p=0.186), *Stat3* (p=0.913), and *Cox2* (p=0.307) in the visceral adipose tissue (Figure 3.16).

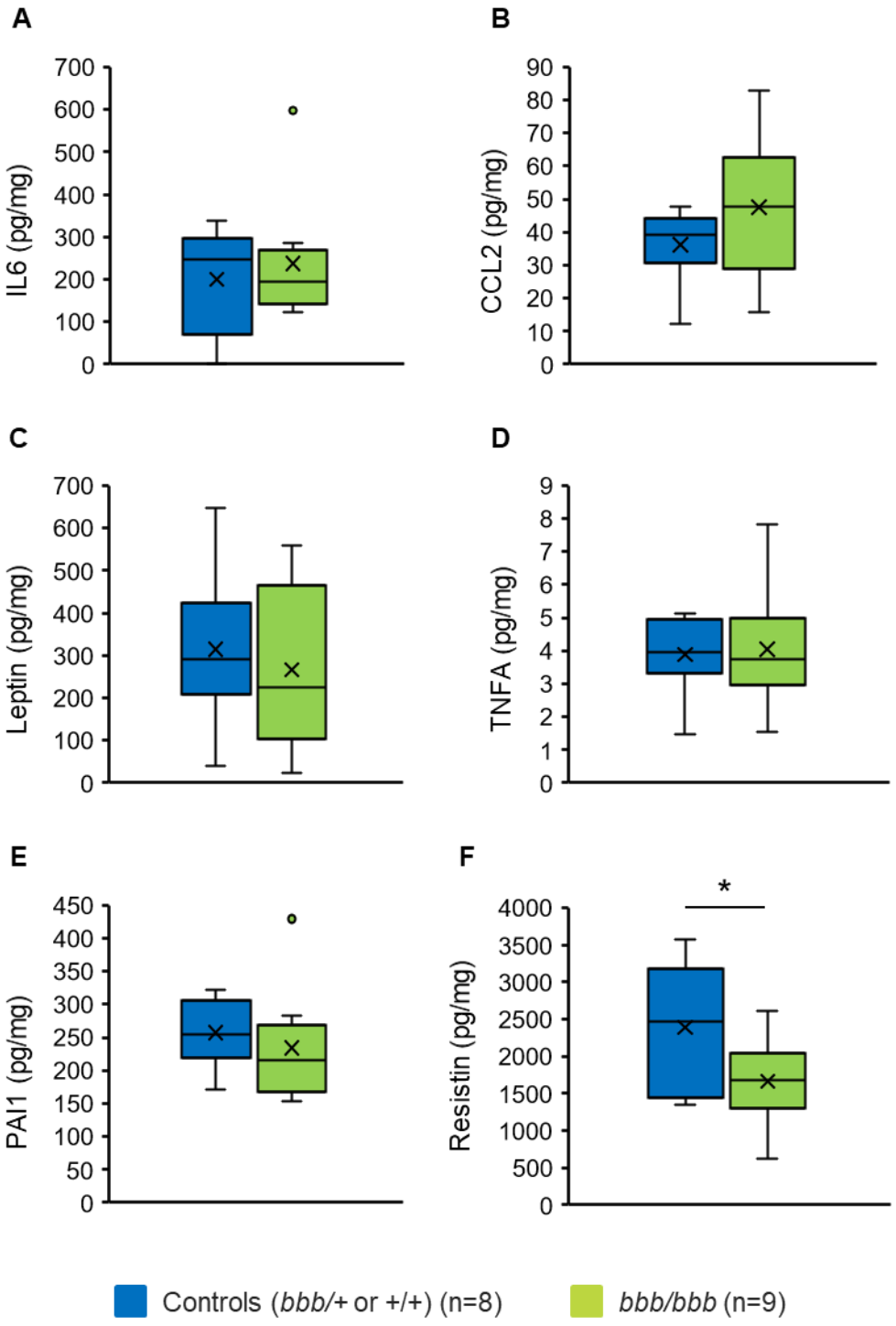

Figure 3.14. Protein abundance of adipokines and proinflammatory cytokines in the mammary glands in control and *bbb/bbb* mice at puberty. Luminex assay assessed the protein levels of (A) IL6, (B) CCL2, (C) leptin, (D) TNFA, (E) PAI1 and (F) resistin in third pair mammary glands. Colour code - Blue: Controls (*bbb/+* or +/+) (n=8) and Green: *bbb/bbb* (n=9). IL6: interleukin 6; CCL2: C-C motif chemokine ligand 2; TNFA: tumour necrosis factor alpha; PAI1: plasminogen activator inhibitor 1. Data are presented as box-plots with median in between the first quartile and third quartile and analysed using a linear regression model. * indicates statistical significance at $p<0.05$.

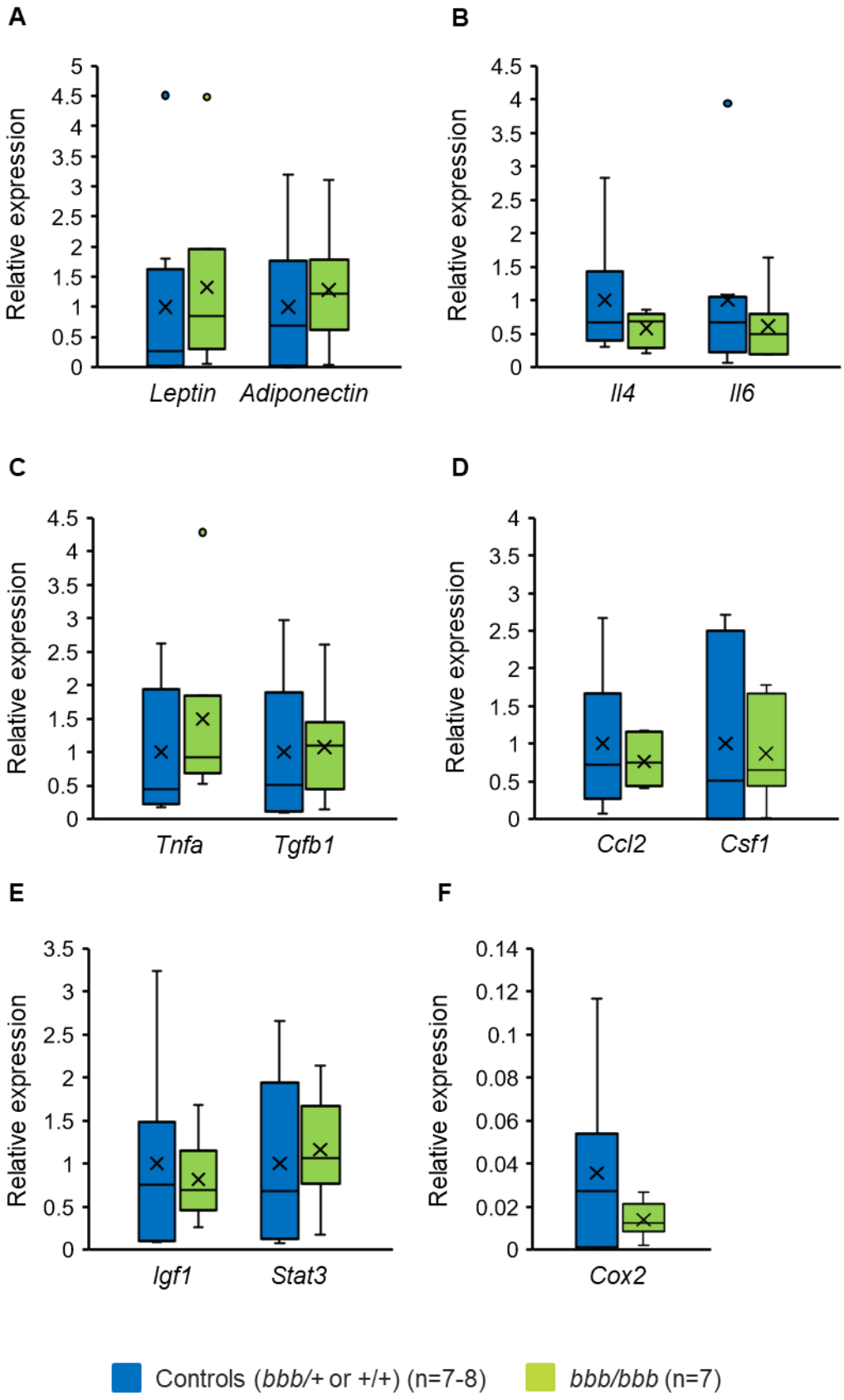
A
Relative expression
Leptin
Adiponectin
B
Relative expression
Il4
Il6
C
Relative expression
Tnfa
Tgfb1
D
Relative expression
Ccl2
Csf1
E
Relative expression
Igf1
Stat3
F
Relative expression
Cox2
Controls (bbb/+ or +/+) (n=7-8)
bbb/bbb (n=7)

Figure 3.15. Gene expression profile of adipokines and proinflammatory cytokines in the mammary glands in control and *bbb/bbb* mice at puberty. Quantification of mRNA encoding (A) leptin, adiponectin, (B) IL4, IL6, (C) TNFA, TGFB1, (D) CCL2, CSF1, (E) IGF1, STAT3, and (F) COX2 by real-time PCR analysis using comparative Ct method (i.e., 2^(-ΔΔCt) method). The abundance of mRNA was normalised to abundance of mRNA encoding the housekeeping gene *Rpl13a* in each mouse. Colour code - Blue: Controls (*bbb/+* or *+/+*) (n=7-8) and Green: *bbb/bbb* (n=7). *Il4*: interleukin 4; *Il6:* interleukin 6; *Tnfa:* tumour necrosis factor alpha; *Tgfb1:* transforming growth factor beta 1; *Ccl2:* C-C motif chemokine ligand 2; *Csf1:* colony-stimulating factor 1; *Igf1:* insulin-like growth factor 1; *Stat3:* signal transducer and activator of transcription 3*; Cox2:* cyclooxygenase 2. Data are presented as box-plots with median in between the first quartile and third quartile and analysed using a linear regression model with statistical significance at $p<0.05$.

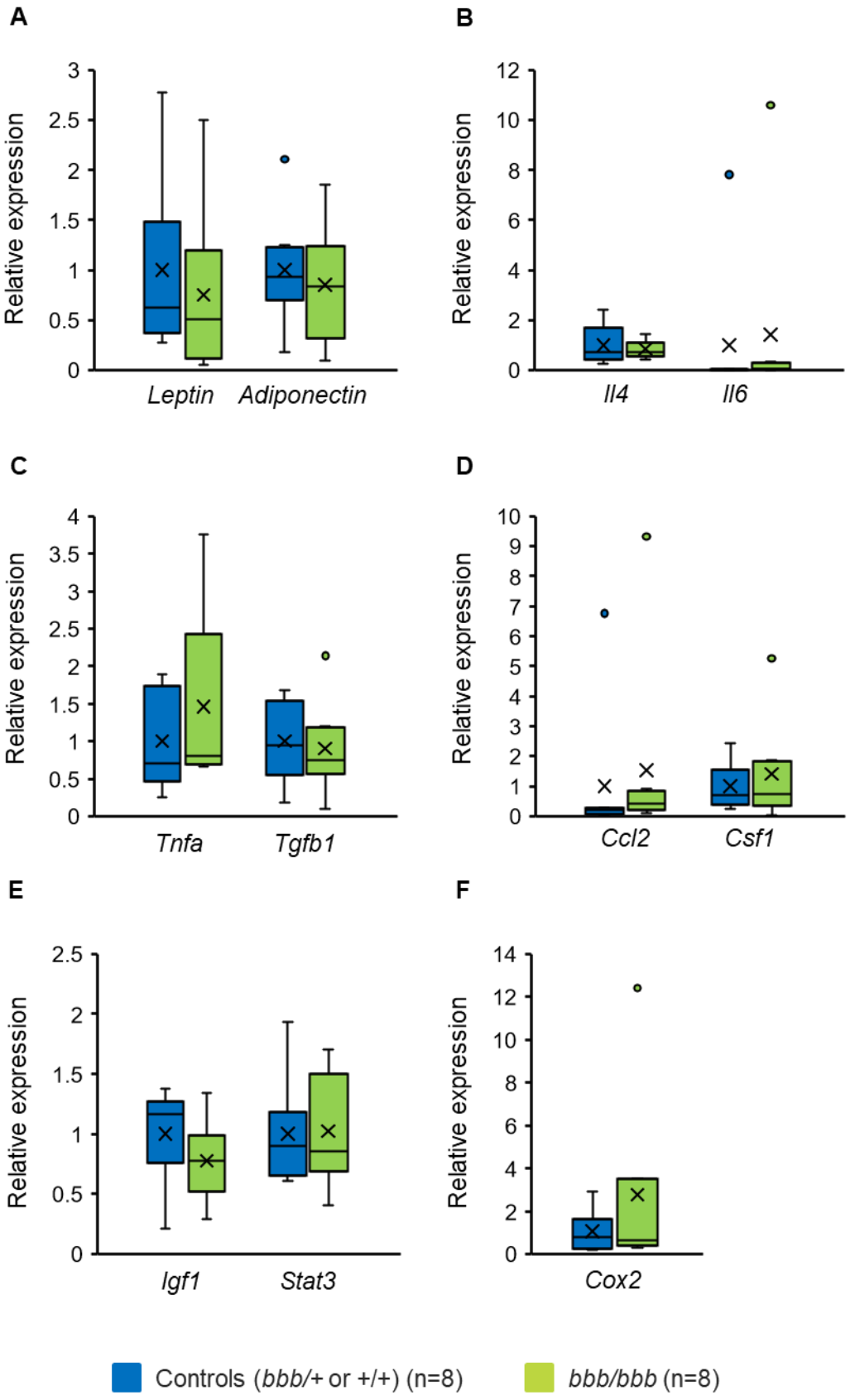
A
Relative expression
Leptin
Adiponectin
B
Relative expression
Il4
Il6
C
Relative expression
Tnfa
Tgfb1
D
Relative expression
Ccl2
Csf1
E
Relative expression
Igf1
Stat3
F
Relative expression
Cox2
Controls (bbb/+ or +/+) (n=8)
bbb/bbb (n=8)

Figure 3.16. Gene expression profile of adipokines and proinflammatory cytokines in the visceral adipose tissue in control and *bbb/bbb* mice at puberty. Quantification of mRNA encoding (A) leptin, adiponectin, (B) IL4, IL6, (C) TNFA, TGFB1, (D) CCL2, CSF1, (E) IGF1, STAT3, and (F) COX2 by real-time PCR analysis using comparative Ct method (i.e., 2^(-ΔΔCt) method). The abundance of mRNA was normalised to abundance of mRNA encoding the housekeeping gene *Rpl13a* in each mouse. Colour code - Blue: Controls (bbb/+ or +/+) (n=8) and Green: *bbb/bbb* (n=8). *Il4*: interleukin 4; *Il6*: interleukin 6; *Tnfa*: tumour necrosis factor alpha; *Tgfb1*: transforming growth factor beta 1; *Ccl2*: C-C motif chemokine ligand 2; *Csf1*: colony-stimulating factor 1; *Igf1*: insulin-like growth factor 1; *Stat3*: signal transducer and activator of transcription 3; *Cox2*: cyclooxygenase 2. Data are presented as box-plots with median in between the first quartile and third quartile and analysed using a linear regression model with statistical significance at $p<0.05$.

3.3 Discussion

Puberty is a key developmental stage in the establishment of mammographic density. Pubertal adiposity is proposed to impact adult mammographic density and breast cancer risk. However, the extent to which increased adiposity during puberty affects mammary gland development and function remains unclear.

The experiments described in this chapter examined the impact of increased pubertal adiposity on mammary gland development in a mouse model. We demonstrated that *bbb/bbb* mice exhibited increased mammary gland adiposity during puberty indicated by increased adipocyte size specifically in adipose tissue in the mammary gland and not visceral fat depots. This increased mammary gland adiposity was associated with increased number of TEBs, increased proliferation of epithelial cells, and increased abundance of macrophages around TEBs and in the mammary gland adipose tissue. Hence, our results suggest that increased mammary gland adiposity during puberty promotes mammary gland development, potentially through the crosstalk between mammary gland adipose tissue, epithelium, and macrophages.

3.3.1 Increased mammary gland adiposity in *bbb/bbb* mice

In this study, *Alms1 bbb/bbb* mice, a genetic model of adiposity, was used instead of a high-fat diet-induced obesity model to explore the impact of adiposity during puberty on mammary gland development. These mice carry a recessive homozygous genetic mutation that causes them to overeat compared to wildtype controls, even when fed a normal mouse chow diet. In this study, no significant gain in body weight at the age of 6 weeks was observed. In addition, no difference was detected in the weight of visceral adipose tissue and weight of total fourth pair mammary glands. This suggests that *bbb/bbb* mice exhibit overtly normal weight gain and growth during puberty, similar to controls. A high-fat diet usually increases BMI and therefore, it is not possible to investigate how diet and increased BMI independently affect breast cancer risk (300). However, *Alms1 bbb/bbb* mouse model ensured that increased adiposity during puberty was derived from a healthy diet and avoided the confounding factors of a high-fat diet.

The finding of overtly normal body weight in *bbb/bbb* mice is in contrast to the finding of Wu et al., (290) where *bbb/bbb* mice exhibited significantly increased body weight compared to controls from the age of 5 weeks onward. This previous study was conducted in the same animal house as the current study, using the same animal colony. The difference in findings may be due to changes in the mouse chow diet in the intervening time between the two studies, or due to changes in the animal environment such as the onset of using individually ventilated cages (IVCs) rather than open top cages. Nonetheless, significant, albeit subtle, differences in

mammary gland adipose tissue were observed, which suggests that the *bbb/bbb* mutation did indeed result in increased food intake consistent with the anticipated phenotype. Mice carrying the *bbb/bbb* mutation exhibited increased mammary gland adipocyte size suggesting increased lipid deposition in this fat depot. This may not have been a large enough increase to be reflected in a statistical difference in mammary gland weight, particularly as this tissue can vary in weight between animals of the same genotype. Interestingly, no change was observed in the expansion of visceral adipose tissue. The differential degree of adipose tissue deposition between the two adipose depots in *bbb/bbb* mice highlight the differences in the function of these depots. The finding of increased adipocyte size in the mammary gland demonstrates a significant, yet subtle increased adiposity in *bbb/bbb* mice during puberty.

3.3.2 Effect of increased mammary gland adiposity on mammary gland development during puberty

Mammary gland development is a well-regulated process. It is largely dependent on endocrine regulators and the paracrine interactions between epithelial stromal cells present within the mammary gland (301). Whilst essential for a functional mammary gland, the precise role of adipose tissue in normal development of the mammary gland during puberty is not well understood. From the perspective of investigating the impact of increased adiposity on mammary gland development during puberty, female *bbb/bbb* mice offer an ideal model; these mice exhibit increased mammary gland adiposity while other adipose tissue depots appear to be minimally affected.

Whole mount analysis of the mammary glands demonstrated that controls and *bbb/bbb* mice have similar ductal development including ductal invasion and branching. Strikingly, *bbb/bbb* mice exhibited increased number of TEBs and increased number of proliferating epithelial cells in TEBs, suggesting that mammary gland adiposity promotes TEB development. The underlying mechanisms of how mammary gland adipose tissue regulates the development of terminal end buds is still not clear but may involve interactions between mammary gland adipose tissue, epithelium, and macrophages.

TEBs are highly proliferative structures that drive mammary gland development during puberty. This involves continuous interaction of TEBs with the stroma within the gland. Our results are consistent with a previous study that demonstrated reduced pace of mammary gland development in mice with adipocyte-ablated mammary glands (301). These mice exhibited reduced branching points, decreased number of TEBs, and decreased proliferation and

apoptosis of epithelial cells. This suggests that adipose tissue deposition in the mammary gland during puberty is a critical factor in driving mammary gland development.

The mammary gland is comprised of fibroglandular and adipose tissue, which affect mammary gland density; the more fibroglandular tissue there is in relation to adipose tissue the higher the density (302). Furthermore, high density mammary tissue is characterised by increased deposition of collagen, compared to low density breast tissue (215). We investigated the impact of increased of mammary gland adiposity on mammary gland density. No significant difference was observed in percent fibroglandular density or abundance of collagen around mammary ducts between controls and *bbb/bbb* mice. It is interesting to note that increased mammary gland adiposity and increased epithelial cell proliferation in TEBs was not associated with altered mammary gland density during puberty. At 6 weeks, the mammary gland is still undergoing development, and assessment of density may not be an appropriate measure of mammary gland function at this stage.

Macrophages are capable of multiple functions including tissue homeostasis and immunity, and also have roles in promoting mammary gland development during puberty, ovarian cycling and pregnancy/lactation. Immunohistochemical analysis using F4/80-antibody demonstrated recruitment of macrophages to the stroma along the neck of TEBs during puberty in mice (227, 303, 304). We investigated the impact of increased mammary gland adiposity on recruitment of macrophages around TEBs using F4/80-antibody immunostaining. Strikingly, increased abundance of macrophages in the stroma around TEBs was observed in *bbb/bbb* mice, which might be responsible for the increased number and proliferation of TEBs we observed. This finding is consistent with a previous study that showed that mice lacking CSF1, a cytokine essential to the differentiation and survival of macrophages, exhibited reduced recruitment of macrophages to the stroma around TEBs resulting in impaired TEB formation and reduced proliferation of TEB epithelial cells (227).

The consequences of the adipose tissue expansion include influx of fatty acids, increased leptin secretion, hypoxia, and adipocyte cell death (305). These consequences are all possible factors that can initiate macrophage recruitment. Immunohistochemical analysis of abundance of macrophages in the mammary gland adipose tissue using F4/80-antibody revealed increased abundance of macrophages in mammary gland adipose tissue of *bbb/bbb* mice. In contrast, no significant difference was observed in the infiltration of macrophages in the visceral adipose tissue. Differences in the infiltration of macrophages in mammary gland adipose tissue and visceral adipose tissue may be attributed to differences in the degree of adiposity and function of these depots.

Increased adipose tissue deposition in obesity is strongly associated with chronic low-grade inflammation and is characterised with infiltration of immune cells that produce and secrete pro-inflammatory cytokines and chemokines (306, 307). In obese adipose tissue, macrophages are located around dead adipocytes and form so-called crown-like structures, which is a proinflammatory feature (308). We did not observe crown-like structures in the mammary gland adipose tissue in either control or *bbb/bbb* mice (data not shown). In addition, the profile of key inflammatory cytokines associated with obesity was not altered in *bbb/bbb* mice. Therefore, we suggest that increased abundance of macrophages in the mammary gland adipose tissue of pubertal *bbb/bbb* mice is not an indicator of an obesity phenotype, but instead it is part of normal pubertal mammary gland development. The lack of an obesity-associated mammary gland microenvironment in this model is discussed further in the following section.

3.3.3 Effect of increased mammary gland adiposity on the mammary gland microenvironment

We investigated the impact of increased mammary gland adiposity on the abundance of adipokines and proinflammatory cytokines in the mammary glands using Luminex assay. Increased adipose tissue deposition is known to increase the secretion of adipokines and cytokines by the stromal cells. No change in the abundance of leptin is consistent with the observation of no increase in the body weight of *bbb/bbb* mice compared to controls. Cytokine concentrations of IL6, CCL2 and TNFA also showed no significant difference.

Plasminogen activator inhibitor (PAI1) is a physiological inhibitor of plasminogen activators. It is synthesised in the adipose tissue. Plasma concentration of PAI1 is elevated in obesity (309). Macrophages infiltrating the adipose tissue are also shown to express PAI1 (310, 311). It has been proposed that production of PAI1 by macrophages and adipocytes is an underlying biological factor that contributes to the strong association between high plasma concentration of PAI1 and visceral obesity (312). In our study, we observed that *bbb/bbb* mice show no sign of significant increase in the levels of PAI1.

We observed that protein abundance of resistin was significantly reduced in the mammary glands of *bbb/bbb* mice compared to controls. Resistin is an adipokine, secreted by adipose tissue, and is suggested to be a link between obesity and insulin resistance (313). Elevation of serum levels of resistin are reported in obese humans as well as in diet-induced obese mice (314, 315). Decreased levels of resistin in the mammary glands of *bbb/bbb* mice, suggests that mammary gland adiposity in these mice is not an obesity state. However, the exact role of resistin in mammary gland development during puberty is still not elucidated.

In addition to investigation of protein abundance of key adipokines and cytokines in the mammary gland, we investigated expression of mRNA encoding leptin, adiponectin, IL4, IL6, TNFA, TGFB1, CCL2, CSF1, IGF1, STAT3, and COX2. Our findings demonstrated a high degree of variability in the expression of these genes and none of them showed a significant difference between control and *bbb/bbb* mice. This high degree of variability could be attributed to varying degree of adiposity in each mouse during puberty. Similarly, we investigated the expression of these genes in visceral adipose tissue by RT-PCR analysis. Consistent with no change in the adiposity of visceral adipose tissue, we observed no significant difference in the expression of these genes.

The above analysed adipokines and proinflammatory cytokines are all related to the state of obesity or inflammatory insults such as infection or necrosis. The *bbb/bbb* mutation led to a subtle increase in mammary gland adiposity which is not an inflammatory or obese state. Thus, it is not surprising that there was a similar abundance of these adipokines and cytokines in the mammary glands compared to controls.

3.3.4 Limitations and future directions

The role of the *Alms1* gene in mammary gland development has not been previously investigated, and it is possible that the *Alms1* gene, or the ENU-induced *bbb* mutation, might impact the mammary gland independent of the finding of increased mammary gland adiposity. Transplantation of mammary gland epithelium between control and *bbb/bbb* mice could reveal whether the epithelium is directly affected by the *bbb* mutation. In addition, other *Alms1* null mutant models exist in the literature (316, 317) and could provide alternative models to investigate the relative roles of *Alms1*, the ENU-induced *bbb* mutation, and mammary adiposity on the pubertal mammary gland phenotype reported here.

Further studies are required to investigate the underlying mechanisms that link mammary gland adiposity to altered mammary gland development. Interactions between adipose tissue and epithelium are crucial for the normal mammary gland development during puberty. For example, absence of mammary gland adipose tissue in pubertal mice resulted in fewer branching points and TEBs (301). Future studies may investigate interactions between epithelium and mammary gland adipose tissue, generating further understanding on possible factors responsible for increased TEB development and infiltration of macrophages in *bbb/bbb* mice. In addition, we did not investigate the concentration of circulating ovarian hormones estradiol and progesterone which are crucial for pubertal mammary gland development. Future studies may investigate ovarian hormones in these mice and their impact on mammary gland

development. High degree of variability in the gene expression of adipokines and proinflammatory cytokines reported in our study possibly highlight the contribution of both epithelium and stroma to affect their expression in the mammary gland. Future studies might unravel the cellular source of each cytokine to better understand the impact of increased adiposity on the mammary gland microenvironment during puberty.

3.4 Conclusion

Increased pubertal mammary gland adiposity in the *Alms1 bbb/bbb* mouse model is associated with increased number and proliferative activity of terminal end buds as well as increased abundance of macrophages in the mammary gland. It is important to note that the increased mammary gland adiposity in this mouse model is not an inflammatory or obesity state, rather it appears to be a subtle expansion in the size of healthy adipocytes. In the following chapter, we use this mouse model to explore how pubertal adiposity affects mammary gland development and density in adulthood.

CHAPTER FOUR

Impact of increased pubertal adiposity on mammary gland development and density in adulthood

4.1 Introduction

Epidemiological studies have consistently demonstrated an inverse association between pubertal adiposity and mammographic density in adult women when adjusted for adult BMI (13, 14, 16-19). High BMI-percentile (75th BMI-percentile) at age 18 is associated with a 45% decrease in adult mammographic density, compared to median BMI-percentile, adjusted for adult BMI and timing of menarche (88). Higher BMI percentile in adolescence is also associated with reduced risk of breast cancer (71, 89, 90). These studies suggest that increased pubertal body adiposity is associated with reduced mammographic density and reduced breast cancer risk in adult women. However, causal relationships between healthy pubertal weight gain and adult breast health are yet to be investigated.

Previous mouse experiments have shown that pubertal C57BL/6 mice fed a high-fat diet exhibit increased body weight and adiposity, and reduced epithelial cell proliferation and stunted mammary duct elongation (318). However, healthy weight gain during puberty is part of normal physiological development in teenage girls, and mice fed a high fat diet is not an appropriate approach to model this. In Chapter three, studies using the *Alms1 bbb/bbb* mouse model, where mice gain weight eating normal mouse chow, suggested that increased adiposity promoted mammary gland development during puberty in mice. The question now arises whether the subtle developmental changes we observed during puberty affect mammary gland density in adulthood. To address this, we investigated the impact of increased pubertal adiposity on mammary gland development and density during adulthood in the *Alms1 bbb/bbb* mouse model.

The experimental design for this study is illustrated in Figure 4.1. Controls (*bbb*/+ or +/+) and *bbb/bbb* mice were fed a normal mouse diet ad libitum from weaning age to 7 weeks of age. After 7 weeks (i.e., end of puberty), a group of *bbb/bbb* mice were calorie-matched to controls until 12 weeks, such that the amount of food eaten by *bbb/bbb* mice was the same as that consumed by the controls. These mice will be referred to as 'matched *bbb/bbb* mice'. Due to consuming mouse chow ad libitum until puberty, matched *bbb/bbb* mice will exhibit increased pubertal adiposity, as described in Chapter 3, but then they will not increasingly gain adipose tissue as adults because they are calorie-matched with control mice. Another cohort of mice was used in this study. They are *bbb/bbb* mice that ate ad libitum throughout the study. These mice will be referred to as 'ad lib *bbb/bbb* mice'. This cohort allowed us to specifically isolate the effect of pubertal adiposity and compare it to the effect of adult obesity. Ad lib *bbb/bbb* mice exhibited increased adiposity during puberty and became progressively overweight in adulthood.

Based on the known epidemiological association between pubertal adiposity and adult mammographic density, we hypothesised that matched *bbb/bbb* mice would exhibit reduced mammary fibroglandular density compared to controls. As ad lib *bbb/bbb* mice would also exhibit an abundance of adipose tissue, they are also anticipated to exhibit reduced fibroglandular density compared to controls. However, we hypothesised that ad lib *bbb/bbb* mice would also exhibit an obesity-associated state of chronic inflammation within the mammary gland.

Mammary glands and visceral adipose tissue were dissected from controls, matched *bbb/bbb*, and ad lib *bbb/bbb* mice at 12 weeks at the estrus phase of ovarian cycle. Mammary gland adipose tissue and visceral adipose tissue were characterised for degree of adiposity, and for infiltration of macrophages. Mammary gland density in terms of percent fibroglandular density and collagen deposition, was quantified. To investigate the impact of perturbation of mammary gland adiposity on the mammary gland microenvironment, we assessed the protein concentration and gene expression of adipokines and proinflammatory cytokines in the mammary glands. Results from this chapter suggest that increased pubertal mammary adiposity alters mammary gland density in adulthood and alters expression of adipokines and proinflammatory cytokines within the mammary gland microenvironment.

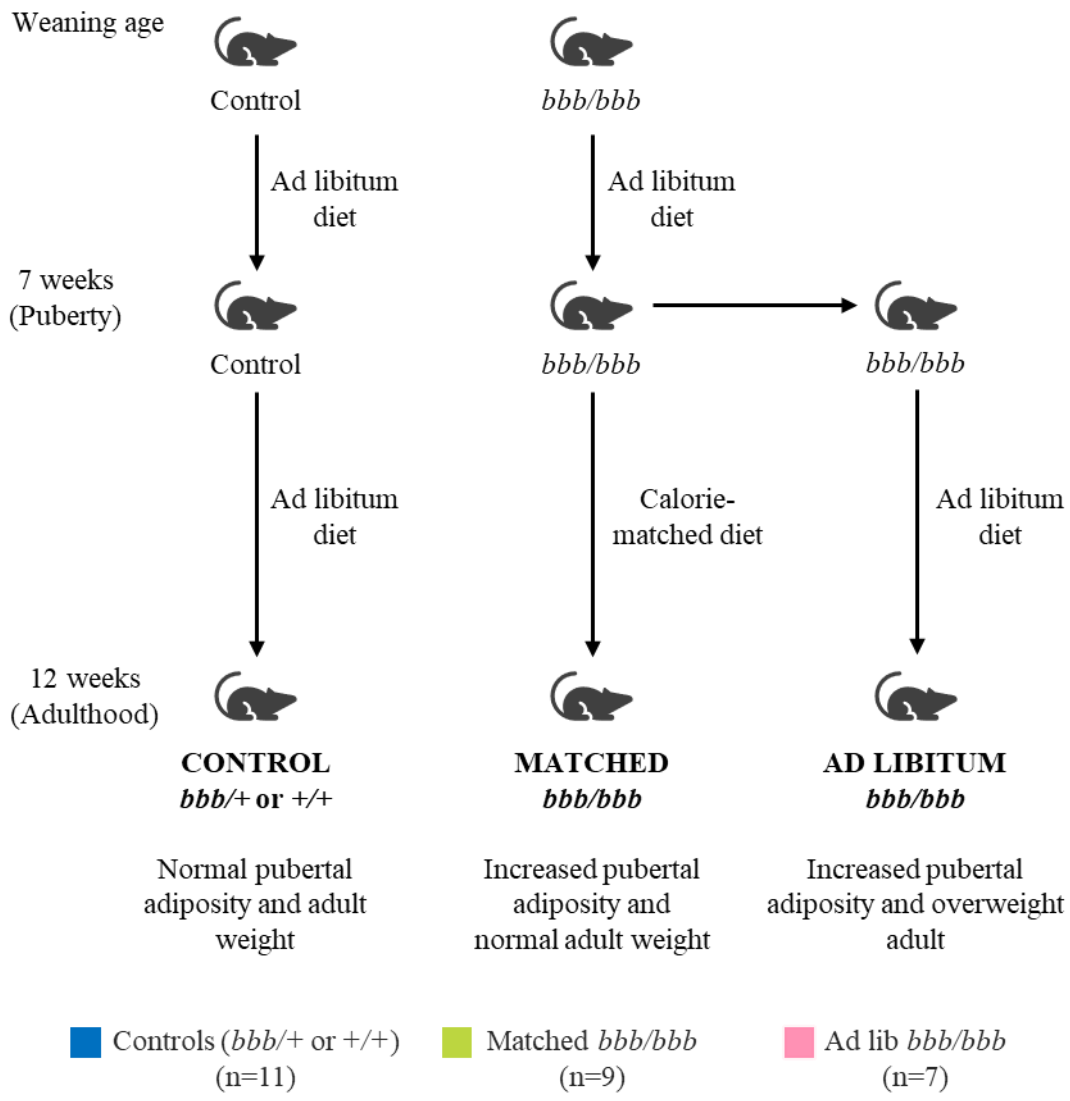

Figure 4.1. Illustration of experimental design to study the impact of pubertal adiposity on mammary gland development and density in adulthood. Controls and *bbb/bbb* mice were fed normal mouse diet ad libitum from weaning age until 7 weeks. After 7 weeks (i.e., end of puberty), a group of *bbb/bbb* mice were calorie-matched to controls until 12 weeks (adulthood), such that the amount of food eaten by *bbb/bbb* mice is same as that eaten by the controls. These mice will be referred to as 'matched *bbb/bbb* mice'. Another cohort of mice in this study are *bbb/bbb* mice that ate ad libitum from 4 weeks to 12 weeks. These mice will be referred to as 'ad lib *bbb/bbb* mice'. Colour code: Blue – Controls (*bbb/+* or +/+) (n=11), Green - matched *bbb/bbb* (n=9), Pink - ad lib *bbb/bbb* (n=7).

4.2 Results

4.2.1 Selection of 7 weeks as the end of pubertal mammary gland growth period

In Chapter 3, it was shown that *bbb/bbb* and control mice exhibited similar ductal elongation but different terminal end bud number and proliferation during puberty at the age of 6 weeks. In order to study the impact of pubertal adiposity on adult mammary fibroglandular density, we needed to set an age where pubertal mammary gland development was complete, so that we could at this point match food intake in the *bbb/bbb* mice such that they would not gain further excess weight and instead exhibit growth more similar to that of control mice. A small pilot study was conducted to confirm whether the age of 7 weeks was an appropriate developmental stage to distinguish pubertal mammary gland development from adult mammary gland function. Control and *bbb/bbb* mice (n=4 per group) were euthanised and mammary glands were dissected at age 7 weeks. Mammary gland whole-mounts were carmine alum-stained and observed. Puberty initiates TEB development and branching morphogenesis, and by the end of pubertal development, a ductal tree is established that fully invades the mammary adipose tissue (206). Mammary gland ducts had fully extended through the mammary gland fat pad by 7 weeks of age (data not shown) suggesting this is an appropriate age at which to switch mice in the matched *bbb/bbb* group from an ad libitum diet to a calorie-matched diet.

4.2.2 Estrous cycling in control and *bbb/bbb* mice during adulthood

The adult mammary gland is under hormonal regulation and can undergo developmental changes across the estrous cycle as the concentration of circulating estradiol and progesterone fluctuate (319). Before assessing adiposity and mammary gland structure and function in these mice, estrous cycles in adult mice were observed by daily vaginal smears between the ages of 7 and 12 weeks. No significant difference was observed in the estrous cycle length between any of the groups (Figure 4.2). The same number of mice were allocated to the matched and ad lib *bbb/bbb* mouse cohorts (n=9). However, 2 mice from the ad lib *bbb/bbb* cohort exhibited very high deposition of adipose tissue in the mammary gland such that visualisation of the mammary glands in whole-mounts was obscured and could not be assessed. Furthermore, extraction of mammary RNA was more difficult due to high lipid content, requiring more rounds of centrifugation to remove the lipid, and there were concerns that the results for these mice would not be comparable to other mice in the cohort. For these reasons, these mice were excluded from the ad lib *bbb/bbb* cohort.

4.2.3 Female *bbb/bbb* mice exhibit increased adiposity during adulthood

To investigate the impact of increased adiposity during puberty on adult mammary gland development, controls, matched *bbb/bbb*, and ad lib *bbb/bbb* female mice were euthanised at 12 weeks of age at the estrus stage of the estrous cycle. After recording body weight, mammary glands and visceral adipose tissue were dissected from these mice. At 12 weeks, due to the calorie-matched diet, matched *bbb/bbb* mice showed similar body weight compared to the controls (Figure 4.3.A). Ad lib *bbb/bbb* mice exhibited a significant increase in body weight, compared to controls ($p<0.001$) and matched *bbb/bbb* mice ($p<0.001$) (Figure 4.3.A).

Further, there was a significant increase in the weight of visceral adipose tissue in ad lib *bbb/bbb* mice, compared to controls ($p<0.001$) and matched *bbb/bbb* mice ($p<0.001$) (Figure 4.3.B). Interestingly, though matched *bbb/bbb* mice had similar body weight as controls, visceral adipose tissue was significantly increased, compared to controls ($p<0.001$) (Figure 4.3.B).

The weight of the total fourth pair mammary glands was significantly increased in ad lib *bbb/bbb* mice, in comparison to controls ($p<0.001$) and matched *bbb/bbb* mice ($p<0.001$) (Figure 4.3.C). Compared to controls, matched *bbb/bbb* mice had significantly increased total fourth pair mammary glands weight ($p=0.038$) (Figure 4.3.C).

To determine whether controls, matched *bbb/bbb*, and ad lib *bbb/bbb* mice exhibit differences in adiposity, we characterised hematoxylin-eosin stained sections of mammary gland and visceral adipose tissue. Ad lib *bbb/bbb* mice exhibited a significant increase in adipocyte size in the mammary gland adipose tissue, in comparison to controls ($p<0.001$) and matched *bbb/bbb* mice ($p=0.008$) (Figure 4.4.A-D). Matched *bbb/bbb* mice also exhibited significantly increased mammary adipocyte size compared to controls ($p<0.01$) (Figure 4.4.A-D).

Consistent with the above result, we observed a significant decrease in the number of adipocytes per area of mammary gland adipose tissue in ad lib *bbb/bbb* mice ($p<0.001$) and matched *bbb/bbb* mice ($p<0.001$), compared to controls (Figure 4.4.E).

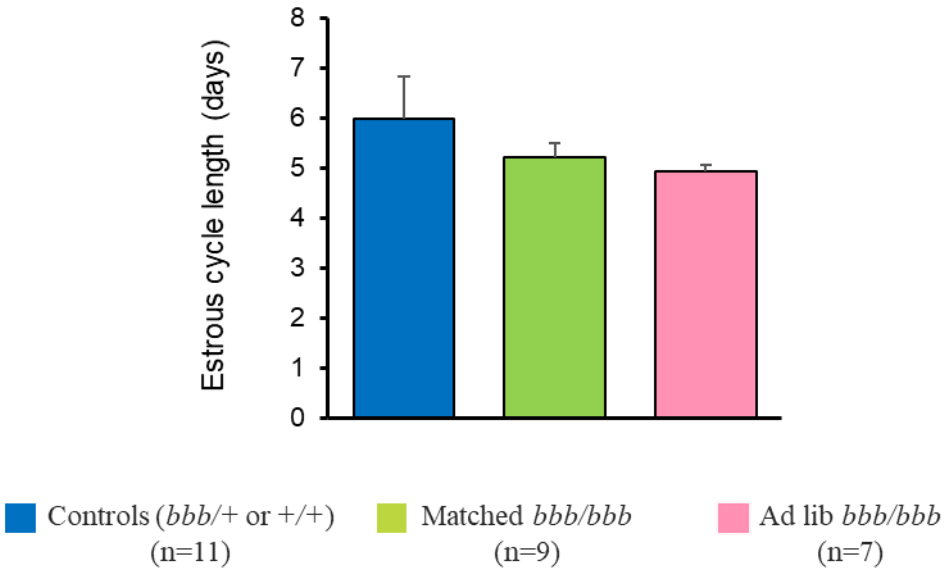

Figure 4.2. Estrous cycle length in female controls, matched *bbb/bbb*, and ad lib *bbb/bbb* mice at adulthood. Estrous cycles in adult mice were observed by daily vaginal smears between the ages of 7 and 12 weeks. Colour code – Blue: Controls (*bbb*/+ or +/+) (n=11), Green: matched *bbb/bbb* (n=9), and Pink: ad lib *bbb/bbb* (n=7). Data are presented as mean+SEM and analysed using linear regression model with statistical significance at $p<0.05$.

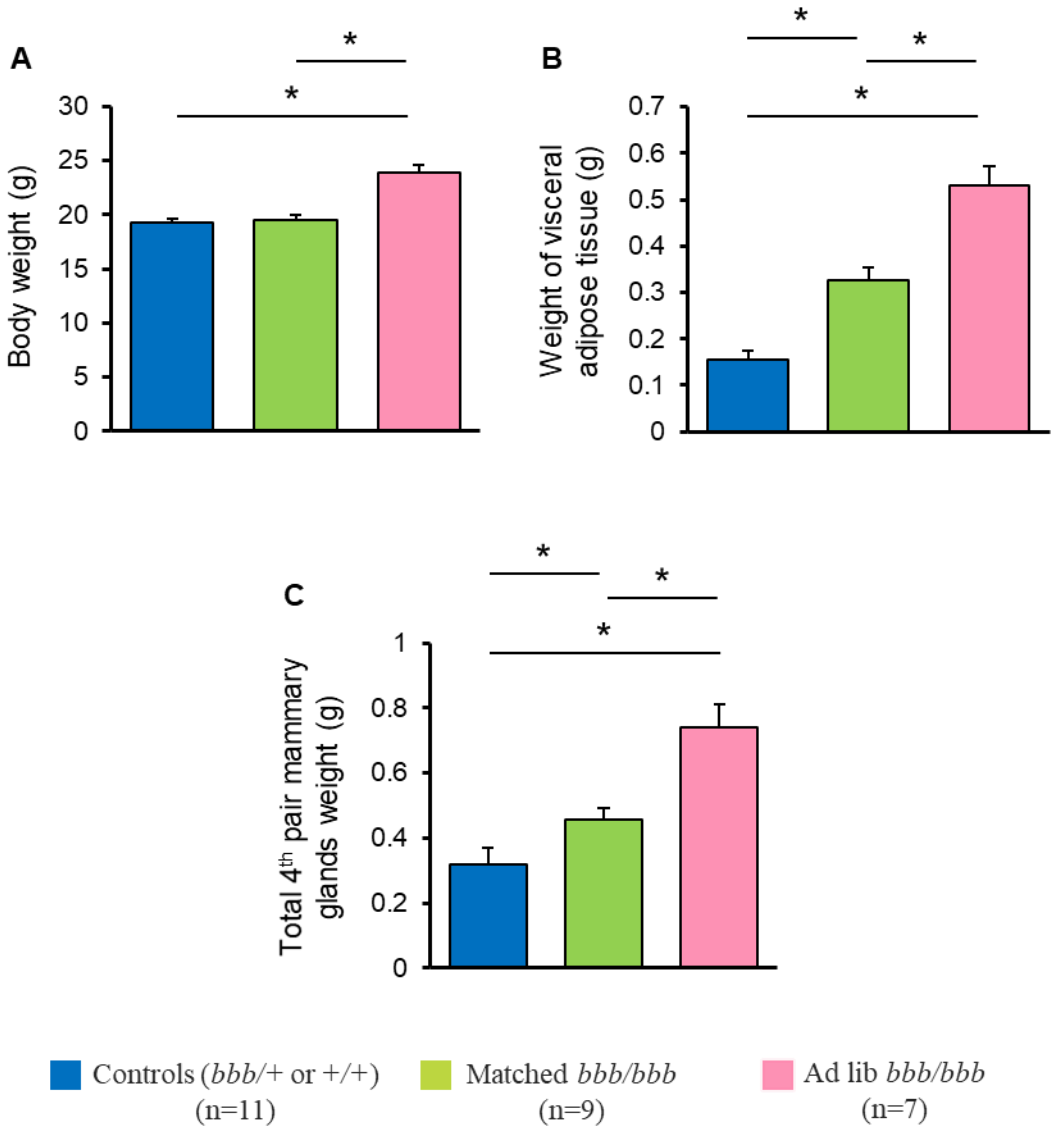

Figure 4.3. Relative weights of female controls, matched *bbb/bbb*, and ad lib *bbb/bbb* mice at adulthood. At 12 weeks of age, mice were weighed, and fourth pair mammary glands and visceral adipose tissue were dissected at the estrus phase of the ovarian cycle. (A) Total body weight. (B) Weight of visceral adipose tissue. (C) Total fourth pair mammary glands weight. Total fourth pair mammary glands weight is the combined weight of left and right fourth mammary glands. Colour code – Blue: Controls (*bbb/+* or +/+) (n=11), Green: matched *bbb/bbb* (n=9), and Pink: ad lib *bbb/bbb* (n=7). Data are presented as mean+SEM and analysed using linear regression model. * indicates statistical significance at $p<0.05$.

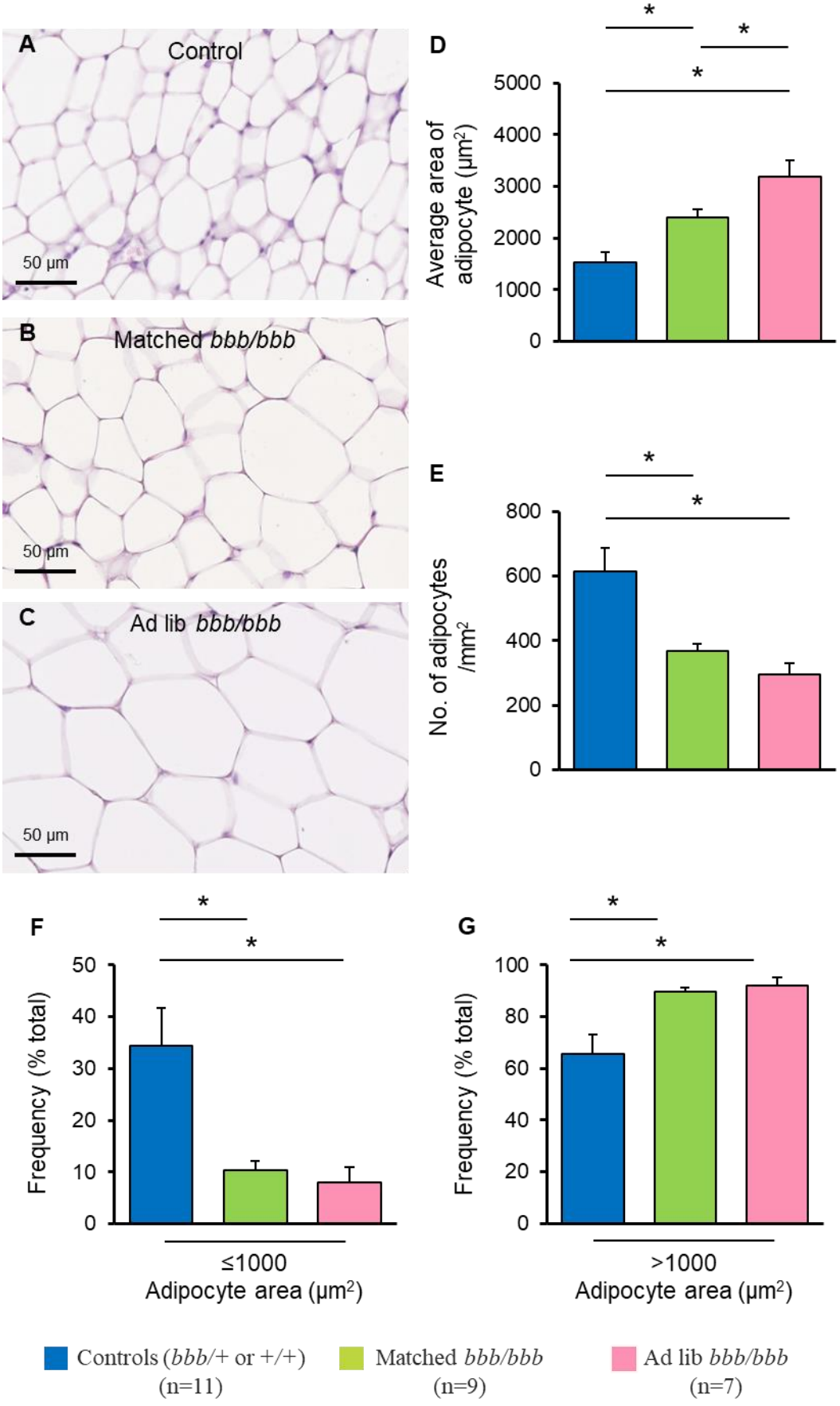
A
Control
50 µm
B
Matched bbb/bbb
50 µm
C
Ad lib bbb/bbb
50 µm
D
Average area of adipocyte (µm²)
5000
4000
3000
2000
1000
0
*
*
*
E
No. of adipocytes /mm²
800
600
400
200
0
*
*
F
Frequency (% total)
50
40
30
20
10
0
*
*
≤1000
Adipocyte area (µm²)
G
Frequency (% total)
100
80
60
40
20
0
*
*
>1000
Adipocyte area (µm²)
Controls (bbb/+ or +/+)
(n=11)
Matched bbb/bbb
(n=9)
Ad lib bbb/bbb
(n=7)

Figure 4.4. Mammary gland adiposity in controls, matched *bbb/bbb*, and ad lib *bbb/bbb* mice at adulthood. Representative images of hematoxylin-eosin stained mammary gland adipose tissue of fourth pair mammary glands of (A) controls, (B) matched *bbb/bbb*, and (C) ad lib *bbb/bbb* mice. Scale bars: 50 µm. (D) Average adipocyte area. (E) Number of adipocytes per area. (F) Percent frequency of smaller adipocytes (≤1000 μm^2). (G) Frequency of larger adipocytes (>1000 μm^2). Colour code – Blue: Controls (*bbb/+* or +/+) (n=11), Green: matched *bbb/bbb* (n=9), and Pink: ad lib *bbb/bbb* (n=7). Data are presented as mean+SEM and analysed using linear regression model. * indicates statistical significance at $p<0.05$.

Further, percent frequency of smaller adipocytes (≤1000 μm^2) versus larger adipocytes (>1000 μm^2) was calculated in mammary gland adipose tissue. The mammary gland adipose tissue of controls was predominantly populated with smaller adipocytes compared to matched *bbb/bbb* ($p<0.01$) and ad lib *bbb/bbb* ($p<0.001$) mice (Figure 4.4.F). On the other hand, the mammary gland adipose tissue of matched *bbb/bbb* ($p<0.01$) and ad lib *bbb/bbb* ($p<0.001$) mice was predominantly occupied by larger adipocytes compared to controls (Figure 4.4.G). These results demonstrate that matched *bbb/bbb* and ad lib *bbb/bbb* mice exhibit increased mammary gland adiposity during adulthood.

Similar to mammary adipose tissue, ad lib *bbb/bbb* mice exhibited a significant increase in adipocyte size in the visceral adipose tissue, in comparison to controls ($p<0.001$) and matched *bbb/bbb* mice ($p<0.001$) (Figure 4.5.A-D). Matched *bbb/bbb* mice also exhibited significantly increased visceral adipocyte size compared to controls ($p<0.001$) (Figure 4.5.A-D).

We found a significant decrease in the number of adipocytes per area of visceral adipose tissue in ad lib *bbb/bbb* mice ($p<0.001$) and matched *bbb/bbb* mice ($p<0.001$), compared to controls (Figure 4.5.E). There was also a significant difference in the number of adipocytes per area between matched *bbb/bbb* mice and ad lib *bbb/bbb* mice ($p=0.035$) (Figure 4.5.E).

Further, percent frequency of smaller adipocytes (≤1000 μm^2) versus larger adipocytes (>1000 μm^2) was estimated in the visceral adipose tissue. Similar to mammary gland adipose tissue, visceral adipose tissue of controls was predominantly populated with smaller adipocytes compared to matched *bbb/bbb* ($p<0.001$) and ad lib *bbb/bbb* ($p<0.001$) mice (Figure 4.5.F). On the other hand, the visceral adipose tissue of matched *bbb/bbb* ($p<0.001$) and ad lib *bbb/bbb* ($p<0.001$) mice was predominantly occupied by larger adipocytes compared to controls (Figure 4.5.G). These results demonstrate that matched *bbb/bbb* and ad lib *bbb/bbb* mice exhibited increased deposition of visceral adipose tissue during adulthood.

4.2.4 Increased development of mammary gland ducts in adult *bbb/bbb* mice

To investigate the impact of increased pubertal mammary adiposity on adult mammary gland development, mammary gland whole-mounts were stained with carmine alum and analysed (Figure 4.6.A-C). Ductal invasion area was significantly increased in matched *bbb/bbb* ($p<0.001$) and ad lib *bbb/bbb* ($p<0.001$) mice, compared to controls (Figure 4.6.D). Ad lib *bbb/bbb* mice exhibited significantly greater ductal invasion area than matched *bbb/bbb* ($p=0.009$) (Figure 4.6.D).

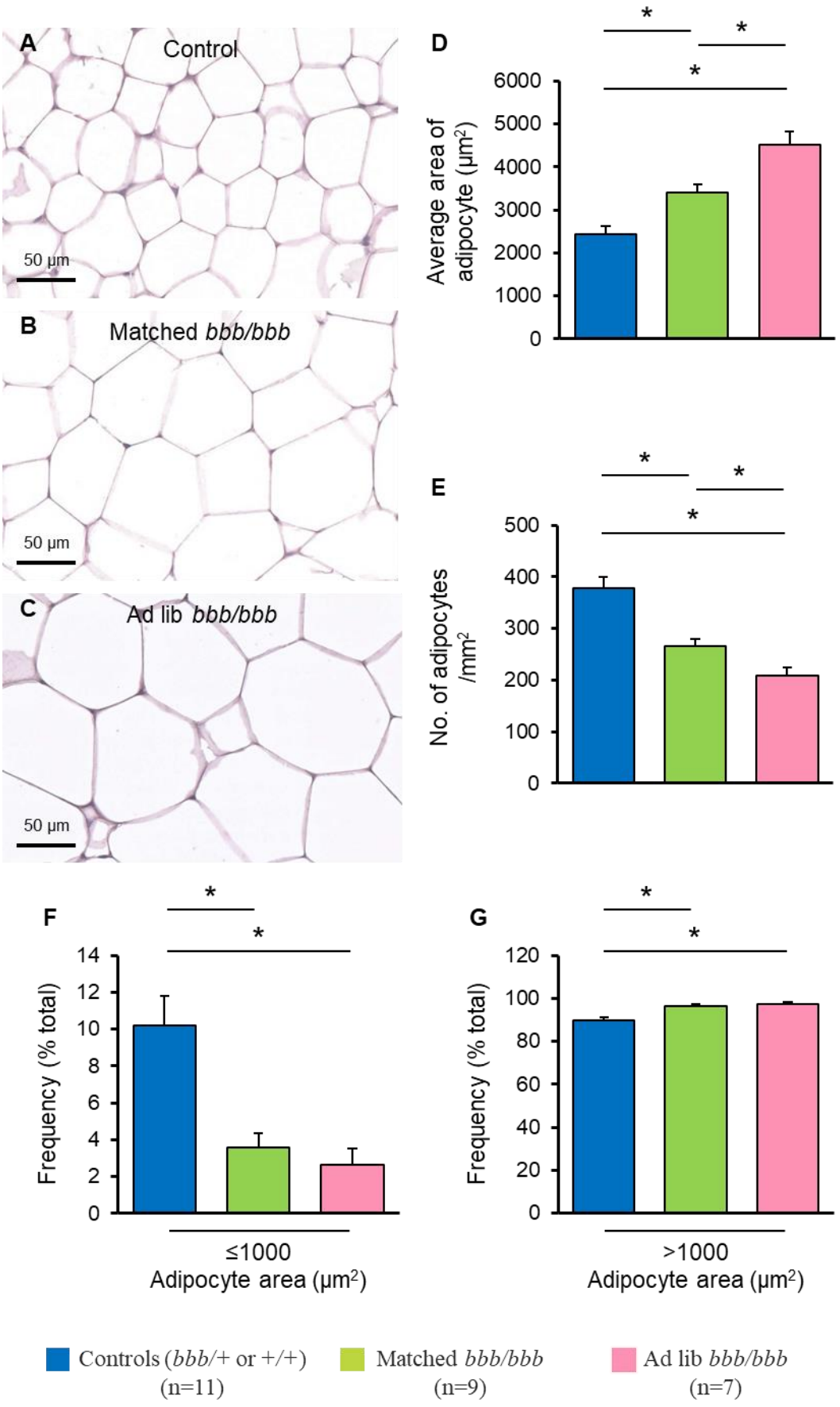
A
Control
50 µm
B
Matched bbb/bbb
50 µm
C
Ad lib bbb/bbb
50 µm
D
Average area of adipocyte (µm²)
6000
5000
4000
3000
2000
1000
0
*
*
*
E
No. of adipocytes /mm²
500
400
300
200
100
0
*
*
*
F
Frequency (% total)
14
12
10
8
6
4
2
0
*
*
≤1000
Adipocyte area (µm²)
G
Frequency (% total)
120
100
80
60
40
20
0
*
*
>1000
Adipocyte area (µm²)
Controls (bbb/+ or +/+)
(n=11)
Matched bbb/bbb
(n=9)
Ad lib bbb/bbb
(n=7)

Figure 4.5. Deposition of visceral adipose tissue in controls, matched *bbb/bbb*, and ad lib *bbb/bbb* mice at adulthood. Representative images of hematoxylin-eosin stained visceral adipose tissue collected from abdominal cavity of (A) controls, (B) matched *bbb/bbb*, and (C) ad lib *bbb/bbb* mice. Scale bars: 50 µm. (D) Average adipocyte area. (E) Number of adipocytes per area. (F) Percent frequency of smaller adipocytes (≤1000 μm^2). (G) Frequency of larger adipocytes (>1000 μm^2). Colour code – Blue: Controls (*bbb/+* or +/+) (n=11), Green: matched *bbb/bbb* (n=9), and Pink: ad lib *bbb/bbb* (n=7). Data are presented as mean+SEM and analysed using linear regression model. * indicates statistical significance at $p<0.05$.

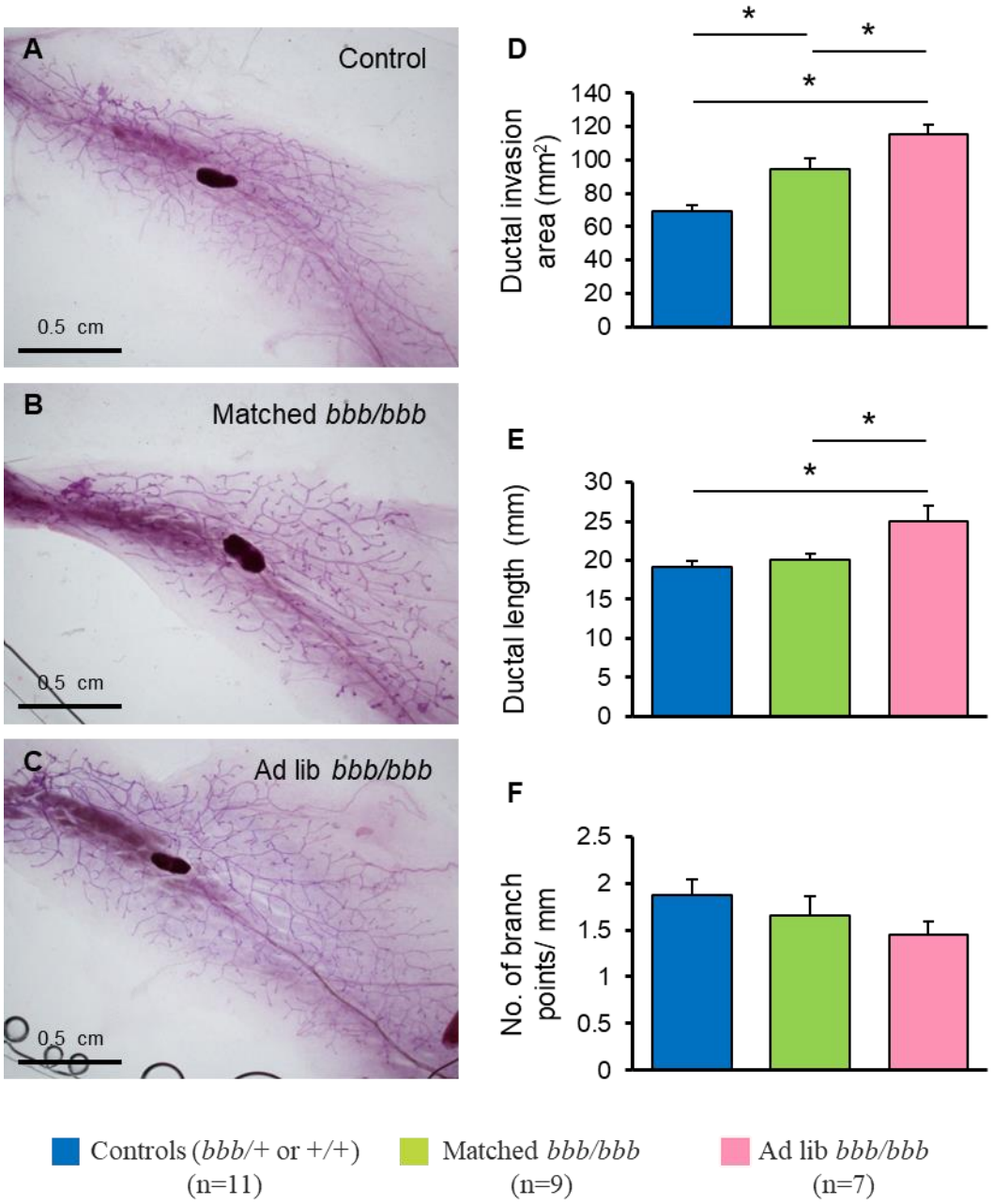

Figure 4.6. Whole-mount analysis of developing mammary glands in controls, matched *bbb/bbb*, and ad lib *bbb/bbb* mice at adulthood. Representative images of alum-carmine stained whole-mounts of fourth pair mammary glands of (A) controls, (B) matched *bbb/bbb*, and (C) ad lib *bbb/bbb* mice. Scale bars: 0.5 cm. (D) Ductal invasion area. It is estimated by calculating the area covered by ducts from the lymph node. (E) Ductal length. It is calculated as the length from the nipple to the furthest duct. (F) Branching. It is calculated as the number of branch points per millimetres. Colour code – Blue: Controls (*bbb/+* or *+/+*) (n=11), Green: matched *bbb/bbb* (n=9), and Pink: ad lib *bbb/bbb* (n=7). Data are presented as mean+SEM and analysed using linear regression model. * indicates statistical significance at $p<0.05$.

Further, we assessed ductal elongation, in terms of ductal length in these mice. The mammary glands of ad lib *bbb/bbb* mice exhibit significantly greater ductal length than matched *bbb/bbb* ($p<0.01$) and controls ($p<0.001$) (Figure 4.6.E). Ductal branching analysis demonstrated that there was no significant difference in the degree of branching in these mice (Figure 4.6.F). These results suggest that increased mammary adiposity promotes ductal development in the mammary glands during adulthood.

4.2.5 Decrease in mammary gland fibroglandular density in adult *bbb/bbb* mice

To investigate the impact of increased pubertal mammary adiposity on mammary gland density, percent fibroglandular density was calculated in haematoxylin-eosin stained mammary glands. Percent fibroglandular density was significantly reduced in matched *bbb/bbb* ($p<0.001$) and ad lib *bbb/bbb* ($p<0.001$), compared to controls (Figure 4.7.A-D). Further, stroma/epithelium ratio was assessed by quantifying the area of stroma occupied around the epithelium. Stroma/epithelium ratio was also significantly decreased in matched *bbb/bbb* ($p=0.003$) and ad lib *bbb/bbb* ($p<0.001$) mice, compared to controls (Figure 4.7.E-H).

Collagen is an important extracellular matrix component that has been shown to be increased in human breast tissue of high mammographic density (215). Masson's trichrome-stained mammary glands were assessed to analyse collagen deposition around mammary ducts. We observed that collagen deposition around the ducts was significantly decreased in matched *bbb/bbb* ($p<0.001$) and ad lib *bbb/bbb* ($p<0.001$) mice, compared to controls (Figure 4.8).

4.2.6 Altered abundance of mammary gland macrophages in adult *bbb/bbb* mice

Macrophages are key immune cells in mammary gland development and function during adulthood (320). To investigate the impact of increased pubertal mammary adiposity on abundance of macrophages around ducts in adult mammary gland, F4/80-antibody immunostaining of the mammary glands was performed. F4/80-positive cells (Figure 4.9.A-C, arrows indicated) represented the F4/80-positive macrophages around ducts of controls, matched *bbb/bbb* and ad lib *bbb/bbb* mice. Negative control showed no F4/80-positive staining (Figure 4.9.D). Abundance of F4/80-positive macrophages around ducts was significantly decreased in matched *bbb/bbb* ($p<0.001$) and ad lib *bbb/bbb* ($p<0.001$) mice, compared to controls (Figure 4.10).

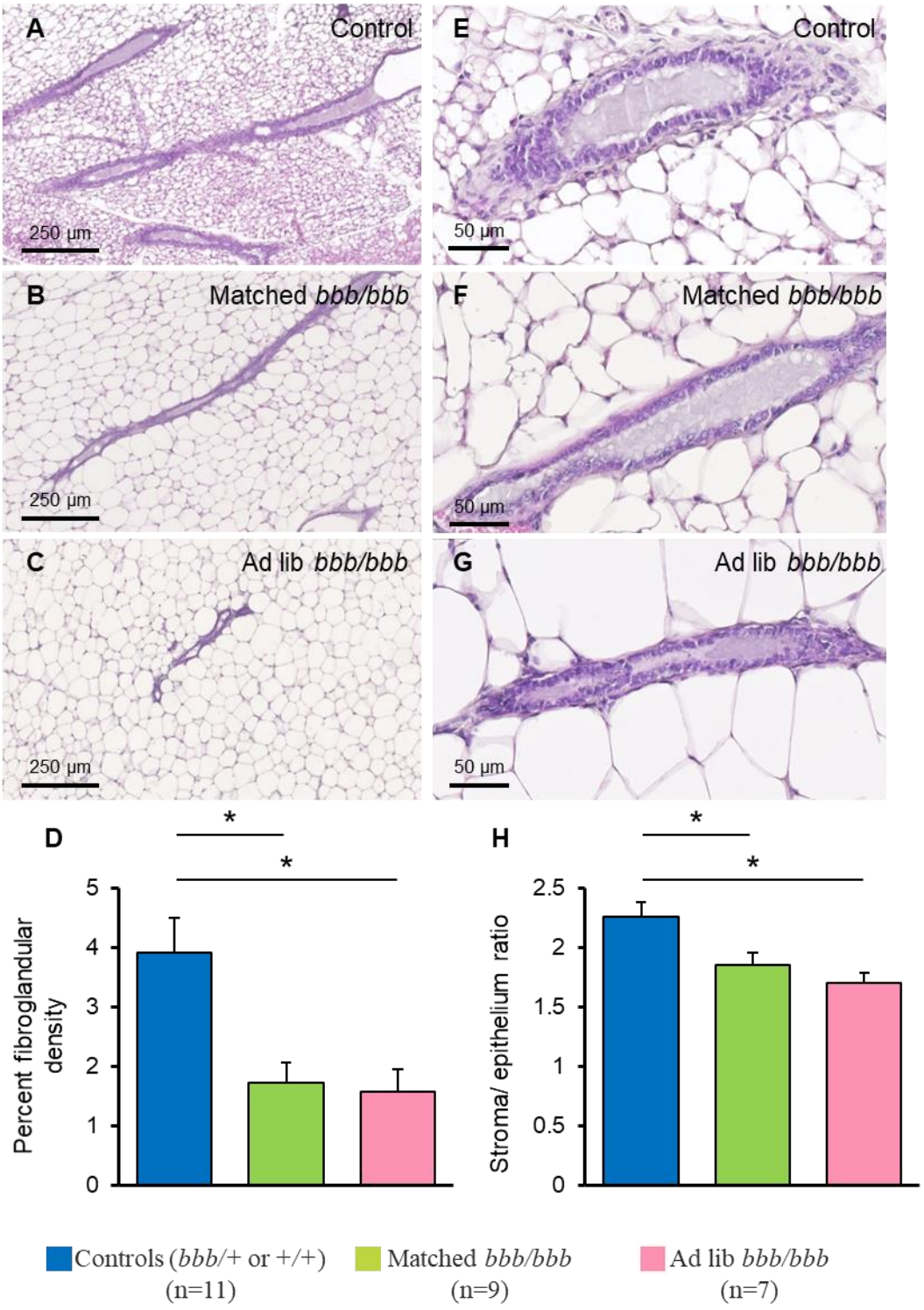
A
Control
250 µm
E
Control
50 µm
B
Matched bbb/bbb
250 µm
F
Matched bbb/bbb
50 µm
C
Ad lib bbb/bbb
250 µm
G
Ad lib bbb/bbb
50 µm
D
Percent fibroglandular density
0
1
2
3
4
5
*
*
H
Stroma/ epithelium ratio
0
0.5
1
1.5
2
2.5
*
*
Controls (bbb/+ or +/+)
(n=11)
Matched bbb/bbb
(n=9)
Ad lib bbb/bbb
(n=7)

Figure 4.7. Percent mammary gland fibroglandular density in controls, matched *bbb/bbb*, and ad lib *bbb/bbb* mice at adulthood. Representative images of hematoxylin-eosin stained fourth pair mammary gland sections of (A) controls, (B) matched *bbb/bbb*, and (C) ad lib *bbb/bbb* mice. Scale bars: 250 µm. (D) Quantification of percent fibroglandular density. It is calculated as the percentage of area occupied by fibroglandular tissue per area in the mammary gland. Representative images of hematoxylin-eosin stained epithelium surrounded by stroma in (E) controls, (F) matched *bbb/bbb* mice, and (G) ad lib *bbb/bbb*. Scale bars: 50 µm. (H) Quantification of stroma/epithelium ratio. It is calculated as the area of stroma occupied around the epithelium in the mammary gland. Colour code – Blue: Controls (*bbb*/+ or +/+) (n=11), Green: matched *bbb/bbb* (n=9), and Pink: ad lib *bbb/bbb* (n=7). Data are presented as mean+SEM and analysed using linear regression model. * indicates statistical significance at $p<0.05$.

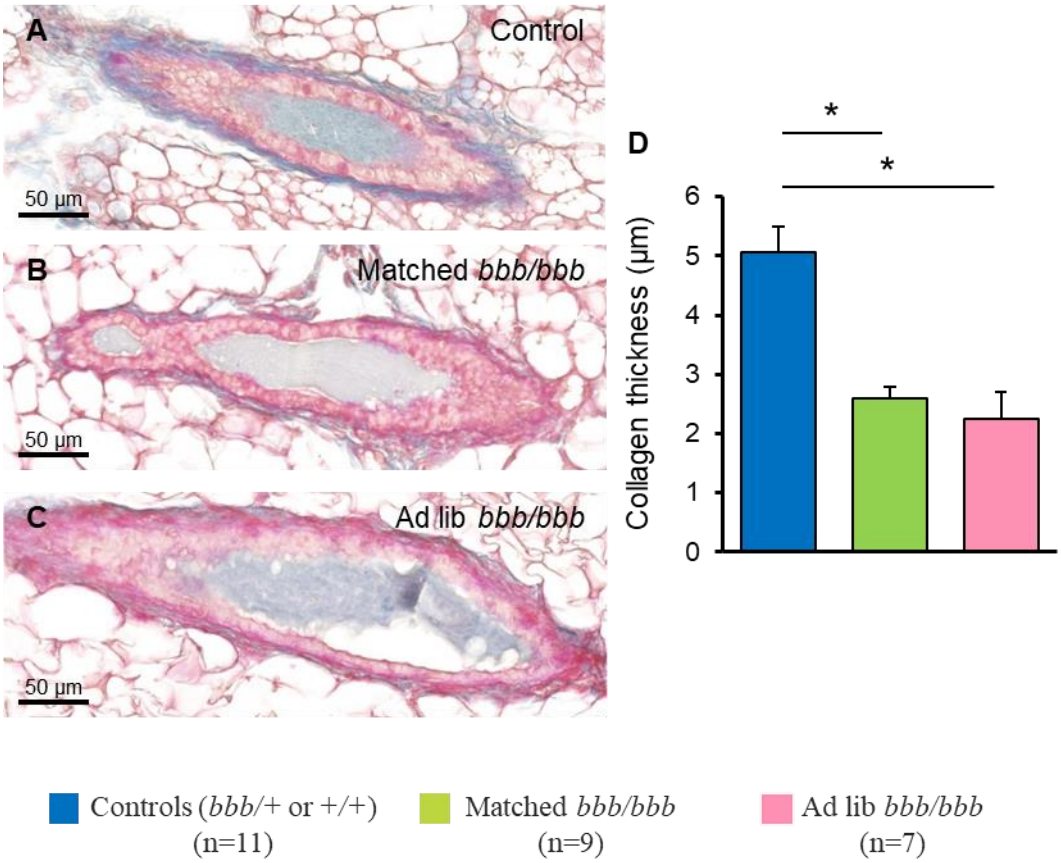

Figure 4.8. Collagen deposition around the mammary gland ducts in controls, matched *bbb/bbb*, and ad lib *bbb/bbb* mice at adulthood. Representative images of Masson's trichrome-stained mammary gland sections of (A) controls, (B) matched *bbb/bbb* mice, and (C) ad lib *bbb/bbb*. Scale bars: 50 µm. (D) Quantification of collagen deposition around ducts. It is measured as the thickness of collagen (blue stain) deposited around the ducts. Colour code – Blue: Controls (*bbb*/+ or +/+) (n=11), Green: matched *bbb/bbb* (n=9), and Pink: ad lib *bbb/bbb* (n=7). Data are presented as mean+SEM and analysed using linear regression model. * indicates statistical significance at $p<0.05$.

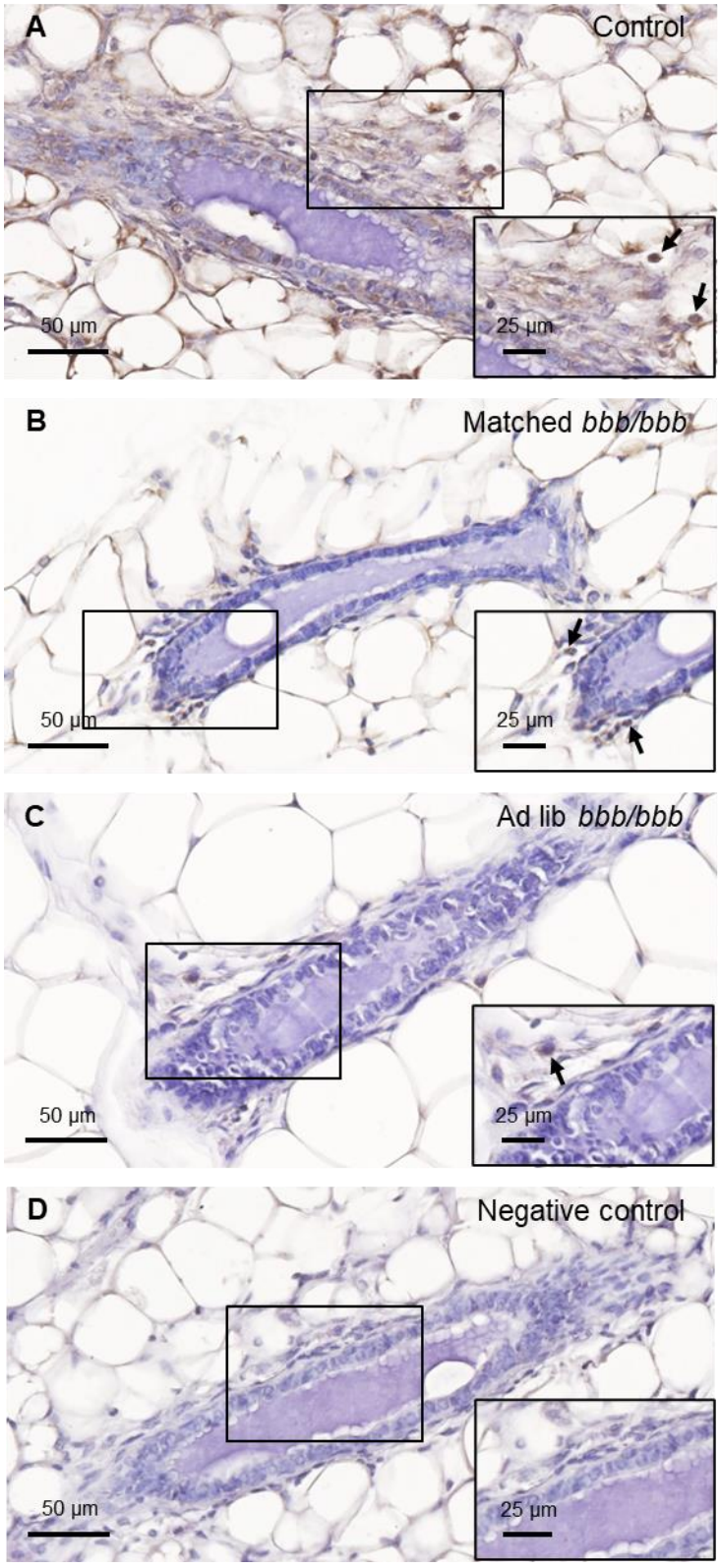

Figure 4.9. F4/80-positive macrophages around mammary gland ducts in controls, matched *bbb/bbb*, and ad lib *bbb/bbb* mice at adulthood. Representative images of F4/80-positive cells (arrows indicated) are the F4/80-positive macrophages in the stroma around mammary ducts in (A) controls, (B) matched *bbb/bbb*, and (C) ad lib *bbb/bbb* mice. (D) Negative control without primary antibody shows no F4/80-positive staining. Images at original magnification of 40X and scale bars: 50 µm, with inset images at original magnification of 80X and scale bars: 25 µm.

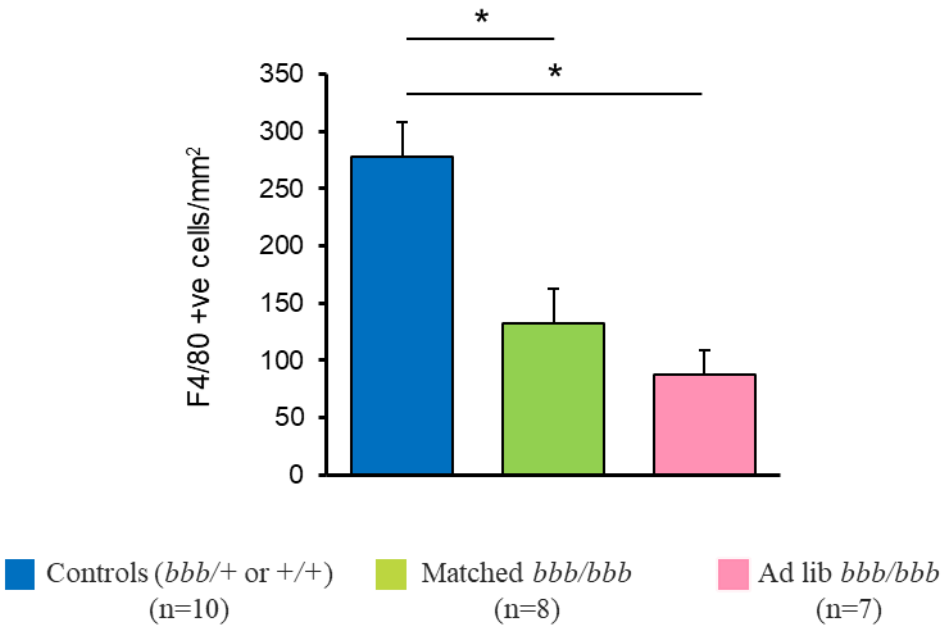

Figure 4.10. Abundance of macrophages around mammary gland ducts in controls, matched *bbb/bbb*, and ad lib *bbb/bbb* mice at adulthood. Quantification of F4/80-positive macrophages per area around mammary ducts of controls, matched *bbb/bbb*, and ad lib *bbb/bbb* female mice. Colour code – Blue: Controls (*bbb/+* or *+/+*) (n=10), Green: matched *bbb/bbb* (n=8), and Pink: ad lib *bbb/bbb* (n=7). Data are presented as mean+SEM and analysed using linear regression model. * indicates statistical significance at $p<0.05$.

To examine the effect of increased adiposity on macrophages residing in the mammary gland adipose tissue, F4/80-antibody immunostaining of the mammary adipose tissue was performed. F4/80-positive cells (Figure 4.11.A-C, arrows indicated) represented the F4/80-positive macrophages in mammary adipose tissue of controls, matched *bbb/bbb*, and ad lib *bbb/bbb* female mice. Negative control showed no F4/80-positive staining (Figure 4.11.D). Interestingly, the mammary gland adipose tissue of ad lib *bbb/bbb* mice was significantly infiltrated with F4/80-positive macrophages, compared to matched *bbb/bbb* mice ($p=0.005$) and controls ($p=0.007$) (Figure 4.12.A).

As previously mentioned, there was a significant decrease in the number of adipocytes per area in matched *bbb/bbb* and ad lib *bbb/bbb* mice. To assess whether the decreased number of adipocytes was associated with a decreased number of macrophages, the number of macrophages per 100 adipocytes in each group was quantified. Consistent with the above result, the number of macrophages per 100 adipocytes was significantly increased in ad lib *bbb/bbb* mice, compared to matched *bbb/bbb* mice ($p<0.001$) and controls ($p<0.001$) (Figure 4.12.B). This demonstrates that the adipose tissue microenvironment of ad lib *bbb/bbb* mice is comprised of more macrophages, irrespective of whether this is measured as macrophages per unit area, or macrophages per number of adipocytes.

Similarly, abundance of macrophages in the visceral adipose tissue was quantified. F4/80-antibody immunostaining of the visceral adipose tissue was performed. F4/80-positive cells (Figure 4.13.A-C, arrows indicated) represented the F4/80-positive macrophages in visceral adipose tissue of controls, matched *bbb/bbb*, and ad lib *bbb/bbb* mice. Negative control showed no F4/80-positive staining (Figure 4.13.D). The visceral adipose tissue of ad lib *bbb/bbb* mice was significantly infiltrated with F4/80-positive macrophages, compared to matched *bbb/bbb* ($p=0.005$) and controls ($p=0.002$) (Figure 4.14.A). The number of macrophages per 100 adipocytes was also observed to be significantly increased in ad lib *bbb/bbb* mice, compared to matched *bbb/bbb* mice ($p=0.003$) and controls ($p<0.001$) (Figure 4.14.B).

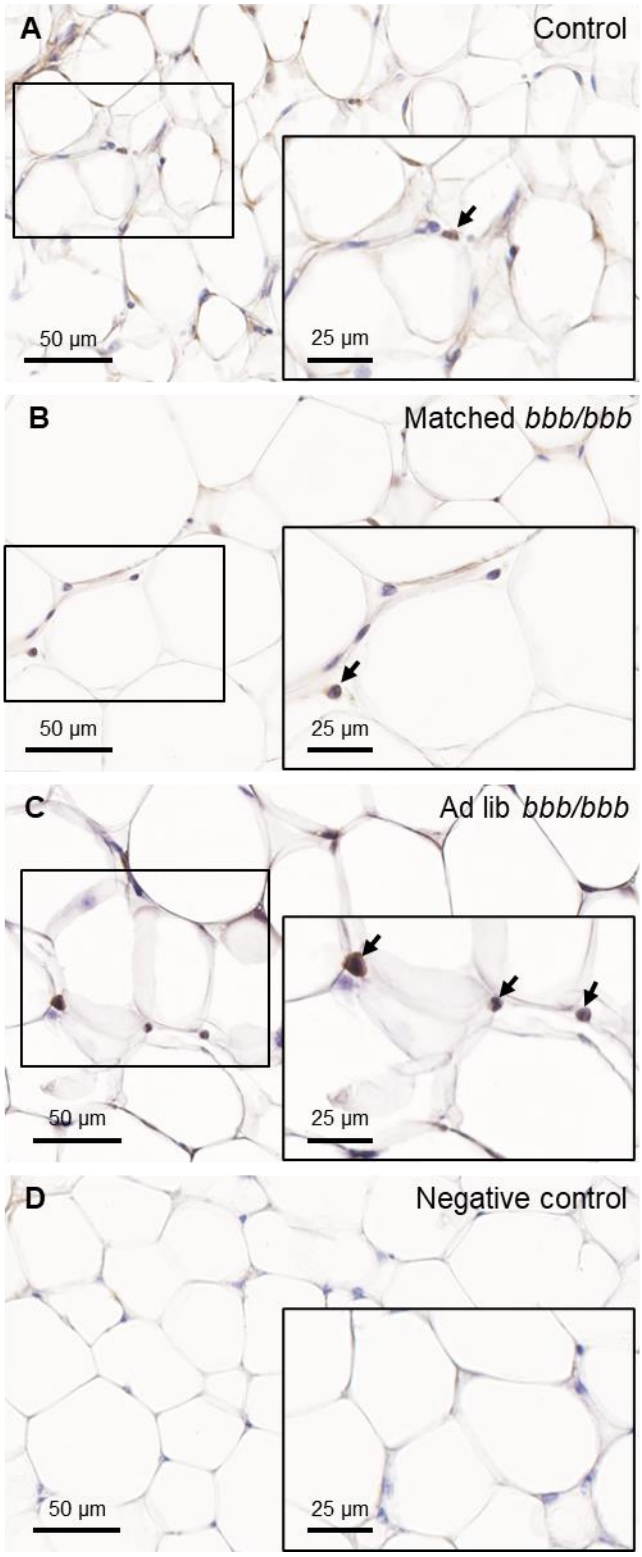

Figure 4.11. F4/80-positive macrophages in the mammary gland adipose tissue in controls, matched *bbb/bbb*, and ad lib *bbb/bbb* mice at adulthood. Representative images of F4/80-positive cells (arrows indicated) are the F4/80-positive macrophages in the mammary adipose tissue from (A) controls, (B) matched *bbb/bbb* mice, and (C) ad lib *bbb/bbb*. (D) Negative control without primary antibody shows no F4/80-positive staining. Images at original magnification of 40X and scale bars: 50 µm, with inset images at original magnification of 80X and scale bars: 25 µm.

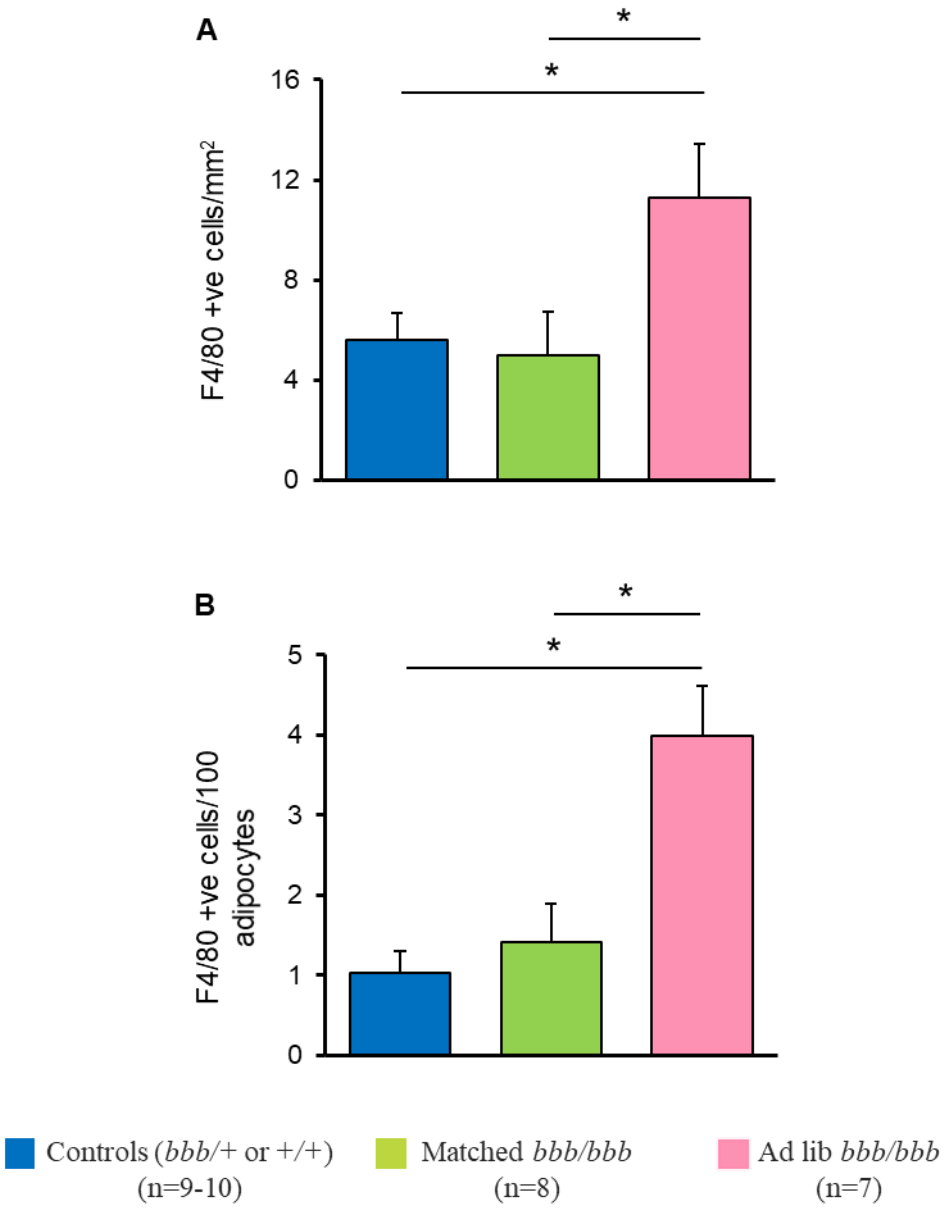

Figure 4.12. Abundance of macrophages in the mammary gland adipose tissue in controls, matched *bbb/bbb*, and ad lib *bbb/bbb* mice at adulthood. Quantification of F4/80-positive macrophages (A) per area and (B) per 100 adipocytes in the mammary gland adipose tissue of controls, matched *bbb/bbb*, and ad lib *bbb/bbb* female mice. Colour code – Blue: Controls (*bbb/+* or +/+) (n=9-10), Green: matched *bbb/bbb* (n=8), and Pink: ad lib *bbb/bbb* (n=7). Data are presented as mean+SEM and analysed using linear regression model. * indicates statistical significance at $p<0.05$.

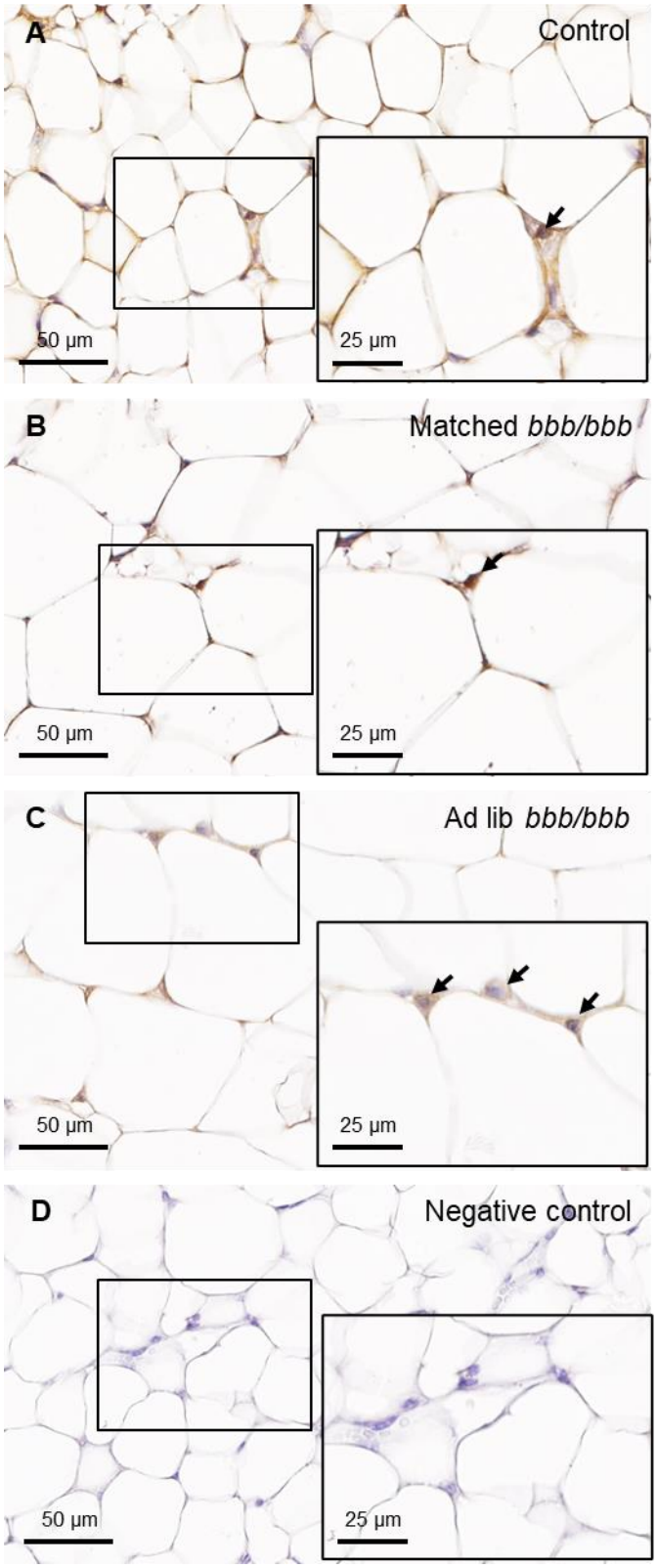

Figure 4.13. F4/80-positive macrophages in the visceral adipose tissue in controls, matched *bbb/bbb*, and ad lib *bbb/bbb* mice at adulthood. Representative images of F4/80-positive cells (arrows indicated) are the F4/80-positive macrophages in visceral adipose tissue from (A) controls, (B) matched *bbb/bbb*, and (C) ad lib *bbb/bbb* mice. (D) Negative control without primary antibody shows no F4/80-positive staining. Images at original magnification of 40X and scale bars: 50 µm, with inset images at original magnification of 80X and scale bars: 25 µm.

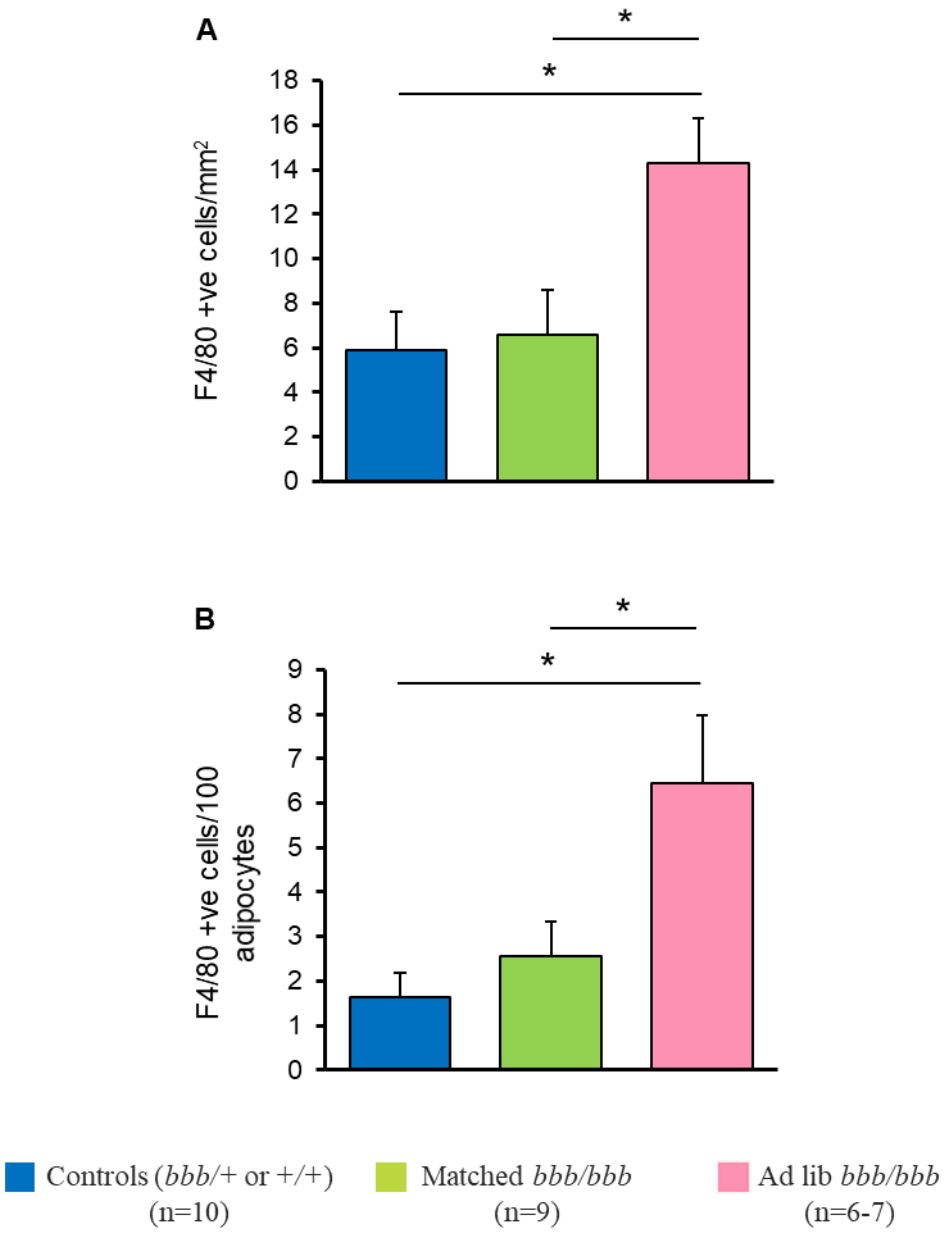

Figure 4.14. Abundance of macrophages in the visceral adipose tissue in controls, matched *bbb/bbb*, and ad lib *bbb/bbb* mice at adulthood. Quantification of F4/80-positive macrophages (A) per area and (B) per 100 adipocytes in visceral adipose tissue of controls, matched *bbb/bbb*, and ad lib *bbb/bbb* female mice. Colour code – Blue: Controls (*bbb*/+ or +/+) (n=10), Green: matched *bbb/bbb* (n=9), and Pink: ad lib *bbb/bbb* (n=6-7). Data are presented as mean+SEM and analysed using linear regression model. * indicates statistical significance at $p<0.05$.

4.2.7 Altered abundance of adipokines and proinflammatory cytokines in adult *bbb/bbb* mice

To investigate the impact of perturbation of adipose tissue on the mammary gland microenvironment, we assessed the protein concentration and gene expression of the most well characterised markers of obesity and tumour development in the mammary glands.

Firstly, Luminex assay was performed to measure the serum concentration of IL6, CCL2, leptin, TNFA, PAI1 and resistin. No significant difference was observed in the concentration of IL6, CCL2, TNFA, PAI1, and resistin (Figure 4.15). However, we observed a significant increase in the circulating concentration of leptin in ad lib *bbb/bbb* mice, compared to matched *bbb/bbb* mice ($p=0.025$) and controls ($p=0.002$) (Figure 4.15.C).

Next, protein concentration of IL6, CCL2, leptin, TNFA, PAI1 and resistin were measured in third pair mammary glands (Figure 4.16). Ad lib *bbb/bbb* mice exhibit increased protein levels of CCL2 ($p=0.002$), leptin ($p<0.001$), and TNFA ($p=0.002$), compared to controls (Figure 4.16.B, C, D). Interestingly, matched *bbb/bbb* mice demonstrated increased protein concentration of IL6 ($p=0.007$), TNFA ($p=0.028$), and PAI1 ($p<0.01$), compared to controls (Figure 4.16.A, D, E). Compared to matched *bbb/bbb* mice, ad lib *bbb/bbb* mice exhibit increased leptin ($p<0.01$) and decreased PAI1 ($p<0.01$) in the mammary glands (Figure 4.16. C, E). No significant difference was observed in resistin concentration in these mice (Figure 4.16.F).

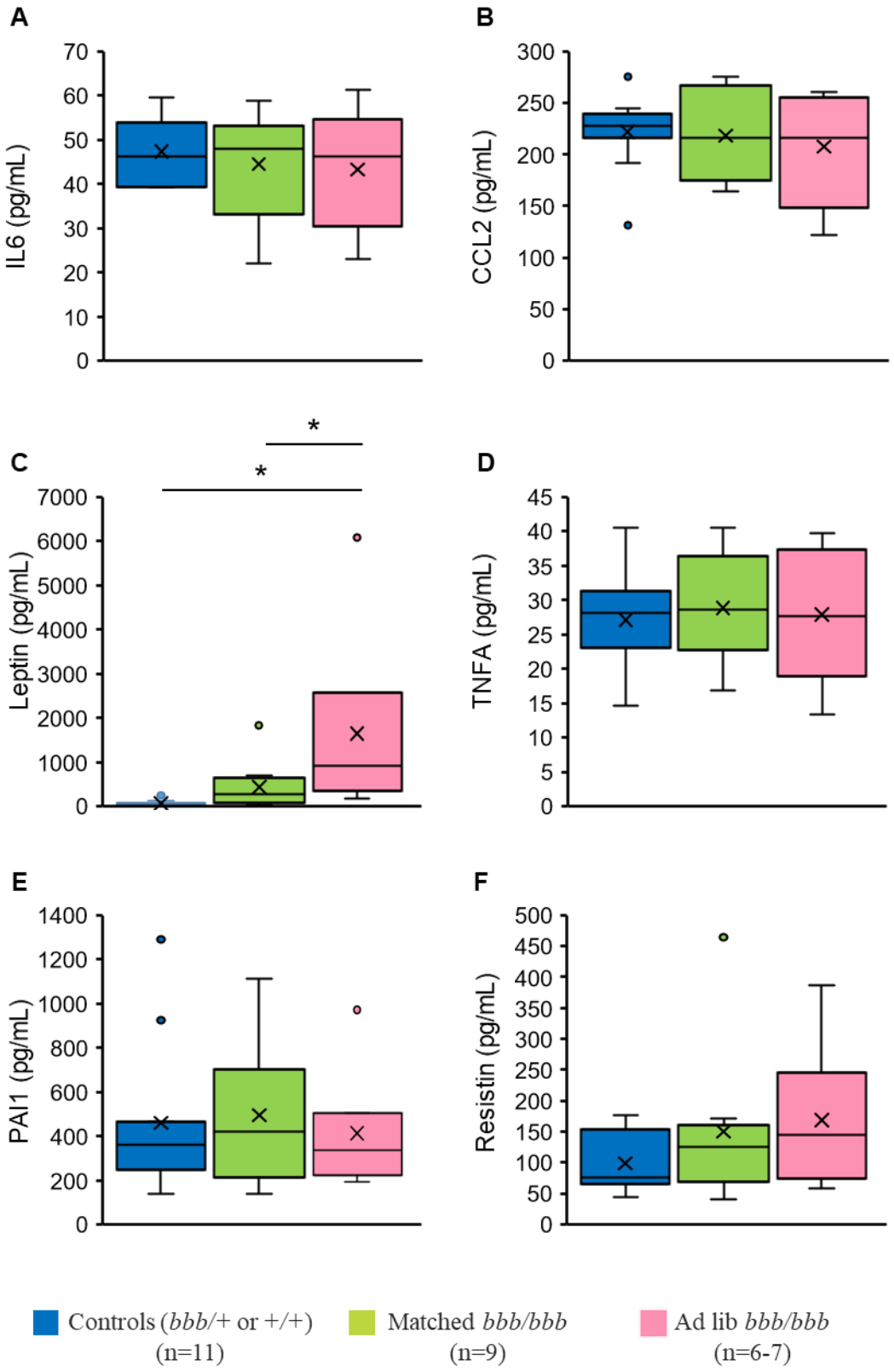
A
IL6 (pg/mL)
70
60
50
40
30
20
10
0
B
CCL2 (pg/mL)
300
250
200
150
100
50
0
C
*
*
Leptin (pg/mL)
7000
6000
5000
4000
3000
2000
1000
0
D
TNFA (pg/mL)
45
40
35
30
25
20
15
10
5
0
E
PAI1 (pg/mL)
1400
1200
1000
800
600
400
200
0
F
Resistin (pg/mL)
500
450
400
350
300
250
200
150
100
50
0
Controls (bbb/+ or +/+) (n=11)
Matched bbb/bbb (n=9)
Ad lib bbb/bbb (n=6-7)

Figure 4.15. Serum concentration of adipokines and proinflammatory cytokines in controls, matched *bbb/bbb*, and ad lib *bbb/bbb* mice at adulthood. Luminex assay assessed the serum concentration of (A) IL6, (B) CCL2, (C) leptin, (D) TNFA, (E) PAI1, and (F) resistin. Colour code – Blue: Controls (*bbb/+* or +/+) (n=11), Green: matched *bbb/bbb* (n=9), and Pink: ad lib *bbb/bbb* (n=6-7). IL6: interleukin 6, CCL2: C-C motif chemokine ligand 2, TNFA: tumour necrosis factor alpha, PAI1: plasminogen activator inhibitor 1. Data are presented as box-plots with median in between the first quartile and third quartile and analysed using a linear regression model. * indicates statistical significance at $p<0.05$.

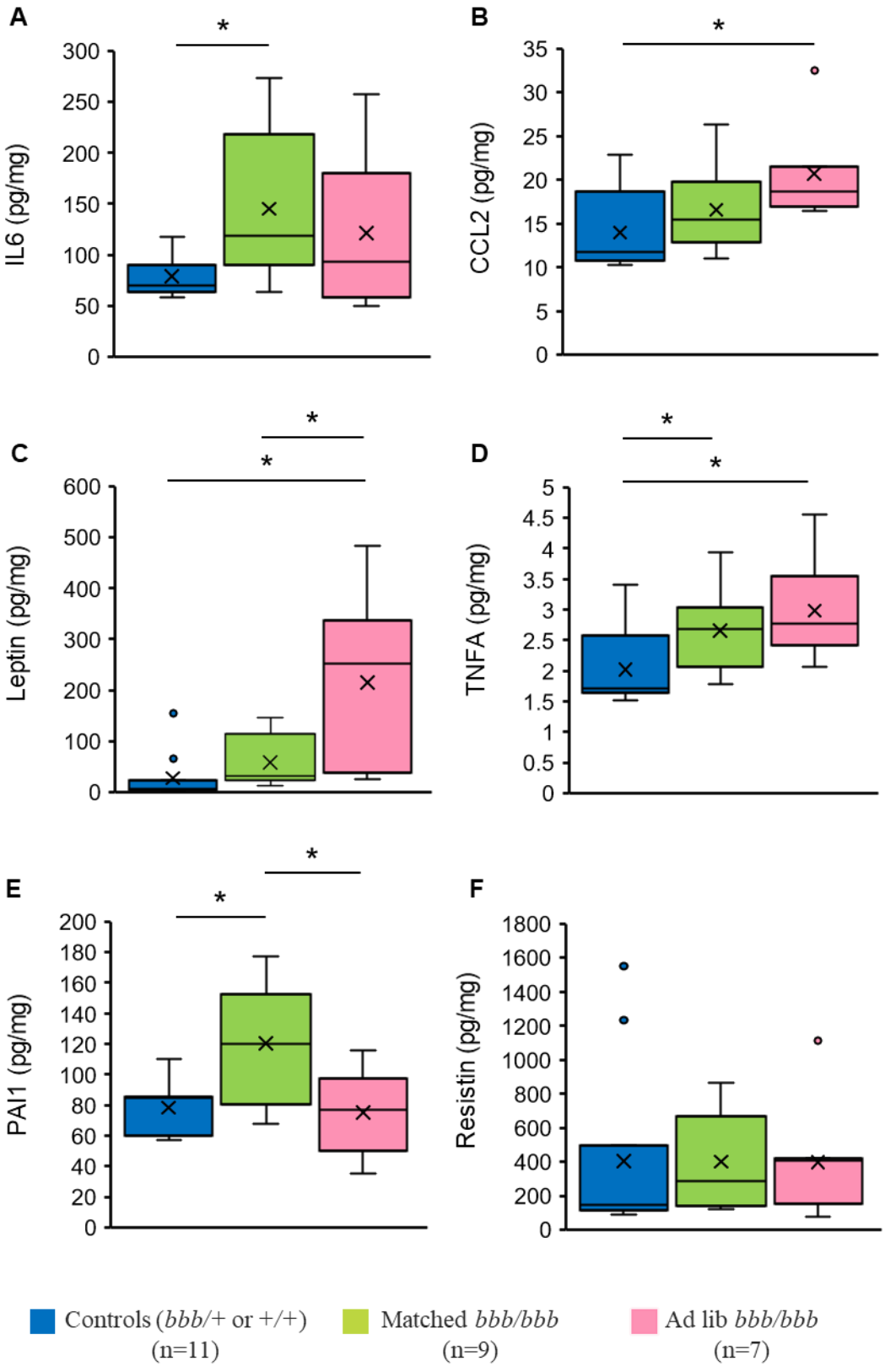
A
IL6 (pg/mg)
300
250
200
150
100
50
0
*
B
CCL2 (pg/mg)
35
30
25
20
15
10
5
0
*
C
Leptin (pg/mg)
600
500
400
300
200
100
0
*
*
D
TNFA (pg/mg)
5
4.5
4
3.5
3
2.5
2
1.5
1
0.5
0
*
*
E
PAI1 (pg/mg)
200
180
160
140
120
100
80
60
40
20
0
*
*
F
Resistin (pg/mg)
1800
1600
1400
1200
1000
800
600
400
200
0
Controls (bbb/+ or +/+) (n=11)
Matched bbb/bbb (n=9)
Ad lib bbb/bbb (n=7)

Figure 4.16. Protein abundance of adipokines and proinflammatory cytokines in the mammary glands in controls, matched *bbb/bbb*, and ad lib *bbb/bbb* mice at adulthood. Luminex assay assessed the protein concentration of (A) IL6, (B) CCL2, (C) leptin, (D) TNFA, (E) PAI1 and (F) resistin in third pair mammary glands. Colour code – Blue: Controls (*bbb/+* or +/+) (n=11), Green: matched *bbb/bbb* (n=9), and Pink: ad lib *bbb/bbb* (n=7). IL6: interleukin 6, CCL2: C-C motif chemokine ligand 2, TNFA: tumour necrosis factor alpha, PAI1: plasminogen activator inhibitor 1. Data are presented as box-plots with median in between the first quartile and third quartile and analysed using a linear regression model. * indicates statistical significance at $p<0.05$.

Further, we investigated gene expression of adipokines and inflammatory cytokines such as leptin, adiponectin, *Il4*, *Il6*, *Tnfa*, *Tgfb1*, *Ccl2*, *Csf1*, *Igf1*, *Stat3*, and *Cox2* in mammary glands by real-time PCR analysis.

Ad lib *bbb/bbb* mice exhibited increased expression of mRNA encoding leptin ($p<0.001$), adiponectin ($p<0.001$), TNFA, ($p<0.001$), TGFB1 ($p<0.001$), CCL2 ($p<0.001$), CSF1 ($p<0.001$), IGF1 ($p<0.001$), and STAT3 ($p<0.001$), compared to controls (Figure 4.17.A, B, E, F, 4.18.A-E). On the other hand, mammary glands of matched *bbb/bbb* mice demonstrate increased expression of mRNA encoding adiponectin ($p<0.01$), TGFB1 ($p=0.044$), CSF1 ($p=0.033$), IGF1 ($p=0.007$), and STAT3 ($p=0.033$), compared to controls (Figure 4.17. B, F, 4.18.B-D). Further, ad lib *bbb/bbb* mice also had increased expression of mRNA encoding leptin ($p<0.001$), adiponectin ($p=0.011$), TNFA, ($p<0.001$), TGFB1 ($p<0.001$), CCL2 ($p<0.001$), CSF1 ($p=0.041$), IGF1 ($p<0.001$), and STAT3 ($p<0.001$), compared to matched *bbb/bbb* mice (Figure 4.17.A, B, E, F, 4.18.A-D). No significant difference was observed in the expression of mRNA encoding IL4, IL6 or COX2 in these mice (Figure 4.17.C, D, 4.18.E).

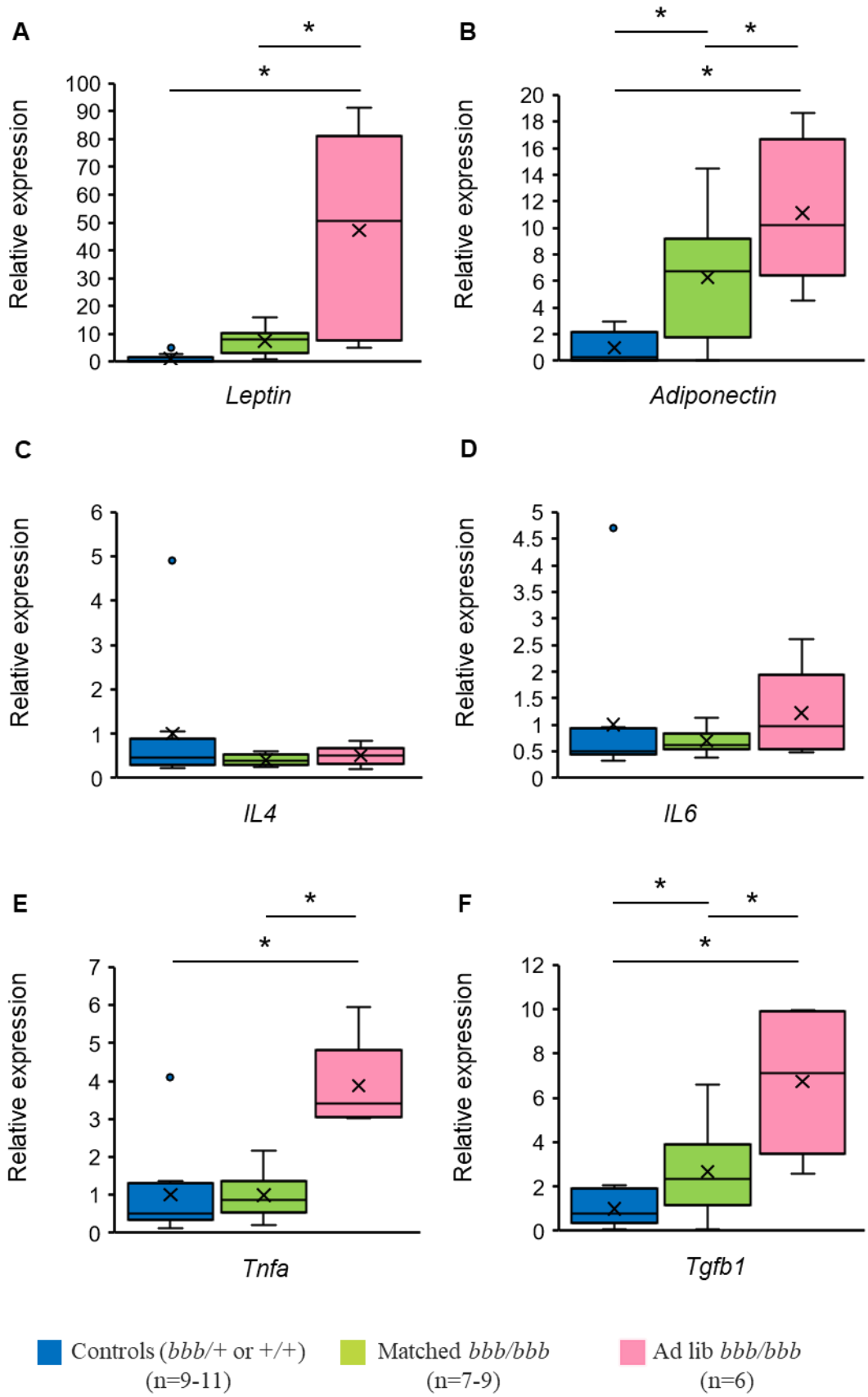
A
Relative expression
Leptin
B
Relative expression
Adiponectin
C
Relative expression
IL4
D
Relative expression
IL6
E
Relative expression
Tnfa
F
Relative expression
Tgfb1
Controls (bbb/+ or +/+) (n=9-11)
Matched bbb/bbb (n=7-9)
Ad lib bbb/bbb (n=6)

Figure 4.17. Gene expression profile of adipokines and proinflammatory cytokines in the mammary glands in controls, matched *bbb/bbb*, and ad lib *bbb/bbb* mice at adulthood. Quantification of mRNA encoding (A) leptin, (B) adiponectin, (C) IL4, (D) IL6, (E) TNFA, and (F) TGFB1 by real-time PCR analysis using comparative Ct method (i.e., 2^(-ΔΔCt) method). The abundance of mRNA was normalised to abundance of mRNA encoding the housekeeping gene *Rpl13a* in each sample. Colour code – Blue: Controls (*bbb/+* or *+/+*) (n=9-11), Green: matched *bbb/bbb* (n=7-9), and Pink: ad lib *bbb/bbb* (n=6). *Il4*: interleukin 4; *Il6:* interleukin 6; *Tnfa:* tumour necrosis factor alpha; *Tgfb1:* transforming growth factor beta 1. Data are presented as box-plots with median in between the first quartile and third quartile and analysed using a linear regression model. * indicates statistical significance at $p<0.05$.

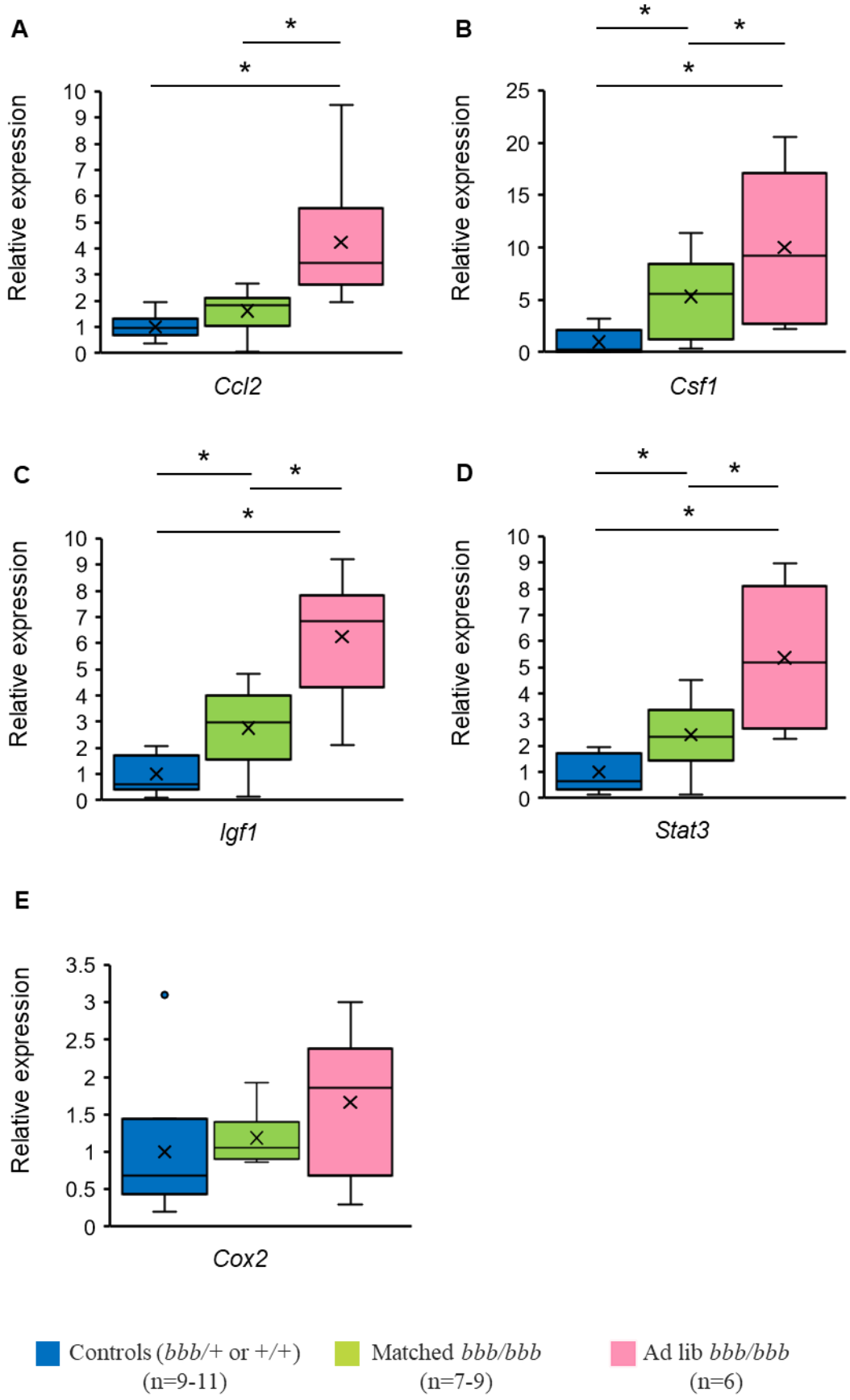
A
Relative expression
Ccl2
B
Relative expression
Csf1
C
Relative expression
Igf1
D
Relative expression
Stat3
E
Relative expression
Cox2
Controls (bbb/+ or +/+) (n=9-11)
Matched bbb/bbb (n=7-9)
Ad lib bbb/bbb (n=6)

Figure 4.18. Gene expression profile of adipokines and proinflammatory cytokines in the mammary glands in controls, matched *bbb/bbb*, and ad lib *bbb/bbb* mice at adulthood. Quantification of mRNA encoding (A) CCL2, (B) CSF1, (C) IGF1, (D) STAT3, and (E) COX2 by real-time PCR analysis using comparative Ct method (i.e., 2^(-ΔΔCt) method). The abundance of mRNA was normalised to abundance of mRNA encoding the housekeeping gene *Rpl13a* in each sample. Colour code – Blue: Controls (*bbb/+* or *+/+*) (n=9-11), Green: matched *bbb/bbb* (n=7-9), and Pink: ad lib *bbb/bbb* (n=6). *Ccl2:* C-C motif chemokine ligand 2; *Csf1:* colony-stimulating factor 1; *Igf1:* insulin-like growth factor 1; *Stat3:* signal transducer and activator of transcription 3*; Cox2:* cyclooxygenase 2. Data are presented as box-plots with median in between the first quartile and third quartile and analysed using a linear regression model. * indicates statistical significance at $p<0.05$.

Different fat depots are proposed to have different roles in endocrine regulation and maintaining homeostasis due to diverse gene expression profiles and differences in the release of adipokines and cytokines (321). To investigate whether increased visceral adiposity vary in its impact from the mammary gland adiposity, we performed real-time PCR analysis to estimate the gene expression of leptin, adiponectin, *Il4*, *Il6*, *Tnfa*, *Tgfb1*, *Ccl2*, *Csf1*, *Igf1*, *Stat3*, and *Cox2* (Figure 4.19, 4.20) in visceral adipose tissue.

Compared to controls, ad lib *bbb/bbb* mice had increased expression of mRNA encoding leptin ($p=0.037$), and decreased expression of mRNA encoding adiponectin ($p=0.017$), IL4 ($p<0.001$), IL6 ($p=0.004$), IGF1 ($p=0.003$), and COX2 ($p=0.004$) (Figure 4.19.A-D, 4.20.C, E). Matched *bbb/bbb* mice exhibited increased expression of mRNA encoding leptin ($p=0.021$) but decreased expression of IL4 ($p=0.039$), in comparison to controls (Figure 4.19.A, C). Interestingly, ad lib *bbb/bbb* mice demonstrated reduced expression of mRNA encoding adiponectin ($p=0.006$), IL4 ($p=0.011$), TGFB1 ($p=0.023$), and COX2 ($p=0.008$), compared to matched *bbb/bbb* mice (Figure 4.19.B, C, F, 4.20.E). No significant difference was observed in the expression of mRNA encoding TNFA, CCL2, CSF1, and STAT3 in these mice (Figure 4.19.E, 4.20.A, B, D).

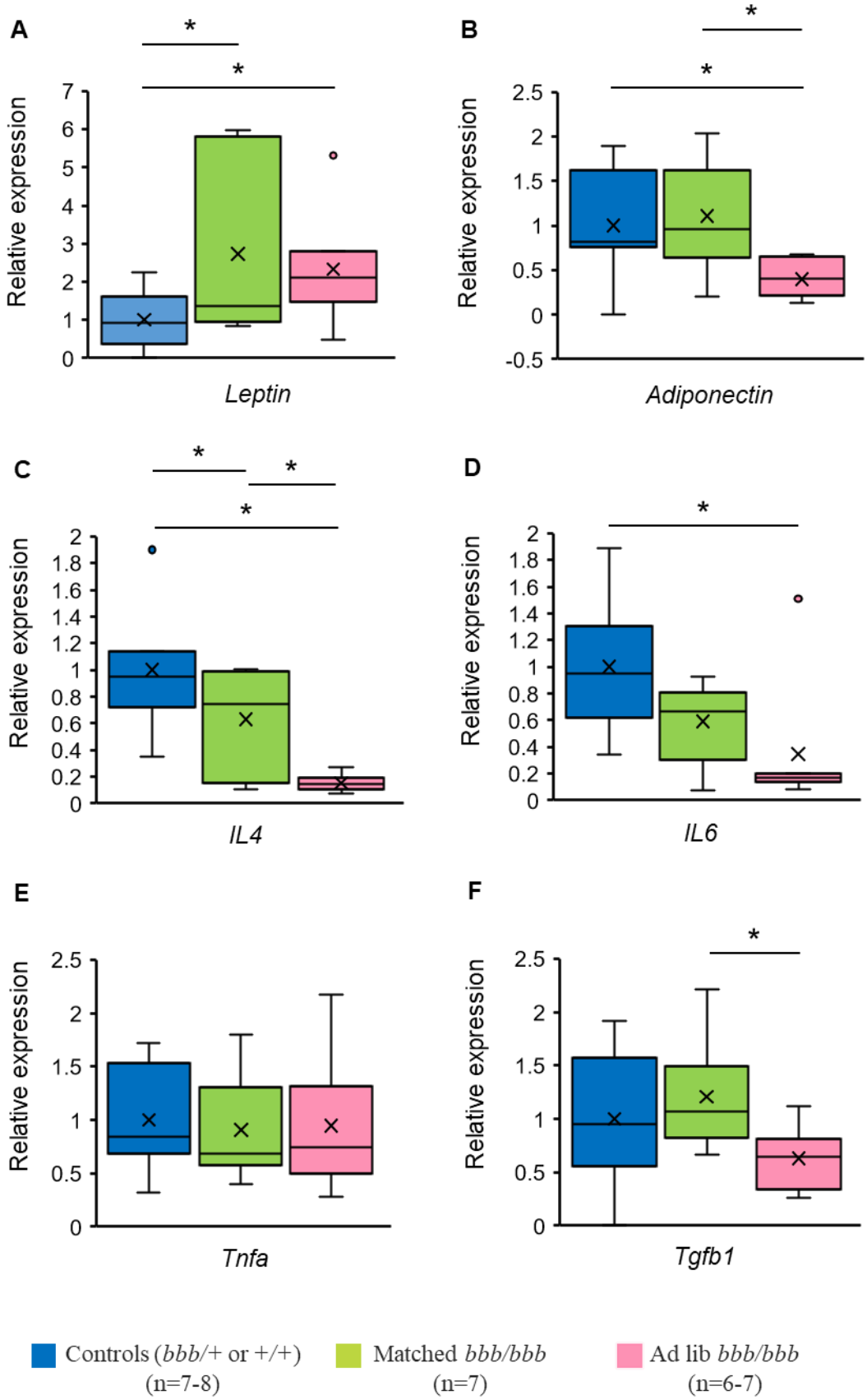
A
Relative expression
Leptin
B
Relative expression
Adiponectin
C
Relative expression
IL4
D
Relative expression
IL6
E
Relative expression
Tnfa
F
Relative expression
Tgfb1
Controls (bbb/+ or +/+) (n=7-8)
Matched bbb/bbb (n=7)
Ad lib bbb/bbb (n=6-7)

Figure 4.19. Gene expression profile of adipokines and proinflammatory cytokines in the visceral adipose tissue in controls, matched *bbb/bbb*, and ad lib *bbb/bbb* mice at adulthood. Quantification of mRNA encoding (A) leptin, (B) adiponectin, (C) IL4, (D) IL6, (E) TNFA, and (F) TGFB1 by real-time PCR analysis using comparative Ct method (i.e., 2^(-ΔΔCt) method). The abundance of mRNA was normalised to abundance of mRNA encoding the housekeeping gene *Rpl13a* in each sample. Colour code – Blue: Controls (*bbb/+* or *+/+*) (n=7-8), Green: matched *bbb/bbb* (n=7), and Pink: ad lib *bbb/bbb* (n=6-7). *Il4*: interleukin 4; *Il6*: interleukin 6; *Tnfa*: tumour necrosis factor alpha; *Tgfb1*: transforming growth factor beta 1. Data are presented as box-plots with median in between the first quartile and third quartile and analysed using a linear regression model. * indicates statistical significance at $p<0.05$.

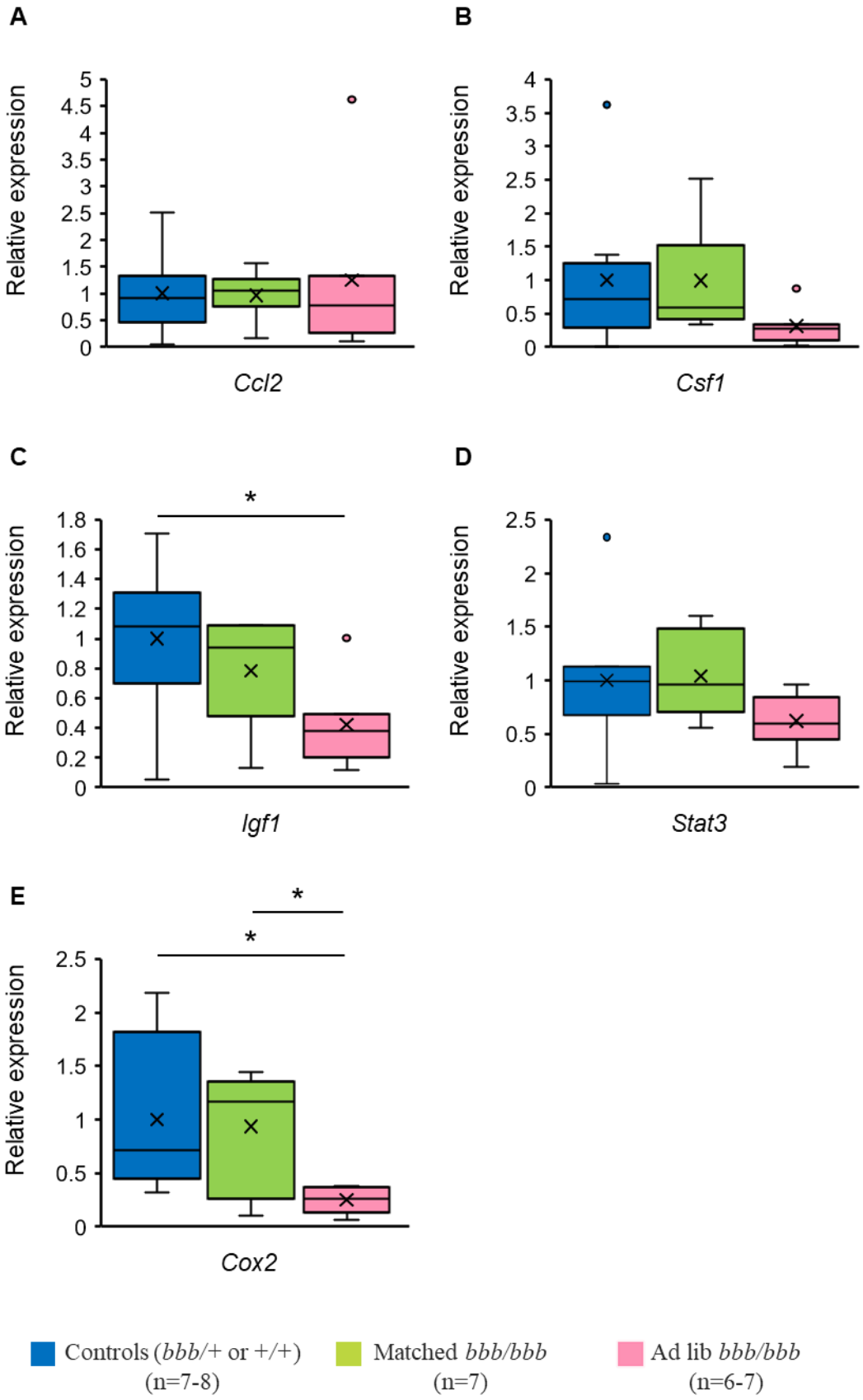
A
Relative expression
Ccl2
B
Relative expression
Csf1
C
Relative expression
*
Igf1
D
Relative expression
Stat3
E
Relative expression
*
*
Cox2
Controls (bbb/+ or +/+) (n=7-8)
Matched bbb/bbb (n=7)
Ad lib bbb/bbb (n=6-7)

Figure 4.20. Gene expression profile of adipokines and proinflammatory cytokines in the visceral adipose tissue in controls, matched *bbb/bbb,* and ad lib *bbb/bbb* mice at adulthood. Quantification of mRNA encoding (A) CCL2, (B) CSF1, (C) IGF1, (D) STAT3, and (E) COX2 by real-time PCR analysis using comparative Ct method (i.e., 2^(-ΔΔCt) method). The abundance of mRNA was normalised to abundance of mRNA encoding the housekeeping gene *Rpl13a* in each sample. Colour code – Blue: Controls (*bbb/+* or *+/+*) (n=7-8), Green: matched *bbb/bbb* (n=7), and Pink: ad lib *bbb/bbb* (n=6-7). *Ccl2*: C-C motif chemokine ligand 2; *Csf1*: colony-stimulating factor 1; *Igf1*: insulin-like growth factor 1; *Stat3*: signal transducer and activator of transcription 3; *Cox2*: cyclooxygenase 2. Data are presented as box-plots with median in between the first quartile and third quartile and analysed using a linear regression model. * indicates statistical significance at $p<0.05$.

4.3 Discussion

The experiments described in this chapter examined the impact of pubertal adiposity on mammary gland development and density during adulthood in a mouse model. We demonstrated that matched *bbb/bbb* and ad lib *bbb/bbb* mice exhibited increased mammary gland and visceral adiposity during adulthood. Increased mammary adiposity in matched *bbb/bbb* and ad lib *bbb/bbb* mice was associated with decreased abundance of macrophages around the ducts, decreased mammary gland density, and reduced deposition of stroma and collagen around the ducts. Overweight adult ad lib *bbb/bbb* mice exhibit increased abundance of macrophages in the mammary gland adipose tissue and visceral adipose tissue. Increased mammary adiposity resulted in altered abundance of adipokines and cytokines within the mammary gland microenvironment. Hence, overall, our results suggest that increased mammary adiposity during puberty reduces mammary gland density in adulthood, possibly through the crosstalk between mammary adipose tissue, epithelium, and stromal cells by altering the concentration of adipokines and cytokines.

4.3.1 Increased mammary gland adiposity in adult *bbb/bbb* mice

Mice that overeat in puberty due to their *bbb/bbb* mutation i.e., matched *bbb/bbb* and ad lib *bbb/bbb* mice both exhibited increased mammary gland adipocyte size suggesting increased lipid deposition in this fat depot. This was a large enough increase to be reflected in a statistical difference in mammary gland weight; thus clearly there was significantly increased adiposity in matched *bbb/bbb* and ad lib *bbb/bbb* mice during adulthood. As expected, ad lib *bbb/bbb* mice had increased visceral adipose tissue and heavier fourth pair mammary glands, which is consistent with their significant gain in body weight. Matched *bbb/bbb* mice have similar body weight as controls but exhibited increased weights of mammary glands. This could be due to either ENU-induced *bbb* mutation or the increased mammary adiposity that occurred during puberty in this model. This can be further investigated in future by utilising alternative *Alms1* null mutant models of which a number exist (316, 317).

4.3.2 Effect of increased mammary gland adiposity on mammary gland density during adulthood

Whole mount analysis of the mammary glands demonstrated that matched *bbb/bbb* and ad lib *bbb/bbb* mice exhibit increased ductal invasion area. Interestingly, increased ductal length was observed in ad lib *bbb/bbb* mice, compared to controls. However, we observed no significant difference in branching. This suggests that increased mammary gland adiposity promotes ductal elongation and development but has minimal effect on ductal branching during adulthood.

We then investigated the impact of increased of pubertal mammary adiposity on mammary gland density. It is striking to observe that matched *bbb/bbb* and ad lib *bbb/bbb* mice exhibit reduced percent fibroglandular density. High mammographic density breast tissue is characterised with increased stroma around epithelium and increased deposition of collagen, compared to low mammographic density breast tissue (215). Matched *bbb/bbb* and ad lib *bbb/bbb* mice both exhibited decreased stroma around epithelium and decreased collagen deposition around ducts, than controls. These results thus demonstrate that increased mammary adiposity reduces adult mammary gland density in mice. Similarly, increased BMI in women is associated with reduced mammographic density, as the proportion of adipose tissue relative to fibroglandular tissue increases.

As mentioned earlier, macrophages are capable of multiple biological roles in the mammary gland, including tissue development, homeostasis, and immunity. We investigated the impact of increased mammary adiposity on recruitment of macrophages around ducts. Interestingly, decreased abundance of macrophages in the stroma around ducts was observed in matched *bbb/bbb* and ad lib *bbb/bbb* mice. Similarly, human breast tissue with low mammographic density exhibits reduced abundance of stromal macrophages compared to breast tissue with high density (215).

Further, we observed that mammary adipose tissue and visceral adipose tissue of ad lib *bbb/bbb* mice exhibited significantly increased abundance of macrophages. Expansion of adipose tissue in the obese state can promote chronic inflammation with increased infiltration of macrophages (308). Ad lib *bbb/bbb* mice are significantly overweight compared to control and matched bbb/bbb mice and could exhibit a state of chronic inflammation in mammary gland and visceral fat depots. In comparison, matched *bbb/bbb* mice have similar abundance of macrophages in the mammary gland adipose tissue and visceral adipose tissue as the controls. This suggests that though matched *bbb/bbb* mice demonstrate increased adipose tissue expansion in adulthood, the mammary gland adipose tissue and visceral adipose tissue microenvironment is different from that of overweight ad lib *bbb/bbb* mice. Analysis of gene and protein expression of inflammatory cytokines provides evidence that this is indeed the case.

4.3.3 Effect of increased mammary gland adiposity on the mammary gland microenvironment

Increased adiposity is known to alter the abundance of adipokines and cytokines. Increased circulating levels and increased mammary gland gene expression of leptin was observed in ad

lib *bbb/bbb* mice. This is consistent with previous studies that report increased circulating concentration of leptin in mice with excess adiposity (322).

Protein abundance of proinflammatory cytokines IL6 and TNFA was increased in mammary glands of matched *bbb/bbb* mice, compared to controls. However, no significant difference was detected in the serum levels and gene expression of these cytokines in the mammary glands of these mice. Hence, further investigation is required to clarify the role of these cytokines in the mammary glands.

Increased protein abundance of PAI1 was detected in the mammary glands of matched *bbb/bbb* mice. Studies have shown elevated expression of PAI1 in adipose tissue of obese mice and humans (323, 324). Increased PAI1 in primary tumour tissues of breast cancer patients (325) are associated with tumour aggressiveness and poor prognosis (326, 327). In contrast, another study demonstrated that vitamin D inhibits invasiveness of MDA-MB-231 breast carcinoma cells, possibly by reducing plasminogen activator activity, downregulating serine protease uPA, and upregulation of PAI1 in this cell line (328). Very little is known about the role of PAI1 in normal adult mammary gland development and function and further investigation of PAI1 could reveal interesting insights.

Obesity is proposed to induce inflammation in the adipose tissue by elevating proinflammatory cytokines. We observed increased protein and gene expression of proinflammatory cytokines such as CCL2 and TNFA in the mammary glands of overweight ad lib *bbb/bbb* mice. In mice, overexpression of CCL2 caused increased abundance of macrophages and increased susceptibility of mammary cancer development (233). Consistent with these reports, increased expression of *Ccl2* and *Csf1* in the mammary glands of ad lib *bbb/bbb* mice was accompanied with increased abundance of macrophages in the mammary gland adipose tissue. These results suggest that mammary glands of ad lib *bbb/bbb* mice exhibit a state of low-grade inflammation within the mammary gland microenvironment.

Further, expression of genes encoding adiponectin, TGFB1, IGF1, and STAT3 were increased in the mammary glands of matched *bbb/bbb* and ad lib *bbb/bbb* mice. The circulating concentration of adiponectin is inversely associated with obesity-associated disorders (329-331). Obese women have lower serum levels of adiponectin and have increased breast cancer risk (332-334). The increased expression of adiponectin in the mammary glands of matched *bbb/bbb* and ad lib *bbb/bbb* mice might thus be protective against mammary cancer development. However, no study has demonstrated the direct role of adiponectin in mammary gland adiposity, mammary gland development, and cancer development.

TGFB1 is highly expressed during puberty, adulthood, and pregnancy by the mammary epithelium (335). TGFB1 action has been extensively studied in pubertal mammary gland development, particularly branching morphogenesis (211). However, the exact role of TFGB1 in adult mammary gland development is still not fully understood. Matched *bbb/bbb* and ad lib *bbb/bbb* mice, both exhibit ductal elongation; however, no significant difference was observed in branching morphogenesis. Studies have reported increased mRNA encoding TGFB1 in the adipose tissues of *ob/ob* and *db/db* mice, suggesting increased TGFB1 production with increasing adiposity as seen with leptin (336-338). These in vivo studies support our finding of increased *Tgfb1* expression with increasing adiposity in matched *bbb/bbb* and ad lib *bbb/bbb* mice.

IGF1 expression in the mammary gland is important for ductal development and branching. *Igf1* null mutant female mice have perturbed pubertal mammary gland development, with reduced TEBs and decreased ductal invasion into the mammary gland adipose tissue (339). In an organ culture system for mouse mammary glands, IGF1 promoted ductal growth and elongation (340). These studies further support our result whereby, increased expression of *Igf1* in the mammary glands of matched *bbb/bbb* and ad lib *bbb/bbb* mice is accompanied with increased ductal invasion through the mammary gland adipose tissue. Mammographic density is positively associated with plasma concentration of IGF1 among premenopausal women (183). Interestingly, a study shows that it is the paracrine effect and not the endocrine effect of IGF1 that is important for branching morphogenesis (170). However, it is still unknown whether IGF1 regulates biological mechanisms that affect both branching morphogenesis and mammographic density.

STAT3 is widely studied in the process of involution of the mammary glands. Its role is in the regulation of apoptosis of mammary epithelial cells and modulation of the immune cell microenvironment within the mammary gland (341-343). Deletion of STAT3 results in early embryonic lethality (344), therefore, the role of STAT3 in mammary gland development is still not fully understood. However, several studies have shown the role of leptin-STAT3 signalling in mammary gland development. Mice specifically lacking leptin-STAT3 signalling exhibit impaired growth of mammary ducts into the mammary gland adipose tissue (345). Our observation of increase in the expression of *Stat3* in matched *bbb/bbb* and ad lib *bbb/bbb* mice is also accompanied with increased ductal growth into the mammary gland adipose tissue. Though previous studies support our findings, future studies might unravel the role of STAT3 in mammary gland development during the non-pregnant non-lactating adult state.

Overall, these findings indicate that the mammary gland microenvironment of matched *bbb/bbb* mice with increased pubertal mammary adiposity is different from that of overweight ad lib *bbb/bbb* mice with lifelong increased adiposity. Increased mammary adiposity in adult ad lib *bbb/bbb* mice induced a state of chronic inflammation within the mammary gland which is evident by the increased infiltration of F4/80-positive macrophages in the mammary adipose tissue and elevated expression of multiple adipokines and proinflammatory cytokines, compared to matched *bbb/bbb* mice.

4.3.4 Effect of increased adiposity on the visceral adipose tissue microenvironment

In overweight ad lib *bbb/bbb* mice, the gene expression profile of cytokines in visceral adipose tissue is strikingly different from that in the mammary glands, except for leptin. Expression of genes encoding cytokines such as adiponectin, IL4, IL6, IGF1, and COX2 was found to be decreased in the visceral adipose tissue of ad lib *bbb/bbb* mice. On the other hand, mRNA encoding IL4 was decreased in matched *bbb/bbb* mice, compared to controls. Our observation of reduced expression of adiponectin is consistent with previous studies that demonstrate decreased adiponectin in obese mice (346-348).

IL4 and IL6 have been extensively studied as inflammatory cytokines, however, more recent studies have suggested their role in metabolic abnormalities associated with the adipose tissue. Lower circulating IL4 is reported in obese 145E mice and mice fed a high-fat diet, compared to wildtype and lean mice (349). Interestingly, IL4 is shown to promote macrophage polarization into M2 phenotypes (350, 351). Decreased expression of IL4 in matched *bbb/bbb* and ad lib *bbb/bbb* mice might be due to the increased visceral adiposity in these mice. However, we did not detect significant differences in the abundance of F4/80-positive macrophages between the visceral adipose tissue of matched *bbb/bbb* mice and controls. On the other hand, IL6 expression is reported to be increased in the adipose tissue in obese, insulin resistant animals (352). However, the inflammatory role of IL6 still remains conflicted and instead, studies suggest the positive effect of IL6 in immuno-metabolic conditions (353). In support of this, IL6-deficient mice develop late onset obesity (354), and when fed a high-fat diet exhibit enhanced inflammation compared to controls (355). Further, an acute bout of exercise increases IL6 signalling markers and reduces F4/80- and CD11c-positive cells in the adipose tissue, which suggests a reduction in M1 macrophage polarization (353). Our findings are consistent with these studies whereby decreased IL6 expression in the visceral adipose tissue is accompanied with increased infiltration of F4/80-positive macrophages in ad lib

bbb/bbb mice. However, further investigation is required to understand the precise role of IL4 and IL6 in the adipose tissue development and function in mice.

IGF1 has been proposed to play a key role in obesity. Obese humans and animal models generally have abnormal circulating IGF1 (356) and an inverse relationship of circulating IGF1 with visceral adipose tissue mass had been proposed (357-361). We have also found reduced expression of *Igf1* in overweight ad lib *bbb/bbb* mice. However, the role of IGF1 in the visceral adipose tissue is still unknown.

COX enzymes are involved in prostaglandin production. While high-fat diet feeding in rats increases expression of COX1 and COX2 (362), high-fat diet feeding in C57BL/6 mice decreases COX-derived products (363). In addition, high-fat diet in C57BL/6 mice suppresses COX2 but not COX1 expression in inguinal white adipose tissue (364). Overexpression of COX2 in mature adipocytes resulted in reduced inguinal white adipose tissue and altered adipocyte size in C57BL/6 mice (365). These studies are consistent with our findings of decreased *Cox2* expression with increased visceral adipose tissue and increased adipocyte size in ad lib *bbb/bbb* mice. Unlike the mice mentioned in the above studies, ad lib *bbb/bbb* mice were not fed a high-fat diet, but exhibit similar obesity. Future studies might unravel the effect of COX2 activity in the adipose tissue.

Interestingly, compared to matched *bbb/bbb* mice, reduced expression of mRNA encoding TGFB1 was detected in visceral adipose tissue of ad lib *bbb/bbb* mice. Constitutive overexpression of an active human *TGFB1* transgene in white adipose tissue resulted in severe reduction of white adipose depots (366). Further, the expression of this transgene in *ob/ob* mice prevented morbid obesity that is typically associated with these mice (366). However, mRNA encoding TGFB1 is increased in the adipose tissue of *ob/ob* and *db/db* mice (337). TGFB1 is known to promote expansion of the preadipocyte population, while preventing their subsequent differentiation (367). High expression of TGFB1 in obese animal models could possibly support undifferentiated population of preadipocytes (368). However, when the differentiation process is initiated possibly by other factors, the inhibitory effect of TGFB1 on adipogenesis would be reduced and would allow for expansion of adipose tissue mass (369). These studies suggest that the lower expression of *Tgfb1* in overweight ad lib *bbb/bbb* mice possibly promotes visceral adiposity.

Overall, these findings suggest that the visceral adipose tissue microenvironment of matched *bbb/bbb* mice is different from that of overweight ad lib *bbb/bbb* mice. Increased visceral adiposity in ad lib *bbb/bbb* mice is associated with a proinflammatory and pro-adipogenic

microenvironment, which is evident by the increased infiltration of F4/80-positive macrophages and reduced expression of anti-adipogenesis factors such as IL4, IL6, and TGFB1.

4.3.5 Limitations and future directions

The expansion of adipose tissue is associated with changes to ovarian hormones estradiol and progesterone; and thus, future research may investigate whether these hormones play any role in the mammary gland density and inflammatory changes observed with obesity in these mice. Further, we also observed high degree of variability in the gene expression of adipokines and proinflammatory cytokines reported in our study which possibly highlight the contribution of both epithelium and stroma to affect their expression in the mammary gland. In addition, the differential gene expression profile of mammary glands from that of visceral adipose tissue can be attributed to the crosstalk of adipose tissue with the epithelium in the mammary glands. Contribution of epithelium in the adult mammary gland with increased mammary adiposity, is still not clearly understood. Our experimental design could not allow us to evaluate the role of the epithelium specifically in adult mammary gland development and function. Therefore, future studies may investigate the role of the epithelium in the adult mammary gland with increased mammary adiposity in mice using a mammary gland transplant approach.

4.4 Conclusion

Increased mammary gland adiposity in the *Alms1 bbb/bbb* mouse model is associated with decreased mammary gland density with reduced deposition of stroma and collagen around mammary ducts, and decreased abundance of macrophages. The significant increase in body weight in ad lib *bbb/bbb* mice in adulthood was associated with a state of chronic inflammation within the mammary gland. On the other hand, matched *bbb/bbb* mice with normal body weight and increased mammary gland adiposity in adulthood did not exhibit these inflammatory phenotypes. Overall, these findings demonstrate that increased pubertal adiposity is a causative factor in regulating mammary fibroglandular density in adulthood. In the following chapter, we investigate how these above alterations in the adult mammary gland impact mammary cancer development.

CHAPTER FIVE

Impact of increased pubertal adiposity on mammary cancer development during adulthood

5.1 Introduction

In Chapter four, we provided evidence that increased pubertal adiposity is causative in regulating mammary gland density in adulthood. However, whether there is a relationship between increased pubertal adiposity and development of mammary cancer in adulthood is still unclear. This study investigates links between adiposity during puberty and mammary cancer development in adulthood in a mouse model.

The MMTV-PyMT transgenic mouse model was used in these studies. The PyMT transgene is an oncogene that causes hyperplasia of the mammary epithelial cells and progression to carcinoma. The resulting tumours spontaneously progress to metastasis and recapitulate the stages of human breast cancer progression (370). These mammary tumours arise with 100% penetrance and align with the basal epithelial subtype of human breast cancer (371, 372). Basal epithelial subtype of human breast cancer is associated with clinically aggressive nature and poor prognosis (373). For this study, the MMTV-PyMT tumour model was crossed with *Alms1 bbb/+* mice to generate female PyMT-control (PyMT-*bbb/+* or PyMT-+/+) and PyMT-*bbb/bbb* mice.

The experimental design of this study is illustrated in Figure 5.1. PyMT-control and PyMT-*bbb/bbb* mice were fed normal mouse diet ad libitum from weaning age to 7 weeks of age. After 7 weeks (i.e., end of puberty), a group of PyMT-*bbb/bbb* mice were calorie-matched to PyMT-control mice until 18 weeks, such that the amount of food eaten by PyMT-*bbb/bbb* mice was the same as that consumed by the PyMT-control. These mice will be referred to as 'matched PyMT-*bbb/bbb* mice'. Due to consuming mouse chow ad libitum until puberty, matched PyMT-*bbb/bbb* mice will exhibit increased pubertal adiposity, as described in Chapter 3, but then they will not increasingly gain adipose tissue as adults because they are calorie-matched with PyMT-control mice. Another cohort of mice was used in parallel. They are PyMT-*bbb/bbb* mice that ate ad libitum throughout the study. These mice will be referred to as 'ad lib PyMT-*bbb/bbb* mice'. This cohort allowed us to specifically isolate the effect of pubertal adiposity and compare it to the effect of adult obesity. Ad lib PyMT-*bbb/bbb* mice exhibited increased adiposity during puberty and became obese in adulthood.

Based on the known epidemiological association between pubertal adiposity and breast cancer risk, we hypothesised that matched PyMT-*bbb/bbb* mice would exhibit reduced mammary cancer development in adulthood, compared to PyMT-control mice. As ad lib PyMT-*bbb/bbb* mice would exhibit obesity in adulthood, we hypothesised that they would exhibit increased mammary cancer development compared to matched PyMT-*bbb/bbb* mice.

Mammary tumours and visceral adipose tissue were dissected from PyMT-control, matched PyMT-*bbb/bbb*, and ad lib PyMT-*bbb/bbb* mice at 18 weeks. The number of mice required for this study was determined by power analysis for MMTV-PyMT tumour model, preformed in previous studies in our lab (data not shown). The MMTV-PyMT tumour model on C57BL/6 background exhibit an average tumour latency of 14 weeks, compared to the shorter latency of 7 weeks in MMTV-PyMT tumour model on FVB background (374). However, to account for C57BL/6 background, *bbb/bbb* mutation, and hypothesised delayed tumour development in matched PyMT-*bbb/bbb* mice, these mice were monitored till 18 weeks. Tumour latency and tumour development was analysed in these mice. Primary tumours were characterised based on histopathological grading assessment. To investigate the impact of perturbation of mammary gland adiposity on the mammary tumour microenvironment, we assessed gene expression of adipokines and proinflammatory cytokines in the mammary tumours. Results from this chapter suggest that increased pubertal mammary adiposity alters tumour latency and tumour development during adulthood. Furthermore, altered expression of adipokines and proinflammatory cytokines was observed within the mammary tumour microenvironment and this could be responsible for altered mammary cancer development in these mice.

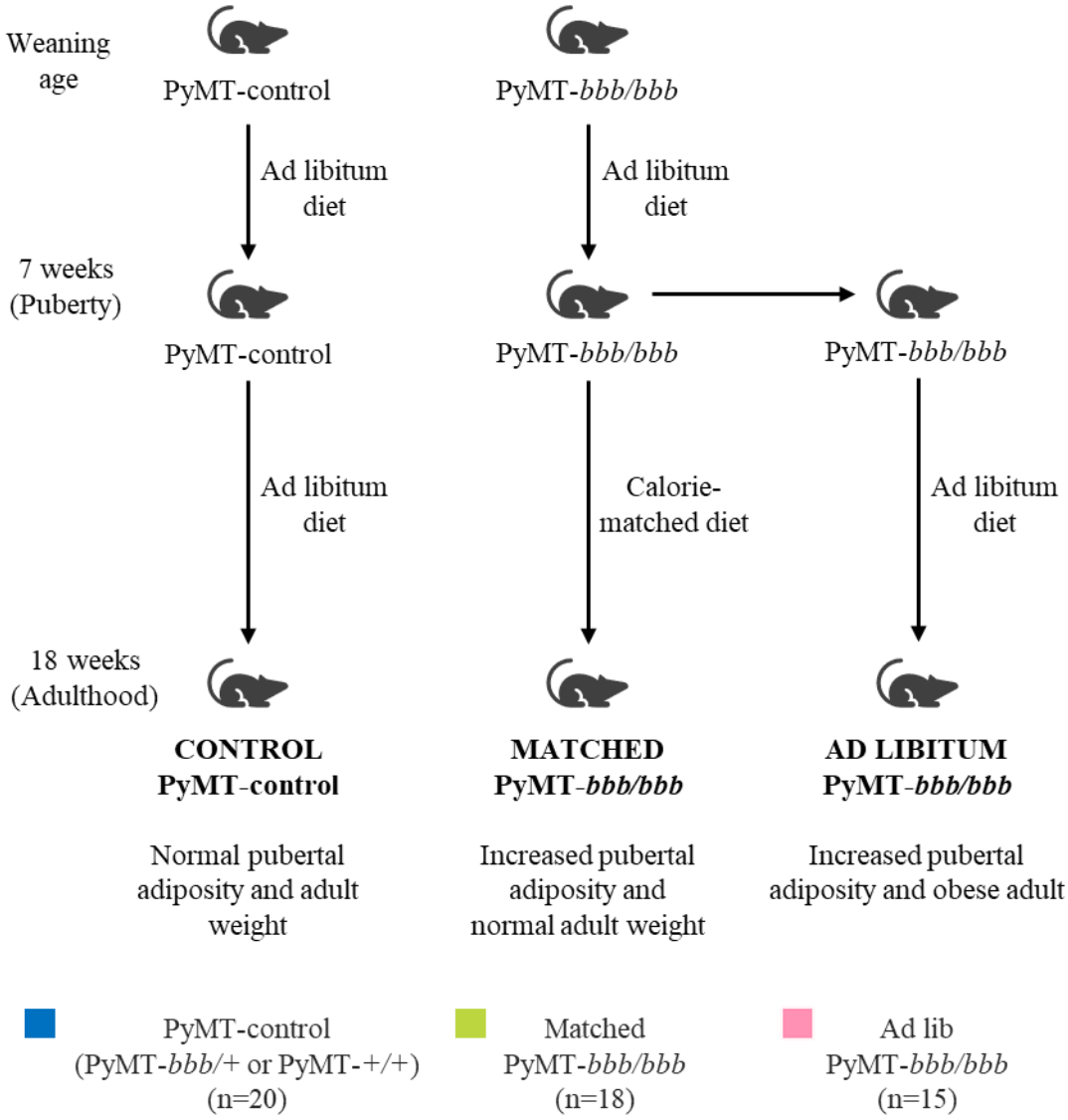

Figure 5.1. Illustration of experimental design to study the impact of pubertal adiposity on mammary cancer development in adulthood. PyMT-control and PyMT-*bbb/bbb* mice were fed normal mouse diet ad libitum from weaning age until 7 weeks. After 7 weeks (i.e., end of puberty), a group of PyMT-*bbb/bbb* mice were calorie-matched to PyMT-control mice until 18 weeks (adulthood), such that the amount of food eaten by PyMT-*bbb/bbb* mice is same as that eaten by the controls. These mice will be referred to as 'matched PyMT-*bbb/bbb* mice'. Another cohort of mice in this study are PyMT-*bbb/bbb* mice that ate ad libitum from 4 weeks to 18 weeks. These mice will be referred to as 'ad lib PyMT-*bbb/bbb* mice'. Colour code: Blue - PyMT-control (PyMT-*bbb*/+ or PyMT-+/+) (n=20), Green - matched PyMT-*bbb/bbb* (n=18), Pink - ad lib PyMT-*bbb/bbb* (n=15).

5.2 Results

5.2.1 Female matched PyMT-*bbb/bbb* mice exhibit greater tumour latency in adulthood

To investigate the impact of increased adiposity during puberty on mammary cancer development in adulthood, matched PyMT-*bbb/bbb*, ad lib PyMT-*bbb/bbb* and PyMT-control female mice were euthanised and then weighed at 18 weeks of age. Mammary tumours and visceral adipose tissue were dissected from these mice. At 18 weeks, matched PyMT-*bbb/bbb* mice showed similar body weight compared to the PyMT-control mice (Figure 5.2.A). Ad lib PyMT-*bbb/bbb* mice exhibited a significant increase in body weight, compared to PyMT-control mice ($p<0.001$) and matched PyMT-*bbb/bbb* mice ($p<0.001$) (Figure 5.2.A). Consistent with body weight, there was significant increase in the weight of visceral adipose tissue in ad lib PyMT-*bbb/bbb* mice, compared to PyMT-control ($p<0.001$) and matched PyMT-*bbb/bbb* mice ($p<0.001$) (Figure 5.2.B).

PyMT-control and PyMT-*bbb/bbb* mice were monitored daily and palpated twice a week to check for tumours from 8 weeks of age to determine latency to mammary tumour development. A significant increase in tumour free survival was observed in matched PyMT-*bbb/bbb* mice, compared to PyMT-control and ad lib PyMT-*bbb/bbb* mice (LogRank $p=0.002$) (Figure 5.3.A). Matched PyMT-*bbb/bbb* mice exhibited a significant increase in tumour latency (age at the time of detection of the first palpable tumour) compared to PyMT-control mice ($p<0.01$) (Figure 5.3.B).

5.2.2 Matched PyMT-*bbb/bbb* mice exhibit decreased mammary cancer development in adulthood

The primary tumour is defined as the first palpable tumour and has the highest weight at dissection. There was significant reduction in the weight of the primary tumour of matched PyMT-*bbb/bbb* mice, compared to ad lib PyMT-*bbb/bbb* mice ($p=0.019$) (Figure 5.4.A). Further, matched PyMT-*bbb/bbb* mice exhibited a significant decrease in the number of tumours, compared to PyMT-control ($p=0.006$) and ad lib PyMT-*bbb/bbb* ($p=0.018$) mice (Figure 5.4.B).

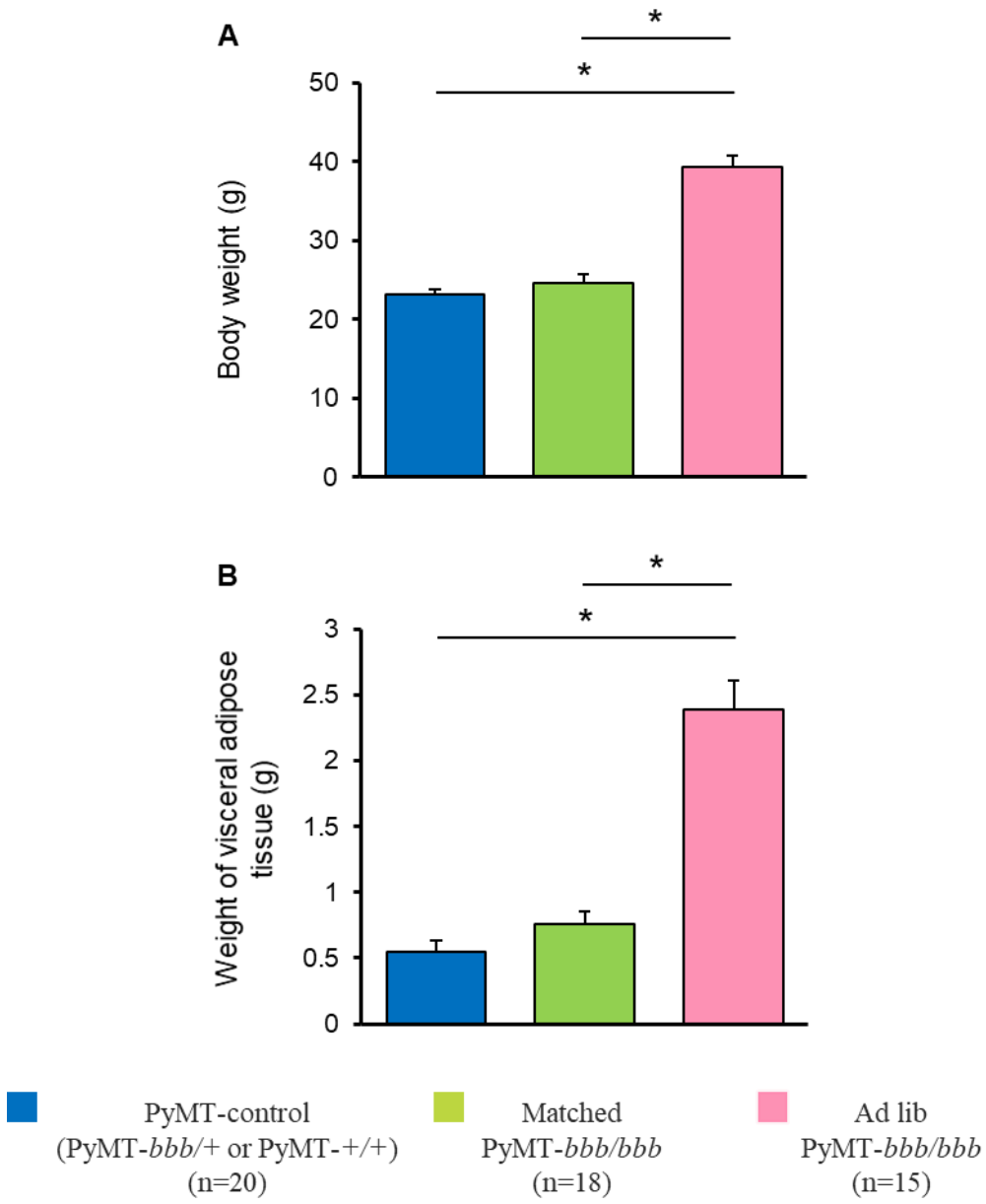

Figure 5.2. Body and adipose tissue weights of female PyMT-control, matched PyMT-*bbb/bbb*, and ad lib PyMT-*bbb/bbb* mice at adulthood. At 18 weeks, mice were weighed, and mammary tumours and visceral adipose tissue was dissected. (A) Total body weight. (B) Weight of visceral adipose tissue. Colour code: Blue - PyMT-control (PyMT-*bbb*/+ or PyMT-+/+) (n=20), Green - matched PyMT-*bbb/bbb* (n=18), Pink - ad lib PyMT-*bbb/bbb* (n=15). Data are presented as mean+SEM and analysed using linear regression model. * indicates statistical significance at $p<0.05$.

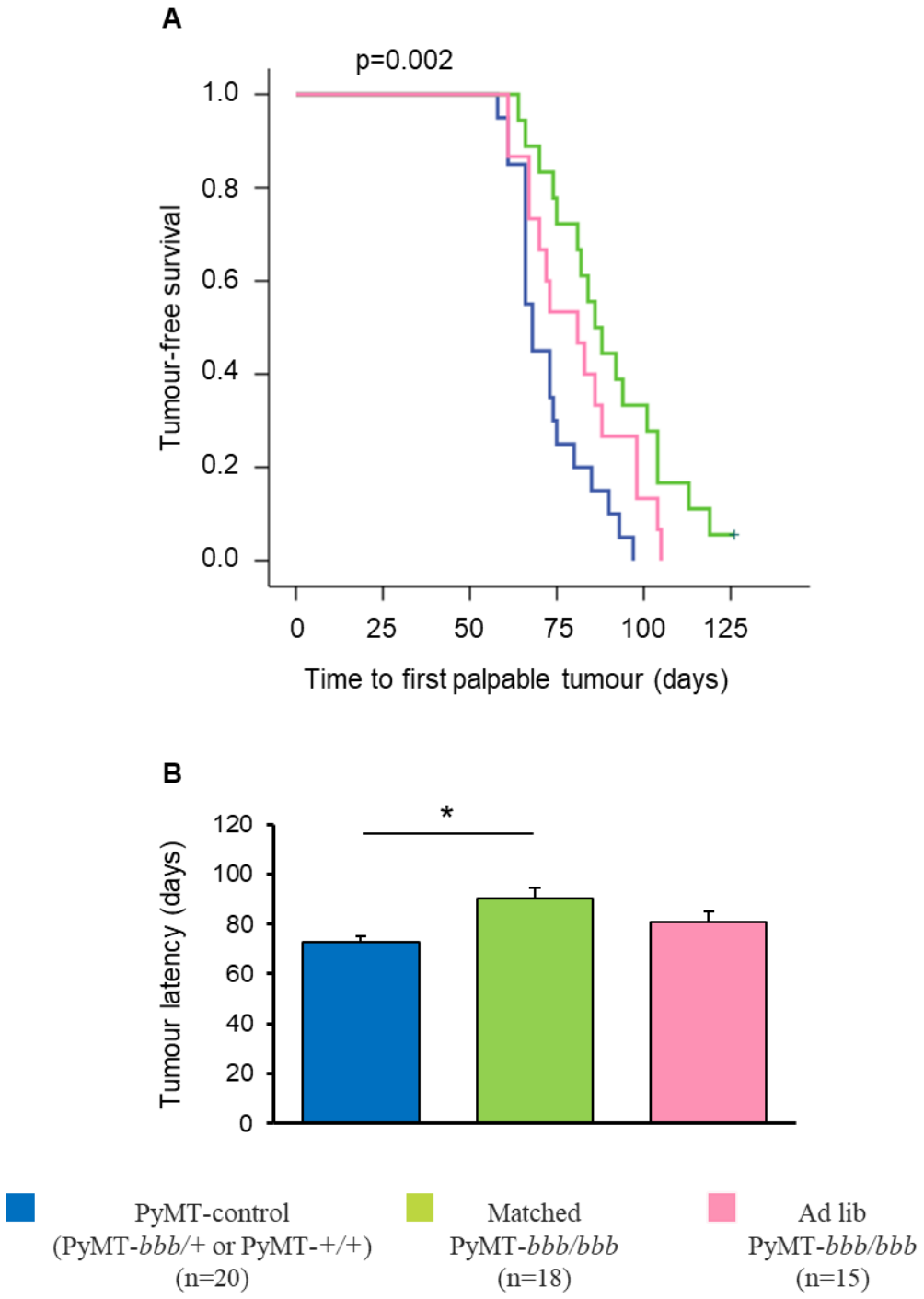

Figure 5.3. Tumour latency in PyMT-control, matched PyMT-*bbb/bbb*, and ad lib PyMT-*bbb/bbb* female mice at adulthood. PyMT-control and PyMT-*bbb/bbb* female mice were monitored twice a week from 8 weeks of age by palpation to determine tumour latency. Mice were either euthanised at 18 weeks or when tumour volume exceeded 2000mm^3. (A) Kaplan-Meier tumour-free survival plot. Statistical significance at Log Rank $p<0.05$. (B) Tumour latency. Colour code: Blue - PyMT-control (PyMT-*bbb/+* or PyMT-+/+) (n=20), Green - matched PyMT-*bbb/bbb* (n=18), Pink - ad lib PyMT-*bbb/bbb* (n=15). Data are presented as mean+SEM and analysed using linear regression model. * indicates statistical significance at $p<0.05$.

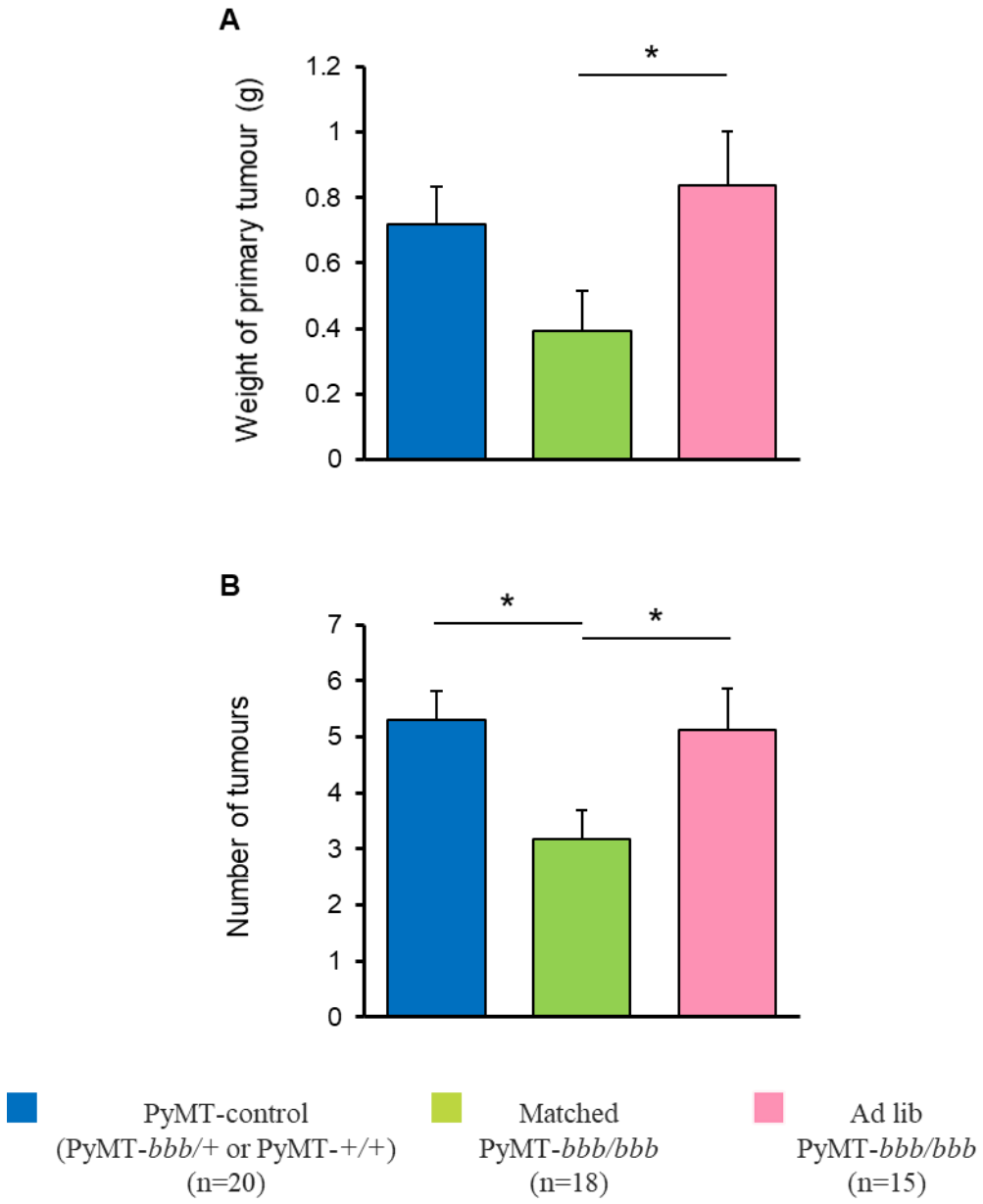

Figure 5.4. Tumour development in PyMT-control, matched PyMT-*bbb/bbb*, and ad lib PyMT-*bbb/bbb* female mice at adulthood. Mammary tumours were dissected from PyMT-control and PyMT-*bbb/bbb* female mice and weighed. (A) Weight of primary tumour. The first palpable tumour with the highest weight is presented as the primary tumour weight. (B) Total number of mammary tumours for each mouse was calculated. Colour code: Blue - PyMT-control (PyMT-*bbb/+* or PyMT-+/+) (n=20), Green - matched PyMT-*bbb/bbb* (n=18), Pink - ad lib PyMT-*bbb/bbb* (n=15). Data are presented as mean+SEM and analysed using linear regression model. * indicates statistical significance at $p<0.05$.

Total tumour burden was determined as the sum of weight of all tumours in each mouse. We observed a significant increase in total tumour burden in ad lib PyMT-*bbb/bbb* mice, compared to PyMT-control ($p=0.008$) and matched PyMT-*bbb/bbb* ($p<0.01$) mice (Figure 5.5.A). Percent tumour burden was calculated as percentage for body weight of each mouse. Matched PyMT-*bbb/bbb* mice exhibited a significant decrease in percent tumour burden, compared to ad lib PyMT-*bbb/bbb* mice ($p=0.006$) (Figure 5.5.B).

5.2.3 No difference in the tumour progression in PyMT-*bbb/bbb* mice

To investigate the impact of pubertal mammary adiposity on tumour progression, haematoxylin-eosin stained sections of primary tumours from PyMT-control, matched PyMT-*bbb/bbb*, and ad lib PyMT-*bbb/bbb* mice were assessed for tumour grade and other pathological markers by veterinary pathologist Dr Lucy Woolford.

Primary tumours were classified into four tumour grades according to their morphology. Late carcinoma is the most advanced tumour stage. No significant difference was observed in tumour grade of the primary tumours in these mice (Figure 5.6). All (100%) of the primary tumours from PyMT-control (20 out of 20 mice) and matched PyMT-*bbb/bbb* mice (17 out of 17 mice) were at late carcinoma. Of all primary tumours dissected from ad lib PyMT-*bbb/bbb* mice, 93.3% were at late carcinoma (14 out of 15 mice) and 6.7% were at early carcinoma (1 out of 15 mice).

Primary tumours were also assessed for cytological atypia. Cytological atypia indicates degree of variation in cell size, nuclear size, nuclear to cytoplasmic ratio, and in cellular and nuclear shape. Four classifications of cytological atypia are: none or minimal, mild, moderate, and marked. All primary tumours from PyMT-control, matched PyMT-*bbb/bbb*, and ad lib PyMT-*bbb/bbb* mice exhibited same degree of cytological atypia and therefore, there was no significant difference between mouse genotypes (Figure 5.7). All (100%) of the primary tumours from PyMT-control mice (20 out of 20 mice), matched PyMT-*bbb/bbb* mice (17 out of 17 mice), and ad lib PyMT-*bbb/bbb* mice (15 out of 15 mice) exhibited marked cytological atypia. Furthermore, primary tumours of PyMT-control, matched PyMT-*bbb/bbb*, and ad lib PyMT-*bbb/bbb* mice were assessed for presence of necrosis. Necrosis, degeneration and death of neoplastic cells within the tumour are key features of malignancy and rapid tumour growth. Primary tumours from PyMT-control, matched PyMT-*bbb/bbb*, and ad lib PyMT-*bbb/bbb* mice exhibited no significant difference in degree of necrosis (Figure 5.8).

Overall, these findings suggest that increased pubertal adiposity is associated with reduced tumour development but does not affect mammary tumour progression.

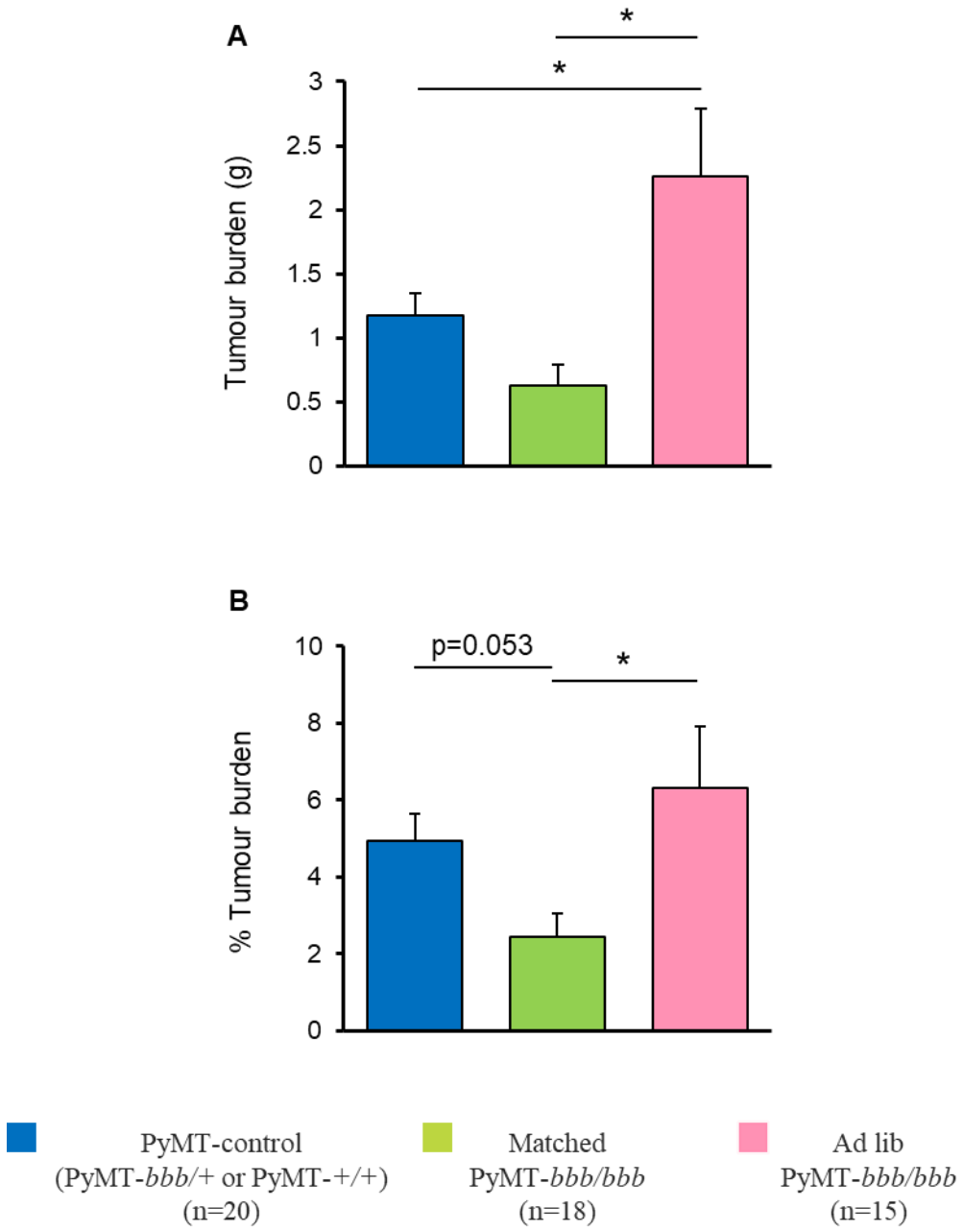

Figure 5.5. Tumour development in PyMT-control, matched PyMT-*bbb/bbb*, and ad lib PyMT-*bbb/bbb* female mice at adulthood. Mammary tumours were dissected from PyMT-control and PyMT-*bbb/bbb* female mice and weighed. (A) Total tumour burden. Total tumour burden was determined by the sum of weight of all tumours in each mouse. (B) Percent tumour burden. It is determined by total tumour burden as a percentage for body weight of each mouse. Colour code: Blue - PyMT-control (PyMT-*bbb*/+ or PyMT-+/+) (n=20), Green - matched PyMT-*bbb/bbb* (n=18), Pink - ad lib PyMT-*bbb/bbb* (n=15). Data are presented as mean+SEM and analysed using linear regression model. * indicates statistical significance at $p<0.05$.

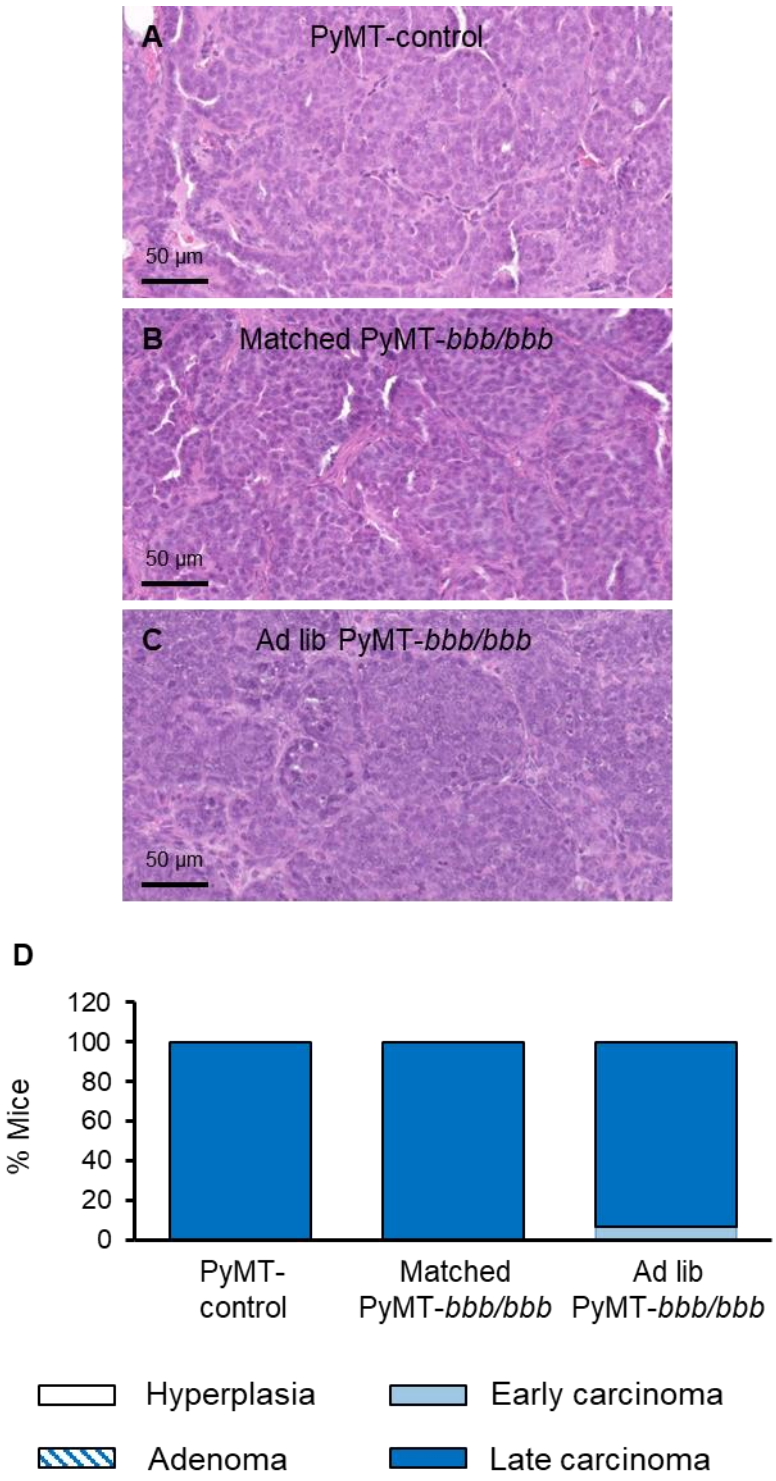

Figure 5.6. Histopathological stage of mammary tumours in PyMT-control, matched PyMT-*bbb/bbb*, and ad lib PyMT-*bbb/bbb* female mice at adulthood. Primary mammary tumours were paraffin-fixed, sectioned, and stained with haematoxylin and eosin. The mammary tumours were classified into four categories – hyperplasia, adenoma, early carcinoma, and late carcinoma. Representative images of haematoxylin eosin-stained primary tumours of (A) PyMT-control, (B) matched PyMT-*bbb/bbb*, and (C) ad lib PyMT-*bbb/bbb* mice. Scale bars: 50 µm. (D) Percent distribution of primary tumours into four histopathological tumour stages. Colour code: Blue - PyMT-control (PyMT-*bbb*/+ or PyMT-+/+) (n=20), Green - matched PyMT-*bbb/bbb* (n=17), Pink - ad lib PyMT-*bbb/bbb* (n=15). Data are presented as percent distribution and analysed using linear regression model with statistical significance at $p<0.05$.

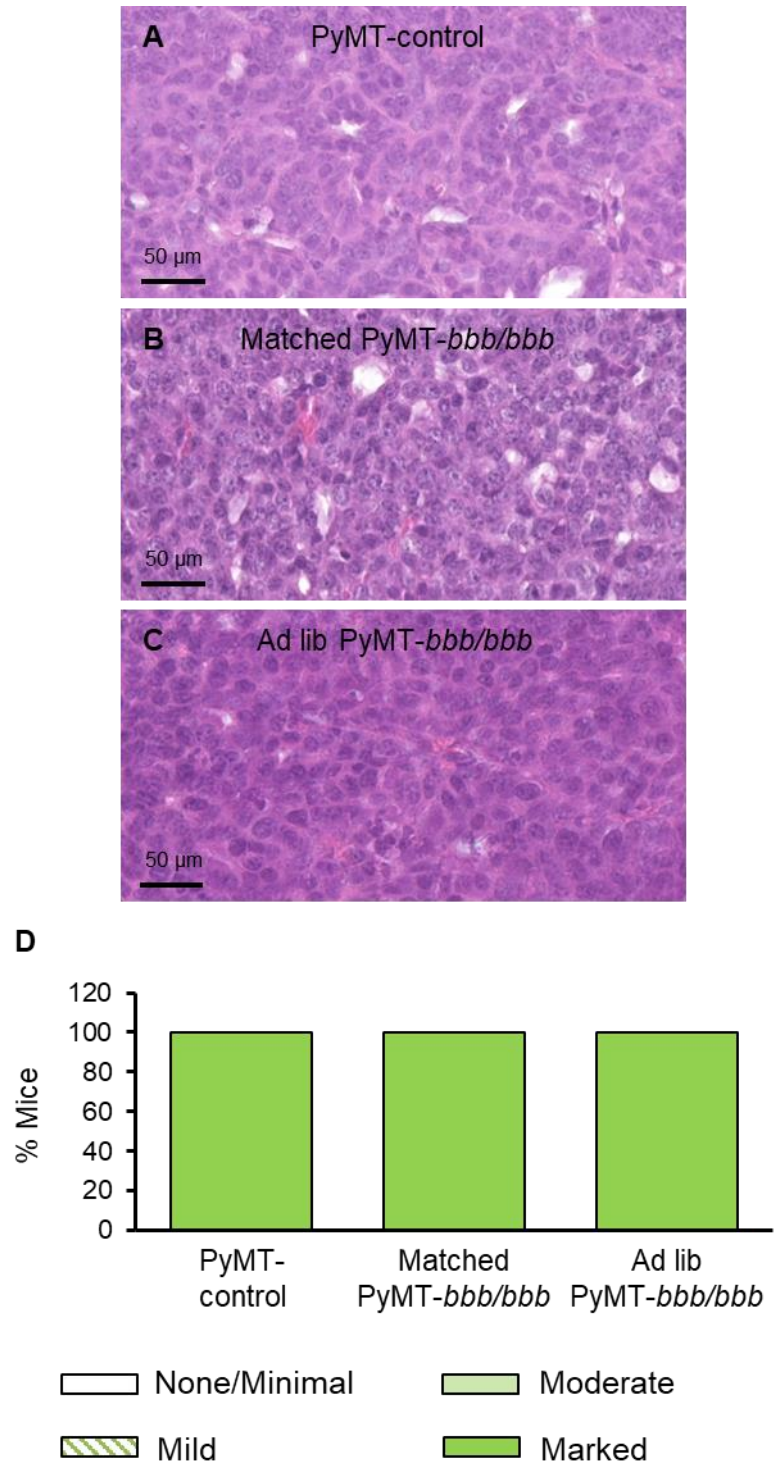

Figure 5.7. Presence of cytological atypia in mammary tumours in PyMT-control, matched PyMT-*bbb/bbb*, and ad lib PyMT-*bbb/bbb* female mice at adulthood. Primary mammary tumours were paraffin-fixed, sectioned, and stained with haematoxylin and eosin. The mammary primary tumours were classified into four categories – no atypia, mild, moderate, and marked atypia. Representative images of cytological atypia present in haematoxylin eosin-stained primary tumours of (A) PyMT-control, (B) matched PyMT-*bbb/bbb*, and (C) ad lib PyMT-*bbb/bbb* mice. Scale bars: 50 µm. (D) Percent distribution of primary tumours into four categories of cytological atypia. Colour code: Blue - PyMT-control (PyMT-*bbb/*+ or PyMT-+/+) (n=20), Green - matched PyMT-*bbb/bbb* (n=17), Pink - ad lib PyMT-*bbb/bbb* (n=15). Data are presented as percent distribution and analysed using linear regression model with statistical significance at $p<0.05$.

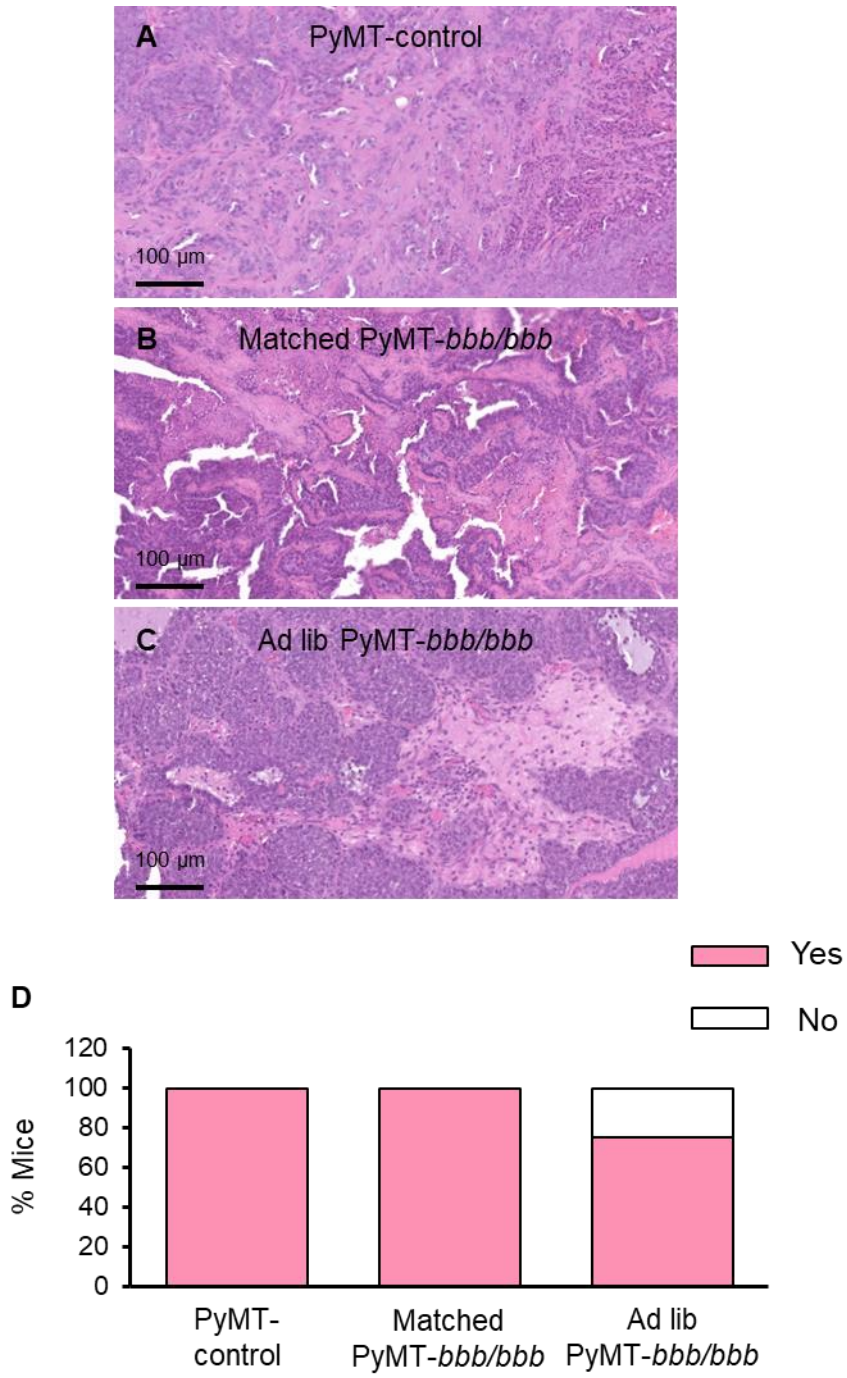

Figure 5.8. Presence of necrosis in mammary tumours in PyMT-control, matched PyMT-*bbb/bbb*, and ad lib PyMT-*bbb/bbb* female mice at adulthood. Primary mammary tumours were paraffin-fixed, sectioned, and stained with haematoxylin and eosin. The mammary primary tumours were assessed for presence of necrosis. Representative images of necrosis present in haematoxylin eosin-stained primary tumours of (A) PyMT-control, (B) matched PyMT-*bbb/bbb*, and (C) ad lib PyMT-*bbb/bbb* mice. Scale bars: 100 µm. (D) Percent distribution of primary tumours for the presence of tumour necrosis. Colour code: Blue - PyMT-control (PyMT-*bbb/+* or PyMT-+/+) (n=15), Green - matched PyMT-*bbb/bbb* (n=15), Pink - ad lib PyMT-*bbb/bbb* (n=4). Data are presented as percent distribution and analysed using linear regression model with statistical significance at $p<0.05$.

5.2.4 Altered abundance of adipokines and proinflammatory cytokines in PyMT-*bbb/bbb* mice

To investigate the impact of perturbation of adipose tissue on the mammary tumour microenvironment, we assessed the gene expression of the most well characterised markers of obesity and tumour development including leptin, adiponectin, IL4, IL6, TNFA, TGFB1, CCL2, CSF1, IGF1, STAT3, and COX2 in mammary tumours by real-time PCR analysis.

Ad lib PyMT-*bbb/bbb* mice exhibited increased expression of mRNA encoding leptin, compared to PyMT-control (p=0.002) and matched PyMT-*bbb/bbb* (p=0.006) mice (Figure 5.9.A). Further, mammary tumours of ad lib PyMT-*bbb/bbb* mice demonstrate significantly increased expression of mRNA encoding IL4, compared to PyMT-control mice (p=0.029) (Figure 5.9.C). Interestingly, matched PyMT-*bbb/bbb* mice exhibited significantly increased expression of mRNA encoding TGFB1, compared to PyMT-control mice (p=0.037) (Figure 5.9.F). No significant difference was observed in the expression of mRNA encoding adiponectin, IL6, TNFA, CCL2, CSF1, IGF1, and COX2 in these mice (Figure 5.9.B, D, E, 5.10.A-C, E). Strikingly, ad lib PyMT-*bbb/bbb* mice exhibited increased expression of mRNA encoding STAT3 in mammary tumours, compared to PyMT-control (p=0.026) and matched PyMT-*bbb/bbb* (p=0.043) mice (Figure 5.10.D).

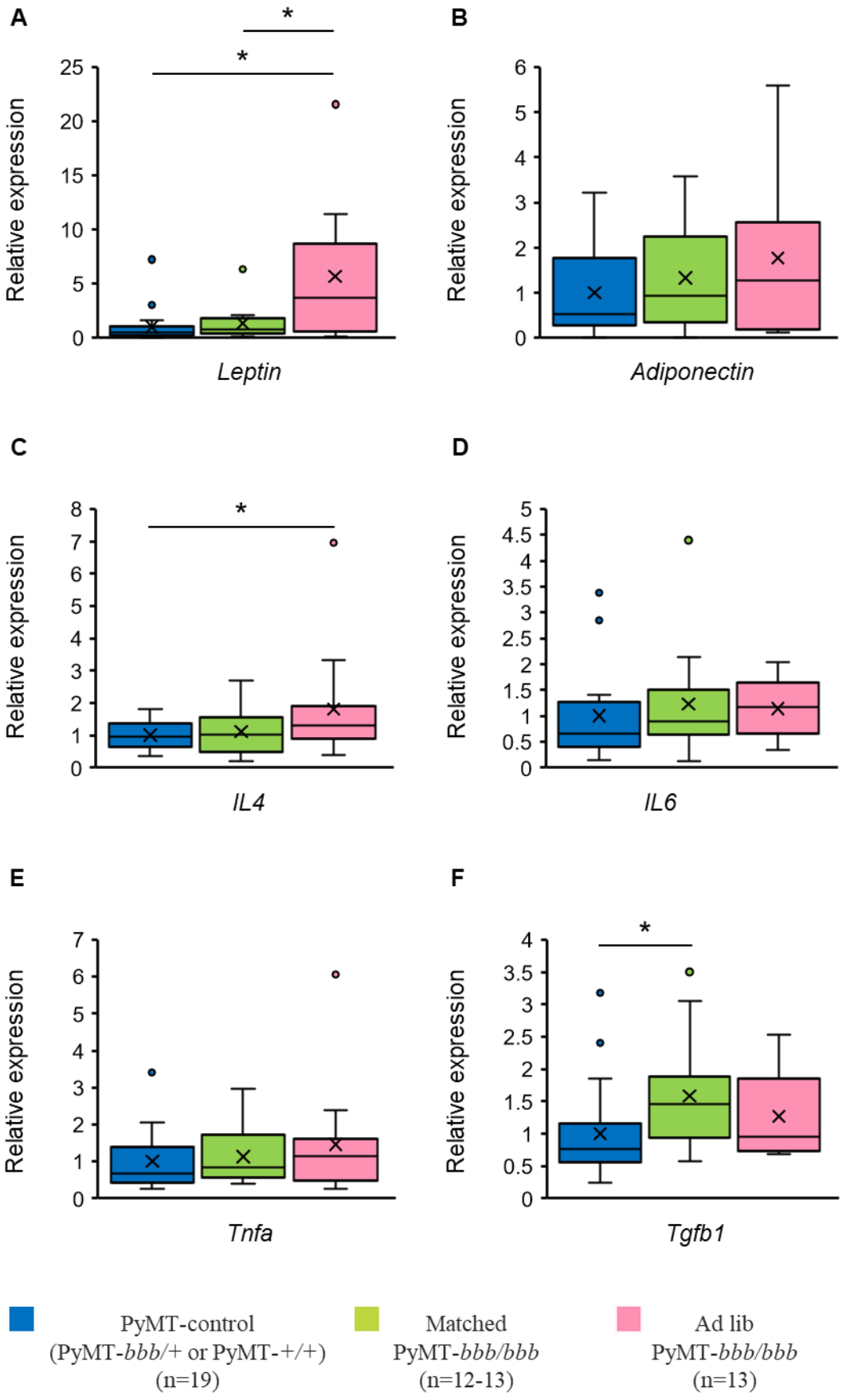
A
B
C
D
E
F
Relative expression
Leptin
Adiponectin
IL4
IL6
Tnfa
Tgfb1
*
PyMT-control
(PyMT-bbb/+ or PyMT-+/+)
(n=19)
Matched
PyMT-bbb/bbb
(n=12-13)
Ad lib
PyMT-bbb/bbb
(n=13)

Figure 5.9. Gene expression profile of adipokines and proinflammatory cytokines in the mammary tumours of PyMT-control, matched PyMT-*bbb/bbb*, and ad lib PyMT-*bbb/bbb* mice at adulthood. Quantification of mRNA encoding (A) leptin, (B) adiponectin, (C) IL4, (D) IL6, (E) TNFA, and (F) TGFB1 in mammary tumours by real-time PCR analysis using comparative Ct method (i.e., 2^(-ΔΔCt) method). The abundance of mRNA was normalised to abundance of mRNA encoding the housekeeping gene *Rpl13a* in each mouse. Colour code: Blue – PyMT-control (n=19), Green - matched PyMT-*bbb/bbb* (n=12-13), Pink - ad lib PyMT-*bbb/bbb* (n=13). *Il4*: interleukin 4; *Il6:* interleukin 6; *Tnfa:* tumour necrosis factor alpha; *Tgfb1:* transforming growth factor beta 1. Data are presented as box-plots with median in between the first quartile and third quartile and analysed using a linear regression model. * indicates statistical significance at $p<0.05$.

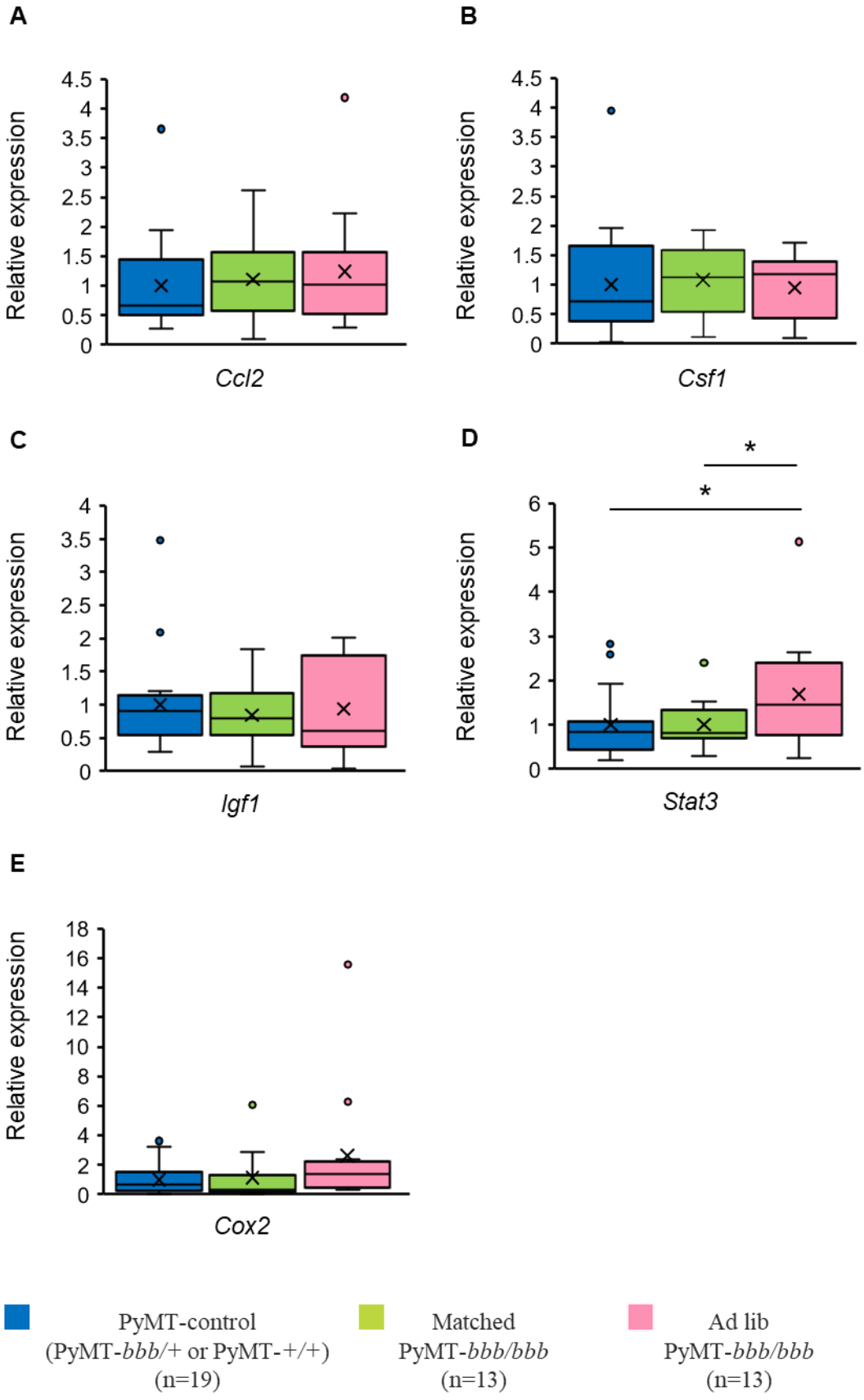
A
Relative expression
Ccl2
B
Relative expression
Csf1
C
Relative expression
Igf1
D
Relative expression
Stat3
*
*
E
Relative expression
Cox2
PyMT-control
(PyMT-bbb/+ or PyMT-+/+)
(n=19)
Matched
PyMT-bbb/bbb
(n=13)
Ad lib
PyMT-bbb/bbb
(n=13)

Figure 5.10. Gene expression profile of adipokines and proinflammatory cytokines in the mammary tumours of PyMT-control, matched PyMT-*bbb/bbb,* and ad lib PyMT-*bbb/bbb* mice at adulthood. Quantification of mRNA encoding (A) CCL2, (B) CSF1, (C) IGF1, (D) STAT3, and (E) COX2 in the mammary tumours by real-time PCR analysis using comparative Ct method (i.e., 2^(-ΔΔCt) method). The abundance of mRNA was normalised to abundance of mRNA encoding the housekeeping gene *Rpl13a* in each mouse. Colour code: Blue – PyMT-control (n=19), Green - matched PyMT-*bbb/bbb* (n=13), Pink - ad lib PyMT-*bbb/bbb* (n=13). *Ccl2:* C-C motif chemokine ligand 2; *Csf1:* colony-stimulating factor 1; *Igf1:* insulin-like growth factor 1; *Stat3:* signal transducer and activator of transcription 3*; Cox2:* cyclooxygenase 2. Data are presented as box-plots with median in between the first quartile and third quartile and analysed using a linear regression model. * indicates statistical significance at $p<0.05$.

5.3 Discussion

The experiments described in this chapter examined the impact of pubertal adiposity on mammary cancer development during adulthood in a mouse model. We demonstrated that matched PyMT-*bbb/bbb* mice exhibited overall better tumour-free survival and reduced tumour development, compared to controls. On the other hand, obese ad lib *bbb/bbb* mice exhibited worse tumour-free survival with increased total tumour burden, and increased expression of mRNA encoding leptin, IL4, and STAT3 in the mammary tumours. Interestingly, matched ad lib PyMT-*bbb/bbb* mice exhibited increased expression of mRNA encoding TGFB1 in the mammary tumours. Overall, our results suggest that increased mammary adiposity during puberty affects mammary cancer development in adulthood, possibly by altering the concentration of adipokines and cytokines in the mammary gland microenvironment in adulthood.

5.3.1 Effect of increased pubertal adiposity on mammary cancer development during adulthood

Matched PyMT-*bbb/bbb* mice with increased pubertal adiposity, compared to PyMT-control mice, exhibited overall better tumour-free survival. This difference was not due to the presence of the *bbb* homozygous mutation, as ad lib PyMT-*bbb/bbb* mice exhibited worse tumour-free survival. Furthermore, ad lib PyMT-*bbb/bbb* mice exhibited increased primary tumour weight, number of tumours, and total tumour burden, compared to matched PyMT-*bbb/bbb* mice. These findings suggest that in this mouse model using the PyMT transgene, which is an aggressive tumour model with 100% penetrance, a subtle change in pubertal adiposity plays a critical role in altering tumour development in adulthood.

We observed no significant difference in histological tumour grade, cytological atypia, and necrosis of the primary tumours from PyMT-control, matched PyMT-*bbb/bbb*, and ad lib PyMT-*bbb/bbb* mice. This suggests that tumour progression was not affected by increased pubertal adiposity. Taken together, these findings suggest that the impact of increased pubertal adiposity in matched PyMT-*bbb/bbb* mice occurs early in tumour development. However, the exact mechanism of this profoundly altered mammary cancer development observed in matched PyMT-*bbb/bbb* mice is yet to be understood.

5.3.2 Effect of increased pubertal adiposity on the mammary tumour microenvironment

Increased expression of mRNA encoding leptin was observed in the tumour microenvironment of ad lib PyMT-*bbb/bbb* mice. This is consistent with previous studies that report increased

circulating leptin with increasing adiposity (322). Breast carcinoma cells express higher levels of leptin and its receptor, than normal mammary cells (375). Further, higher circulating leptin is linked to breast cancer aggressiveness and related to poor prognosis (376, 377). Moreover, leptin has been suggested as a biomarker associated with type, grade, stage, involvement of lymph node, hormone receptors, and recurrence in breast cancer through immunohistochemical analysis (378) Studies on leptin *(ob/ob)* and leptin receptor (*db/db)* mutant mice have consistently supported the role of leptin in mammary cancer development (379, 380) These studies support our findings of increased *leptin* expression in ad lib PyMT-*bbb/bbb* mice with increased incidence of mammary tumours.

Constitutive activation of STAT3 is reported in breast cancer (381). STAT3 is known to affect proliferation and apoptosis (382) Further, in a human epidermal growth factor receptor 2 (HER2) induced mouse model of mammary carcinoma, STAT3 is demonstrated to promote tumour progression (383). Moreover, MMTV-PyMT tumours without STAT3 exhibit impaired immune responses and defective metastasis (384). Interestingly, leptin signalling is reported to be mediated through activation of STAT3, phosphorylated extracellular signal-regulated kinase, and transcript activator protein 1 pathways (385-387). An *in vitro* study (388) demonstrated that leptin increased expression of phosphorylated *Stat3* in the T47D human breast carcinoma cell line. Our findings of increased expression of mRNA encoding STAT3 in obese ad lib PyMT-*bbb/bbb* mice with increased mammary cancer development is consistent with previous studies. However, we did not investigate the expression of phosphorylated STAT3 in the tumours of these mice. Consequently, leptin-STAT3 signalling pathway may be further studied to understand the impact of excess adiposity on mammary cancer development in obese ad lib PyMT-*bbb/bbb* mice.

Increased expression of IL4 in tumours has been reported in several human malignancies, including breast, colon, pancreatic, ovarian, and lung cancer (389-392). It is proposed that IL4 promotes tumorigenesis through an immunosuppressive effect on T cells (393), increased cancer cell proliferation (390), and resistance to apoptosis (394). In contrast, IL4 is also reported to have anti-tumour effects *in vitro* (393). Further, the role of IL4 is proposed to be highly context-dependent, influenced by the cytokine levels and specific population of immune cells in the tumour microenvironment (395). We observed a significant increase in *Il4* expression in ad lib PyMT-*bbb/bbb* tumours. However, the exact role of IL4 in mammary cancer development in these mice is still unknown.

TGFB1 is proposed to act as both stimulatory and inhibitory in tumour development and progression (396-398). The tumour-suppressive effect of TGFB1 inhibits cell proliferation,

induces apoptosis, and suppresses growth factors and production of cytokines and chemokines (396-398). However, with tumour progression, there is an increase in the abundance of TGFB1, which imposes pro-tumorigenic effects including impaired immune responses, promotion of angiogenesis, and metastasis (396-398). Our finding that matched PyMT-*bbb/bbb* mice with increased *Tgfb1* expression in primary tumours, exhibit decreased tumour development, suggests a tumour-suppressive effect of TGFB1 in these mice.

Overall, these findings suggest that obesity in ad lib PyMT-*bbb/bbb* mice creates a tumour-promoting microenvironment that mediates tumour development and survival, possibly by elevating IL4 and activating leptin-STAT3 signalling pathway. On the other hand, the decreased mammary cancer development seen in matched PyMT-*bbb/bbb* mice could potentially be due to an unfavourable microenvironment for tumour development, which helps to protect the mammary gland from tumorigenesis in adulthood.

5.3.3 Limitations and future directions

TGFB1 targets immune cells, including macrophages (399), and macrophages play multiple roles in tumour development in breast cancer (Reviewed in (400)). Therefore, it would be interesting to investigate the impact of TGFB1 signalling on local macrophage populations in primary tumours of PyMT-control, matched PyMT-*bbb/bbb*, and ad lib PyMT-*bbb/bbb* mice. This study did not examine pulmonary metastasis in these mice, which could be investigated in the future. However, significant differences in pulmonary metastasis in these mice are unlikely, as we did not find any difference in the histopathological classification of primary tumours. Moreover, it is important to analyse the expression of phosphorylated STAT3 to unravel the role of leptin-STAT3 signalling pathway in mammary cancer development in our mouse model. Our study suggests that increased pubertal adiposity in matched PyMT-*bbb/bbb* tumour mouse model resulted in reduced mammary cancer development in adulthood. In future, a transplant study will provide further evidence of whether this relationship is the result of changes that have occurred specifically in the mammary gland during puberty. The mammary glands from PyMT-control and PyMT-*bbb/bbb* mice will be transplanted into wildtype female mice lacking the PyMT transgene. These recipient mice will be monitored for tumour latency and tumour development.

5.4 Conclusion

Increased mammary gland adiposity in the PyMT-*bbb/bbb* mouse model is associated with decreased mammary cancer development with greater tumour latency, decreased tumour burden, and overall better tumour-free survival. The significant increase in body weight in ad

lib PyMT-*bbb/bbb* mice in adulthood was associated with shorter tumour latency and increased tumour burden, with a state of chronic inflammation within the tumours. On the other hand, matched PyMT-*bbb/bbb* mice exhibited increased expression of mRNA encoding TGFB1 in the tumours, which possibly suggests a tumour-suppressive role of TGFB1 in these mice. We propose that decreased mammary cancer development in mice with normal adult body weight and increased pubertal mammary gland adiposity, could potentially be due to an unfavourable microenvironment for tumour development. Overall, these findings suggest that increased pubertal adiposity is causative in affecting mammary cancer development in adulthood.

CHAPTER SIX
General discussion and conclusions

6.1 Introduction

Mammographic density, one of the most significant risk factors for breast cancer, is established in girls during pubertal breast development. Adiposity during pubertal growth appears to be a significant factor that impacts adult breast health. Epidemiological studies have consistently shown that increased BMI in adolescence is associated with reduced adult mammographic density as well as reduced lifetime risk of breast cancer. However, the nature of this association and whether there are underlying causal mechanisms are still unknown.

The studies described in this thesis aimed to investigate whether increased adiposity during puberty is causal in mammary gland density and cancer development in adulthood. We have used different mouse models to address this, including the *Alms1 bbb/bbb* model of adiposity and the PyMT tumour model. Results from this thesis suggest that increased mammary adiposity promotes pubertal mammary gland development. Further, increased pubertal adiposity was associated with reduced mammary gland density and cancer development in adulthood. These results provide strong evidence that pubertal mammary gland adiposity induces a long-term effect on the mammary gland microenvironment that alters mammary gland density in adulthood, and subsequently affects mammary cancer development.

The results in this thesis are the first to show in mice that pubertal adiposity is causative in altering mammary gland density and cancer development during adulthood. In this chapter, we highlight the implications of our findings for a new paradigm on the developmental origins of mammographic density and breast cancer risk. We also present opportunities for future research to improve our understanding of the biological underpinning of the relationships between pubertal growth, adult mammographic density, and cancer risk. Finally, we propose key considerations required to understand what optimal adolescent growth for long-term breast health is, and how that can potentially reduce subsequent breast cancer risk in adulthood.

6.2 Pubertal adiposity alters adult mammary gland density

Puberty is a unique stage of breast development that can affect future breast health. Early onset of puberty and thelarche in girls is associated with increased adolescent BMI (104, 106, 108-111). Increased adiposity during childhood and puberty is associated with reduced lifetime breast cancer risk (21-26, 70), whereas early menarche is associated with increased risk (401). The apparent contradiction in the relationship between pubertal adiposity, menarche, and breast cancer risk suggest that pubertal adiposity and menarche affect different biological pathways to alter breast cancer risk.

Mammographic density is proposed to mediate the association of pubertal adiposity with adult breast cancer risk (20, 79, 80). High BMI-percentile in girls at 18 years is associated with reduced mammographic density in adulthood, compared to girls with median BMI-percentile, when adjusted for adult BMI and timing of menarche (88). Higher BMI percentile in adolescence is also associated with reduced risk of breast cancer (71, 89, 90). One study demonstrated that mammographic density mediates the association of childhood BMI with breast cancer risk in premenopausal women (83). However, these studies have demonstrated epidemiological associations; causal relationships between pubertal adiposity with adult mammographic density and breast cancer risk have not been investigated at the biological level.

Previous mouse experiments have shown that pubertal C57BL/6 mice fed high-fat diet exhibit increased body weight and adiposity, reduced mammary epithelial cell proliferation, and stunted mammary duct elongation (318). Further, pubertal C57BL/6 mice fed an obesogenic diet until 20 weeks of age exhibit enlarged mammary adipose tissue deposits, and a less dense and branched ductal tree (402). Importantly, consumption of an extremely high-fat diet is not the same as the normal physiological weight gain that commonly occurs during puberty. Therefore, we used the *Alms1 bbb/bbb* mouse model where mice gain weight eating normal mouse chow to more directly investigate this relationship. Results from this thesis suggest that increased adiposity promotes mammary gland development during puberty and reduces mammary gland density and cancer development in adulthood. This suggests that pubertal mammary gland adiposity induces a long-term effect on the mammary gland microenvironment that alters mammary gland biology in adulthood. We propose that this relationship is restricted to adipose tissue deposition during puberty, not weight gain during adulthood. Ad lib *bbb/bbb* mice exhibited reduced mammary gland density, similar to matched *bbb/bbb* mice, but exhibited increased adult body weight and an obesity-associated state of chronic inflammation within the mammary gland. Critically, this could mean that obesity in adulthood overrides the protective effect of pubertal adiposity on lifetime breast cancer risk.

6.3 Pubertal adiposity is causative in mammary cancer development

The origins of breast cancer are widely recognised to occur early in development, particularly during pubertal breast development (71). Diet during puberty can alter mammary gland development and tumour development (403-405). It is well established that a high-fat diet increases mammary tumour development in rodents, depending upon types of dietary fat and period of exposure (Reviewed in (406)). Further, obesity was found to increase both spontaneous tumours and transplanted tumour burden in mice (407, 408). A high-fat diet increases BMI and therefore, it is usually not possible to investigate how diet and increased

BMI independently affect breast cancer risk (300). However, our study ensured that increased adiposity during puberty was derived from a healthy diet and avoided the confounding factors of a high-fat diet. Results from this thesis demonstrated that increased pubertal adiposity is associated with a greater tumour latency and delayed tumour development in adulthood. This suggests that pubertal mammary adiposity could potentially induce an unfavourable microenvironment for tumour development; and this will protect the mammary gland from tumorigenesis in adulthood. On the other hand, obese ad lib *bbb/bbb* mice exhibited shorter tumour latency and greater tumour burden, with increased expression of mRNA encoding leptin, STAT3, and IL4. We propose that excess adiposity in ad lib *bbb/bbb* mice induced obesity-associated inflammation in the mammary gland microenvironment that increased mammary cancer development in these mice.

The hallmarks of cancer have been described in detail by Hanahan and Weinberg (60, 409). It is still not clear whether pubertal adiposity contributes to these biological hallmarks or follows unknown biological mechanisms to alter mammary cancer development. However, our findings support the epidemiological evidence that high BMI during adolescence is associated with reduced mammographic density and breast cancer risk. Taken together, results from this thesis provide strong evidence that pubertal adiposity is causative in altering mammary gland density and cancer development in adulthood.

6.4 Proposed mechanism

Using the *Alms1 bbb/bbb* mouse model of adiposity, we demonstrated that increased adiposity during puberty is associated with reduced mammary gland density in adulthood, similar to epidemiological studies in women. Understanding and possibly manipulating the link between pubertal adiposity, mammary gland density, and mammary cancer development, could lead to potential interventions during puberty to prevent subsequent breast cancer.

Several factors work in concert to regulate the risk of mammary cancer development including ECM, immune cells, adipokines, and cytokines. Pubertal adiposity and obesity both possibly have different mechanisms to affect mammary cancer development. Adult control mice (*bbb/+* or +/+) with normal adiposity throughout life exhibit mammary gland density with a high degree of stroma and collagen deposition, and increased abundance of macrophages around ducts, compared to mice with increased pubertal adiposity. These factors reflect the histological composition of high mammographic density breast tissue in women. Increased stroma and collagen are the major contributing factors for high mammographic density, and studies have shown that modifications in the stromal composition can cause epithelial cancers (217, 410-

412). ECM present in stroma is consistently shown to promote breast cancer tumorigenesis and progression (413-415). In addition, increased abundance of macrophages around ducts in these mice may also promote increased organisation of collagen around ducts, as macrophages have been identified as key cells in fibrillogenesis of collagen during mammary gland development (229). Further, PyMT-control mice with normal adiposity exhibited overall worse tumour-free survival with greater tumour burden. Therefore, we propose that a pro-tumour microenvironment exists in mammary glands of control mice with high mammary gland density, which subsequently increased mammary cancer development (Figure 6.1.A).

Adult *bbb/bbb* mice with increased pubertal adiposity exhibited reduced mammary gland density, with decreased stroma and collagen deposition around ducts, and decreased abundance of macrophages around ducts. These factors capture the histological composition of low mammographic density breast tissue in women. Matched PyMT-*bbb/bbb* mice with increased pubertal adiposity and normal adult weight had reduced mammary cancer development with overall better tumour-free survival. Although the exact underlying biological mechanism is not known, we propose that the mammary gland microenvironment in these mice is less favourable for tumour development, which decreases mammary cancer development (Figure 6.1.B). However, excess adult body weight in ad lib *bbb/bbb* mice increased the abundance of inflammatory cytokines and adipokines, and increased infiltration of macrophages in the mammary adipose tissue; and obese ad lib PyMT-*bbb/bbb* mice ultimately exhibited overall worse tumour-free survival with reduced tumour latency. We propose that an obesity-associated state of chronic inflammation within the mammary gland of ad libitum fed *bbb/bbb* mice increased mammary cancer development (Figure 6.1.C). However, these proposed mechanisms require critical investigation to unravel the exact mechanisms underlying the relationship of pubertal adiposity, mammary gland density, and mammary cancer development.

6.5 Developmental origins of breast cancer risk

A wealth of research has demonstrated that adverse growth conditions during fetal and childhood development have a significant impact on risk of chronic non-communicable diseases including obesity, diabetes, and heart disease (416). This is known as the 'Developmental origins of health and disease' (DOHaD) paradigm. We propose to adapt the DOHaD paradigm to breast cancer and suggest that mammographic density-associated breast cancer risk has origins in breast development during puberty. Breast cancer, like other malignancies, can be considered a chronic non-communicable disease; molecular and cellular changes precede clinically detectable cancer and can be present many years before a diagnosis. We propose that puberty is a critical developmental window that impacts lifetime breast cancer

risk through affecting mammographic density. We propose that interventions that modify breast development during puberty could have a greater impact on lifetime breast cancer risk than interventions that modify breast cancer risk in later life.

Predominant risk factors have been identified in some cancers, e.g., smoking and lung cancer (417) and human papillomavirus and cervical cancer (418). Currently, there are no preventative measures that can dramatically decrease the incidence of breast cancer. Radical surgery such as prophylactic mastectomy can reduce breast cancer risk, however this is not appealing for the majority of women. The breast cancer prevention guidelines by The American Cancer Society suggest increasing physical activity, limiting alcohol intake, maintaining healthy body weight, eating healthy diet, and avoiding postmenopausal hormone use (419). However, these lifestyle modifications have a minor impact on breast cancer risk, and even after considering these factors, a significant proportion of breast cancer risk remains unexplained (420, 421). Prevention of breast cancer in the future could hinge on a better understanding of the developmental and environmental factors that individually and in combination lead to increased breast cancer risk.

(A) <u>Normal pubertal adiposity and normal adult weight</u>:
High mammary gland density

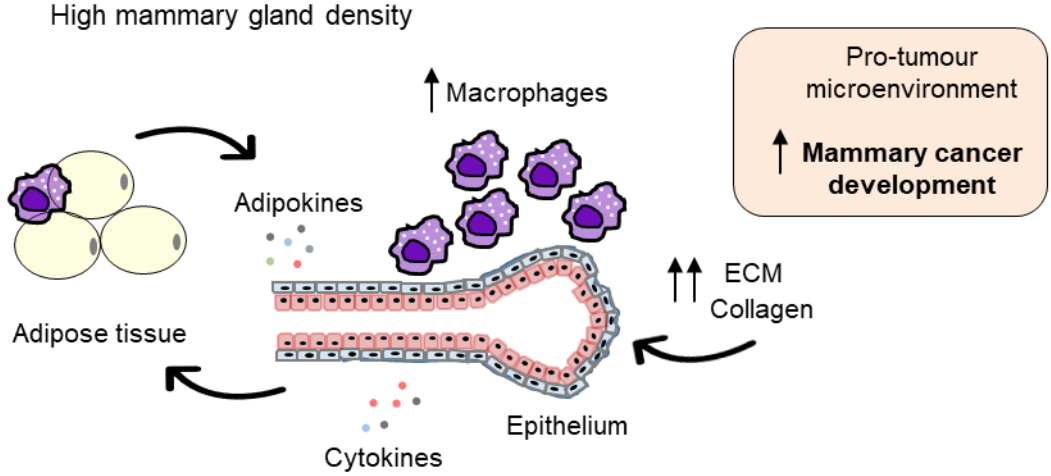

(B) <u>High pubertal adiposity and normal adult weight</u>:
Low mammary gland density

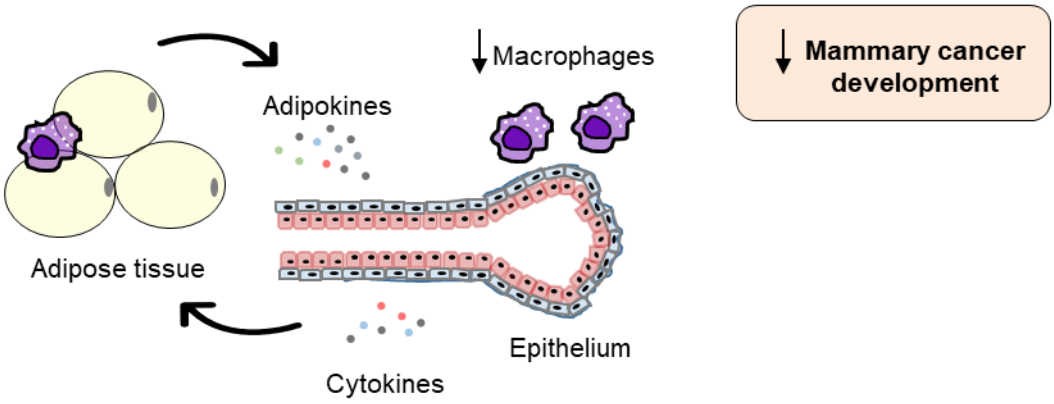

(C) <u>High pubertal adiposity and obese adult</u>:
Low mammary gland density

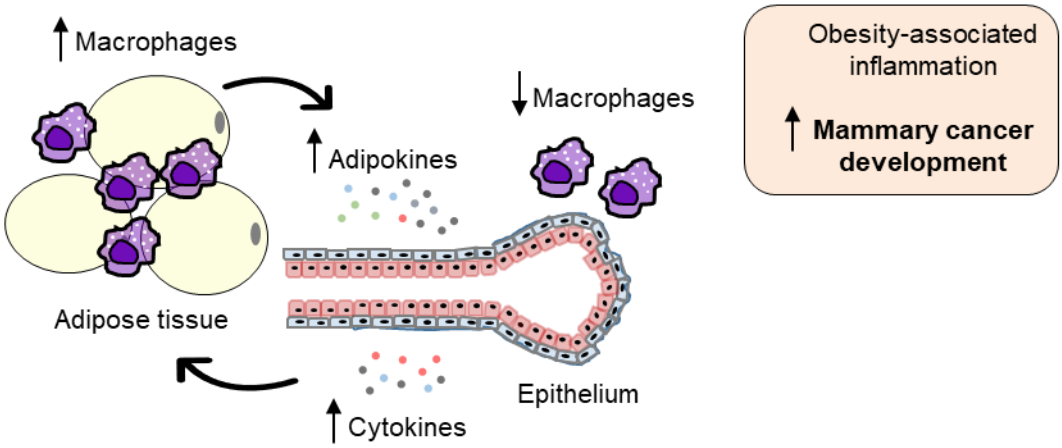

Figure 6.1. Schematic illustration of proposed mechanism linking pubertal adiposity to mammary gland density and mammary cancer development in adulthood. (A) Normal pubertal adiposity resulted in increased mammary gland density and mammary cancer development during adulthood. Normal pubertal adiposity led to increased stroma and collagen around ducts, and increased abundance of macrophages around ducts in the mammary gland during adulthood. These factors created a pro-tumour microenvironment that subsequently increased mammary cancer development. (B) High pubertal adiposity and normal adult weight resulted in low mammary gland density and reduced mammary cancer development in adulthood. (C) Obesity in adulthood increased infiltration of macrophages in the mammary gland adipose tissue and increased adipokines and proinflammatory cytokines. This created an obesity-associated inflammatory state in the mammary glands that led to increased mammary cancer development.

An early first full-term birth is shown to be effective in reducing a woman's lifetime breast cancer risk (422). Compared to nulliparous women, women who had a first full-term pregnancy before the age of 20 had a 50% reduced breast cancer risk (423). This is especially concerning as the average age for a woman's first birth has been steadily increasing over many years. The proportion of women in the US who had a first full-term pregnancy between the ages of 30 and 34 rose 28% and those over 35 years of age rose 23% between 2000 and 2014 (424). Strikingly, women who had a first full-term pregnancy above the age of 33 years were not protected against breast cancer (424).

Mammographic density is a modifiable risk factor (425-428) and contributes to 29% of all breast cancer cases. Breast tissue undergoes rapid changes between menarche and first full-term pregnancy, and risk accumulates most rapidly during this period (429, 430). This makes menarche-to-first pregnancy a window of susceptibility when breast tissue is particularly vulnerable to cancer development (431). Therefore, potential interventions as early as puberty hold promise as significant breast cancer prevention approaches. We have provided evidence that mammographic density could be modifiable during adolescent breast development by pubertal adiposity. We propose that interventions during puberty that reduce mammographic density could be more significant in their impact on adult breast cancer risk than the known impact of mid-term interventions such as age at first full term pregnancy, and late-term lifestyle modifications in adulthood (Figure 6.2).

Nutrition is a major contributing factor for adiposity. In just a few studies, diet during puberty is demonstrated to be associated with mammographic density in adulthood. High intake of red meat at 12-17 years is shown to be associated with increased percent dense area in women (432). However, a clinical study (The Dietary Intervention Study in Children (DISC)) found that dietary intervention to high fibre and low-fat diet during childhood and adolescence is not associated with dense tissue volume and percent dense volume (433). Interestingly, famine exposure at 2-9 years of age was found to be associated with increased percent dense area and decreased nondense tissue area (434). The availability of only a few studies limits the inferences that can be drawn, and therefore further research is required to understand the role of nutrition during puberty in determining mammographic density.

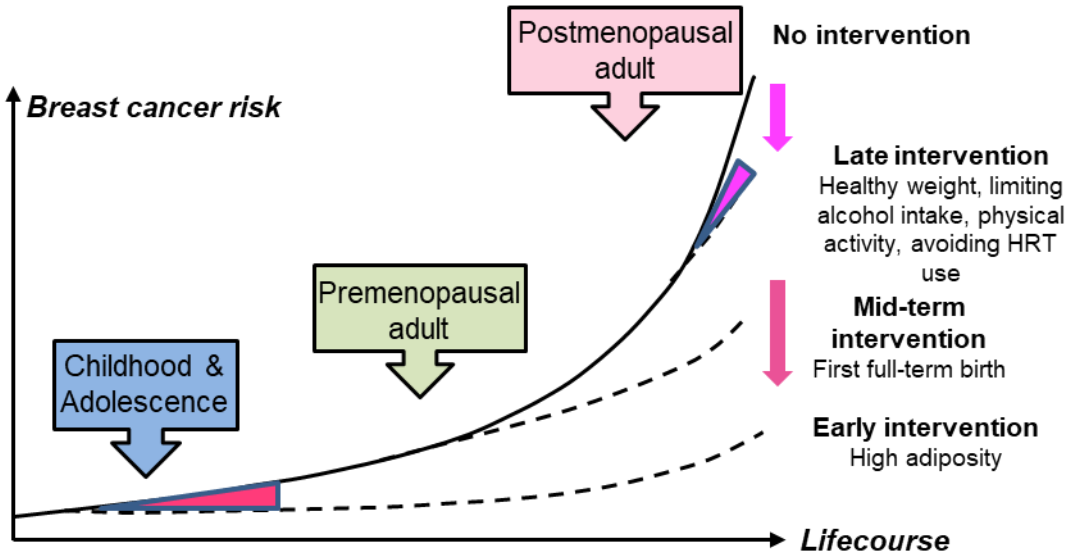

Figure 6.2. Life course model for breast cancer risk. Diagram illustrating the potential significance of interventions during childhood and adolescence to reduce breast cancer risk. We propose that potential interventions targeting pubertal development could be an effective method to reduce mammographic density and subsequent breast cancer risk. An early first full-term pregnancy is also shown to be effective in reducing a woman's lifetime breast cancer risk. Possible interventions during the postmenopausal period include increasing physical activity, maintaining healthy body weight, limiting alcohol intake, and avoiding postmenopausal hormone replacement therapy (HRT) use. Figure inspired by (435).

6.6 What is optimal adolescent growth for long-term breast health?

It is still unknown to what extent adiposity during puberty is healthy or unhealthy. The complex interplay between nutrition, adiposity, and pubertal growth may involve many endocrine and metabolic pathways. As discussed earlier, an appropriate level of adiposity is necessary for the onset of puberty (121). However, too much adiposity is an unhealthy condition, and there is much concern worldwide on the growing problem of childhood obesity, which is known to lead to poor health outcomes in adulthood.

Pubertal girls with excess adiposity have lower circulating concentration of IGF1 (193, 194). IGF1 slows energy expenditure and may induce protein-sparing effects during feeding by indirectly affecting energy metabolism (436-438). This pathway is possibly exaggerated in the condition of excess adiposity, which creates a loop between nutrition and body adiposity. Leptin is suggested to be a crucial link between body adiposity and onset of puberty. Decreased leptin levels are associated with caloric restriction and weight loss (439, 440). Thus, low concentrations of leptin in condition of food deprivation can explain the starvation-induced suppression of HPG axis (441). Further, Kisspeptins and the G-protein coupled receptor-54 system are the recently identified gatekeepers of pubertal development. In the condition of undernutrition, there is marked reduction in central KISS1 tone, which in turn, inhibits the HPG axis (442). Based on these studies, we propose that there exists a crucial link between body adiposity, energy homeostasis, and HPG axis to drive the normal pubertal growth.

The relationship between obesity and pubertal development are quite widely explored. However, the impact of malnutrition or undernutrition is not well studied in this context. Anorexia nervosa is an eating disorder with self-induced food restriction. During puberty, anorexia nervosa causes stunting of growth, arrest of pubertal development, and amenorrhea (443-445). Growth failure in girls with anorexia nervosa has been shown to be related to GH resistance, low serum levels of GH-binding protein, IGF1 and IGFBP3 (446). However, these changes are demonstrated to be reversible with weight gain, a decrease in GH and cortisol levels, and a gradual increase in the levels of thyroid hormones, gonadotropins, and IGF1 (447, 448).

These studies thus, suggest the link between nutrition, adiposity, and pubertal growth. However, the mechanisms through which nutrition, adiposity, and pubertal development interact to determine mammographic density still remains unexplored.

6.7 Future studies

Our experiments suggested a causative role for pubertal adiposity in mammary gland density and cancer development in adulthood. However, the precise molecular mechanisms through which pubertal adiposity affects mammary gland density and cancer development are still far from clear. There are several aspects of the crosstalk between mammary adipose tissue, epithelium, and macrophages in the mammary gland that need to be explored. We found that increased pubertal adiposity altered the abundance of proinflammatory cytokines and adipokines in the mammary gland microenvironment. However, the exact role of these proinflammatory cytokines and adipokines in mammary gland development is still not known. Further, we did not investigate the ovarian hormones, estradiol and progesterone, in pubertal and adult mice. The whole organ culture of mouse mammary gland provides an excellent model to study the effects of hormones on growth, differentiation, and regression of the mammary gland (449). In future studies, whole organ culture of the mouse mammary gland can be employed to study the role of proinflammatory cytokines and adipokines in mammary gland development during puberty and adulthood. Moreover, transgenic and knockout mouse models can be used to investigate the interplay between ovarian hormones, proinflammatory cytokines and adipokines in the mammary gland and their influence on mammary cancer development. High throughput sequencing would be more beneficial to determine entire mechanistic pathways rather than analysis of individual factors mediating the causal mechanism of pubertal adiposity, mammary gland density, and mammary cancer development.

Due to the experimental design of the studies in this thesis, we could not investigate the source of each cytokine in the mammary gland. In future, mammary gland adipose tissue can be isolated from epithelium by laser capture microdissection and levels of proinflammatory cytokines can be analysed in each of these tissue compartments. This will allow us to better understand the intercellular roles of these proinflammatory cytokines in the link between pubertal adiposity, mammary gland density and mammary cancer development.

We have demonstrated that increased pubertal adiposity reduces mammary cancer development in adulthood. However, in future, a transplant study will be key in providing evidence of whether this relationship is the result of changes that have occurred specifically in the mammary gland during puberty. It is also part of our future study to transplant mammary glands from PyMT-control and PyMT-*bbb/bbb* mice into wildtype female mice lacking the PyMT transgene. These recipient mice will be monitored for tumour latency and tumour development. The tumours collected from these mice will be further characterised on the basis of histopathology. Based on the results from chapter five, we hypothesise that the tumours arising

from PyMT-*bbb/bbb* transplanted mammary glands would exhibit delayed tumour development compared to transplanted mammary glands from PyMT-control mice.

Another important future study is to investigate relationships between pubertal BMI and human breast biology. Our laboratory has a unique tissue bank comprised of human non-neoplastic breast tissue from patients undergoing reduction mammoplasty, mastectomy for breast cancer removal, or prophylactic mastectomy. This tissue collection is approved by Human Ethics Committee at the University of Adelaide and The Queen Elizabeth Hospital. The participating patients were asked to complete a comprehensive medical and personal history questionnaire following their breast surgery. This questionnaire included their recalled height and weight at 18 years of age and their current adult BMI. It will be interesting to use this tissue bank to investigate the abundance of CD68-positive and CD206-positive macrophages, expression of Ki67, aromatase, and hormone receptors in the breast tissue collected from women with high BMI at 18 years and normal adult BMI, compared to that collected from women with normal BMI at 18 years and adulthood. Further, these factors can also be analysed in the breast tissue collected from women with high BMI at 18 years and at adulthood. These experiments will enable us to explore the biological differences in breast tissue collected from women who had high adolescent BMI versus low adolescent BMI.

6.8 Conclusions

Our study in a preclinical model is the first to show that breast cancer risk may indeed be modifiable during pubertal breast development. It is the crucial first step in showing that there is a causative link between teenage weight and adult breast cancer risk. Together with epidemiological studies, this research provides the foundation for a new paradigm for the origins of mammographic density and breast cancer risk during pubertal mammary gland development. These studies suggest that there may be an opportunity to prevent breast cancer through manipulating pubertal adiposity (or its associated cellular factors) to modify mammographic density. Future studies are needed to unravel the molecular mechanisms underlying the link between pubertal adiposity, mammary gland density, and mammary cancer development. The knowledge generated will provide fundamental information that will assist in development of novel early life interventions to prevent breast cancer.

CHAPTER SEVEN
Appendices

APPENDIX A

Journal articles

Ghadge AG, Dasari P, Stone J, Thompson EW, Robker RL and Ingman WV (2021). Pubertal mammary gland development is a key determinant of adult mammographic density. Semin Cell Dev Biol. 114:143-158. doi.org/10.1016/j.semcdb.2020.11.011.

Seminars in Cell and Developmental Biology 114 (2021) 143–158

Contents lists available at ScienceDirect

Seminars in Cell and Developmental Biology

journal homepage: www.elsevier.com/locate/semcdb

Pubertal mammary gland development is a key determinant of adult mammographic density

Amita G. Ghadge [a,b], Pallave Dasari [a,b], Jennifer Stone [c], Erik W. Thompson [d,e,f], Rebecca L. Robker [b], Wendy V. Ingman [a,b,*]

[a] Discipline of Surgery, Adelaide Medical School, University of Adelaide, The Queen Elizabeth Hospital, Adelaide, Australia
[b] Robinson Research Institute, Adelaide Medical School, University of Adelaide, Australia
[c] Genetic Epidemiology Group, School of Population and Global Health, University of Western Australia, Perth, Australia
[d] Queensland University of Technology, School of Biomedical Sciences, Faculty of Health, Gardens Point, 4000, Australia
[e] Queensland University of Technology, Institute of Health and Biomedical Innovation, Kelvin Grove 4059, Australia
[f] Translational Research Institute, Woolloongabba 4102, Australia

ARTICLE INFO

Keywords:
Mammary gland development
Puberty
Mammographic density
Adipose tissue
Thelarche
Menarche

ABSTRACT

Mammographic density refers to the radiological appearance of fibroglandular and adipose tissue on a mammogram of the breast. Women with relatively high mammographic density for their age and body mass index are at significantly higher risk for breast cancer. The association between mammographic density and breast cancer risk is well-established, however the molecular and cellular events that lead to the development of high mammographic density are yet to be elucidated. Puberty is a critical time for breast development, where endocrine and paracrine signalling drive development of the mammary gland epithelium, stroma, and adipose tissue. As the relative abundance of these cell types determines the radiological appearance of the adult breast, puberty should be considered as a key developmental stage in the establishment of mammographic density. Epidemiological studies have pointed to the significance of pubertal adipose tissue deposition, as well as timing of menarche and thelarche, on adult mammographic density and breast cancer risk. Activation of hypothalamic-pituitary axes during puberty combined with genetic and epigenetic molecular determinants, together with stromal fibroblasts, extracellular matrix, and immune signalling factors in the mammary gland, act in concert to drive breast development and the relative abundance of different cell types in the adult breast. Here, we discuss the key cellular and molecular mechanisms through which pubertal mammary gland development may affect adult mammographic density and cancer risk.

1. Introduction

Mammographic density (also known as breast density) is an important risk factor for breast cancer [1,2]. It refers to the proportion of radiologically dense fibroglandular tissue present in the breast in comparison to radiologically non-dense adipose tissue, when observed on a mammogram. At the cellular level, epithelial and stromal cells are the predominant cell types in white dense regions and adipocytes are the predominant cell type in dark non-dense regions [3]. Forty years of epidemiological research has demonstrated that women with 'extremely dense' breasts have a 4–6-fold increased risk of breast cancer in comparison to women with 'mostly fatty' breasts, when adjusted for age and body mass index (BMI) [2–6]. Although the association between mammographic density and breast cancer risk is well-established, the molecular and cellular events that lead to the development of mammographic density, and why this is associated with an increased risk of cancer are yet to be elucidated.

Puberty is a critical time for breast development. Endocrine and paracrine signalling drive development of epithelial, stromal, and adipose tissue in the breast [7–12]. As the relative abundance of these cell types determines the radiological appearance of the adult breast, puberty should be considered as a key developmental stage in the establishment of mammographic density. This important stage of growth and development has a significant impact on both adult mammographic density and breast cancer risk. Epidemiological studies have consistently shown an inverse association between pubertal adiposity measures such

* Correspondence to: Discipline of Surgery, The Queen Elizabeth Hospital, DX465702, 28 Woodville Rd, Woodville 5011, Australia.
E-mail address: wendy.ingman@adelaide.edu.au (W.V. Ingman).

https://doi.org/10.1016/j.semcdb.2020.11.011
Received 28 July 2020; Received in revised form 25 November 2020; Accepted 28 November 2020
Available online 11 December 2020

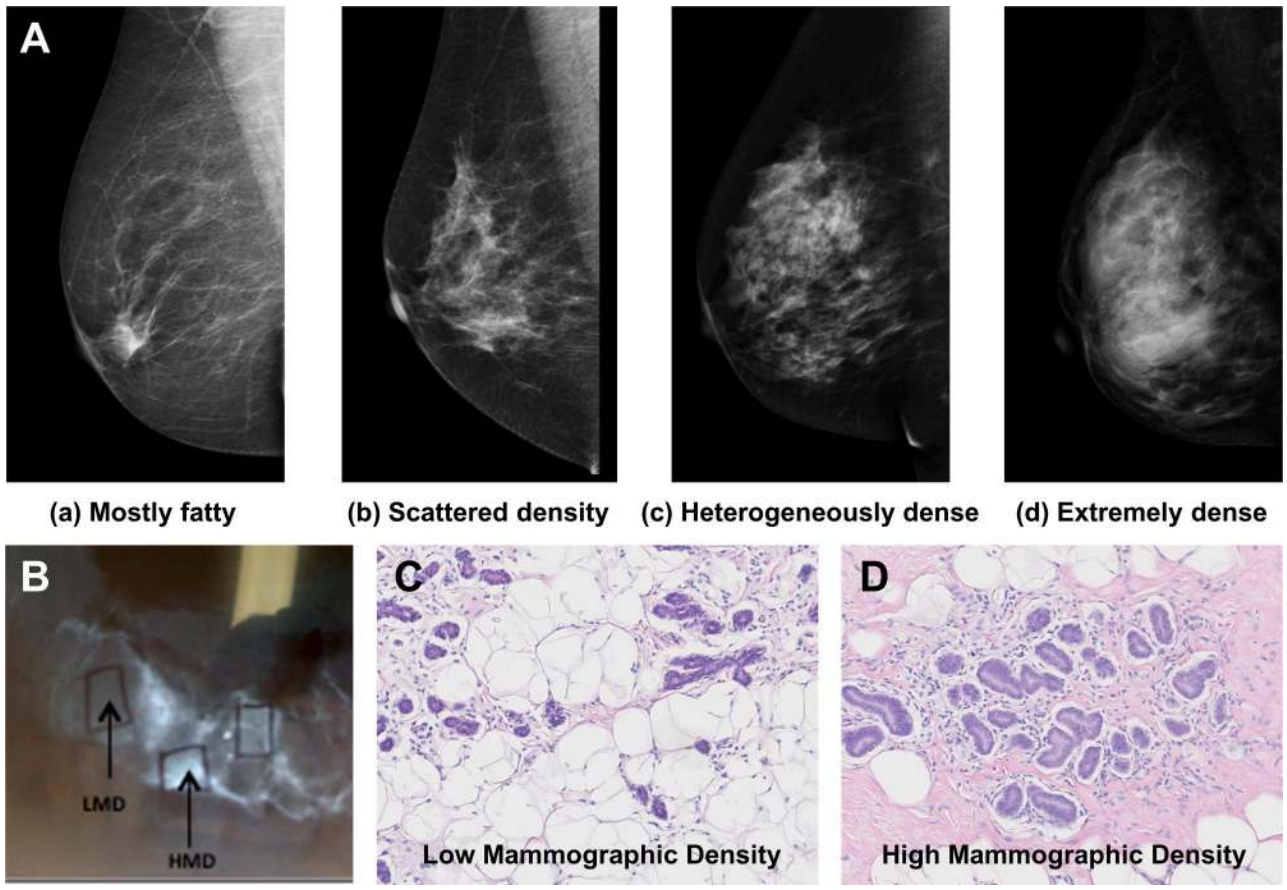

Fig. 1. Mammographic density refers to the radiological appearance of the breast and reflects the relative proportion of fibroglandular and adipose tissue. (A) Four categories of mammographic density are described by the American College of Radiology; (a) mostly fatty, (b) scattered density, (c) heterogeneously dense, and (d) extremely dense, images are reproduced from InforMD (www.informd.org.au). (B) In order to explore the cellular structures associated with high and low mammographic density (HMD and LMD respectively), surgically-excised breast tissue is X-rayed and the image used to guide biopsies of high and low density regions for further analysis. (C, D) Hematoxylin and eosin stained sections of low and high mammographic density respectively from a 35-year old woman undergoing breast reduction surgery. Regions of low mammographic density consist predominantly of adipocytes (large white cells), and regions of high mammographic density consist predominantly of epithelial cells (purple-stained cells) and stroma (pink-stained regions).

as weight, BMI and body shape with percent mammographic density [13–20] as well as adult breast cancer risk [21–26]. Commencement of menstrual cycling – known as menarche, and timing of appearance of breast buds - known as thelarche, also impact adult mammographic density. Later onset of menarche and regular menstrual cycles is associated with increased mammographic density and earlier age at thelarche is associated with lower adult mammographic density [27].

Although these epidemiological studies point to significant associations between pubertal adiposity, adult mammographic density, and breast cancer risk, causal relationships are yet to be established. If it could be shown that adult mammographic density is modifiable during the pubertal growth period, there could be opportunities to intervene during adolescence to reduce lifetime mammographic density-associated breast cancer risk. Therefore, understanding biological mechanisms active during puberty that might drive high mammographic density hold great potential in breast cancer prevention. Here we discuss potential roles of endocrine and paracrine signalling during puberty as well as genetic and epigenetic factors that affect adult mammographic density.

2. Mammographic density is a breast cancer risk factor

The Breast Imaging Reporting and Data System (BI-RADS) developed by the American College of Radiology describes four categories of mammographic density: (a) ‘mostly fatty’; (b) ‘scattered density’; (c) ‘heterogeneously dense’; and (d) ‘extremely dense’ [28] (Fig. 1A). Approximately 8% of women aged 40–74 have breasts classified as ‘extremely dense’ and around 35% have breasts classified as ‘heterogeneously dense’ [29]. Combined, these two categories of density are often termed “high mammographic density” and define what it means for a woman to have “dense breasts”. The cellular components of mammographic density can be identified through image-guided biopsies of X-rayed breast tissue samples (Fig. 1B; [30]). Breast tissue regions with low mammographic density exhibit increased abundance of adipocytes and reduced abundance of epithelium and stroma (Fig. 1C). Conversely, high mammographic density is characterised by abundant stromal and epithelial cells and fewer adipocytes (Fig. 1D).

Thirty nine percent of premenopausal and 26% of postmenopausal breast cancers are attributed to high mammographic density [2]. Mammographic density also masks cancer on a mammogram; dense fibroglandular tissue and breast cancers both appear white on the mammogram, therefore increased mammographic density can reduce the sensitivity of mammography to detect breast cancer [1,31–33]. Early research suggested that the increased risk of breast cancer associated with high mammographic density was the consequence of the masking effect of density [34]. However, the masking effect of mammographic density is only partly responsible for the association of mammographic density with breast cancer risk. A landmark meta-analysis in 2006 demonstrated that women with increased mammographic density, assessed at least 5 years earlier, had a 3.25-fold increased breast cancer

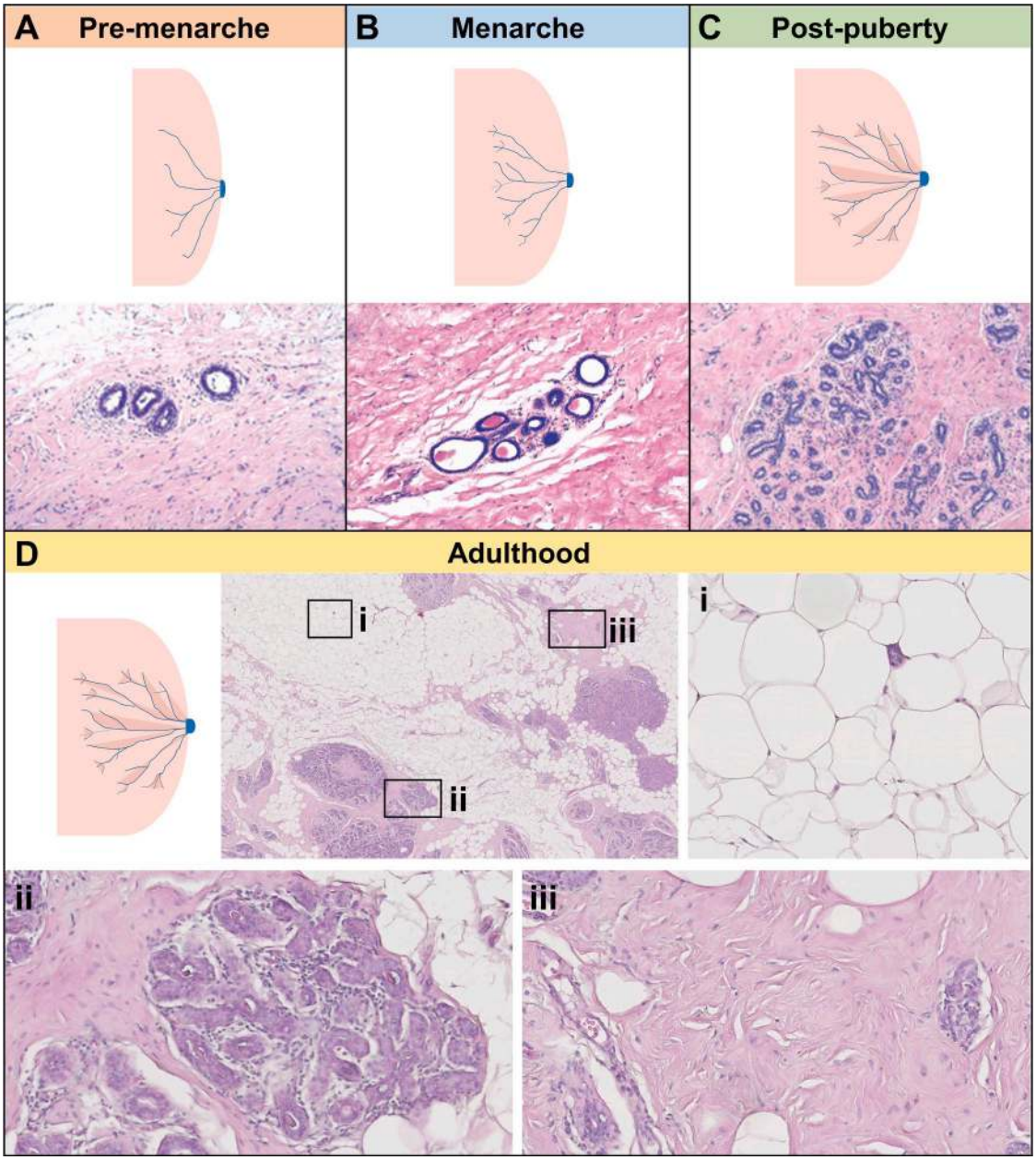

Fig. 2. Development of epithelial, stromal, and adipose tissue in the breasts occurs during puberty. (A-D) Schematic diagrams and hematoxylin and eosin (H&E)-stained sections of ductal morphology in the breast in the pre-menarche, menarche, post-puberty stages, and adult stages respectively. (A) H&E-stained section is breast tissue of an 11-year old pre-menarcheal girl with no lobular differentiation; (B) H&E-stained section is breast tissue showing initiation of lobular differentiation and development of intralobular stroma in an 11-year old girl at menarche; (C) H&E-stained section is breast tissue showing lobular structures observed in the follicular phase of the menstrual cycle in a 15-year old girl; and (D) H&E-stained sections are of breast tissue from a 27-year old woman undergoing mastectomy for inherited high breast cancer risk of unknown genetic origin, boxes show magnified regions predominantly containing (i) adipocytes, (ii) epithelial cells, and (iii) stroma. H&E-stained sections in A and C are reproduced from Hoda et al., Rosen's Breast Pathology 3rd edition, Wolters Kluwer Health Inc, 2008; H&E-stained section in B is reproduced from Hoda et al., Rosen's Diagnosis of Breast Pathology by Needle Core Biopsy 3rd edition, Wolters Kluwer Health Inc, 2010.

risk, in comparison to women of similar age with low mammographic density [4]. In another study, the association between high mammographic density and breast cancer risk remained intact for an average of 7 years after mammographic screening [35].

High mammographic density appears to be associated with an increased risk of all breast cancer subtypes although there are still mixed findings in the literature (comprehensively reviewed by [36]). Breast cancer is 5 times more likely to develop in dense breast tissue regions compared to non-dense regions [37]. An autopsy study of women without clinically detectable breast cancer demonstrated that precancerous microscopic columnar cell lesions are found in 1 of 4 women with dense breasts [38]. This suggests that the cellular and molecular components that comprise high mammographic density could be associated with a pro-tumorigenic microenvironment that increases the susceptibility of the breast to all cancer subtypes [3,39]. The breast is a highly heterogeneous tissue containing 3 distinct tissue compartments; (1) epithelium (containing epithelial cells), (2) stroma (containing a combination of fibroblasts, immune cells, and extracellular matrix), and (3) adipose tissue (containing adipocytes and immune cells). All of these cell types, as well as the extracellular matrix, contribute to the mammographic density of the breast, and could also affect breast cancer risk. However, the molecular and cellular mechanisms that link high

Table 1
Summary of studies reporting association of early life growth measures with mammographic density. Somatotype assessment is based on 9-level figure pictogram, participants recall the figure that best represented their body shape at a particular age (1 represented extremely lean and 9 represented extremely obese). The correlation of recalled somatotype and BMI measured at approximately same ages range from 0.60 to 0.75 [286]. BMI Z-scores are BMI expressed as a Z-score relative to Centres for Disease Control and Prevention (CDC) 2000 growth charts [287]. Breast water is the water content of the breast measured by magnetic resonance imaging, provides measurement of amount of fibroglandular breast tissue, without exposure of young women to radiation [288]. Breast water is strongly correlated to mammographic density [289]. MRI: Magnetic resonance imaging; DXA: Dual energy X-ray absorptiometry.

Reference	Number of participants	Growth measure	Age at growth measure	Mammographic density measure	Menopausal status at mammographic density assessment	Association of adiposity with mammographic density
Samimi et al. [13]	1398	Recalled somatotype	5, 10 years	Percent mammographic density	Pre-, Post-	Inverse association
Sellers et al. [14]	1893	Recalled somatotype	12 years	Percent mammographic density	Pre-, Post-	Inverse association
Jeffreys et al. [16]	608	BMI	Young adult at University	Percent mammographic density	Pre-, Post-	Inverse association
Lope et al. [17]	3557	Self reported relative weight	Before menarche	Percent mammographic density	Pre-, Post-	Inverse association
McCormack et al. [18]	1298	BMI	2–53 years	Wolfe grade	Peri-	Inverse association
Andersen et al. [19]	13,572	BMI	7–13 years	Mixed/dense or fatty	Post-	Inverse association
Yochum et al. [81]	Review of 9 epidemiologic studies	Direct measurement or self-reported BMI, recalled somatotype relative to peers	$\leq$ 18 years	Percent mammographic density	Pre-	No association
Rice et al. [82]	1531	Recalled somatotype	Before menarche, two years after menarche, 18–20 years	Percent mammographic density	Pre-, Post-	No association
Bertrand et al. [84]	182	Age-specific BMI Z-scores	8–10 years	Percent mammographic density (MRI)	Pre-	Inverse association
Boyd et al. [85]	400	Measured weight	15–30 years	Percent breast water (MRI)	Pre-	Inverse association
Alexeeff et al. [88]	24,840	BMI-percentile	18 years	Percent mammographic density	Pre-, Post-	Inverse association
Novotny et al. [98]	113	BMI	10–16 years	Percent fibroglandular volume (DXA)	Adolescence	Inverse association

mammographic density with increased breast cancer risk are yet to be elucidated.

The prevalence of high mammographic density in the population is greatest in younger women and gradually decreases with increasing age [29]. Studies have shown that percent mammographic density decreases an average of 1% per year [40,41] and more (~ 5%) over menopause [41]. High mammographic density is associated with increased breast cancer risk across all age groups, with the strongest association in premenopausal women and women receiving postmenopausal hormone therapy [42]. Although mammographic density declines as women age, young women with high density tend to have high density throughout life relative to their peers [43,44]. Therefore, mammographic density tends to be at its highest in young women following breast development during puberty, and this sets the trajectory for mammographic density over the life course.

3. Pubertal breast development

Puberty is a critical time for breast development when endocrine and paracrine factors drive development of epithelial, stromal, and adipose tissue in the breast [7–12,45] (Fig. 2). Prior to puberty, the mammary gland consists of a rudimentary framework, with ductal elongation occurring at a rate proportional to general growth of the body [46]. At this stage, the epithelium is two-layered, and the dense supporting stroma can be distinguished from the less dense periductal connective tissue, with these different tissue compartments having been established around the age of 8 months [47]. Thelarche occurs prior to menarche. During puberty, with activation of the hypothalamus and pituitary gland leading to increased secretion of ovarian, adrenal, and somatotropic hormones, the rudimentary mammary gland begins to show active responses and there are changes in both the epithelium and the stroma [48]. Solid epithelial buds form along the already laid ducts, which with the progression of development become canalised [46]. The growth and branching of the solid epithelial buds are supported by proliferation of connective tissue that replaces the fatty tissue [47]. This results in the formation of groups of small ductules surrounded by loose connective tissue, which finally form typical terminal duct lobular structures seen by the end of puberty. After the completion of puberty, there is minimal development in the epithelium and stromal components of the adult breast until the first pregnancy [48]. The adult breast is thus comprised of three broad tissue compartments; epithelium, stroma and adipose tissue. As the relative abundance of these cell types determines the radiological appearance of the adult breast, puberty therefore can be considered as a key developmental stage in the establishment of mammographic density.

4. Adiposity, mammographic density, and breast cancer risk

There is compelling evidence of associations between measures of adiposity over the life course with adult mammographic density and breast cancer risk. However, the relationships are complex; increased adiposity at different developmental stages affects breast cancer risk

Table 2
Summary of studies reporting association of timing of puberty onset with mammographic density. DXA: Dual energy X-ray absorptiometry.

Reference	Number of participants	Timing of puberty onset	Mammographic density measure	Association of pubertal stages with mammographic density
Lope et al. [17]	3557	Menarche	Percent mammographic density	Positive association
McCormack et al. [18]	1298	Menarche	Wolfe grade	Positive association
Schoemaker et al. [27]	1105	Menarche	Percent mammographic density, absolute dense area	Positive association
		Thelarche	Percent mammographic density	
		Pubertal tempo	Absolute dense area	
Butler et al. [92]	801	Menarche	Percent mammographic density	Positive association
Dite et al. [93]	571 monozygotic, 380 dizygotic	Menarche	Dense area	Positive association
Dorgan et al. [94]	176	Menarche	Percent dense breast volume	No association
Heng et al. [95]	803	Menarche	Percent mammographic density	No association
Titus-Ernstoff et al. [96]	144,018	Menarche	Dichotomised as dense versus not dense	Positive association
Tehranifar et al. [97]	191	Menarche	Dense area	Inverse association
Novotny et al. [98]	113	Menarche	Adolescent percent fibroglandular volume (DXA)	Positive association
Houghton et al. [99]	182	Pubertal tempo	Percent dense breast volume	Positive association

differently. Adiposity is often expressed in terms of BMI, and calculated as the ratio of weight (in kilograms) to square of height (in metres). In the literature linking pubertal growth measures with adult mammographic density, weight and recalled body shape or somatotype are also used as measures of adiposity. The association between BMI and mammographic density is dependent on how mammographic density is expressed (percent or absolute) and measured (area or volume). Increased BMI often increases breast size [49–51] and the relative abundance of non-dense adipose breast tissue compared to dense fibroglandular tissue influences percent mammographic density simply by its calculation. BMI has been shown to be inversely associated with absolute dense area, which is the two-dimensional dense tissue area projected on the mammogram, but positively associated with dense volume, which takes into account the thickness of dense tissue [52–55]. This highlights the importance of adjusting for confounding adiposity measures when investigating associations between mammographic density and breast cancer risk.

Adult BMI affects breast cancer risk, however the direction of this relationship varies by menopausal status. Premenopausal women with high BMI have lower risk of breast cancer, but postmenopausal women with high BMI have increased risk [56,57]. In obese premenopausal women, increased frequency of anovulatory menstrual cycles results in reduced exposure to ovarian hormones, which may contribute to the reduced risk of breast cancer [57]. On the other hand, there can be an increased concentration of oestrogen in obese postmenopausal women due to increased aromatisation of adrenal androgens in adipose tissue, which increases breast cancer risk [58]. Obesity also increases inflammatory markers in adipose tissue which could drive increased breast cancer risk [59–64].

Several studies have shown an inverse association of pubertal body adiposity with breast cancer risk [21–26], however, there are other studies that do not support this association [65–67]. Prospective data from a British birth cohort [68,69] showed that women diagnosed with breast cancer had been consistently thinner during childhood than women without breast cancer [70]. Interestingly, a post-hoc analysis within the earlier Nurses' Health Study showed that gain in body adiposity between ages 5–10 years was associated with lower postmenopausal breast cancer risk, but gain in body adiposity between ages 10–20 years was associated with greater risk [71]. Epidemiological studies show that excess body adiposity or abnormal leanness in adolescents, both associated with decreased risk of breast cancer, also have an association with ovulatory dysfunction [72–77]. With abnormal leanness, child gymnasts, athletes, and ballet dancers who commonly experience delayed menarche and irregular menstrual cycles, have reduced breast cancer risk [78]. Although the biological basis of the association between childhood and pubertal adiposity and adult breast cancer risk is not clearly understood, it may be mediated through mammographic density [20,79,80].

There is a growing body of evidence for a relationship between pubertal growth measures and adult mammographic density (Table 1). A number of studies show consistent inverse associations between pubertal adiposity using measures such as BMI, weight and recalled body shape, and percent mammographic density in adult women when adjusted for adult BMI [13,14,16–19], while there are few studies that oppose this association [81,82]. One study demonstrated that mammographic density mediates the association of childhood BMI with breast cancer risk in premenopausal women [83]. In a register-based cohort study, the significant inverse association of BMI at age 13 with breast cancer risk was weakened when adjusted for mammographic density [19], which further supports the notion that mammographic density could mediate the association between pubertal BMI and breast cancer risk. Other studies have suggested the mediating effect of mammographic density on the association of pubertal adiposity with breast cancer risk is weak [15]. However, these studies have examined mammographic density in older, predominantly postmenopausal women where the impact of pubertal growth could be mitigated by other factors during adulthood.

Mammographic density in girls and younger women has not been well characterised because routine radiographic screening is not implemented until age 40 or older. When mammographic density is measured by magnetic resonance imaging (MRI) in women aged less than 30, it is found to be inversely associated with childhood body size [84,85]. A limitation in some studies investigating relationships between pubertal BMI and adult mammographic density is that the pubertal BMI is self-reported, however, the accuracy of this is thought to be reasonably good [86]. A further degree of caution is needed when assessing pubertal body adiposity using the adult BMI scale. Weight and height can change in adolescents as part of normal pubertal growth and development. Therefore, it is important to use a BMI scale that is age appropriate, such as BMI-percentiles [87]. Compared to the median BMI-percentile (20.7 kg/m^2), a BMI over 22.3 kg/m^2 (75th BMI-percentile) at age 18 is associated with a 45% decrease in adult mammographic density, adjusted for adult BMI and timing of menarche [88]. Higher BMI percentile in adolescence is also associated with reduced risk of breast cancer [71,89,90]. Overall, these studies demonstrate that increased pubertal body adiposity is associated with reduced mammographic density and breast cancer risk in adult women.

5. Timing of puberty onset affects adult mammographic density

In humans, puberty is marked by maturation of reproductive organs, linear growth acceleration, development of secondary sex characteristics, and, in females, the occurrence of menarche. The transition into puberty is driven by two physiological processes: gonadarche and adrenarche. In females, gonadarche is the growth and maturation of the ovary with secretion of oestrogen and progesterone, initiation of ovulation, and menarche. Adrenarche, which typically precedes gonadarche, is associated with increased secretion of adrenal androgens, such as dehydroepiandrosterone (DHEA), dehydroepiandrosterone sulphate (DHEAS), and androstenedione [91]. In females, increased secretion of ovarian and adrenal hormones cause thelarche and menarche. The age at onset of puberty and the time interval between thelarche and menarche, known as pubertal tempo, are dependent on many factors and highly varied between individuals.

Onset of pubertal breast development, onset of menstrual cycling, and pubertal tempo, all impact adult mammographic density (Table 2). Most studies analysing the association of age at puberty onset with adult mammographic density have utilised age at menarche [17,18,92–97]. A recent study [27] found that later onset of menarche and later onset of regular cycles are associated with increased mammographic density. Most studies show a positive association between age at menarche with mammographic density [17,18,27,92,93,96,98], but not all [94,95,97]. Similarly, age at thelarche and pubertal tempo are also found to be associated with adult mammographic density. Early age at thelarche has been shown to be associated with lower adult mammographic density [27]. Women who experienced a longer interval between thelarche and menarche (ie tempo), and between thelarche and regular menstrual cycles, have increased dense breast area, independent of age at onset of menarche [27]. Women whose pubertal tempo was 2.9 years or longer, had 40% higher percent dense breast volume than women whose pubertal tempo was less than 1.6 years [99].

Childhood weight is likely to be an important factor in the association between puberty onset and adult mammographic density [18,27,98]. Multiple longitudinal and cross-sectional studies demonstrate that girls with higher body adiposity during childhood, undergo earlier pubertal development [100–104]. A recent pooled analysis of five cohort studies [100,102,105–107] indicated that the proportion of obese girls with early puberty was significantly greater than girls with average weight [108]. A number of studies add support to the notion that increased adiposity may be a significant driving factor for early onset of puberty in girls [109–111]. However, the relationship between excess adiposity and early menarche is not universal. A meta-analysis based on two cohorts [112,113] indicated no statistical difference in the age of menarche between obese and normal-weight girls. Another study reported no correlation between age at menarche and pubertal BMI [114]. Like menarche, onset of thelarche is also dependent on body adiposity during puberty. Studies have shown that girls with thelarche exhibit greater body adiposity compared to age-matched girls without thelarche [102,104], and similarly, that girls with excessive adiposity more commonly have earlier thelarche compared to girls with normal BMI [115]. However, more accurate assessment of breast development in obese girls is needed, as excessive subcutaneous adiposity in the breasts can be mistaken for breast development and thus, errors can occur in estimating the onset of puberty [116].

Despite some minor controversy around the relationship between obesity and early menarche, it is clear that a certain amount and distribution of adipose tissue is necessary for the onset of menarche [117] and increased body adiposity is associated with earlier pubertal development [100–104]. Body adiposity is thought to increase in mammalian females during puberty as it guarantees a healthy future pregnancy and maternal survival [113]. Interestingly, adipose tissue localised to the gluteofemoral depots is associated with onset of menarche, and this specific fat deposit appears to be more closely associated with puberty initiation than the amount of total body fat [118–120]. Thus, adiposity is a significant regulator of puberty onset in healthy children affecting the timing of thelarche and menarche (Fig. 3). In turn, these key pubertal milestones, and the time interval between them, appear to affect the relative abundance of fibroglandular and adipose tissue within the breast. Pubertal changes in mammary gland development may persist into adulthood where they are observed on a mammogram as altered mammographic density.

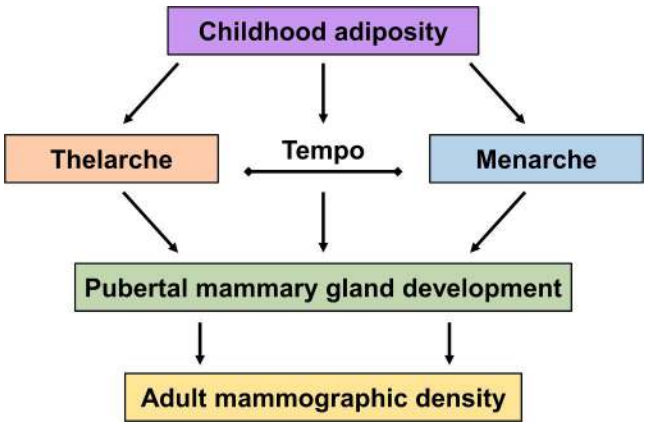

Fig. 3. Puberty is a key developmental stage in the establishment of adult mammographic density. Adiposity during childhood affects the timing of thelarche, menarche, and the time interval between these developmental stages (tempo). These factors collectively affect pubertal mammary gland development, which in turn affects the establishment of adult mammographic density.

6. Endocrine regulators of pubertal breast development and mammographic density

The onset of puberty and mammary gland development is a consequence of activation of the hypothalamic-pituitary axes, with the timing influenced by nutrition and genetic factors that affect adipose tissue deposition (Fig. 4). The hypothalamus is activated by the production of kisspeptin resulting in the release of gonadotropin releasing hormone (GnRH) and growth hormone-releasing hormone (GHRH). In females, the anterior pituitary secretes growth hormone (GH) that acts on the liver to form the hypothalamic-pituitary-somatotropic axis; and adrenocorticotropic hormone (ACTH) that stimulates the adrenal gland to form the hypothalamic-pituitary-adrenal axis. In addition, luteinising hormone (LH) and follicle-stimulating hormone (FSH) act on the ovaries to form the hypothalamic–pituitary–gonadal (HPG) axis. FSH promotes ovarian biosynthesis of oestrogen and LH induces ovulation [121,122]. Rising oestrogen acts on the hypothalamus creating a negative feedback loop in this cycle [123]. Breast development typically starts around 9 years of age and is well-progressed by the time of menarche [124–127]. Thus, breast tissue in pre-pubertal and early pubertal girls is exposed to relatively lower levels of estradiol [128]. However, increased body adiposity is shown to affect the abundance of sex hormones in girls. Increased total and free testosterone, in association with lower concentration of sex hormone binding globulin (SHBG), and higher fasting insulin, have been reported in peripubertal obese girls [129]. In addition, around the time of thelarche, girls with higher BMI had lower circulating concentration of estradiol [124].

6.1. Sex hormones

Few studies have investigated the role of peripubertal hormones on determination of adult mammographic density. Irrespective of menarche status, oestrogens [85,130–134], progesterone [85,130,132,134], testosterone [85,131,133–141] and androstenedione [131,135,138,141,142] measured during puberty were found to be non-significantly associated with mammographic density in adult

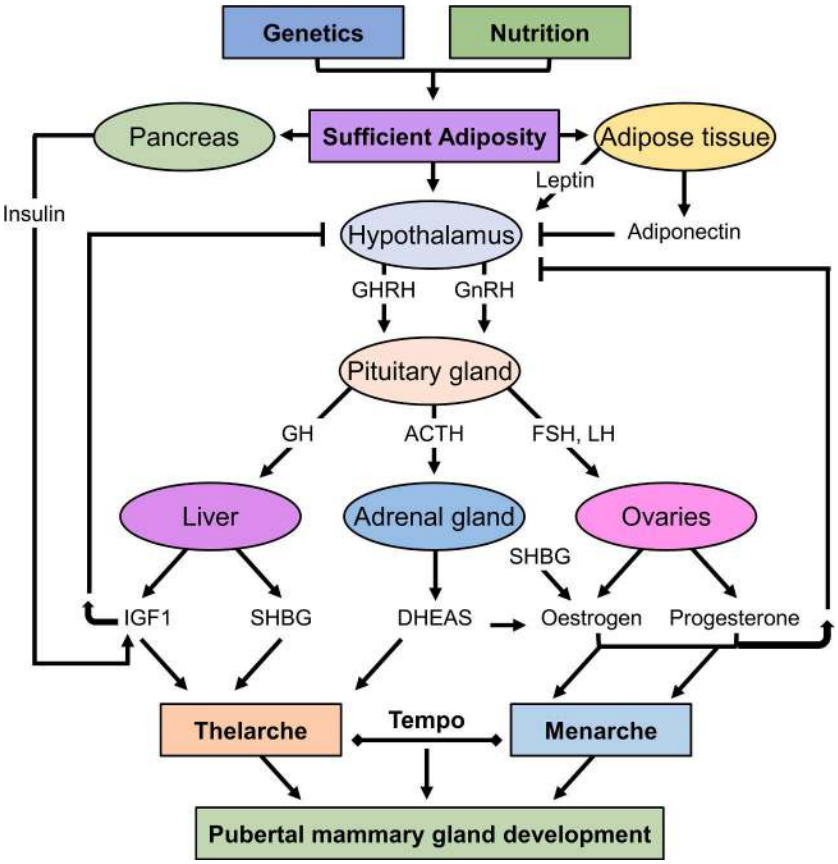

Fig. 4. Schematic diagram of the factors that initiate pubertal mammary gland development in girls. Nutrition and inherited genetic factors regulate the abundance of childhood adipose tissue and govern secretion of insulin by the pancreas, secretion of leptin, and adiponectin by adipose tissue, and activation of hypothalamic-pituitary axes. Activation of the hypothalamic-pituitary-somatotropic axis results in secretion of growth hormone-releasing hormone (GHRH) from the hypothalamus, followed by release of growth hormone (GH) from the anterior pituitary gland. The secretion of insulin-like growth factor 1 (IGF1) from the liver then creates a negative feedback loop in this cycle. Activation of the hypothalamic-pituitary-adrenal axis results in secretion of adrenocorticotropic hormone (ACTH) from the anterior pituitary gland and dehydroepiandrosterone sulphate (DHEAS) from the adrenal gland. Activation of hypothalamic-pituitary-ovarian axis results in secretion of gonadotropin-releasing hormone (GnRH) from the hypothalamus, followed by release of luteinising hormone (LH) and follicle-stimulating hormone (FSH) from the anterior pituitary gland. The secretion of sex hormones, oestrogen and progesterone, then create a negative feedback loop in this cycle. Secretion of sex hormone-binding globulin (SHBG) from the liver and DHEAS from the adrenal gland regulates the activity of oestrogen. This whole process, starting from the activated hypothalamus and pituitary gland, results in thelarche, menarche, and pubertal mammary gland development.

women. In contrast, elevated premenarcheal concentration of circulating DHEAS is associated with increased breast dense area during adulthood [143]. DHEAS is also found to be positively associated with growth factors during puberty [144], which can have substantial impact on pubertal breast development [145–147]. DHEAS can have estradiol-like proliferative effects in an environment of low oestrogen [148], which is typical during early puberty in girls [128]. In pre-pubertal girls, prior to the activation of the HPG axis, DHEAS can be metabolised to oestrogens in adipose tissue [124]. This could explain the early breast development, mediated independent of ovarian hormones, in girls with excess adiposity [125,149].

Premenarcheal SHBG is also shown to be positively associated with adult percent dense breast volume in premenopausal [130,131,133,143,150] and postmenopausal women [130,142,151], although other studies do not support this association [135–138,141,152]. Further, cell surface SHBG receptors and intracellular SHBG are detected in the breasts, which further suggest that SHBG could influence mammographic density via other mechanisms [153] besides controlling steroid hormone bioavailability. Hence, both SHBG and DHEAS could be potential candidates to mediate the effect of pubertal adiposity on development of adult breasts with low mammographic density.

6.2. *Growth hormone and insulin-like growth factor 1*

Growth hormone (GH) acts on both the stromal and epithelial cell components of the mammary gland to promote the formation of terminal end buds and ductal elongation [147,154–156]. In addition to pituitary secretion, GH is also produced locally in the mammary gland [157,158]. In mice, expression of GH mRNA and protein is detected in mammary gland epithelium, with maximum expression observed during puberty [156]. Over-expression of GH in a transgenic mouse model results in precocious mammary gland development [159], while deficiency of functional GH leads to severe impairment of mammary gland development [160]. In humans, autocrine GH and GH receptor mRNA and protein expression are primarily observed in the luminal epithelial and myoepithelial ductal cells [157,158,161,162].

Insulin-like growth factor 1 (IGF1) is believed to be a key mediator of GH signalling in mammary gland development [147,154–156]. This is demonstrated by the inability of GH to have any effect on mammary gland development in animals unable to produce IGF1 [163]. Rodent studies have demonstrated that locally-derived IGF1 promotes pubertal mammary gland development [164–166]. Further, the expression of GH receptor is also observed in the stroma [167] and it is hypothesised that the presence of GH activates the GH receptor within the stromal cells leading to the expression of IGF1, which further activates IGF1 receptors in the epithelium [168]. Lower circulating concentrations of both GH and IGF1 are observed in pubertal girls with excess adiposity [169], however this may not reflect levels within the breast tissue.

In adult women, case-control and cohort studies have demonstrated a positive association between elevated circulating concentration of IGF1 with breast cancer risk [170–175], however other studies have found no association [176,177]. The GH/IGF1 axis is also shown to be associated with mammographic density. IGF1 and GH are positively associated with percent mammographic density in both premenopausal and postmenopausal women, without adjustment for other risk factors [178]. However, another study adjusted for waist circumference and only IGF1 remained significantly associated with percent mammographic density, and only in premenopausal women [130], supporting other findings that circulating concentration of IGF1 is positively correlated with percent mammographic density in premenopausal women, but not in postmenopausal women [179]. Within breast tissue, IGF1 is elevated in tissue of high density compared to low density, with greater differences observed in women under the age of 50 compared to older women [180].

6.3. Endocrine function of adipose tissue

Adipose tissue is an active endocrine organ that secretes adipokines including leptin, adiponectin, tumour necrosis factor alpha (TNFA) and interleukin 6 (IL6). The abundance of adipose tissue can affect the circulating concentration of these adipokines and thus influence tissue development and homoeostasis. Circulating leptin concentration is strongly correlated with abundance of gluteofemoral fat depots in human females [119], can stimulate the secretion of kisspeptin, and subsequently activate the HPG axis [117]. On the other hand, obese individuals exhibit low circulating concentration of adiponectin [181, 182], an insulin-sensitising adipokine, which affects the HPG axis via adiponectin receptors present in the hypothalamus, pituitary gland, and gonads [182,183]. Adiponectin acts as a negative regulator of puberty onset through inhibition of kisspeptin and GnRH secretion in the hypothalamus and inhibition of GH and LH in the pituitary gland [182–185]. These findings suggest that adipose tissue-derived leptin and adiponectin affect initiation of puberty [117].

Studies in animal models suggest leptin may regulate mammary gland development and function through direct effects on the mammary gland and also indirectly through inhibition of IGF1. Leptin inhibits IGF1-mediated proliferation in a bovine mammary epithelial cell line [186] as well as in the bovine mammary gland [187]. Heavier girls have elevated circulating leptin [188] and lower IGF1 [189,190], and these factors in adulthood are shown to be associated with lower mammographic density [130,179,191–193]. In addition, leptin might act directly on mammary fibroblasts [194], thereby altering the stromal compartment of the breast and mammographic density [195].

Excess adiposity is also known to establish a state of chronic low-grade inflammation characterised by increased inflammatory cytokines such as TNFA and IL6 [196] as well as other adipokines, including omentin, visfatin, resistin, and chemerin [197–200]. These factors affect ovarian function with downstream consequences for pubertal mammary gland development and potentially mammographic density. In addition, immune signalling cytokines can act as paracrine regulators of pubertal mammary gland development and mammographic density.

7. Paracrine regulators of pubertal breast development and mammographic density

7.1. Stromal fibroblasts and extracellular matrix

Fibroblasts are one of the main cell types in the mammary stroma and significantly contribute to the fibroglandular tissue compartment that comprises high mammographic density. During puberty, mammary fibroblasts around the terminal end buds become activated by oestrogen and growth hormones and interact with epithelial cells to promote mammary gland morphogenesis [201]. These fibroblasts actively produce factors such as TGFB, IGF1, and hepatocyte growth factor (HGF), which regulate epithelial cell proliferation [202–208]. TGFB also regulates the growth and activity of fibroblasts, modulating expression of tissue remodelling factors including extracellular matrix (ECM) proteins, proteases, and angiogenic factors [209,210].

In situ, fibroblasts proliferate slowly and synthesise low levels of ECM proteins, matrix metalloproteinases (MMPs) that degrade ECM, and tissue inhibitor of metalloproteinases (TIMPs) that inhibit MMP-mediated degradation to maintain breast tissue integrity [201]. Mammographic density is positively associated with extracellular matrix proteins produced by fibroblasts such as collagen, lumican, decorin, and syndecan-1 [180,195,211,212]. ECM proteins can be active players in promotion of tumorigenesis and metastasis, for example, a highly dense collagen matrix promotes tumour formation and progression in a mouse model associated with increased neutrophils and inflammatory cyclooxygenase 2 (COX2) [213–215]. High mammographic density tissue is associated with increased TIMP3, compared to low mammographic density tissue in adult women [180], although this association was not found in another study [216]. TIMP3 is expressed in the mammary stroma and acts on epithelial cells to promote cancer onset in mouse models [217]. Further, a study in mice xenografted with human breast tissue [218] found that high mammographic density breast tissue significantly increased tumour weight, had greater proportions of high grade ductal carcinoma in situ (DCIS) and metastasis of DCIS.com cells compared to the low mammographic density breast tissue from the same woman, suggesting that high mammographic density promotes tumour development and progression.

Using in vitro and in vivo screening of human and murine mammary tissue samples, gene expression profiling of fibroblasts associated with high and low mammographic density tissue revealed that CD36 expression was reduced in high mammographic density-associated fibroblasts [219]. CD36, also known as fatty acid translocase, is involved in adipocyte differentiation, immune signalling, TGFB activation, and cell–ECM interactions [220,221]. CD36 knockout in mice caused decrease in fat accumulation and increase matrix accumulation [219]. Taken together, these studies suggest that fibroblast-associated CD36 may be actively involved in regulating the abundance of adipocytes versus abundance of stromal ECM that determines mammographic density.

7.2. Immune cells and signalling molecules

Immune system cells and signalling molecules are essential components of the mammary gland, with macrophages, eosinophils, neutrophils, mast cells, and lymphocytes (T and B cells) all contributing to mammary gland development and function [201,222–224]. Of particular significance in pubertal mammary gland development, macrophages promote collagen fibrillogenesis, which supports the development of terminal end buds and ductal elongation [225]. Colony stimulating factor 1 (CSF1) is a key factor responsible for the proliferation and survival of macrophages [226]. The mammary glands of mice homozygous for a null mutation in *Csf1* exhibit reduced number of macrophages, lower numbers of terminal end buds as well as reduced ductal branching and elongation [223]. CC-chemokine ligand 2 (CCL2) is an inflammatory cytokine known to be a chemoattractant for monocytes and macrophages to the sites of inflammation [227,228]. In CCL2-overexpressing mice, the mammary gland exhibits increased abundance of macrophages, elevated deposition of stroma and collagen, and increased susceptibility to carcinogen-induced mammary cancer [229]. Human and murine studies reported that increased abundance of inflammatory CCL2, COX2, IL4, and IL6, as well as macrophages, dendritic cells, and B cells are all observed in high mammographic density breast tissue, in comparison to tissue with low mammographic density, suggestive of a protumor inflammatory microenvironment [211, 229–231].

Eosinophils are detected around the developing terminal end buds (TEBs) in pubertal mouse mammary glands, where they promote ductal elongation and branching [223]. Similarly, IL5, a key cytokine that promotes eosinophil differentiation and survival, is also required for ductal elongation [232,233]. However, overabundance of eosinophils due to transgenic expression of IL5 results in delayed onset of ovarian cycling accompanied by perturbed pubertal mammary gland development [234]. Therefore, the abundance and activity of mammary gland eosinophils during puberty appear to be critical for appropriate development. Eosinophils secrete eosinophil peroxidase, an enzyme that promotes fibroblast recruitment and establishment of collagen-rich ECM [235]. While the role of eosinophils in establishment of mammographic density is yet to be explored, eosinophil peroxidase promotes breast cancer progression in a mouse model, associated with increased collagen deposition and elevated COX2 [236].

Excess adiposity enhances bioavailability of TGFB [237,238], an anti-inflammatory cytokine with diverse roles in pubertal mammary gland development in mice. Epithelial cell-derived TGFB limits both proliferation and cell death of mammary epithelium as well as

regulating local immune cell populations [239]. The mammary glands of mice heterozygous for a null mutation in *Tgfb1* exhibit increased ductal invasion, with increased epithelial cell proliferation during puberty [208]. Stromal- or endocrine-derived TGFB promotes mammary gland development possibly through regulation of the HPG axis or through regulation of macrophage function [207,240]. TGFB signalling is reduced in breast tissue with high mammographic density in adult women [241,242].

8. Molecular determinants of pubertal mammary gland development and mammographic density

8.1. Heritability and genetics

Twin studies have provided strong evidence that percent mammographic density is partially heritable [243–245] and that a large proportion of variation in absolute dense area and absolute non-dense area is also attributed to genetic factors [246]. A study comparing 571 pairs of monozygotic twins to 380 pairs of dizygotic twins from Australia and North America suggests that genetics accounts for 60–67% of the variability in all three of the mammographic density measures (percent, absolute dense and absolute non-dense area) when adjusted for other major breast cancer risk factors [243]. The overlap between genetic determinants of both breast cancer risk and mammographic density measures is estimated to be around 14–18% [247,248]. Twin studies have also shown that the circulating concentration of IGF1 is strongly heritable [249,250]. Excess pubertal adiposity is associated with lower IGF1 and lower mammographic density [169], suggesting this may be one role of genetic factors in regulation of pubertal adipose tissue deposition and development of mammographic density. A number of common genetic variants are associated with mammographic density including rs3817198, which is a polymorphism of the gene encoding lymphocyte-specific protein 1, and rs2241716, a polymorphism of the gene encoding TGFB1 [248,251–254].

Surprisingly, elevated concentration of androgens have been observed in girls with breast cancer family history in comparison to girls without breast cancer family history [255]. This suggests that elevated concentration of hormones during puberty may be an important factor explaining the familial clustering of breast cancer [256]. Hence, it has been postulated that association of elevated androgen concentrations and increased breast cancer risk is established during puberty and modified by breast cancer family history [256], which indicates that both pubertal development and genetic factors play a crucial role in breast cancer risk. However, the interaction between genetic factors and environmental factors in pubertal development that could determine adult mammographic density is still not known and will surely be multi-factorial.

8.2. Epigenetic basis

DNA methylation can modulate gene expression without altering the DNA sequence and is believed to play a role in regulating homoeostasis and risk of disease. Peripheral blood DNA hypermethylation in breast cancer susceptibility genes, such as *BRCA1* and *ATM* is shown to be associated with increased breast cancer risk [257–259]. Several genome-wide DNA methylation studies have suggested that peripheral blood DNA methylation, at both global and site-specific levels, is associated with breast cancer risk [260–263]. An analysis of the association of genome-wide average methylation and epigenetic age acceleration within participants of the Australian Mammographic Density Twins and Sisters Study [251] found that genome-wide average methylation was associated with hormone-related risk factors (number of live births and age at first live birth), while epigenetic age acceleration was associated with lifestyle risk factors (BMI, smoking, and alcohol intake) and hormone-related risk factors (age at menarche and age at first live birth) [264].

The association between lifestyle risk factors and epigenetic age acceleration points to the proposition that an unhealthy lifestyle can impact epigenetic ageing to modify breast cancer risk [264]. Although there appears to be no association between blood DNA methylation and mammographic density in adult women [265], peripheral blood DNA methylation at several genomic locations show association with current BMI, BMI at ages 18–21 years, and BMI change, suggesting adiposity through the life course can impact on future breast cancer risk through epigenetic modifications [266]. Environmental factors such as exposure to synthetic oestrogens may also be responsible for these DNA modifications [267,268]. Twin pair correlations in genome-wide average DNA methylation at birth, decrease with age during adolescence, suggesting individual environmental exposures during early life can affect DNA methylation [269]. Use of oral contraceptives during puberty [94,270] or before pregnancy [271] is associated with increased rates of breast tissue proliferation [271], increased dense breast volume [94], and higher breast cancer risk [270]. Thus, environmental and lifestyle factors, as well as endogenous and exogenous sex hormone exposure during puberty, possess the potential to induce epigenetic changes to modify the composition of breast tissue.

Epigenetic age acceleration is also postulated to predict onset of puberty. Increased epigenetic age acceleration was observed to be strongly associated with decreased pubertal tempo and earlier menarche [272]. Previous studies have shown the association of timing of puberty and pubertal tempo with pubertal percent fibroglandular volume [98]. Another study, however, observed that epigenetic age acceleration was positively associated with pubertal percent fibroglandular volume in adjusted models, but was weakened after adjusting for cellular heterogeneity [272]. Through the existing literature, the role of epigenetic age acceleration in determining pubertal mammographic density is still not clear and thus needs further investigation.

Oestrogen receptor alpha (ERA) is a crucial transcriptional regulator that mediates the action of oestrogen in regulating mammary gland development and function [273,274]. Variants in the gene encoding ERA (*ESR1*) are associated with increased percent fibroglandular volume in both premenopausal and postmenopausal women [275–277]. A recent study observed that average *ESR1* DNA methylation pattern at Tanner stage B4 is inversely associated with total breast volume and fibroglandular volume measured at Tanner stage B4, after adjustment of breast fat percentage, *ESR1* DNA methylation pattern at Tanner stage B2, and cellular heterogeneity [278]. It is hypothesised that *ESR1* downregulation might increase expression of inhibitory factors, such as TGFB, to cause cell cycle arrest and this may result in reduced mammary epithelial proliferation in the later stages of breast maturation [279–281].

Recently, a study identified that breast tissue in healthy women ages faster than blood, as measured by DNA methylation [282]. Further, women with luminal breast cancer were observed to have significant epigenetic age acceleration in normal adjacent breast tissue, in comparison to healthy women [283]. These studies suggest that breast tissue age is determined by exposure to endogenous and exogenous factors during a women's lifetime. Taken together, the limited studies available do not provide enough evidence to support an epigenetic basis of mammographic density during puberty. However, if we could understand the impact of pubertal body adiposity on epigenetic ageing of breast tissue, epigenetic age of the breast tissue during puberty could be used to understand the changing internal milieu of the breasts and establishment of mammographic density during puberty.

9. Current controversies, conclusions and outlook

Adolescence is a time of developmental plasticity [284,285], and as breast tissue develops there is the potential for environmental and lifestyle exposures to have a significant influence on future breast cancer risk. Pubertal adiposity, timing of menarche, and timing of thelarche are all demonstrated to affect mammographic density, an important risk

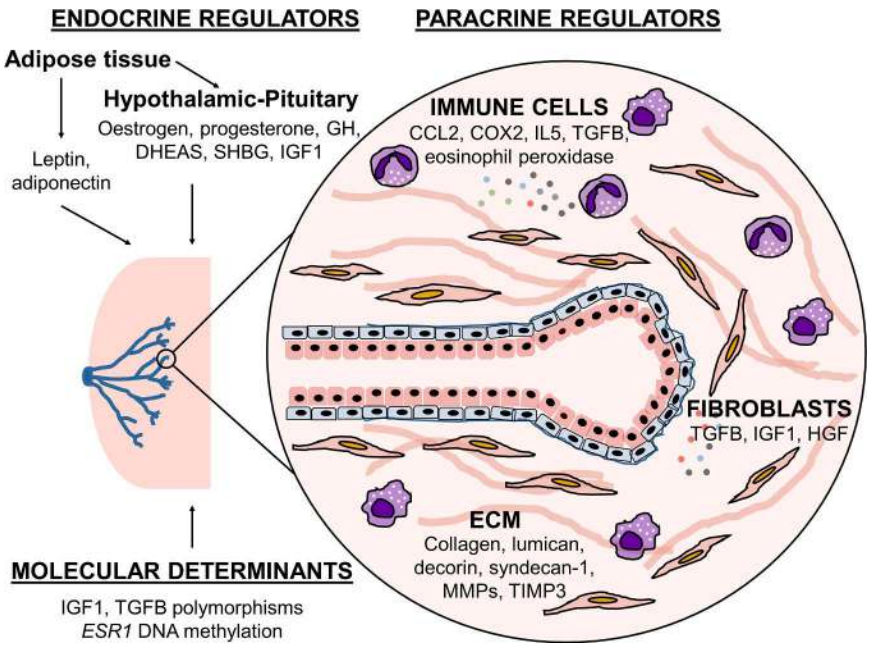

Fig. 5. Schematic diagram of endocrine, paracrine, and molecular regulators of pubertal mammary gland development that may affect adult mammographic density. Endocrine hormones from adipose tissue and hypothalamic-pituitary axes, combined with genetic and epigenetic determinants, regulate pubertal mammary gland development and may affect adult mammographic density. Within the pubertal mammary gland, paracrine regulators associated with immune cells, stromal fibroblasts and the extracellular matrix direct the development of the epithelial, stromal and adipose tissue compartments that determine adult mammographic density.

factor for breast cancer. Activation of hypothalamic-pituitary axes during puberty, genetic and epigenetic molecular determinants, together with stromal fibroblasts, extracellular matrix, and immune signalling factors in the mammary gland are likely to act in concert to drive breast development and ultimately the histological structure of the adult breast (Fig. 5).

The interaction between established risk factors for breast cancer and mammographic density is currently somewhat paradoxical, and further research is required to address these complexities. For example, epidemiological studies suggest that earlier menarche, which is an established breast cancer risk factor, is associated with reduced mammographic density, which is protective against breast cancer. This complicated relationship between age at onset of menarche, mammographic density, and breast cancer risk has not been sufficiently explored in the published literature. However, it is possible that age at menstrual onset affects breast development and establishment of mammographic density via the simultaneous increase in adiposity, while independently increasing breast cancer risk through longer term exposure to ovarian hormones oestrogen and progesterone with menstrual cycling.

Another paradox lies in the relationship between adipose tissue at different stages of the life course and breast cancer risk. Obesity is a risk factor for breast cancer in postmenopausal women, but might be protective during adolescence. A key uncertainty resides in the assessment of pubertal body size and shape, making it difficult to discriminate between healthy adolescent weight gain and excessive weight gain. Whilst adipose tissue deposition is a key driver of puberty onset, it can be difficult to distinguish healthy pubertal weight gain from overweight/obesity in the published literature. For instance, the mass component of BMI reflects the accumulation of adipose tissue, but does not distinguish between localised deposition in gluteofemoral or breast depots, which is indicative of healthy pubertal weight gain, versus abdominal and subcutaneous depots, which characterise obesity. Thus, varied study approaches using different growth measures remain a barrier in synthesising a clear understanding of the relationship between adipose tissue deposition and mammographic density. Further research that specifically investigates the association between pubertal adipose tissue deposition at localised depots and adult mammographic density is required to address this uncertainty.

Beyond these complexities, a critical research question yet to be addressed is whether interventions that modify body adiposity during puberty alter adult breast cancer risk. Given the limitations of human studies, controlled animal experiments can provide clues regarding possible biological mechanisms through which pubertal development might affect adult mammographic density and long-term changes in risk of breast cancer. Future research in understanding how pubertal mammary gland development might determine adult breast composition and mammographic density could be a new key to reducing the incidence of breast cancer.

Declaration of Competing Interest

None.

Acknowledgements

Fig. 1A is reproduced with permission from InforMD (www.informd.org.au); H&E-stained tissue sections in Fig. 2A–C are reproduced with permission from Wolters Kluwer Health, Inc. Images not credited elsewhere were obtained from author's own research with ethics approval from The Queen Elizabeth Hospital Human Research Ethics Committee and Peter MacCallum Human Research Ethics Committee, informed consent was obtained from study participants. Thank you to Leigh Hodson, University of Adelaide, Adelaide for preparation of H&E-stained sections and Dexing Huang, St. Vincent's Institute, Melbourne for image of X-rayed breast tissue. JS is a National Breast Cancer Foundation Early Career Fellow. EWT is Professor of Breast Cancer Research at Queensland University of Technology and receives support for Mammographic Density research from the Princess Alexandra Research Foundation, Brisbane. The Translational Research Institute receives support from the Australian Government. RLR is supported by a Senior Research Fellowship from the National Health and Medical Research Council. WVI is The Hospital Research Foundation Associate Professor of Breast Cancer Research.

References

[1] N.F. Boyd, H. Guo, L.J. Martin, L. Sun, J. Stone, E. Fishell, R.A. Jong, G. Hislop, A. Chiarelli, S. Minkin, M.J. Yaffe, Mammographic density and the risk and detection of breast cancer, N. Engl. J. Med. 356 (3) (2007) 227–236.

[2] N.J. Engmann, M.K. Golmakani, D.L. Miglioretti, B.L. Sprague, K. Kerlikowske, Breast cancer surveillance C: **population-attributable risk proportion of clinical risk factors for breast cancer**, JAMA Oncol. 3 (9) (2017) 1228–1236.

[3] C.W. Huo, G.L. Chew, K.L. Britt, W.V. Ingman, M.A. Henderson, J.L. Hopper, E. W. Thompson, Mammographic density-a review on the current understanding of its association with breast cancer, Breast Cancer Res. Treat. 144 (3) (2014) 479–502.

[4] V.A. McCormack, I. dos Santos Silva, Breast density and parenchymal patterns as markers of breast cancer risk: a meta-analysis, Cancer Epidemiol. Biomark. Prev. 15 (6) (2006) 1159–1169.

[5] J.N. Wolfe, Risk for breast cancer development determined by mammographic parenchymal pattern, Cancer 37 (5) (1976) 2486–2492.

[6] D. Bond-Smith, J. Stone, Methodological challenges and updated findings from a meta-analysis of the association between mammographic density and breast cancer, Cancer Epidemiol. Biomark. Prev. 28 (1) (2019) 22–31.

[7] G.W. Robinson, A.B. Karpf, K. Kratochwil, Regulation of mammary gland development by tissue interaction, J. Mammary Gland Biol. Neoplasia 4 (1) (1999) 9–19.

[8] T.S., Mammary Embryogenesis, Plenum Press, New York, 1987, pp. 37–66.

[9] A. Propper, L. Gomot, Tissue interactions during organogenesis of the mammary gland in the rabbit embryo, C. R. Acad. Hebd. Seances Acad. Sci. D 264 (22) (1967) 2573–2575.

[10] G.R. Cunha, P. Young, K. Christov, R. Guzman, S. Nandi, F. Talamantes, G. Thordarson, Mammary phenotypic expression induced in epidermal cells by embryonic mammary mesenchyme, Acta Anat. 152 (3) (1995) 195–204 (Basel).

[11] B.A. Gusterson, T. Stein, Human breast development, Semin. Cell Dev. Biol. 23 (5) (2012) 567–573.

[12] A. Javed, A. Lteif, Development of the human breast, Semin. Plast. Surg. 27 (1) (2013) 5–12..

[13] G. Samimi, G.A. Colditz, H.J. Baer, R.M. Tamimi, Measures of energy balance and mammographic density in the Nurses' Health Study, Breast Cancer Res. Treat. 109 (1) (2008) 113–122.

[14] T.A. Sellers, C.M. Vachon, V.S. Pankratz, C.A. Janney, Z. Fredericksen, K. R. Brandt, Y. Huang, F.J. Couch, L.H. Kushi, J.R. Cerhan, Association of childhood and adolescent anthropometric factors, physical activity, and diet with adult mammographic breast density, Am. J. Epidemiol. 166 (4) (2007) 456–464.

[15] H.R. Harris, R.M. Tamimi, W.C. Willett, S.E. Hankinson, K.B. Michels, Body size across the life course, mammographic density, and risk of breast cancer, Am. J. Epidemiol. 174 (8) (2011) 909–918.

[16] M. Jeffreys, R. Warren, D. Gunnell, P. McCarron, G.D. Smith, Life course breast cancer risk factors and adult breast density (United Kingdom), Cancer Causes Control 15 (9) (2004) 947–955.

[17] V. Lope, B. Pérez-Gómez, M.P. Moreno, C. Vidal, D. Salas-Trejo, N. Ascunce, I. G. Román, C. Sánchez-Contador, M.C. Santamariña, J.A.V. Carrete, F. Collado-García, C. Pedraz-Pingarrón, M. Ederra, F. Ruiz-Perales, M. Peris, S. Abad, A. Cabanes, M. Pollán, Childhood factors associated with mammographic density in adult women, Breast Cancer Res. Treat. 130 (3) (2011) 965–974.

[18] V.A. McCormack, I. dos Santos Silva, B.L. De Stavola, N. Perry, S. Vinnicombe, A. J. Swerdlow, R. Hardy, D. Kuh, Life-course body size and perimenopausal mammographic parenchymal patterns in the MRC 1946 British birth cohort, Br. J. Cancer 89 (5) (2003) 852–859.

[19] Z.J. Andersen, J.L. Baker, K. Bihrmann, I. Vejborg, T.I. Sorensen, E. Lynge, Birth weight, childhood body mass index, and height in relation to mammographic density and breast cancer: a register-based cohort study, Breast Cancer Res. 16 (1) (2014) R4.

[20] J.L. Hopper, T.L. Nguyen, J. Stone, K. Aujard, M.C. Matheson, M.J. Abramson, J. A. Burgess, E.H. Walters, G.S. Dite, M. Bui, C. Evans, E. Makalic, D.F. Schmidt, G. Ward, M.A. Jenkins, G.G. Giles, S.C. Dharmage, C. Apicella, Childhood body mass index and adult mammographic density measures that predict breast cancer risk, Breast Cancer Res. Treat. 156 (1) (2016) 163–170.

[21] C. Magnusson, J. Baron, I. Persson, A. Wolk, R. Bergstrom, D. Trichopoulos, H. O. Adami, Body size in different periods of life and breast cancer risk in post-menopausal women, Int. J. Cancer 76 (1) (1998) 29–34.

[22] T.G. Hislop, A.J. Coldman, J.M. Elwood, G. Brauer, L. Kan, Childhood and recent eating patterns and risk of breast cancer, Cancer Detect. Prev. 9 (1–2) (1986) 47–58.

[23] L.A. Brinton, C.A. Swanson, Height and weight at various ages and risk of breast cancer, Ann. Epidemiol. 2 (5) (1992) 597–609.

[24] A.J. Swerdlow, B.L. De Stavola, B. Floderus, N.V. Holm, J. Kaprio, P.K. Verkasalo, T. Mack, Risk factors for breast cancer at young ages in twins: an international population-based study, J. Natl. Cancer Inst. 94 (16) (2002) 1238–1246.

[25] L. Le Marchand, L.N. Kolonel, M.E. Earle, M.P. Mi, Body size at different periods of life and breast cancer risk, Am. J. Epidemiol. 128 (1) (1988) 137–152.

[26] L. Hilakivi-Clarke, T. Forsen, J.G. Eriksson, R. Luoto, J. Tuomilehto, C. Osmond, D.J. Barker, Tallness and overweight during childhood have opposing effects on breast cancer risk, Br. J. Cancer 85 (11) (2001) 1680–1684.

[27] M.J. Schoemaker, M.E. Jones, S. Allen, J. Hoare, A. Ashworth, M. Dowsett, A. J. Swerdlow, Childhood body size and pubertal timing in relation to adult mammographic density phenotype, Breast Cancer Res. 19 (1) (2017) 13.

[28] Radiology ACo: The American College of Radiology Breast Imaging Reporting and Data System (BI-RADS), American College of Radiology, Reston, VA, 4th ed. 2003.

[29] B.L. Sprague, R.E. Gangnon, V. Burt, A. Trentham-Dietz, J.M. Hampton, R. D. Wellman, K. Kerlikowske, D.L. Miglioretti, Prevalence of mammographically dense breasts in the United States, J. Natl. Cancer Inst. 106 (2014) 10.

[30] S.J. Lin, J. Cawson, P. Hill, I. Haviv, M. Jenkins, J.L. Hopper, M.C. Southey, I. G. Campbell, E.W. Thompson, Image-guided sampling reveals increased stroma and lower glandular complexity in mammographically dense breast tissue, Breast Cancer Res. Treat. 128 (2) (2011) 505–516.

[31] P.A. Carney, D.L. Miglioretti, B.C. Yankaskas, K. Kerlikowske, R. Rosenberg, C. M. Rutter, B.M. Geller, L.A. Abraham, S.H. Taplin, M. Dignan, G. Cutter, R. Ballard-Barbash, Individual and combined effects of age, breast density, and hormone replacement therapy use on the accuracy of screening mammography, Ann. Intern. Med. 138 (3) (2003) 168–175.

[32] J.A. Harvey, V.E. Bovbjerg, Quantitative assessment of mammographic breast density: relationship with breast cancer risk, Radiology 230 (1) (2004) 29–41.

[33] M.T. Mandelson, N. Oestreicher, P.L. Porter, D. White, C.A. Finder, S.H. Taplin, E. White, Breast density as a predictor of mammographic detection: comparison of interval- and screen-detected cancers, J. Natl. Cancer Inst. 92 (13) (2000) 1081–1087.

[34] R.L. Egan, R.C. Mosteller, Breast cancer mammography patterns, Cancer 40 (5) (1977) 2087–2090.

[35] C.M. Vachon, K.R. Brandt, K. Ghosh, C.G. Scott, S.D. Maloney, M.J. Carston, V. S. Pankratz, T.A. Sellers, Mammographic breast density as a general marker of breast cancer risk, Cancer Epidemiol. Biomark. Prev. 16 (1) (2007) 43–49.

[36] M.S. Shawky, C.W. Huo, M.A. Henderson, A. Redfern, K. Britt, E.W. Thompson, A review of the influence of mammographic density on breast cancer clinical and pathological phenotype, Breast Cancer Res. Treat. 177 (2) (2019) 251–276.

[37] I.H. Kanbayti, W.I.D. Rae, M.F. McEntee, M. Al-Foheidi, S. Ashour, S.A. Turson, E. U. Ekpo, Is mammographic density a marker of breast cancer phenotypes? Cancer Causes Control 31 (8) (2020) 749–765.

[38] G. Turashvili, S. McKinney, L. Martin, K.A. Gelmon, P. Watson, N. Boyd, S. Aparicio, Columnar cell lesions, mammographic density and breast cancer risk, Breast Cancer Res. Treat. 115 (3) (2009) 561–571.

[39] C.W. Huo, P. Hill, G. Chew, P.J. Neeson, H. Halse, E.D. Williams, M.A. Henderson, E.W. Thompson, K.L. Britt, High mammographic density in women is associated with protumor inflammation, Breast Cancer Res. 20 (1) (2018), 92.

[40] M. Lokate, R.K. Stellato, W.B. Veldhuis, P.H. Peeters, C.H. van Gils, Age-related changes in mammographic density and breast cancer risk, Am. J. Epidemiol. 178 (1) (2013) 101–109.

[41] N. Boyd, L. Martin, J. Stone, L. Little, S. Minkin, M. Yaffe, A longitudinal study of the effects of menopause on mammographic features, Cancer Epidemiol. Biomark. Prev. 11 (10) (2002) 1048.

[42] K. Kerlikowske, A.J. Cook, D.S. Buist, S.R. Cummings, C. Vachon, P. Vacek, D. L. Miglioretti, Breast cancer risk by breast density, menopause, and postmenopausal hormone therapy use, J. Clin. Oncol. 28 (24) (2010) 3830–3837.

[43] K. Krishnan, L. Baglietto, J. Stone, J.A. Simpson, G. Severi, C.F. Evans, R. J. MacInnis, G.G. Giles, C. Apicella, J.L. Hopper, Longitudinal study of mammographic density measures that predict breast cancer risk, Cancer Epidemiol. Biomark. Prev. 26 (4) (2017) 651–660.

[44] V.A. McCormack, N.M. Perry, S.J. Vinnicombe, I. Dos Santos Silva, Changes and tracking of mammographic density in relation to Pike's model of breast tissue aging: a UK longitudinal study, Int. J. Cancer 127 (2) (2010) 452–461.

[45] S.X. Sun, Z. Bostanci, R.B. Kass, A.T. Mancino, A.L. Rosenbloom, V.S. Klimberg, K. I. Bland, Breast physiology: normal and abnormal development and function. The Breast: Comprehensive Management of Benign and Malignant Diseases, Elsevier Inc., 2018, pp. 37–56, e36.

[46] E.K. Dawson, A histological study of the normal mamma in relation to tumour growth. I.-Early development to maturity, Edinb. Med. J. 41 (12) (1934) 653–682.

[47] A. Dabelow, Die Milchdruse, in: Handbuch der Mikroskopischen Anatomie des Menschen, 3, Springer-Verlag, Berlin, 1957, pp. 277–512.

[48] J.O. Drife, Breast development in puberty, Ann. N. Y. Acad. Sci. 464 (1986) 58–65.

[49] N. Brown, J. White, A. Milligan, D. Risius, B. Ayres, W. Hedger, J. Scurr, The relationship between breast size and anthropometric characteristics, Am. J. Hum. Biol. 24 (2) (2012) 158–164.

[50] L.Y. Lim, P.J. Ho, J. Liu, W.Y. Chay, M.H. Tan, M. Hartman, J. Li, Determinants of breast size in Asian women, Sci. Rep. 8 (1) (2018) 1201.

[51] C.E. Coltman, J.R. Steele, D.E. McGhee, Breast volume is affected by body mass index but not age, Ergonomics 60 (11) (2017) 1576–1585.

[52] M. Lokate, M.G. Kallenberg, N. Karssemeijer, M.A. Van den Bosch, P.H. Peeters, Van, C.H. Gils, Volumetric breast density from full-field digital mammograms and its association with breast cancer risk factors: a comparison with a threshold method, Cancer Epidemiol. Biomark. Prev. 19 (12) (2010) 3096–3105.

[53] V.A. McCormack, R. Highnam, N. Perry, I. dos Santos Silva, Comparison of a new and existing method of mammographic density measurement: intramethod reliability and associations with known risk factors, Cancer Epidemiol. Biomark. Prev. 16 (6) (2007) 1148–1154.

[54] M. Jeffreys, R. Warren, R. Highnam, G. Davey Smith, Breast cancer risk factors and a novel measure of volumetric breast density: cross-sectional study, Br. J. Cancer 98 (1) (2008) 210–216.

[55] Z. Aitken, V.A. McCormack, R.P. Highnam, L. Martin, A. Gunasekara, O. Melnichouk, G. Mawdsley, C. Peressotti, M. Yaffe, N.F. Boyd, I. dos Santos Silva, Screen-film mammographic density and breast cancer risk: a comparison of the volumetric standard mammogram form and the interactive threshold measurement methods, Cancer Epidemiol. Biomark. Prev. 19 (2) (2010) 418–428.

[56] P.A. van den Brandt, Pooled analysis of prospective cohort studies on height, weight, and breast cancer risk, Am. J. Epidemiol. 152 (6) (2000) 514–527.

[57] C.M. Friedenreich, Review of anthropometric factors and breast cancer risk, Eur. J. Cancer Prev. 10 (1) (2001) 15–32.

[58] L. Bernstein, Epidemiology of endocrine-related risk factors for breast cancer, J. Mammary Gland Biol. Neoplasia 7 (1) (2002) 3–15.

[59] S.B. Matthews, H.J. Thompson, The obesity-breast cancer conundrum: an analysis of the issues, Int. J. Mol. Sci. 17 (6) (2016) 989.

[60] D. Hanahan, R.A. Weinberg, Hallmarks of cancer: the next generation, Cell 144 (5) (2011) 646–674.
[61] S.I. Grivennikov, F.R. Greten, M. Karin, Immunity, inflammation, and cancer, Cell 140 (6) (2010) 883–899.
[62] T. Deng, C.J. Lyon, S. Bergin, M.A. Caligiuri, W.A. Hsueh, Obesity, inflammation, and cancer, Annu. Rev. Pathol. 11 (2016) 421–449.
[63] K. Subbaramaiah, L.R. Howe, P. Bhardwaj, B. Du, C. Gravaghi, R.K. Yantiss, X. K. Zhou, V.A. Blaho, T. Hla, P. Yang, L. Kopelovich, C.A. Hudis, A.J. Dannenberg, Obesity is associated with inflammation and elevated aromatase expression in the mouse mammary gland, Cancer Prev. Res. (Phila.) 4 (3) (2011) 329–346.
[64] K. Subbaramaiah, P.G. Morris, X.K. Zhou, M. Morrow, B. Du, D. Giri, L. Kopelovich, C.A. Hudis, A.J. Dannenberg, Increased levels of COX-2 and prostaglandin E2 contribute to elevated aromatase expression in inflamed breast tissue of obese women, Cancer Discov. 2 (4) (2012) 356–365.
[65] M. Pryor, M.L. Slattery, L.M. Robison, M. Egger, Adolescent diet and breast cancer in Utah, Cancer Res. 49 (8) (1989) 2161–2167.
[66] S. Franceschi, A. Favero, C. La Vecchia, A.E. Baron, E. Negri, L. Dal Maso, A. Giacosa, M. Montella, E. Conti, D. Amadori, Body size indices and breast cancer risk before and after menopause, Int. J. Cancer 67 (2) (1996) 181–186.
[67] R.J. Coates, R.J. Uhler, H.I. Hall, N. Potischman, L.A. Brinton, R. Ballard-Barbash, M.D. Gammon, D.R. Brogan, J.R. Daling, K.E. Malone, J.B. Schoenberg, C. A. Swanson, Risk of breast cancer in young women in relation to body size and weight gain in adolescence and early adulthood, Br. J. Cancer 81 (1) (1999) 167–174.
[68] M.E. Wadsworth, S.L. Mann, B. Rodgers, D.J. Kuh, W.S. Hilder, E.J. Yusuf, Loss and representativeness in a 43 year follow up of a national birth cohort, J. Epidemiol. Community Health 46 (3) (1992) 300–304.
[69] M.E. Wadsworth, S.L. Butterworth, R.J. Hardy, D.J. Kuh, M. Richards, C. Langenberg, W.S. Hilder, M. Connor, The life course prospective design: an example of benefits and problems associated with study longevity, Soc. Sci. Med. 57 (11) (2003) 2193–2205.
[70] B.L. De Stavola, I. dos Santos Silva, V. McCormack, R.J. Hardy, D.J. Kuh, M. E. Wadsworth, Childhood growth and breast cancer, Am. J. Epidemiol. 159 (7) (2004) 671–682.
[71] C.S. Berkey, A.L. Frazier, J.D. Gardner, G.A. Colditz, Adolescence and breast carcinoma risk, Cancer 85 (11) (1999) 2400–2409.
[72] M. LA, Menstrual dysfunction in anorexia nervosa, J. Pediatr. Adolesc. Gynecol. 17 (2) (2004) 81–85.
[73] H. Xu, P. Li, T.M. Barrow, E. Colicino, C. Li, R. Song, H. Liu, N. Tang, S. Liu, L. Guo, H.M. Byun, Obesity as an effect modifier of the association between menstrual abnormalities and hypertension in young adult women: results from Project ELEFANT, PLoS One 13 (11) (2018), e0207929.
[74] Z. Tauqeer, G. Gomez, F.C. Stanford, Obesity in women: insights for the clinician, J. Women's Health 27 (4) (2018) 444–457 (Larchmt.).
[75] J.W. Rich-Edwards, M.B. Goldman, W.C. Willett, D.J. Hunter, M.J. Stampfer, G. A. Colditz, J.E. Manson, Adolescent body mass index and infertility caused by ovulatory disorder, Am. J. Obstet. Gynecol. 171 (1) (1994) 171–177.
[76] A.J. Hartz, P.N. Barboriak, A. Wong, K.P. Katayama, A.A. Rimm, The association of obesity with infertility and related menstural abnormalities in women, Int. J. Obes. 3 (1) (1979) 57–73.
[77] K.L.B.C. Radimer, Breast cancer risks associated with obesity, in: B.A. Stoll (Ed.), Reducing Breast Cancer Risk in Women, Kluwer Academic, Dordrecht, 1995, p. 145.
[78] R.E. Frisch, G. Wyshak, N.L. Albright, T.E. Albright, I. Schiff, J. Witschi, M. Marguglio, Lower lifetime occurrence of breast cancer and cancers of the reproductive system among former college athletes, Am. J. Clin. Nutr. 45 (Suppl. 1) (1987) S328–S335.
[79] M.S.R. Shawon, M. Eriksson, J. Li, Body size in early life and risk of breast cancer, Breast Cancer Res. 19 (1) (2017) 84.
[80] L. Eriksson, K. Czene, L. Rosenberg, K. Humphreys, P. Hall, The influence of mammographic density on breast tumor characteristics, Breast Cancer Res. Treat. 134 (2) (2012) 859–866.
[81] L. Yochum, R.M. Tamimi, S.E. Hankinson, Birthweight, early life body size and adult mammographic density: a review of epidemiologic studies, Cancer Causes Control 25 (10) (2014) 1247–1259.
[82] M.S. Rice, K.A. Bertrand, M. Lajous, R.M. Tamimi, G. Torres-Mejia, C. Biessy, R. Lopez-Ridaura, I. Romieu, Body size throughout the life course and mammographic density in Mexican women, Breast Cancer Res. Treat. 138 (2) (2013) 601–610.
[83] M.S. Rice, K.A. Bertrand, T.J. VanderWeele, B.A. Rosner, X. Liao, H.O. Adami, R. M. Tamimi, Mammographic density and breast cancer risk: a mediation analysis, Breast Cancer Res. 18 (1) (2016) 94.
[84] K.A. Bertrand, H.J. Baer, E.J. Orav, C. Klifa, J.A. Shepherd, L. Van Horn, L. Snetselaar, V.J. Stevens, N.M. Hylton, J.F. Dorgan, Body fatness during childhood and adolescence and breast density in young women: a prospective analysis, Breast Cancer Res. 17 (2015) 95.
[85] N. Boyd, L. Martin, S. Chavez, A. Gunasekara, A. Salleh, O. Melnichouk, M. Yaffe, C. Friedenreich, S. Minkin, M. Bronskill, Breast-tissue composition and other risk factors for breast cancer in young women: a cross-sectional study, Lancet Oncol. 10 (6) (2009) 569–580.
[86] A. Must, S.M. Phillips, E.N. Naumova, M. Blum, S. Harris, B. Dawson-Hughes, W. M. Rand, Recall of early menstrual history and menarcheal body size: after 30 years, how well do women remember? Am. J. Epidemiol. 155 (7) (2002) 672–679.
[87] D.S.S.B. Freedman, The validity of BMI as an indicator of body fatness and risk among children, Pediatrics 124 (2009) S23–S34.
[88] S.E. Alexeeff, N.U. Odo, J.A. Lipson, N. Achacoso, J.H. Rothstein, M.J. Yaffe, R. Y. Liang, L. Acton, V. McGuire, A.S. Whittemore, D.L. Rubin, W. Sieh, L.A. Habel, Age at menarche and late adolescent adiposity associated with mammographic density on processed digital mammograms in 24,840 women, Cancer Epidemiol. Biomark. Prev. 26 (9) (2017) 1450–1458.
[89] A. Bardia, C.M. Vachon, J.E. Olson, R.A. Vierkant, A.H. Wang, L.C. Hartmann, T. A. Sellers, J.R. Cerhan, Relative weight at age 12 and risk of postmenopausal breast cancer, Cancer Epidemiol. Biomark. Prev. 17 (2) (2008) 374–378.
[90] H.J. Baer, S.S. Tworoger, S.E. Hankinson, W.C. Willett, Body fatness at young ages and risk of breast cancer throughout life, Am. J. Epidemiol. 171 (11) (2010) 1183–1194.
[91] E.O. Reiter, V.G. Fuldauer, A.W. Root, Secretion of the adrenal androgen, dehydroepiandrosterone sulfate, during normal infancy, childhood, and adolescence, in sick infants, and in children with endocrinologic abnormalities, J. Pediatr. 90 (5) (1977) 766–770.
[92] L.M. Butler, E.B. Gold, G.A. Greendale, C.J. Crandall, F. Modugno, N. Oestreicher, C.P. Quesenberry Jr., L.A. Habel, Menstrual and reproductive factors in relation to mammographic density: the Study of Women's Health Across the Nation (SWAN), Breast Cancer Res. Treat. 112 (1) (2008) 165–174.
[93] G.S. Dite, L.C. Gurrin, G.B. Byrnes, J. Stone, A. Gunasekara, M.R.E. McCredie, D. R. English, G.G. Giles, J. Cawson, R.A. Hegele, A.M. Chiarelli, M.J. Yaffe, N. F. Boyd, J.L. Hopper, Predictors of mammographic density: insights gained from a novel regression analysis of a twin study, Cancer Epidemiol. Biomark. Prev. 17 (12) (2008) 3474–3481.
[94] J.F. Dorgan, C. Klifa, S. Deshmukh, B.L. Egleston, J.A. Shepherd, P. O. Kwiterovich Jr., L. Van Horn, L.G. Snetselaar, V.J. Stevens, A.M. Robson, N. L. Lasser, N.M. Hylton, Menstrual and reproductive characteristics and breast density in young women, Cancer Causes Control 24 (11) (2013) 1973–1983.
[95] D. Heng, F. Gao, R. Jong, E. Fishell, M. Yaffe, L. Martin, T. Li, J. Stone, L. Sun, J. Hopper, et al., Risk factors for breast cancer associated with mammographic features in Singaporean chinese women, Cancer Epidemiol. Biomark. Prev. 13 (11 Pt. 1) (2004) 1751–1758.
[96] L. Titus-Ernstoff, A.N. Tosteson, C. Kasales, J. Weiss, M. Goodrich, E.E. Hatch, P. A. Carney, Breast cancer risk factors in relation to breast density (United States), Cancer Causes Control 17 (10) (2006) 1281–1290.
[97] P. Tehranifar, D. Reynolds, J. Flom, L. Fulton, Y. Liao, E. Kudadjie-Gyamfi, M. B. Terry, Reproductive and menstrual factors and mammographic density in African American, Caribbean, and white women, Cancer Causes Control 22 (4) (2011) 599–610.
[98] R. Novotny, Y. Daida, Y. Morimoto, J. Shepherd, G. Maskarinec, Puberty, body fat, and breast density in girls of several ethnic groups, Am. J. Hum. Biol. 23 (3) (2011) 359–365.
[99] L.C. Houghton, S. Jung, R. Troisi, E.S. LeBlanc, L.G. Snetselaar, N.M. Hylton, C. Klifa, L. Van Horn, K. Paris, J.A. Shepherd, R.N. Hoover, J.F. Dorgan, Pubertal timing and breast density in young women: a prospective cohort study, Breast Cancer Res. 21 (1) (2019) 122.
[100] J.M. Lee, D. Appugliese, N. Kaciroti, R.F. Corwyn, R.H. Bradley, J.C. Lumeng, Weight status in young girls and the onset of puberty, Pediatrics 119 (3) (2007) e624–e630.
[101] K.K.S.E. Davison, L.L. Birch, Percent body fat at age 5 predicts earlier pubertal development among girls at age 9, Pediatrics 111 (4 Pt. 1) (2003) 815–821.
[102] Y. Wang, Is obesity associated with early sexual maturation? A comparison of the association in American boys versus girls, Pediatrics 110 (5) (2002) 903–910.
[103] L.S. Adair, P. Gordon-Larsen, Maturational timing and overweight prevalence in US adolescent girls, Am. J. Public Health 91 (4) (2001) 642–644.
[104] P.B. Kaplowitz, E.J. Slora, R.C. Wasserman, S.E. Pedlow, M.E. Herman-Giddens, Earlier onset of puberty in girls: relation to increased body mass index and race, Pediatrics 108 (2) (2001) 347–353.
[105] L. Zhai, J. Liu, J. Zhao, J. Liu, Y. Bai, L. Jia, X. Yao, Association of obesity with onset of puberty and sex hormones in Chinese girls: a 4-year longitudinal study, PLoS One 10 (8) (2015), e0134656.
[106] R.B. Leitao, L.P. Rodrigues, L. Neves, G.S. Carvalho, Development of adiposity, obesity and age at menarche: an 8-year follow-up study in Portuguese schoolgirls, Int. J. Adolesc. Med. Health 25 (1) (2013) 55–63.
[107] L. Tremblay, J.Y. Frigon, The interaction role of obesity and pubertal timing on the psychosocial adjustment of adolescent girls: longitudinal data, Int. J. Obes. 29 (10) (2005) 1204–1211 (Lond.).
[108] W. Li, Q. Liu, X. Deng, Y. Chen, S. Liu, M. Story, Association between obesity and puberty timing: a systematic review and meta-analysis, Int. J. Environ. Res. Public Health 14 (2017) 1266.
[109] I.F. Barcellos Gemelli, E.D.S. Farias, O.F. Souza, Age at menarche and its association with excess weight and body fat percentage in girls in the southwestern region of the Brazilian Amazon, J. Pediatr. Adolesc. Gynecol. 29 (5) (2016) 482–488.
[110] I.M. St George, S. Williams, P.A. Silva, Body size and the menarche: the Dunedin Study, J. Adolesc. Health 15 (7) (1994) 573–576.
[111] A.M. Bau, A. Ernert, L. Schenk, S. Wiegand, P. Martus, A. Gruters, H. Krude, Is there a further acceleration in the age at onset of menarche? A cross-sectional study in 1840 school children focusing on age and bodyweight at the onset of menarche, Eur. J. Endocrinol. 160 (1) (2009) 107–113.
[112] T. Gavela-Perez, C. Garces, P. Navarro-Sanchez, L. Lopez Villanueva, L. Soriano-Guillen, Earlier menarcheal age in Spanish girls is related with an increase in body mass index between pre-pubertal school age and adolescence, Pediatr. Obes. 10 (6) (2015) 410–415.

[113] F. Ramezani Tehrani, P. Mirmiran, R. Gholami, N. Moslehi, F. Azizi, Factors influencing menarcheal age: results from the cohort of tehran lipid and glucose study, Int. J. Endocrinol. Metab. 12 (3) (2014), e16130.
[114] B. García Cuartero, A. Gónzalez Vergaz, E. Frías García, C. Arana Cañete, E. Díaz Martínez, M.D. Tolmo, Assessment of the secular trend in puberty in boys and girls, An. Pediatr. 73 (6) (2010) 320–326 (Barc).
[115] R.L. Rosenfield, R.B. Lipton, M.L. Drum, Thelarche, pubarche, and menarche attainment in children with normal and elevated body mass index, Pediatrics 123 (1) (2009) 84–88.
[116] C. Chen, Y. Zhang, W. Sun, Y. Chen, Y. Jiang, Y. Song, Q. Lin, L. Zhu, Q. Zhu, X. Wang, S. Liu, F. Jiang, Investigating the relationship between precocious puberty and obesity: a cross-sectional study in Shanghai, China, BMJ Open 7 (4) (2017), e014004.
[117] D. Nieuwenhuis, N. Pujol-Gualdo, I.A.C. Arnoldussen, A.J. Kiliaan, Adipokines: A gear shift in puberty, Obes. Rev. 21 (2020).
[118] C.M. de Ridder, J.H. Thijssen, P.F. Bruning, J.L. Van den Brande, M. L. Zonderland, W.B. Erich, Body fat mass, body fat distribution, and pubertal development: a longitudinal study of physical and hormonal sexual maturation of girls, J. Clin. Endocrinol. Metab. 75 (2) (1992) 442–446.
[119] W. Lassek, S. Gaulin, Brief communication: menarche is related to fat distribution, Am. J. Phys. Anthropol. 133 (2007) 1147–1151.
[120] L. Loomba-Albrecht, D. Styne, Effect of puberty on body composition, Curr. Opin. Endocrinol. Diabetes Obes. 16 (2009) 10–15.
[121] M.F. Alotaibi, Physiology of puberty in boys and girls and pathological disorders affecting its onset, J. Adolesc. 71 (2019) 63–71.
[122] V. Simonneaux, T. Bahougne, A multi-oscillatory circadian system times female reproduction, Front. Endocrinol. 6 (2015), 157-157.
[123] P. Marques, K. Skorupskaite, J.T. George, R.A. Anderson, Physiology of GNRH and gonadotropin secretion, in: K.R. Feingold, B. Anawalt, A. Boyce, G. Chrousos, K. Dungan, A. Grossman, J.M. Hershman, G. Kaltsas, C. Koch, P. Kopp (Eds.), Endotext, MDText.com, Inc., South Dartmouth MA, 2000.
[124] F.M. Biro, S.M. Pinney, B. Huang, E.R. Baker, D. Walt Chandler, L.D. Dorn, Hormone changes in peripubertal girls, J. Clin. Endocrinol. Metab. 99 (10) (2014) 3829–3835.
[125] L. Aksglaede, K. Sorensen, J.H. Petersen, N.E. Skakkebaek, A. Juul, Recent decline in age at breast development: the Copenhagen puberty study, Pediatrics 123 (5) (2009) e932–e939.
[126] S.M.B. Cabrera, M. George, Frane, W. James, Blethen, L. Sandra, Peter Lee, Age of the larche and menarche in contemporary US females: a cross-sectional analysis, J. Pediatr. Endocrinol. Metab. (2014) 47–51.
[127] J.M. Tanner, Issues and advances in adolescent growth and development, J. Adolesc. Health Care 8 (6) (1987) 470–478.
[128] K. Bay, A.M. Andersson, N.E. Skakkebaek, Estradiol levels in prepubertal boys and girls–analytical challenges, Int. J. Androl. 27 (5) (2004) 266–273.
[129] C.R. McCartney, S.K. Blank, K.A. Prendergast, S. Chhabra, C.A. Eagleson, K. D. Helm, R. Yoo, R.J. Chang, C.M. Foster, S. Caprio, J.C. Marshall, Obesity and sex steroid changes across puberty: evidence for marked hyperandrogenemia in pre- and early pubertal obese girls, J. Clin. Endocrinol. Metab. 92 (2) (2007) 430–436.
[130] N.F. Boyd, J. Stone, L.J. Martin, R. Jong, E. Fishell, M. Yaffe, G. Hammond, S. Minkin, The association of breast mitogens with mammographic densities, Br. J. Cancer 87 (8) (2002) 876–882.
[131] M. Yong, C. Atkinson, K.M. Newton, E.J. Aiello Bowles, F.Z. Stanczyk, K. C. Westerlind, V.L. Holt, S.M. Schwartz, W.M. Leisenring, J.W. Lampe, Associations between endogenous sex hormone levels and mammographic and bone densities in premenopausal women, Cancer Causes Control 20 (7) (2009) 1039–1053.
[132] J.J. Noh, G. Maskarinec, I. Pagano, L.W. Cheung, F.Z. Stanczyk, Mammographic densities and circulating hormones: a cross-sectional study in premenopausal women, Breast 15 (1) (2006) 20–28.
[133] M.J. Borugian, J.J. Spinelli, P.B. Gordon, Z. Abanto, A. Brooks-Wilson, M. N. Pollak, L.J. Warren, T.G. Hislop, R.P. Gallagher, Fasting insulin and endogenous hormones in relation to premenopausal breast density (Canada), Cancer Causes Control 25 (2014) 385–394.
[134] K. Walker, O. Fletcher, N. Johnson, B. Coupland, V.A. McCormack, E. Folkerd, L. Gibson, S.G. Hillier, J.M. Holly, S. Moss, M. Dowsett, J. Peto, I. dos Santos Silva, Premenopausal mammographic density in relation to cyclic variations in endogenous sex hormone levels, prolactin, and insulin-like growth factors, Cancer Res. 69 (16) (2009) 6490–6499.
[135] M. Verheus, P.H. Peeters, P.A. van Noord, Y.T. van der Schouw, D.E. Grobbee, C. H. van Gils, No relationship between circulating levels of sex steroids and mammographic breast density: the prospect-EPIC cohort, Breast Cancer Res. 9 (4) (2007) R53.
[136] V.A. McCormack, M. Dowsett, E. Folkerd, N. Johnson, C. Palles, B. Coupland, J. M. Holly, S.J. Vinnicombe, N.M. Perry, I. dos Santos Silva, Sex steroids, growth factors and mammographic density: a cross-sectional study of UK postmenopausal Caucasian and Afro-Caribbean women, Breast Cancer Res. 11 (3) (2009) R38.
[137] B.L. Sprague, A. Trentham-Dietz, R.E. Gangnon, D.S. Buist, E.S. Burnside, E. J. Bowles, F.Z. Stanczyk, G.S. Sisney, Circulating sex hormones and mammographic breast density among postmenopausal women, Horm. Cancer 2 (1) (2011) 62–72.
[138] C.G. Woolcott, K.S. Courneya, N.F. Boyd, M.J. Yaffe, A. McTiernan, R. Brant, C. A. Jones, F.Z. Stanczyk, T. Terry, L.S. Cook, Q. Wang, C.M. Friedenreich, Association between sex hormones, glucose homeostasis, adipokines, and inflammatory markers and mammographic density among postmenopausal women, Breast Cancer Res. Treat. 139 (1) (2013) 255–265.
[139] G.A. Greendale, S.L. Palla, G. Ursin, G.A. Laughlin, C. Crandall, M.C. Pike, B. A. Reboussin, The association of endogenous sex steroids and sex steroid binding proteins with mammographic density: results from the postmenopausal estrogen/progestin interventions mammographic density study, Am. J. Epidemiol. 162 (9) (2005) 826–834.
[140] M.J. Schoemaker, E.J. Folkerd, M.E. Jones, M. Rae, S. Allen, A. Ashworth, M. Dowsett, A.J. Swerdlow, Combined effects of endogenous sex hormone levels and mammographic density on postmenopausal breast cancer risk: results from the Breakthrough Generations Study, Br. J. Cancer 110 (7) (2014) 1898–1907.
[141] R.M. Tamimi, S.E. Hankinson, G.A. Colditz, C. Byrne, Endogenous sex hormone levels and mammographic density among postmenopausal women, Cancer Epidemiol. Biomark. Prev. 14 (11 Pt. 1) (2005) 2641–2647.
[142] Y. Bremnes, G. Ursin, N. Bjurstam, S. Rinaldi, R. Kaaks, I.T. Gram, Endogenous sex hormones, prolactin and mammographic density in postmenopausal Norwegian women, Int. J. Cancer 121 (11) (2007) 2506–2511.
[143] S. Jung, L. Brian Egleston, D. Walt Chandler, Linda Van Horn, M. Nola Hylton, C. Catherine Klifa, Norman L. Lasser, Erin S. LeBlanc, Kenneth Paris, John A. Shepherd, Linda G. Snetselaar, Frank Z. Stanczyk, Victor J. Stevens, Joanne F. Dorgan, Adolescent endogenous sex hormones and breast density in early adulthood, Breast Cancer Res. 17 (1) (2015) 77.
[144] G. Guercio, M.A. Rivarola, E. Chaler, M. Maceiras, A. Belgorosky, Relationship between the growth hormone/insulin-like growth factor-I axis, insulin sensitivity, and adrenal androgens in normal prepubertal and pubertal girls, J. Clin. Endocrinol. Metab. 88 (3) (2003) 1389–1393.
[145] L. Ibanez, C. Valls, K. Ong, D.B. Dunger, F. de Zegher, Metformin therapy during puberty delays menarche, prolongs pubertal growth, and augments adult height: a randomized study in low-birth-weight girls with early-normal onset of puberty, J. Clin. Endocrinol. Metab. 91 (6) (2006) 2068–2073.
[146] D.L. Kleinberg, W. Ruan, IGF-I, GH, and sex steroid effects in normal mammary gland development, J. Mammary Gland Biol. Neoplasia 13 (4) (2008) 353–360.
[147] M.D. Sternlicht, Key stages in mammary gland development: the cues that regulate ductal branching morphogenesis, Breast Cancer Res. 8 (1) (2005) 201.
[148] P.K.V. Ebeling, Physiological importance of dehydroepiandrosterone, Lancet 343 (1994) 1479–1481.
[149] M.L. Ahmed, K.K. Ong, D.B. Dunger, Childhood obesity and the timing of puberty, Trends Endocrinol. Metab. 20 (5) (2009) 237–242.
[150] J.H. Chen, W.P. Chen, S. Chan, D.C. Yeh, M.Y. Su, C.E. McLaren, Correlation of endogenous hormonal levels, fibroglandular tissue volume and percent density measured using 3D MRI during one menstrual cycle, Ann. Oncol. 24 (9) (2013) 2329–2335.
[151] R. Warren, Associations among mammographic density, circulating sex hormones, and polymorphisms in sex hormone metabolism genes in postmenopausal women, Cancer Epidemiol. Biomark. Prev. 15 (8) (2006) 1502–1508.
[152] G.A. Greendale, B.A. Reboussin, A. Sie, H.R. Singh, L.K. Olson, O. Gatewood, L. W. Bassett, C. Wasilauskas, T. Bush, E. Barrett-Connor, Effects of estrogen and estrogen-progestin on mammographic parenchymal density. Postmenopausal estrogen/progestin interventions (PEPI) investigators, Ann. Intern. Med. 130 (4 Pt. 1) (1999) 262–269.
[153] W. Rosner, D.J. Hryb, S.M. Kahn, A.M. Nakhla, N.A. Romas, Interactions of sex hormone-binding globulin with target cells, Mol. Cell. Endocrinol. 316 (1) (2010) 79–85.
[154] D.L. Kleinberg, Early mammary development: growth hormone and IGF-1, J. Mammary Gland Biol. Neoplasia 2 (1) (1997) 49–57.
[155] P.D. Walden, W. Ruan, M. Feldman, D.L. Kleinberg, Evidence that the mammary fat pad mediates the action of growth hormone in mammary gland development, Endocrinology 139 (2) (1998) 659–662.
[156] S. Mukhina, D. Liu, K. Guo, M. Raccurt, S. Borges-Bendris, H.C. Mertani, P. E. Lobie, Autocrine growth hormone prevents lactogenic differentiation of mouse mammary epithelial cells, Endocrinology 147 (4) (2006) 1819–1829.
[157] J.A. Mol, S.C. Henzen-Logmans, P. Hageman, W. Misdorp, M.A. Blankenstein, A. Rijnberk, Expression of the gene encoding growth hormone in the human mammary gland, J. Clin. Endocrinol. Metab. 80 (10) (1995) 3094–3096.
[158] M. Raccurt, P.E. Lobie, E. Moudilou, T. Garcia-Caballero, L. Frappart, G. Morel, H. C. Mertani, High stromal and epithelial human gh gene expression is associated with proliferative disorders of the mammary gland, J. Endocrinol. 175 (2) (2002) 307–318.
[159] O. Bchini, A.C. Andres, B. Schubaur, M. Mehtali, M. LeMeur, R. Lathe, P. Gerlinger, Precocious mammary gland development and milk protein synthesis in transgenic mice ubiquitously expressing human growth hormone, Endocrinology 128 (1) (1991) 539–546.
[160] H. Nagasawa, Y. Noguchi, T. Mori, K. Niki, H. Namiki, Suppression of normal and preneoplastic mammary growth and uterine adenomyosis with reduced growth hormone level in SHN mice given monosodium glutamate neonatally, Eur. J. Cancer Clin. Oncol. 21 (12) (1985) 1547–1551.
[161] H.C. Mertani, M.C. Delehaye-Zervas, J.F. Martini, M.C. Postel-Vinay, G. Morel, Localization of growth hormone receptor messenger RNA in human tissues, Endocrine 3 (2) (1995) 135–142.
[162] H.C. Mertani, T. Garcia-Caballero, A. Lambert, F. Gerard, C. Palayer, J.M. Boutin, B.K. Vonderhaar, M.J. Waters, P.E. Lobie, G. Morel, Cellular expression of growth hormone and prolactin receptors in human breast disorders, Int. J. Cancer 79 (2) (1998) 202–211.
[163] D.L. Kleinberg, W. Ruan, V. Catanese, C.B. Newman, M. Feldman, Non-lactogenic effects of growth hormone on growth and insulin-like growth factor-I messenger ribonucleic acid of rat mammary gland, Endocrinology 126 (6) (1990) 3274–3276.

[164] D.L. Kleinberg, M. Feldman, W. Ruan, IGF-I: an essential factor in terminal end bud formation and ductal morphogenesis, J. Mammary Gland Biol. Neoplasia 5 (1) (2000) 7–17.
[165] C. Couldrey, J. Moitra, C. Vinson, M. Anver, K. Nagashima, J. Green, Adipose tissue: a vital in vivo role in mammary gland development but not differentiation, Dev. Dyn. 223 (4) (2002) 459–468.
[166] R.G. Richards, D.M. Klotz, M.P. Walker, R.P. Diaugustine, Mammary gland branching morphogenesis is diminished in mice with a deficiency of insulin-like growth factor-I (IGF-I), but not in mice with a liver-specific deletion of IGF-I, Endocrinology 145 (7) (2004) 3106–3110.
[167] M.I. Gallego, N. Binart, G.W. Robinson, R. Okagaki, K.T. Coschigano, J. Perry, J. J. Kopchick, T. Oka, P.A. Kelly, L. Hennighausen, Prolactin, growth hormone, and epidermal growth factor activate Stat5 in different compartments of mammary tissue and exert different and overlapping developmental effects, Dev. Biol. 229 (1) (2001) 163–175.
[168] E. Marshman, C.H. Streuli, Insulin-like growth factors and insulin-like growth factor binding proteins in mammary gland function, Breast Cancer Res. 4 (6) (2002) 231–239.
[169] M. Scacchi, A.I. Pincelli, F. Cavagnini, Growth hormone in obesity, Int. J. Obes. Relat. Metab. Disord. 23 (3) (1999) 260–271.
[170] K. Bohlke, D.W. Cramer, D. Trichopoulos, C.S. Mantzoros, Insulin-like growth factor-I in relation to premenopausal ductal carcinoma in situ of the breast, Epidemiology 9 (5) (1998) 570–573.
[171] T. Agurs-Collins, L.L. Adams-Campbell, K.S. Kim, K.J. Cullen, Insulin-like growth factor-1 and breast cancer risk in postmenopausal African-American women, Cancer Detect. Prev. 24 (3) (2000) 199–206.
[172] H. Yu, X.O. Shu, B.D. Li, Q. Dai, Y.T. Gao, F. Jin, W. Zheng, Joint effect of insulin-like growth factors and sex steroids on breast cancer risk, Cancer Epidemiol. Biomark. Prev. 12 (10) (2003) 1067–1073.
[173] R.A. Krajcik, N.D. Borofsky, S. Massardo, N. Orentreich, Insulin-like growth factor I (IGF-I), IGF-binding proteins, and breast cancer, Cancer Epidemiol. Biomark. Prev. 11 (12) (2002) 1566–1573.
[174] S.E. Hankinson, W.C. Willett, G.A. Colditz, D.J. Hunter, D.S. Michaud, B. Deroo, B. Rosner, F.E. Speizer, M. Pollak, Circulating concentrations of insulin-like growth factor-I and risk of breast cancer, Lancet 351 (9113) (1998) 1393–1396.
[175] P. Toniolo, P.F. Bruning, A. Akhmedkhanov, J.M. Bonfrer, K.L. Koenig, A. Lukanova, R.E. Shore, A. Zeleniuch-Jacquotte, Serum insulin-like growth factor-I and breast cancer, Int. J. Cancer 88 (5) (2000) 828–832.
[176] R. Kaaks, E. Lundin, J. Manjer, S. Rinaldi, C. Biessy, S. Söderberg, P. Lenner, L. Janzon, E. Riboli, G. Berglund, G. Hallmans, Prospective study of IGF-I, IGF-binding proteins, and breast cancer risk, in northern and southern Sweden, Cancer Causes Control 13 (4) (2002) 307–316.
[177] M.E. Del Giudice, I.G. Fantus, S. Ezzat, G. McKeown-Eyssen, D. Page, P. J. Goodwin, Insulin and related factors in premenopausal breast cancer risk, Breast Cancer Res. Treat. 47 (2) (1998) 111–120.
[178] C. Mulhall, R.A. Hegele, H. Cao, D. Tritchler, M. Yaffe, N.F. Boyd, Pituitary growth hormone and growth hormone–releasing hormone receptor genes and associations with mammographic measures and serum growth hormone, Cancer Epidemiol. Biomark. Prev. 14 (11) (2005) 2648–2654.
[179] C. Byrne, G.A. Colditz, W.C. Willett, F.E. Speizer, M. Pollak, S.E. Hankinson, Plasma insulin-like growth factor (IGF) I, IGF-binding protein 3, and mammographic density, Cancer Res. 60 (14) (2000) 3744–3748.
[180] Y.P. Guo, L.J. Martin, W. Hanna, D. Banerjee, N. Miller, E. Fishell, R. Khokha, N. F. Boyd, Growth factors and stromal matrix proteins associated with mammographic densities, Cancer Epidemiol. Biomark. Prev. 10 (3) (2001) 243–248.
[181] E. Budak, M. Fernandez Sanchez, J. Bellver, A. Cervero, C. Simon, A. Pellicer, Interactions of the hormones leptin, ghrelin, adiponectin, resistin, and PYY3-36 with the reproductive system, Fertil. Steril. 85 (6) (2006) 1563–1581.
[182] K. Dobrzyn, N. Smolinska, M. Kiezun, K. Szeszko, E. Rytelewska, K. Kisielewska, M. Gudelska, T. Kaminski, Adiponectin: a new regulator of female reproductive system, Int. J. Endocrinol. 2018 (2018) 1–12.
[183] T. Reinehr, C.L. Roth, Is there a causal relationship between obesity and puberty? Lancet Child Adolesc. Health 3 (1) (2019) 44–54.
[184] L. Martin, Implications of adiponectin in linking metabolism to testicular function, Endocrine (2013) 46.
[185] H. Mathew, V.D. Castracane, C. Mantzoros, Adipose tissue and reproductive health, Metabolism 86 (2018) 18–32.
[186] L.F. Silva, M.J. VandeHaar, M.S. Weber Nielsen, G.W. Smith, Evidence for a local effect of leptin in bovine mammary gland, J. Dairy Sci. 85 (12) (2002) 3277–3286.
[187] L.F.P. Silva, B.E. Etchebarne, M.S. Weber Nielsen, J.S. Liesman, M. Kiupel, M. J. VandeHaar, Intramammary infusion of leptin decreases proliferation of mammary epithelial cells in prepubertal heifers, J. Dairy Sci. 91 (8) (2008) 3034–3044.
[188] S.G. Hassink, D.V. Sheslow, E. de Lancey, I. Opentanova, R.V. Considine, J. F. Caro, Serum leptin in children with obesity: relationship to gender and development, Pediatrics 98 (2 Pt. 1) (1996) 201–203.
[189] E.S. Schernhammer, S.S. Tworoger, A.H. Eliassen, S.A. Missmer, J.M. Holly, M. N. Pollak, S.E. Hankinson, Body shape throughout life and correlations with IGFs and GH, Endocr. Relat. Cancer 14 (3) (2007) 721–732.
[190] E.M. Poole, S.S. Tworoger, S.E. Hankinson, E.S. Schernhammer, M.N. Pollak, H. J. Baer, Body size in early life and adult levels of insulin-like growth factor 1 and insulin-like growth factor binding protein 3, Am. J. Epidemiol. 174 (6) (2011) 642–651.
[191] C. Diorio, M. Pollak, C. Byrne, B. Mâsse, N. Hébert-Croteau, M. Yaffe, G. Coté, S. Bérubé, C. Morin, J. Brisson, Insulin-like growth factor-I, IGF-binding protein-3, and mammographic breast density, Cancer Epidemiol. Biomark. Prev. 14 (5) (2005) 1065–1073.
[192] G. Maskarinec, Y. Takata, Z. Chen, I.T. Gram, C. Nagata, I. Pagano, K. Hayashi, L. Arendell, G. Skeie, S. Rinaldi, R. Kaaks, IGF-I and mammographic density in four geographic locations: a pooled analysis, Int. J. Cancer 121 (8) (2007) 1786–1792.
[193] A. Stuedal, G. Ursin, M.B. Veierød, Y. Bremnes, J.E. Reseland, C.A. Drevon, I. T. Gram, Plasma levels of leptin and mammographic density among postmenopausal women: a cross-sectional study, Breast Cancer Res. 8 (5) (2006) R55.
[194] A. Glasow, W. Kiess, U. Anderegg, A. Berthold, A. Bottner, J. Kratzsch, Expression of leptin (Ob) and leptin receptor (Ob-R) in human fibroblasts: regulation of leptin secretion by insulin, J. Clin. Endocrinol. Metab. 86 (9) (2001) 4472–4479.
[195] S. Alowami, S. Troup, S. Al-Haddad, I. Kirkpatrick, P.H. Watson, Mammographic density is related to stroma and stromal proteoglycan expression, Breast Cancer Res. 5 (5) (2003) R129–R135.
[196] U.N. Das, **Is obesity an inflammatory condition?** Nutrition 17 (2001) 953–966 (Burbank, Los Angeles County, Calif).
[197] K. Sejrsen, J.T. Huber, H.A. Tucker, R.M. Akers, Influence of nutrition of mammary development in pre- and postpubertal heifers, J. Dairy Sci. 65 (5) (1982) 793–800.
[198] A.N. Comninos, C.N. Jayasena, W.S. Dhillo, The relationship between gut and adipose hormones, and reproduction, Hum. Reprod. Update 20 (2) (2013) 153–174.
[199] A. Singh, M. Choubey, P. Bora, A. Krishna, Adiponectin and chemerin: contrary adipokines in regulating reproduction and metabolic disorders, Reprod. Sci. 25 (10) (2018) 1462–1473.
[200] C. Tsatsanis, E. Dermitzaki, P. Avgoustinaki, N. Malliaraki, V. Mytaras, A. N. Margioris, The impact of adipose tissue-derived factors on the hypothalamic-pituitary-gonadal (HPG) axis, Hormones 14 (4) (2015) 549–562 (Athens).
[201] A. Unsworth, R. Anderson, K. Britt, Stromal fibroblasts and the immune microenvironment: partners in mammary gland biology and pathology? J. Mammary Gland Biol. Neoplasia 19 (2) (2014) 169–182.
[202] H. Macias, L. Hinck, Mammary gland development, Wiley Interdiscip. Rev. Dev. Biol. 1 (2012) 533–557.
[203] Y. Kojima, A. Acar, E.N. Eaton, K.T. Mellody, C. Scheel, I. Ben-Porath, T.T. Onder, Z.C. Wang, A.L. Richardson, R.A. Weinberg, A. Orimo, Autocrine TGF-beta and stromal cell-derived factor-1 (SDF-1) signaling drives the evolution of tumor-promoting mammary stromal myofibroblasts, Proc. Natl. Acad. Sci. USA 107 (46) (2010) 20009–20014.
[204] A. Orimo, P.B. Gupta, D.C. Sgroi, F. Arenzana-Seisdedos, T. Delaunay, R. Naeem, V.J. Carey, A.L. Richardson, R.A. Weinberg, Stromal fibroblasts present in invasive human breast carcinomas promote tumor growth and angiogenesis through elevated SDF-1/CXCL12 secretion, Cell 121 (3) (2005) 335–348.
[205] B. Niranjan, L. Buluwela, J. Yant, N. Perusinghe, A. Atherton, D. Phippard, T. Dale, B. Gusterson, T. Kamalati, HGF/SF: a potent cytokine for mammary growth, morphogenesis and development, Development 121 (9) (1995) 2897–2908.
[206] G.B. Silberstein, C.W. Daniel, Reversible inhibition of mammary gland growth by transforming growth factor-beta, Science 237 (4812) (1987) 291–293.
[207] W.V. Ingman, S.A. Robertson, Mammary gland development in transforming growth factor Beta1 null mutant mice: systemic and epithelial effects1, Biol. Reprod. 79 (4) (2008) 711–717.
[208] K.B. Ewan, G. Shyamala, S.A. Ravani, Y. Tang, R. Akhurst, L. Wakefield, M. H. Barcellos-Hoff, Latent transforming growth factor-beta activation in mammary gland: regulation by ovarian hormones affects ductal and alveolar proliferation, Am. J. Pathol. 160 (6) (2002) 2081–2093.
[209] W.B. Fang, B. Mafuvadze, M. Yao, A. Zou, M. Portsche, N. Cheng, TGF-β negatively regulates CXCL1 chemokine expression in mammary fibroblasts through enhancement of Smad2/3 and suppression of HGF/c-met signaling mechanisms, PLoS One 10 (8) (2015), e0135063.
[210] Y. Gao, Y. Wang, Y. Li, X. Xia, S. Zhao, Y. Che, Y. Sun, L. Lei, TGF-beta1 promotes bovine mammary fibroblast proliferation through the ERK 1/2 signalling pathway, Cell Biol. Int. 40 (7) (2016) 750–760.
[211] C.W. Huo, G. Chew, P. Hill, D. Huang, W. Ingman, L. Hodson, K.A. Brown, A. Magenau, A.H. Allam, E. McGhee, P. Timpson, M.A. Henderson, E. W. Thompson, K. Britt, High mammographic density is associated with an increase in stromal collagen and immune cells within the mammary epithelium, Breast Cancer Res. 17 (1) (2015) 79.
[212] M.S. Shawky, C. Ricciardelli, M. Lord, J. Whitelock, V. Ferro, K. Britt, E. W. Thompson, Proteoglycans: potential agents in mammographic density and the associated breast cancer risk, J. Mammary Gland Biol. Neoplasia 20 (3–4) (2015) 121–131.
[213] P.P. Provenzano, D.R. Inman, K.W. Eliceiri, J.G. Knittel, L. Yan, C.T. Rueden, J. G. White, P.J. Keely, Collagen density promotes mammary tumor initiation and progression, BMC Med. 6 (1) (2008) 11.
[214] M.G. García-Mendoza, D.R. Inman, S.M. Ponik, J.J. Jeffery, D.S. Sheerar, R.R. Van Doorn, P.J. Keely, Neutrophils drive accelerated tumor progression in the collagen-dense mammary tumor microenvironment, Breast Cancer Res. 18 (1) (2016) 49.
[215] K. Esbona, D. Inman, S. Saha, J. Jeffery, P. Schedin, L. Wilke, P. Keely, COX-2 modulates mammary tumor progression in response to collagen density, Breast Cancer Res. 18 (1) (2016) 35.

[216] J.S. Steude, G. Maskarinec, E. Erber, M. Verheus, B.Y. Hernandez, J. Killeen, J. M. Cline, Mammographic density and matrix metalloproteinases in breast tissue, Cancer Microenviron. 3 (1) (2010) 57–65.
[217] H.W. Jackson, C.V. Hojilla, A. Weiss, O.H. Sanchez, G.A. Wood, R. Khokha, Timp3 deficient mice show resistance to developing breast cancer, PLoS One 10 (3) (2015), e0120107.
[218] C.W. Huo, M. Waltham, C. Khoo, S.B. Fox, P. Hill, S. Chen, G.L. Chew, J.T. Price, C.H. Nguyen, E.D. Williams, M. Henderson, E.W. Thompson, K.L. Britt, Mammographically dense human breast tissue stimulates MCF10DCIS.com progression to invasive lesions and metastasis, Breast Cancer Res. 18 (1) (2016) 106.
[219] R.A. DeFilippis, H. Chang, N. Dumont, J.T. Rabban, Y.-Y. Chen, G.V. Fontenay, H. K. Berman, M.L. Gauthier, J. Zhao, D. Hu, J.J. Marx, J.A. Tjoe, E. Ziv, M. Febbraio, K. Kerlikowske, B. Parvin, T.D. Tlsty, CD36 Repression activates a multicellular stromal program shared by high mammographic density and tumor tissues, Cancer Discov. 2 (9) (2012) 826–839.
[220] F. Gregoire, C. Smas, H.S. Sul, F.M. Gregoire, C.M. Smas, H.S. Sul, Understanding adipocyte differentiation, Physiol. Rev. 78 (1998) 783–809.
[221] Z. Sfeir, A. Ibrahimi, E. Amri, P. Grimaldi, N. Abumrad, CD36 antisense expression in 3T3-F442A preadipocytes, Mol. Cell. Biochem. 192 (1–2) (1999) 3–8.
[222] E.F. Need, V. Atashgaran, W.V. Ingman, P. Dasari, Hormonal regulation of the immune microenvironment in the mammary gland, J. Mammary Gland Biol. Neoplasia 19 (2) (2014) 229–239.
[223] V. Gouon-Evans, M. Rothenberg, J. Pollard, Postnatal mammary gland development requires macrophages and eosinophils, Development 127 (2000) 2269–2282 (Cambridge, England).
[224] X. Sun, W.V. Ingman, Cytokine networks that mediate epithelial cell-macrophage crosstalk in the mammary gland: implications for development and cancer, J. Mammary Gland Biol. Neoplasia 19 (2) (2014) 191–201.
[225] W.V. Ingman, J. Wyckoff, V. Gouon-Evans, J. Condeelis, J.W. Pollard, Macrophages promote collagen fibrillogenesis around terminal end buds of the developing mammary gland, Dev. Dyn. 235 (12) (2006) 3222–3229.
[226] F.J. Pixley, E.R. Stanley, CSF-1 regulation of the wandering macrophage: complexity in action, Trends Cell Biol. 14 (11) (2004) 628–638.
[227] A. Yadav, V. Saini, S. Arora, MCP-1: chemoattractant with a role beyond immunity: a review, Clin. Chim. Acta 411 (21–22) (2010) 1570–1579.
[228] S.L. Deshmane, S. Kremlev, S. Amini, B.E. Sawaya, Monocyte chemoattractant protein-1 (MCP-1): an overview, J. Interferon Cytokine Res. 29 (6) (2009) 313–326.
[229] X. Sun, D.J. Glynn, L.J. Hodson, C. Huo, K. Britt, E.W. Thompson, L. Woolford, A. Evdokiou, J.W. Pollard, S.A. Robertson, W.V. Ingman, CCL2-driven inflammation increases mammary gland stromal density and cancer susceptibility in a transgenic mouse model, Breast Cancer Res. 19 (1) (2017) 4.
[230] C.W. Huo, P. Hill, G. Chew, P.J. Neeson, H. Halse, E.D. Williams, M.A. Henderson, E.W. Thompson, K.L. Britt, High mammographic density in women is associated with protumor inflammation, Breast Cancer Res. 20 (1) (2018), 92.
[231] G.L. Chew, C.W. Huo, D. Huang, P. Hill, J. Cawson, H. Frazer, J.L. Hopper, I. Haviv, M.A. Henderson, K. Britt, E.W. Thompson, Increased COX-2 expression in epithelial and stromal cells of high mammographic density tissues and in a xenograft model of mammographic density, Breast Cancer Res. Treat. 153 (1) (2015) 89–99.
[232] D.C. Colbert, M.P. McGarry, K. O'Neill, N.A. Lee, J.J. Lee, Decreased size and survival of weanling mice in litters of IL-5-/ -mice are a consequence of the IL-5 deficiency in nursing dams, Contemp. Top. Lab. Anim. Sci. 44 (3) (2005) 53–55.
[233] D. Colbert, M. McGarry, K. O'Neill, N. Lee, J. Lee, Decreased size and survival of weanling mice in litters of IL-5 -/- mice are a consequence of the IL-5 deficiency in nursing dams, Contemp. Top. Lab. Anim. Sci. Am. Assoc. Lab. Anim. Sci. 44 (2005) 53–55.
[234] A.N. Sferruzzi-Perri, S.A. Robertson, L.A. Dent, Interleukin-5 transgene expression and eosinophilia are associated with retarded mammary gland development in mice, Biol. Reprod. 69 (1) (2003) 224–233.
[235] M.O. DeNichilo, V. Panagopoulos, T.E. Rayner, R.A. Borowicz, J.E. Greenwood, A. Evdokiou, Peroxidase enzymes regulate collagen extracellular matrix biosynthesis, Am. J. Pathol. 185 (5) (2015) 1372–1384.
[236] V. Panagopoulos, D.A. Leach, I. Zinonos, V. Ponomarev, G. Licari, V. Liapis, W. V. Ingman, P. Anderson, M.O. DeNichilo, A. Evdokiou, Inflammatory peroxidases promote breast cancer progression in mice via regulation of the tumour microenvironment, Int. J. Oncol. 50 (4) (2017) 1191–1200.
[237] M.A. Cichon, D.C. Radisky, Extracellular matrix as a contextual determinant of transforming growth factor-beta signaling in epithelial-mesenchymal transition and in cancer, Cell Adhes. Migr. 8 (6) (2014) 588–594.
[238] J.N. Fain, D.S. Tichansky, A.K. Madan, Transforming growth factor beta1 release by human adipose tissue is enhanced in obesity, Metabolism 54 (11) (2005) 1546–1551.
[239] X. Sun, S.A. Robertson, W.V. Ingman, Regulation of epithelial cell turnover and macrophage phenotype by epithelial cell-derived transforming growth factor beta1 in the mammary gland, Cytokine 61 (2) (2013) 377–388.
[240] W.V. Ingman, S.A. Robertson, Transforming growth factor-β1 null mutation causes infertility in male mice associated with testosterone deficiency and sexual dysfunction, Endocrinology 148 (8) (2007) 4032–4043.
[241] X. Sun, G.L. Gierach, R. Sandhu, T. Williams, B.R. Midkiff, J. Lissowska, E. Wesolowska, N.F. Boyd, N.B. Johnson, J.D. Figueroa, M.E. Sherman, M. A. Troester, Relationship of mammographic density and gene expression: analysis of normal breast tissue surrounding breast cancer, Clin. Cancer Res. 19 (18) (2013) 4972–4982.
[242] W.T. Yang, M.T. Lewis, K. Hess, H. Wong, A. Tsimelzon, N. Karadag, M. Cairo, C. Wei, F. Meric-Bernstam, P. Brown, B. Arun, G.N. Hortobagyi, A. Sahin, J. C. Chang, Decreased TGFbeta signaling and increased COX2 expression in high risk women with increased mammographic breast density, Breast Cancer Res. Treat. 119 (2) (2010) 305–314.
[243] N.F. Boyd, G.S. Dite, J. Stone, A. Gunasekara, D.R. English, M.R.E. McCredie, G. G. Giles, D. Tritchler, A. Chiarelli, M.J. Yaffe, J.L. Hopper, Heritability of mammographic density, a risk factor for breast cancer, N. Engl. J. Med. 347 (12) (2002) 886–894.
[244] J.S. Pankow, C.M. Vachon, C.C. Kuni, R.A. King, D.K. Arnett, D.M. Grabrick, S. S. Rich, V.E. Anderson, T.A. Sellers, Genetic analysis of mammographic breast density in adult women: evidence of a gene effect, J. Natl. Cancer Inst. 89 (8) (1997) 549–556.
[245] G. Ursin, E.O. Lillie, E. Lee, M. Cockburn, N.J. Schork, W. Cozen, Y.R. Parisky, A. S. Hamilton, M.A. Astrahan, T. Mack, The relative importance of genetics and environment on mammographic density, Cancer Epidemiol. Biomark. Prev. 18 (1) (2009) 102–112.
[246] J. Stone, The heritability of mammographically dense and nondense breast tissue, Cancer Epidemiol. Biomark. Prev. 15 (4) (2006) 612–617.
[247] J.S. Varghese, D.J. Thompson, K. Michailidou, S. Lindstrom, C. Turnbull, J. Brown, J. Leyland, R.M.L. Warren, R.N. Luben, R.J. Loos, N.J. Wareham, J. Rommens, A.D. Paterson, L.J. Martin, C.M. Vachon, C.G. Scott, E.J. Atkinson, F. J. Couch, J. Apicella, M.C. Southey, J. Stone, J. Li, L. Eriksson, K. Czene, N. F. Scott, P. Hall, J.L. Hopper, R.M. Tamimi, N. Rahman, D.F. Easton, Mammographic breast density and breast cancer: evidence of a shared genetic basis, Cancer Res. 72 (6) (2012) 1478–1484.
[248] J. Stone, D.J. Thompson, I. Dos Santos Silva, C. Scott, R.M. Tamimi, S. Lindstrom, P. Kraft, A. Hazra, J. Li, L. Eriksson, K. Czene, P. Hall, M. Jensen, J. Cunningham, J.E. Olson, K. Purrington, F.J. Couch, J. Brown, J. Leyland, R.M.L. Warren, R. N. Luben, K.T. Khaw, P. Smith, N.J. Wareham, S.M. Jud, K. Heusinger, M. W. Beckmann, J.A. Douglas, K.P. Shah, H.P. Chan, M.A. Helvie, L. Le Marchand, L.N. Kolonel, C. Woolcott, G. Maskarinec, C. Haiman, G.G. Giles, L. Baglietto, K. Krishnan, M.C. Southey, C. Apicella, I.L. Andrulis, J.A. Knight, G. Ursin, G.I. G. Alnaes, V.N. Kristensen, A.L. Borresen-Dale, I.T. Gram, M.K. Bolla, Q. Wang, K. Michailidou, J. Dennis, J. Simard, P. Pharoah, A.M. Dunning, D.F. Easton, P. A. Fasching, V.S. Pankratz, J.L. Hopper, C.M. Vachon, Novel associations between common breast cancer susceptibility variants and risk-predicting mammographic density measures, Cancer Res. 75 (12) (2015) 2457–2467.
[249] J. Stone, E. Folkerd, D. Doody, C. Schroen, S.A. Treloar, G.G. Giles, M.C. Pike, D. R. English, M.C. Southey, J.L. Hopper, M. Dowsett, Familial correlations in postmenopausal serum concentrations of sex steroid hormones and other mitogens: a twins and sisters study, J. Clin. Endocrinol. Metab. 94 (12) (2009) 4793–4800.
[250] Y. Hong, N.L. Pedersen, K. Brismar, K. Hall, U. de Faire, Quantitative genetic analyses of insulin-like growth factor I (IGF-I), IGF-binding protein-1, and insulin levels in middle-aged and elderly twins, J. Clin. Endocrinol. Metab. 81 (5) (1996) 1791–1797.
[251] F. Odefrey, J. Stone, L.C. Gurrin, G.B. Byrnes, C. Apicella, G.S. Dite, J.N. Cawson, G.G. Giles, S.A. Treloar, D.R. English, J.L. Hopper, M.C. Southey, Common genetic variants associated with breast cancer and mammographic density measures that predict disease, Cancer Res. 70 (4) (2010) 1449–1458.
[252] E. Lee, D. Van Den Berg, C. Hsu, G. Ursin, W.-P. Koh, J.-M. Yuan, D.O. Stram, M. C. Yu, A.H. Wu, Genetic variation in transforming growth factor Beta 1 and mammographic density in Singapore Chinese women, Cancer Res. 73 (6) (2013) 1876–1882.
[253] S. Lindström, D.J. Thompson, A.D. Paterson, J. Li, G.L. Gierach, C. Scott, J. Stone, J.A. Douglas, I. dos-Santos-Silva, P. Fernandez-Navarro, J. Verghase, P. Smith, J. Brown, R. Luben, N.J. Wareham, R.J.F. Loos, J.A. Heit, V. Shane Pankratz, A. Norman, E.L. Goode, J.M. Cunningham, M. deAndrade, R.A. Vierkant, K. Czene, P.A. Fasching, L. Baglietto, M.C. Southey, G.G. Giles, K.P. Shah, H. P. Chan, M.A. Helvie, A.H. Beck, N.W. Knoblauch, A. Hazra, D.J. Hunter, P. Kraft, M. Pollan, J.D. Figueroa, F.J. Couch, J.L. Hopper, P. Hall, D.F. Easton, N.F. Boyd, C.M. Vachon, R.M. Tamimi, Genome-wide association study identifies multiple loci associated with both mammographic density and breast cancer risk, Nat. Commun. 5 (2014) 5303.
[254] C.M. Vachon, C.G. Scott, P.A. Fasching, P. Hall, R.M. Tamimi, J. Li, J. Stone, C. Apicella, F. Odefrey, G.L. Gierach, S.M. Jud, K. Heusinger, M.W. Beckmann, M. Pollan, P. Fernandez-Navarro, A. Gonzalez-Neira, J. Benitez, C.H. van Gils, M. Lokate, N.C. Onland-Moret, P.H.M. Peeters, J. Brown, J. Leyland, J. S. Varghese, D.F. Easton, D.J. Thompson, R.N. Luben, R.M.L. Warren, N. J. Wareham, P. Loos, K.T. Khaw, G. Ursin, E. Lee, S.A. Gayther, S.J. Ramus, R. A. Eeles, M.O. Leach, G. Kwan-Lim, F.J. Couch, G.G. Giles, L. Baglietto, K. Krishnan, M.C. Southey, L. Le Marchand, L.N. Kolonel, C. Woolcott, G. Maskarinec, C.A. Haiman, K. Walker, N. Johnson, V.A. McCormack, M. Biong, G.I.G. Alnaes, I.T. Gram, V.N. Kristensen, A.L. Borresen-Dale, S. Lindstrom, S. E. Hankinson, D.J. Hunter, I.L. Andrulis, J.A. Knight, N.F. Boyd, J.D. Figuero, J. Lissowska, E. Wesolowska, B. Peplonska, A. Bukowska, E. Reszka, J. Liu, L. Eriksson, K. Czene, T. Audley, A.H. Wu, V.S. Pankratz, J.L. Hopper, I. dos-Santos-Silva, Common breast cancer susceptibility variants in LSP1 and RAD51L1 are associated with mammographic density measures that predict breast cancer risk, Cancer Epidemiol. Biomark. Prev. 21 (7) (2012) 1156–1166.
[255] L.C. Houghton, J.A. Knight, Y. Wei, R.D. Romeo, M. Goldberg, I.L. Andrulis, A. R. Bradbury, S.S. Buys, M.B. Daly, E.M. John, W.K. Chung, R.M. Santella, F. Z. Stanczyk, M.B. Terry, Association of prepubertal and adolescent androgen concentrations with timing of breast development and family history of breast cancer, JAMA Netw. Open 2 (2) (2019), e190083.

[256] N.F.H.J. Boyd, Mammographic density of the breast: the authors reply, N. Engl. J. Med. 348 (2) (2003) 174–175.
[257] E.M. Wong, M.C. Southey, S.B. Fox, M.A. Brown, J.G. Dowty, M.A. Jenkins, G. G. Giles, J.L. Hopper, A. Dobrovic, Constitutional methylation of the BRCA1 promoter is specifically associated with BRCA1 mutation-associated pathology in early-onset breast cancer, Cancer Prev. Res. (Phila.) 4 (1) (2011) 23–33.
[258] K. Brennan, M. Garcia-Closas, N. Orr, O. Fletcher, M. Jones, A. Ashworth, A. Swerdlow, H. Thorne, E. Riboli, P. Vineis, M. Dorronsoro, F. Clavel-Chapelon, S. Panico, N.C. Onland-Moret, D. Trichopoulos, R. Kaaks, K.T. Khaw, R. Brown, J. M. Flanagan, Intragenic ATM methylation in peripheral blood DNA as a biomarker of breast cancer risk, Cancer Res. 72 (9) (2012) 2304–2313.
[259] T. Iwamoto, N. Yamamoto, T. Taguchi, Y. Tamaki, S. Noguchi, BRCA1 promoter methylation in peripheral blood cells is associated with increased risk of breast cancer with BRCA1 promoter methylation, Breast Cancer Res. Treat. 129 (1) (2011) 69–77.
[260] G. Severi, M.C. Southey, D.R. English, C.H. Jung, A. Lonie, C. McLean, H. Tsimiklis, J.L. Hopper, G.G. Giles, L. Baglietto, Epigenome-wide methylation in DNA from peripheral blood as a marker of risk for breast cancer, Breast Cancer Res. Treat. 148 (3) (2014) 665–673.
[261] K. van Veldhoven, S. Polidoro, L. Baglietto, G. Severi, C. Sacerdote, S. Panico, A. Mattiello, D. Palli, G. Masala, V. Krogh, C. Agnoli, R. Tumino, G. Frasca, K. Flower, E. Curry, N. Orr, K. Tomczyk, M.E. Jones, A. Ashworth, A. Swerdlow, M. Chadeau-Hyam, E. Lund, M. Garcia-Closas, T.M. Sandanger, J.M. Flanagan, P. Vineis, Epigenome-wide association study reveals decreased average methylation levels years before breast cancer diagnosis, Clin. Epigenet. 7 (1) (2015) 67.
[262] Z. Xu, S.C. Bolick, L.A. DeRoo, C.R. Weinberg, D.P. Sandler, J.A. Taylor, Epigenome-wide association study of breast cancer using prospectively collected sister study samples, J. Natl. Cancer Inst. 105 (10) (2013) 694–700.
[263] H. Heyn, F.J. Carmona, A. Gomez, H.J. Ferreira, J.T. Bell, S. Sayols, K. Ward, O. A. Stefansson, S. Moran, J. Sandoval, J.E. Eyfjord, T.D. Spector, M. Esteller, DNA methylation profiling in breast cancer discordant identical twins identifies DOK7 as novel epigenetic biomarker, Carcinogenesis 34 (1) (2013) 102–108.
[264] M. Chen, E.M. Wong, T.L. Nguyen, G.S. Dite, J. Stone, G.G. Giles, M.C. Southey, J. L. Hopper, S. Li, Associations between environmental breast cancer risk factors and DNA methylation-based risk-predicting measures, bioRxiv (2018), 446484.
[265] S. Li, P.-A. Dugué, L. Baglietto, G. Severi, E.M. Wong, T.L. Nguyen, J. Stone, D. R. English, M.C. Southey, G.G. Giles, J.L. Hopper, R.L. Milne, Genome-wide association study of peripheral blood DNA methylation and conventional mammographic density measures, Int. J. Cancer 145 (7) (2019) 1768–1773.
[266] S. Li, E.M. Wong, M. Bui, T.L. Nguyen, J.-H.E. Joo, J. Stone, G.S. Dite, P.-A. Dugué, R.L. Milne, G.G. Giles, R. Saffery, M.C. Southey, J.L. Hopper, Inference about causation between body mass index and DNA methylation in blood from a twin family study, Int. J. Obes. 43 (2) (2019) 243–252.
[267] S.E. Fenton, C. Reed, R.R. Newbold, Perinatal environmental exposures affect mammary development, function, and cancer risk in adulthood, Annu. Rev. Pharmacol. Toxicol. 52 (2012) 455–479.
[268] L. Hilakivi-Clarke, S. de Assis, A. Warri, Exposures to synthetic estrogens at different times during the life, and their effect on breast cancer risk, J. Mammary Gland Biol. Neoplasia 18 (1) (2013) 25–42.
[269] S. Li, E.M. Wong, P.-A. Dugué, A.F. McRae, E. Kim, J.-H.E. Joo, T.L. Nguyen, J. Stone, G.S. Dite, N.J. Armstrong, K.A. Mather, A. Thalamuthu, M.J. Wright, D. Ames, R.L. Milne, J.M. Craig, R. Saffery, G.W. Montgomery, Y.M. Song, J. Sung, T.D. Spector, P.S. Sachdev, G.G. Giles, M.C. Southey, J.L. Hopper, Genome-wide average DNA methylation is determined in utero, Int. J. Epidemiol. 47 (3) (2018) 908–916.
[270] H. Jernstrom, N. Loman, O.T. Johannsson, A. Borg, H. Olsson, Impact of teenage oral contraceptive use in a population-based series of early-onset breast cancer cases who have undergone BRCA mutation testing, Eur. J. Cancer 41 (15) (2005) 2312–2320.
[271] T.J. Anderson, S. Battersby, R.J. King, K. McPherson, J.J. Going, Oral contraceptive use influences resting breast proliferation, Hum. Pathol. 20 (12) (1989) 1139–1144.
[272] A.M. Binder, C. Corvalan, V. Mericq, A. Pereira, J.L. Santos, S. Horvath, J. Shepherd, K.B. Michels, Faster ticking rate of the epigenetic clock is associated with faster pubertal development in girls, Epigenetics 13 (1) (2018) 85–94.
[273] S. Saji, E.V. Jensen, S. Nilsson, T. Rylander, M. Warner, J.Å. Gustafsson, Estrogen receptors α and β in the rodent mammary gland, Breast Cancer Res. 2 (1) (2000). S.11.
[274] G. Cheng, Z. Weihua, M. Warner, J.-Å. Gustafsson, Estrogen receptors ERα and ERβ in proliferation in the rodent mammary gland, Proc. Natl. Acad. Sci. USA 101 (11) (2004) 3739–3746.
[275] N.F. Gomes-Rochette, L.S. Souza, B.O. Tommasi, D.F. Pedrosa, S.R. Eis, I.d.C. F. Fin, F.L.H. Vieira, J.B. Graceli, L.B.A. Rangel, I.V. Silva, Association of *Pvu*II and *Xba*I polymorphisms on estrogen receptor alpha (ESR1) gene to changes into serum lipid profile of post-menopausal women: effects of aging, body mass index and breast cancer incidence, PLoS One 12 (2) (2017), e0169266.
[276] M.A. Souza, A.d.M.d. Fonseca, V.R. Bagnoli, N.d. Barros, É.M.d. Neves, S.D.T.d. A. Moraes, V.H.S. Hortense, J.M. Soares, E.C. Baracat, The expression of the estrogen receptor in obese patients with high breast density (HBD), Gynecol. Endocrinol. 30 (1) (2014) 78–80.
[277] S. Tchatchou, A. Jung, K. Hemminki, C. Sutter, B. Wappenschmidt, P. Bugert, B.H. F. Weber, D. Niederacher, N. Arnold, R. Varon-Mateeva, N. Ditsch, A. Meindl, R. K. Schmutzler, C.R. Bartram, B. Burwinkel, A variant affecting a putative miRNA target site in estrogen receptor (ESR) 1 is associated with breast cancer risk in premenopausal women, Carcinogenesis 30 (1) (2008) 59–64.
[278] A.M. Binder, L.T. Stiemsma, K. Keller, S.D. van Otterdijk, V. Mericq, A. Pereira, J. L. Santos, J. Shepherd, K.B. Michels, Inverse association between estrogen receptor-α DNA methylation and breast composition in adolescent Chilean girls, Clin. Epigenet. 10 (1) (2018) 122.
[279] J. Russo, X. Ao, C. Grill, I.H. Russo, Pattern of distribution of cells positive for estrogen receptor α and progesterone receptor in relation to proliferating cells in the mammary gland, Breast Cancer Res. Treat. 53 (3) (1999) 217–227.
[280] K.B.R. Ewan, H.A. Oketch-Rabah, S.A. Ravani, G. Shyamala, H.L. Moses, M. H. Barcellos-Hoff, Proliferation of estrogen receptor-α-positive mammary epithelial cells is restrained by transforming growth factor-β1 in adult mice, Am. J. Pathol. 167 (2) (2005) 409–417.
[281] A.M. Band, M. Laiho, Crosstalk of TGF-β and estrogen receptor signaling in breast cancer, J. Mammary Gland Biol. Neoplasia 16 (2) (2011) 109–115.
[282] M.E. Sehl, J.E. Henry, A.M. Storniolo, P.A. Ganz, S. Horvath, DNA methylation age is elevated in breast tissue of healthy women, Breast Cancer Res. Treat. 164 (1) (2017) 209–219.
[283] E.W. Hofstatter, S. Horvath, D. Dalela, P. Gupta, A.B. Chagpar, V.B. Wali, V. Bossuyt, A.M. Storniolo, C. Hatzis, G. Patwardhan, M.K. Von Wahlde, M. Butler, L. Epstein, K. Stavris, T. Sturrock, A. Wali, S. Kwei, L. Pusztai, Increased epigenetic age in normal breast tissue from luminal breast cancer patients, Clin. Epigenet. 10 (1) (2018) 112.
[284] Ze Hochberg, J. Belsky, Evo-devo of human adolescence: beyond disease models of early puberty, BMC Med. 11 (1) (2013) 113.
[285] Z. Hochberg, Developmental plasticity in child growth and maturation, Front. Endocrinol. 2 (2011) 41.
[286] A. Must, W.C. Willett, W.H. Dietz, Remote recall of childhood height, weight, and body build by elderly subjects, Am. J. Epidemiol. 138 (1) (1993) 56–64.
[287] R.J. Kuczmarski, C.L. Ogden, L.M. Grummer-Strawn, K.M. Flegal, S.S. Guo, R. Wei, Z. Mei, L.R. Curtin, A.F. Roche, C.L. Johnson, CDC growth charts: United States, Adv. Data 314 (2000) 1–27.
[288] S.J. Graham, S. Ness, B.S. Hamilton, M.J. Bronskill, Magnetic resonance properties of ex vivo breast tissue at 1.5T, Magn. Reson. Med. 38 (4) (1997) 669–677.
[289] S.J. Graham, M.J. Bronskill, J.W. Byng, M.J. Yaffe, N.F. Boyd, Quantitative correlation of breast tissue parameters using magnetic resonance and X-ray mammography, Br. J. Cancer 73 (2) (1996) 162–168.

APPENDIX B

Copyright licence agreement with Wolters Kluwer Health, Inc for images in Figure 1.2.A, C reproduced from Hoda *et al.,* (2008), Rosen's Breast Pathology.

WOLTERS KLUWER HEALTH, INC. LICENSE
TERMS AND CONDITIONS

Aug 27, 2021

This Agreement between Miss. Amita Ghadge ("You") and Wolters Kluwer Health, Inc. ("Wolters Kluwer Health, Inc.") consists of your license details and the terms and conditions provided by Wolters Kluwer Health, Inc. and Copyright Clearance Center.

The publisher has provided special terms related to this request that can be found at the end of the Publisher's Terms and Conditions.

License Number	5137360027932
License date	Aug 27, 2021
Licensed Content Publisher	Wolters Kluwer Health, Inc.
Licensed Content Publication	WK Health Book
Licensed Content Title	Rosen's Breast Pathology
Licensed Content Author	Syed A. Hoda MD, Paul Peter Rosen MD, Edi Brogi MD, PHD, Frederick C. Koerner MD
Licensed Content Date	Dec 1, 2020
Type of Use	Dissertation/Thesis
Requestor type	University/College
Sponsorship	No Sponsorship
Format	Print and electronic
Will this be posted online?	Yes, on a secure website

Portion	Figures/tables/illustrations
Number of figures/tables/illustrations	2
Author of this Wolters Kluwer article	No
Will you be translating?	No
Intend to modify/change the content	No
Current or previous edition of book	Previous edition
Title	The developmental origins of mammographic density and breast cancer risk
Institution name	The University of Adelaide
Expected presentation date	Nov 2021
Portions	The figures are Fig 1.1B and Fig 1.3B
What edition are you requesting from?	3rd edition
Requestor Location	Miss. Amita Ghadge Unit 604, 304 Waymouth Street Adelaide, South Australia 5000 Australia Attn: Miss. Amita Ghadge
Publisher Tax ID	13-2932696
Billing Type	Invoice
Billing Address	Miss. Amita Ghadge Unit 604, 304 Waymouth Street

Adelaide, Australia 5000
Attn: Miss. Amita Ghadge

Total 0.00 AUD

Terms and Conditions

Wolters Kluwer Health Inc. Terms and Conditions

1. **Duration of License:** Permission is granted for a one time use only. Rights herein do not apply to future reproductions, editions, revisions, or other derivative works. This permission shall be effective as of the date of execution by the parties for the maximum period of 12 months and should be renewed after the term expires.
    i. When content is to be republished in a book or journal the validity of this agreement should be the life of the book edition or journal issue.
    ii. When content is licensed for use on a website, internet, intranet, or any publicly accessible site (not including a journal or book), you agree to remove the material from such site after 12 months, or request to renew your permission license
2. **Credit Line:** A credit line must be prominently placed and include: For book content: the author(s), title of book, edition, copyright holder, year of publication; For journal content: the author(s), titles of article, title of journal, volume number, issue number, inclusive pages and website URL to the journal page; If a journal is published by a learned society the credit line must include the details of that society.
3. **Warranties:** The requestor warrants that the material shall not be used in any manner which may be considered derogatory to the title, content, authors of the material, or to Wolters Kluwer Health, Inc.
4. **Indemnity:** You hereby indemnify and hold harmless Wolters Kluwer Health, Inc. and its respective officers, directors, employees and agents, from and against any and all claims, costs, proceeding or demands arising out of your unauthorized use of the Licensed Material
5. **Geographical Scope:** Permission granted is non-exclusive and is valid throughout the world in the English language and the languages specified in the license.
6. **Copy of Content:** Wolters Kluwer Health, Inc. cannot supply the requestor with the original artwork, high-resolution images, electronic files or a clean copy of content.
7. **Validity:** Permission is valid if the borrowed material is original to a Wolters Kluwer Health, Inc. imprint (J.B Lippincott, Lippincott-Raven Publishers, Williams & Wilkins, Lea & Febiger, Harwal, Rapid Science, Little Brown & Company, Harper & Row Medical, American Journal of Nursing Co, and Urban & Schwarzenberg - English Language, Raven Press, Paul Hoeber, Springhouse, Ovid), and the Anatomical Chart Company
8. **Third Party Material:** This permission does not apply to content that is credited to publications other than Wolters Kluwer Health, Inc. or its Societies. For images credited to non-Wolters Kluwer Health, Inc. books or journals, you must obtain permission from the source referenced in the figure or table legend or credit line before making any use of the image(s), table(s) or other content.
9. **Adaptations:** Adaptations are protected by copyright. For images that have been adapted, permission must be sought from the rightsholder of the original material and the rightsholder of the adapted material.
10. **Modifications:** Wolters Kluwer Health, Inc. material is not permitted to be modified or adapted without written approval from Wolters Kluwer Health, Inc. with the exception of text size or color. The adaptation should be credited as follows: Adapted with permission from Wolters Kluwer Health, Inc.: [the author(s), title of book,

edition, copyright holder, year of publication] or [the author(s), titles of article, title of journal, volume number, issue number, inclusive pages and website URL to the journal page].

11. **Full Text Articles:** Republication of full articles in English is prohibited.
12. **Branding and Marketing:** No drug name, trade name, drug logo, or trade logo can be included on the same page as material borrowed from *Diseases of the Colon & Rectum, Plastic Reconstructive Surgery, Obstetrics & Gynecology (The Green Journal), Critical Care Medicine, Pediatric Critical Care Medicine, the American Heart Association publications and the American Academy of Neurology publications.*
13. **Open Access:** Unless you are publishing content under the same Creative Commons license, the following statement must be added when reprinting material in Open Access journals: "The Creative Commons license does not apply to this content. Use of the material in any format is prohibited without written permission from the publisher, Wolters Kluwer Health, Inc. Please contact permissions@lww.com for further information."
14. **Translations:** The following disclaimer must appear on all translated copies: Wolters Kluwer Health, Inc. and its Societies take no responsibility for the accuracy of the translation from the published English original and are not liable for any errors which may occur.
15. **Published Ahead of Print (PAP):** Articles in the PAP stage of publication can be cited using the online publication date and the unique DOI number.
    i. Disclaimer: Articles appearing in the PAP section have been peer-reviewed and accepted for publication in the relevant journal and posted online before print publication. Articles appearing as PAP may contain statements, opinions, and information that have errors in facts, figures, or interpretation. Any final changes in manuscripts will be made at the time of print publication and will be reflected in the final electronic version of the issue. Accordingly, Wolters Kluwer Health, Inc., the editors, authors and their respective employees are not responsible or liable for the use of any such inaccurate or misleading data, opinion or information contained in the articles in this section.
16. **Termination of Contract:** Wolters Kluwer Health, Inc. must be notified within 90 days of the original license date if you opt not to use the requested material.
17. **Waived Permission Fee:** Permission fees that have been waived are not subject to future waivers, including similar requests or renewing a license.
18. **Contingent on payment:** You may exercise these rights licensed immediately upon issuance of the license, however until full payment is received either by the publisher or our authorized vendor, this license is not valid. If full payment is not received on a timely basis, then any license preliminarily granted shall be deemed automatically revoked and shall be void as if never granted. Further, in the event that you breach any of these terms and conditions or any of Wolters Kluwer Health, Inc.'s other billing and payment terms and conditions, the license is automatically revoked and shall be void as if never granted. Use of materials as described in a revoked license, as well as any use of the materials beyond the scope of an unrevoked license, may constitute copyright infringement and publisher reserves the right to take any and all action to protect its copyright in the materials.
19. **STM Signatories Only:** Any permission granted for a particular edition will apply to subsequent editions and for editions in other languages, provided such editions are for the work as a whole in situ and do not involve the separate exploitation of the permitted illustrations or excerpts. Please view: STM Permissions Guidelines
20. **Warranties and Obligations:** LICENSOR further represents and warrants that, to the best of its knowledge and belief, LICENSEE's contemplated use of the Content as represented to LICENSOR does not infringe any valid rights to any third party.
21. **Breach:** If LICENSEE fails to comply with any provisions of this agreement, LICENSOR may serve written notice of breach of LICENSEE and, unless such breach is fully cured within fifteen (15) days from the receipt of notice by LICENSEE, LICENSOR may thereupon, at its option, serve notice of cancellation on LICENSEE, whereupon this Agreement shall immediately terminate.

22. **Assignment:** License conveyed hereunder by the LICENSOR shall not be assigned or granted in any manner conveyed to any third party by the LICENSEE without the consent in writing to the LICENSOR.
23. **Governing Law:** The laws of The State of New York shall govern interpretation of this Agreement and all rights and liabilities arising hereunder.
24. **Unlawful:** If any provision of this Agreement shall be found unlawful or otherwise legally unenforceable, all other conditions and provisions of this Agreement shall remain in full force and effect.

For Copyright Clearance Center / RightsLink Only:

1. **Service Description for Content Services:** Subject to these terms of use, any terms set forth on the particular order, and payment of the applicable fee, you may make the following uses of the ordered materials:
    i. **Content Rental:** You may access and view a single electronic copy of the materials ordered for the time period designated at the time the order is placed. Access to the materials will be provided through a dedicated content viewer or other portal, and access will be discontinued upon expiration of the designated time period. An order for Content Rental does not include any rights to print, download, save, create additional copies, to distribute or to reuse in any way the full text or parts of the materials.
    ii. **Content Purchase:** You may access and download a single electronic copy of the materials ordered. Copies will be provided by email or by such other means as publisher may make available from time to time. An order for Content Purchase does not include any rights to create additional copies or to distribute copies of the materials

Other Terms and Conditions:
null

v1.18

Questions? customercare@copyright.com or +1-855-239-3415 (toll free in the US) or +1-978-646-2777.

APPENDIX C

Copyright licence agreement with Wolters Kluwer Health, Inc for image in Figure 1.2.B reproduced from Hoda *et al.,* (2010), Rosen's Diagnosis of Breast Pathology by Needle Core Biopsy.

WOLTERS KLUWER HEALTH, INC. LICENSE
TERMS AND CONDITIONS

Aug 27, 2021

This Agreement between Miss. Amita Ghadge ("You") and Wolters Kluwer Health, Inc. ("Wolters Kluwer Health, Inc.") consists of your license details and the terms and conditions provided by Wolters Kluwer Health, Inc. and Copyright Clearance Center.

The publisher has provided special terms related to this request that can be found at the end of the Publisher's Terms and Conditions.

License Number	5137360221678
License date	Aug 27, 2021
Licensed Content Publisher	Wolters Kluwer Health, Inc.
Licensed Content Publication	WK Health Book
Licensed Content Title	Rosen's Diagnosis of Breast Pathology by Needle Core Biopsy
Licensed Content Author	Syed A. Hoda MD, Paul Peter Rosen MD, Edi Brogi MD, PHD, Frederick C. Koerner MD
Licensed Content Date	Jan 31, 2017
Type of Use	Dissertation/Thesis
Requestor type	University/College
Sponsorship	No Sponsorship
Format	Print and electronic
Will this be posted online?	Yes, on a secure website

Portion	Figures/tables/illustrations
Number of figures/tables/illustrations	1
Author of this Wolters Kluwer article	No
Will you be translating?	No
Intend to modify/change the content	No
Current or previous edition of book	Previous edition
Title	The developmental origins of mammographic density and breast cancer risk
Institution name	The University of Adelaide
Expected presentation date	Nov 2021
Portions	The figure is Fig 1.1
What edition are you requesting from?	3rd edition
Requestor Location	Miss. Amita Ghadge Unit 604, 304 Waymouth Street Adelaide, South Australia 5000 Australia Attn: Miss. Amita Ghadge
Publisher Tax ID	13-2932696
Billing Type	Invoice
Billing Address	Miss. Amita Ghadge Unit 604, 304 Waymouth Street

Adelaide, Australia 5000
Attn: Miss. Amita Ghadge

Total 0.00 AUD

Terms and Conditions

Wolters Kluwer Health Inc. Terms and Conditions

1. **Duration of License:** Permission is granted for a one time use only. Rights herein do not apply to future reproductions, editions, revisions, or other derivative works. This permission shall be effective as of the date of execution by the parties for the maximum period of 12 months and should be renewed after the term expires.
    i. When content is to be republished in a book or journal the validity of this agreement should be the life of the book edition or journal issue.
    ii. When content is licensed for use on a website, internet, intranet, or any publicly accessible site (not including a journal or book), you agree to remove the material from such site after 12 months, or request to renew your permission license
2. **Credit Line:** A credit line must be prominently placed and include: For book content: the author(s), title of book, edition, copyright holder, year of publication; For journal content: the author(s), titles of article, title of journal, volume number, issue number, inclusive pages and website URL to the journal page; If a journal is published by a learned society the credit line must include the details of that society.
3. **Warranties:** The requestor warrants that the material shall not be used in any manner which may be considered derogatory to the title, content, authors of the material, or to Wolters Kluwer Health, Inc.
4. **Indemnity:** You hereby indemnify and hold harmless Wolters Kluwer Health, Inc. and its respective officers, directors, employees and agents, from and against any and all claims, costs, proceeding or demands arising out of your unauthorized use of the Licensed Material
5. **Geographical Scope:** Permission granted is non-exclusive and is valid throughout the world in the English language and the languages specified in the license.
6. **Copy of Content:** Wolters Kluwer Health, Inc. cannot supply the requestor with the original artwork, high-resolution images, electronic files or a clean copy of content.
7. **Validity:** Permission is valid if the borrowed material is original to a Wolters Kluwer Health, Inc. imprint (J.B Lippincott, Lippincott-Raven Publishers, Williams & Wilkins, Lea & Febiger, Harwal, Rapid Science, Little Brown & Company, Harper & Row Medical, American Journal of Nursing Co, and Urban & Schwarzenberg - English Language, Raven Press, Paul Hoeber, Springhouse, Ovid), and the Anatomical Chart Company
8. **Third Party Material:** This permission does not apply to content that is credited to publications other than Wolters Kluwer Health, Inc. or its Societies. For images credited to non-Wolters Kluwer Health, Inc. books or journals, you must obtain permission from the source referenced in the figure or table legend or credit line before making any use of the image(s), table(s) or other content.
9. **Adaptations:** Adaptations are protected by copyright. For images that have been adapted, permission must be sought from the rightsholder of the original material and the rightsholder of the adapted material.
10. **Modifications:** Wolters Kluwer Health, Inc. material is not permitted to be modified or adapted without written approval from Wolters Kluwer Health, Inc. with the exception of text size or color. The adaptation should be credited as follows: Adapted with permission from Wolters Kluwer Health, Inc.: [the author(s), title of book,

edition, copyright holder, year of publication] or [the author(s), titles of article, title of journal, volume number, issue number, inclusive pages and website URL to the journal page].

11. **Full Text Articles:** Republication of full articles in English is prohibited.
12. **Branding and Marketing:** No drug name, trade name, drug logo, or trade logo can be included on the same page as material borrowed from *Diseases of the Colon & Rectum, Plastic Reconstructive Surgery, Obstetrics & Gynecology (The Green Journal), Critical Care Medicine, Pediatric Critical Care Medicine, the American Heart Association publications and the American Academy of Neurology publications.*
13. **Open Access:** Unless you are publishing content under the same Creative Commons license, the following statement must be added when reprinting material in Open Access journals: "The Creative Commons license does not apply to this content. Use of the material in any format is prohibited without written permission from the publisher, Wolters Kluwer Health, Inc. Please contact permissions@lww.com for further information."
14. **Translations:** The following disclaimer must appear on all translated copies: Wolters Kluwer Health, Inc. and its Societies take no responsibility for the accuracy of the translation from the published English original and are not liable for any errors which may occur.
15. **Published Ahead of Print (PAP):** Articles in the PAP stage of publication can be cited using the online publication date and the unique DOI number.
    i. Disclaimer: Articles appearing in the PAP section have been peer-reviewed and accepted for publication in the relevant journal and posted online before print publication. Articles appearing as PAP may contain statements, opinions, and information that have errors in facts, figures, or interpretation. Any final changes in manuscripts will be made at the time of print publication and will be reflected in the final electronic version of the issue. Accordingly, Wolters Kluwer Health, Inc., the editors, authors and their respective employees are not responsible or liable for the use of any such inaccurate or misleading data, opinion or information contained in the articles in this section.
16. **Termination of Contract:** Wolters Kluwer Health, Inc. must be notified within 90 days of the original license date if you opt not to use the requested material.
17. **Waived Permission Fee:** Permission fees that have been waived are not subject to future waivers, including similar requests or renewing a license.
18. **Contingent on payment:** You may exercise these rights licensed immediately upon issuance of the license, however until full payment is received either by the publisher or our authorized vendor, this license is not valid. If full payment is not received on a timely basis, then any license preliminarily granted shall be deemed automatically revoked and shall be void as if never granted. Further, in the event that you breach any of these terms and conditions or any of Wolters Kluwer Health, Inc.'s other billing and payment terms and conditions, the license is automatically revoked and shall be void as if never granted. Use of materials as described in a revoked license, as well as any use of the materials beyond the scope of an unrevoked license, may constitute copyright infringement and publisher reserves the right to take any and all action to protect its copyright in the materials.
19. **STM Signatories Only:** Any permission granted for a particular edition will apply to subsequent editions and for editions in other languages, provided such editions are for the work as a whole in situ and do not involve the separate exploitation of the permitted illustrations or excerpts. Please view: STM Permissions Guidelines
20. **Warranties and Obligations:** LICENSOR further represents and warrants that, to the best of its knowledge and belief, LICENSEE's contemplated use of the Content as represented to LICENSOR does not infringe any valid rights to any third party.
21. **Breach:** If LICENSEE fails to comply with any provisions of this agreement, LICENSOR may serve written notice of breach of LICENSEE and, unless such breach is fully cured within fifteen (15) days from the receipt of notice by LICENSEE, LICENSOR may thereupon, at its option, serve notice of cancellation on LICENSEE, whereupon this Agreement shall immediately terminate.

22. **Assignment:** License conveyed hereunder by the LICENSOR shall not be assigned or granted in any manner conveyed to any third party by the LICENSEE without the consent in writing to the LICENSOR.
23. **Governing Law:** The laws of The State of New York shall govern interpretation of this Agreement and all rights and liabilities arising hereunder.
24. **Unlawful:** If any provision of this Agreement shall be found unlawful or otherwise legally unenforceable, all other conditions and provisions of this Agreement shall remain in full force and effect.

For Copyright Clearance Center / RightsLink Only:

1. **Service Description for Content Services:** Subject to these terms of use, any terms set forth on the particular order, and payment of the applicable fee, you may make the following uses of the ordered materials:
    i. **Content Rental:** You may access and view a single electronic copy of the materials ordered for the time period designated at the time the order is placed. Access to the materials will be provided through a dedicated content viewer or other portal, and access will be discontinued upon expiration of the designated time period. An order for Content Rental does not include any rights to print, download, save, create additional copies, to distribute or to reuse in any way the full text or parts of the materials.
    ii. **Content Purchase:** You may access and download a single electronic copy of the materials ordered. Copies will be provided by email or by such other means as publisher may make available from time to time. An order for Content Purchase does not include any rights to create additional copies or to distribute copies of the materials

Other Terms and Conditions:
null

v1.18

Questions? customercare@copyright.com or +1-855-239-3415 (toll free in the US) or +1-978-646-2777.

REFERENCES

1. Boyd NF, Guo H, Martin LJ, Sun L, Stone J, Fishell E, et al. Mammographic density and the risk and detection of breast cancer. N Engl J Med. 2007;356(3):227-36.

2. Engmann NJ, Golmakani MK, Miglioretti DL, Sprague BL, Kerlikowske K. Population-Attributable Risk Proportion of Clinical Risk Factors for Breast Cancer. JAMA oncology. 2017;3(9):1228-36.

3. Huo CW, Chew GL, Britt KL, Ingman WV, Henderson MA, Hopper JL, et al. Mammographic density-a review on the current understanding of its association with breast cancer. Breast Cancer Res Treat. 2014;144(3):479-502.

4. McCormack VA, dos Santos Silva I. Breast density and parenchymal patterns as markers of breast cancer risk: a meta-analysis. Cancer epidemiology, biomarkers & prevention. 2006;15(6):1159-69.

5. Wolfe JN. Risk for breast cancer development determined by mammographic parenchymal pattern. Cancer. 1976;37(5):2486-92.

6. Bond-Smith D, Stone J. Methodological Challenges and Updated Findings from a Meta-analysis of the Association between Mammographic Density and Breast Cancer. Cancer epidemiology, biomarkers & prevention. 2019;28(1):22-31.

7. Robinson GW, Karpf ABC, Kratochwil K. Regulation of Mammary Gland Development by Tissue Interaction. Journal of Mammary Gland Biology and Neoplasia. 1999;4(1):9-19.

8. Sakakura T. Mammary embryogensis. In C. W. Neville and M. C. Daniel (eds.). The Mammary Gland: Development, Regulation, and Function Plenum Press, New York. 1987:37–66.

9. Propper A, Gomot L. Tissue interactions during organogenesis of the mammary gland in the rabbit embryo. C R Acad Hebd Seances Acad Sci D. 1967;264(22):2573-5.

10. Cunha GR, Young P, Christov K, Guzman R, Nandi S, Talamantes F, et al. Mammary phenotypic expression induced in epidermal cells by embryonic mammary mesenchyme. Acta Anat (Basel). 1995;152(3):195-204.

11. Gusterson BA, Stein T. Human breast development. Semin Cell Dev Biol. 2012;23(5):567-73.

12. Javed A, Lteif A. Development of the human breast. Semin Plast Surg. 2013;27(1):5-12.

13. Samimi G, Colditz GA, Baer HJ, Tamimi RM. Measures of energy balance and mammographic density in the Nurses' Health Study. Breast Cancer Res Treat. 2008;109(1):113-22.

14. Sellers TA, Vachon CM, Pankratz VS, Janney CA, Fredericksen Z, Brandt KR, et al. Association of childhood and adolescent anthropometric factors, physical activity, and diet with adult mammographic breast density. Am J Epidemiol. 2007;166(4):456-64.

15. Harris HR, Tamimi RM, Willett WC, Hankinson SE, Michels KB. Body size across the life course, mammographic density, and risk of breast cancer. Am J Epidemiol. 2011;174(8):909-18.

16. Jeffreys M, Warren R, Gunnell D, McCarron P, Smith GD. Life course breast cancer risk factors and adult breast density (United Kingdom). Cancer Causes Control. 2004;15(9):947-55.

17. Lope V, Pérez-Gómez B, Moreno MP, Vidal C, Salas-Trejo D, Ascunce N, et al. Childhood factors associated with mammographic density in adult women. Breast Cancer Res Treat. 2011;130(3):965-74.

18. McCormack VA, dos Santos Silva I, De Stavola BL, Perry N, Vinnicombe S, Swerdlow AJ, et al. Life-course body size and perimenopausal mammographic parenchymal patterns in the MRC 1946 British birth cohort. Br J Cancer. 2003;89(5):852-9.

19. Andersen ZJ, Baker JL, Bihrmann K, Vejborg I, Sorensen TI, Lynge E. Birth weight, childhood body mass index, and height in relation to mammographic density and breast cancer: a register-based cohort study. Breast Cancer Res. 2014;16(1):R4.

20. Hopper JL, Nguyen TL, Stone J, Aujard K, Matheson MC, Abramson MJ, et al. Childhood body mass index and adult mammographic density measures that predict breast cancer risk. Breast Cancer Res Treat. 2016;156(1):163-70.

21. Magnusson C, Baron J, Persson I, Wolk A, Bergstrom R, Trichopoulos D, et al. Body size in different periods of life and breast cancer risk in post-menopausal women. Int J Cancer. 1998;76(1):29-34.

22. Hislop TG, Coldman AJ, Elwood JM, Brauer G, Kan L. Childhood and recent eating patterns and risk of breast cancer. Cancer Detect Prev. 1986;9(1-2):47-58.

23. Brinton LA, Swanson CA. Height and weight at various ages and risk of breast cancer. Ann Epidemiol. 1992;2(5):597-609.

24. Swerdlow AJ, De Stavola BL, Floderus B, Holm NV, Kaprio J, Verkasalo PK, et al. Risk factors for breast cancer at young ages in twins: an international population-based study. J Natl Cancer Inst. 2002;94(16):1238-46.

25. Le Marchand L, Kolonel LN, Earle ME, Mi MP. Body size at different periods of life and breast cancer risk. Am J Epidemiol. 1988;128(1):137-52.

26. Hilakivi-Clarke L, Forsen T, Eriksson JG, Luoto R, Tuomilehto J, Osmond C, et al. Tallness and overweight during childhood have opposing effects on breast cancer risk. Br J Cancer. 2001;85(11):1680-4.

27. Schoemaker MJ, Jones ME, Allen S, Hoare J, Ashworth A, Dowsett M, et al. Childhood body size and pubertal timing in relation to adult mammographic density phenotype. Breast Cancer Res. 2017;19(1):13.

28. Radiology ACo: The American College of Radiology Breast Imaging Reporting and Data System (BI-RADS). American College of Radiology, Reston, VA, 4th ed 2003.

29. Sprague BL, Gangnon RE, Burt V, Trentham-Dietz A, Hampton JM, Wellman RD, et al. Prevalence of mammographically dense breasts in the United States. J Natl Cancer Inst. 2014;106(10).

30. Lin SJ, Cawson J, Hill P, Haviv I, Jenkins M, Hopper JL, et al. Image-guided sampling reveals increased stroma and lower glandular complexity in mammographically dense breast tissue. Breast Cancer Res Treat. 2011;128(2):505-16.

31. Carney PA, Miglioretti DL, Yankaskas BC, Kerlikowske K, Rosenberg R, Rutter CM, et al. Individual and combined effects of age, breast density, and hormone replacement therapy use on the accuracy of screening mammography. Annals of internal medicine. 2003;138(3):168-75.

32. Harvey JA, Bovbjerg VE. Quantitative assessment of mammographic breast density: relationship with breast cancer risk. Radiology. 2004;230(1):29-41.

33. Mandelson MT, Oestreicher N, Porter PL, White D, Finder CA, Taplin SH, et al. Breast density as a predictor of mammographic detection: comparison of interval- and screen-detected cancers. J Natl Cancer Inst. 2000;92(13):1081-7.

34. Egan RL, Mosteller RC. Breast cancer mammography patterns. Cancer. 1977;40(5):2087-90.

35. Vachon CM, van Gils CH, Sellers TA, Ghosh K, Pruthi S, Brandt KR, et al. Mammographic density, breast cancer risk and risk prediction. Breast Cancer Research. 2007;9(6):217.

36. Shawky MS, Huo CW, Henderson MA, Redfern A, Britt K, Thompson EW. A review of the influence of mammographic density on breast cancer clinical and pathological phenotype. Breast Cancer Res Treat. 2019;177(2):251-76.

37. Kanbayti IH, Rae WID, McEntee MF, Al-Foheidi M, Ashour S, Turson SA, et al. Is mammographic density a marker of breast cancer phenotypes? Cancer Causes Control. 2020;31(8):749-65.

38. Turashvili G, McKinney S, Martin L, Gelmon KA, Watson P, Boyd N, et al. Columnar cell lesions, mammographic density and breast cancer risk. Breast Cancer Res Treat. 2009;115(3):561-71.

39. Huo CW, Hill P, Chew G, Neeson PJ, Halse H, Williams ED, et al. High mammographic density in women is associated with protumor inflammation. Breast Cancer Research. 2018;20(1):92.

40. Lokate M, Stellato RK, Veldhuis WB, Peeters PH, van Gils CH. Age-related changes in mammographic density and breast cancer risk. Am J Epidemiol. 2013;178(1):101-9.

41. Boyd N, Martin L, Stone J, Little L, Minkin S, Yaffe M. A longitudinal study of the effects of menopause on mammographic features. Cancer epidemiology, biomarkers & prevention. 2002;11(10 Pt 1):1048-53.

42. Kerlikowske K, Cook AJ, Buist DS, Cummings SR, Vachon C, Vacek P, et al. Breast cancer risk by breast density, menopause, and postmenopausal hormone therapy use. Journal of clinical oncology. 2010;28(24):3830-7.

43. Krishnan K, Baglietto L, Stone J, Simpson JA, Severi G, Evans CF, et al. Longitudinal Study of Mammographic Density Measures That Predict Breast Cancer Risk. Cancer epidemiology, biomarkers & prevention. 2017;26(4):651-60.

44. McCormack VA, Perry NM, Vinnicombe SJ, Dos Santos Silva I. Changes and tracking of mammographic density in relation to Pike's model of breast tissue aging: a UK longitudinal study. Int J Cancer. 2010;127(2):452-61.

45. S.X. Sun ZB, R.B. Kass, A.T. Mancino, A.L. Rosenbloom, V.S. Klimberg, K. , Bland I. Breast physiology: normal and abnormal development and function. The Breast: Comprehensive Management of Benign and Malignant Diseases, Elsevier Inc 2018:37–56, e36.

46. Dawson EK. A Histological Study of the Normal Mamma in Relation to Tumour Growth. I.-Early Development to Maturity. Edinb Med J. 1934;41(12):653-82.

47. Dabelow A. Die Milchdruse, in: Handbuch der Mikroskopischen Anatomie des Menschen 3, Springer-Verlag, Berlin. 1957:277–512.

48. Drife JO. Breast development in puberty. Ann N Y Acad Sci. 1986;464:58-65.

49. Brown N, White J, Milligan A, Risius D, Ayres B, Hedger W, et al. The relationship between breast size and anthropometric characteristics. Am J Hum Biol. 2012;24(2):158-64.

50. Lim LY, Ho PJ, Liu J, Chay WY, Tan MH, Hartman M, et al. Determinants of breast size in Asian women. Sci Rep. 2018;8(1):1201.

51. Coltman CE, Steele JR, McGhee DE. Breast volume is affected by body mass index but not age. Ergonomics. 2017;60(11):1576-85.

52. Lokate M, Kallenberg MG, Karssemeijer N, Van den Bosch MA, Peeters PH, Van Gils CH. Volumetric breast density from full-field digital mammograms and its association with breast cancer risk factors: a comparison with a threshold method. Cancer epidemiology, biomarkers & prevention. 2010;19(12):3096-105.

53. McCormack VA, Highnam R, Perry N, dos Santos Silva I. Comparison of a new and existing method of mammographic density measurement: intramethod reliability and associations with known risk factors. Cancer epidemiology, biomarkers & prevention. 2007;16(6):1148-54.

54. Jeffreys M, Warren R, Highnam R, Davey Smith G. Breast cancer risk factors and a novel measure of volumetric breast density: cross-sectional study. Br J Cancer. 2008;98(1):210-6.

55. Aitken Z, McCormack VA, Highnam RP, Martin L, Gunasekara A, Melnichouk O, et al. Screen-film mammographic density and breast cancer risk: a comparison of the volumetric standard mammogram form and the interactive threshold measurement methods. Cancer epidemiology, biomarkers & prevention. 2010;19(2):418-28.

56. van den Brandt PA, Spiegelman D, Yaun SS, Adami HO, Beeson L, Folsom AR, et al. Pooled analysis of prospective cohort studies on height, weight, and breast cancer risk. Am J Epidemiol. 2000;152(6):514-27.

57. Friedenreich CM. Review of anthropometric factors and breast cancer risk. Eur J Cancer Prev. 2001;10(1):15-32.

58. Bernstein L. Epidemiology of endocrine-related risk factors for breast cancer. J Mammary Gland Biol Neoplasia. 2002;7(1):3-15.

59. Matthews SB, Thompson HJ. The Obesity-Breast Cancer Conundrum: An Analysis of the Issues. Int J Mol Sci. 2016;17(6).

60. Hanahan D, Weinberg RA. Hallmarks of cancer: the next generation. Cell. 2011;144(5):646-74.

61. Grivennikov SI, Greten FR, Karin M. Immunity, inflammation, and cancer. Cell. 2010;140(6):883-99.

62. Deng T, Lyon CJ, Bergin S, Caligiuri MA, Hsueh WA. Obesity, Inflammation, and Cancer. Annu Rev Pathol. 2016;11:421-49.

63. Subbaramaiah K, Howe LR, Bhardwaj P, Du B, Gravaghi C, Yantiss RK, et al. Obesity is associated with inflammation and elevated aromatase expression in the mouse mammary gland. Cancer Prev Res (Phila). 2011;4(3):329-46.

64. Subbaramaiah K, Morris PG, Zhou XK, Morrow M, Du B, Giri D, et al. Increased levels of COX-2 and prostaglandin E2 contribute to elevated aromatase expression in inflamed breast tissue of obese women. Cancer Discov. 2012;2(4):356-65.

65. Pryor M, Slattery ML, Robison LM, Egger M. Adolescent diet and breast cancer in Utah. Cancer Res. 1989;49(8):2161-7.

66. Franceschi S, Favero A, La Vecchia C, Baron AE, Negri E, Dal Maso L, et al. Body size indices and breast cancer risk before and after menopause. Int J Cancer. 1996;67(2):181-6.

67. Coates RJ, Uhler RJ, Hall HI, Potischman N, Brinton LA, Ballard-Barbash R, et al. Risk of breast cancer in young women in relation to body size and weight gain in adolescence and early adulthood. British journal of cancer. 1999;81(1):167-74.

68. Wadsworth ME, Mann SL, Rodgers B, Kuh DJ, Hilder WS, Yusuf EJ. Loss and representativeness in a 43 year follow up of a national birth cohort. J Epidemiol Community Health. 1992;46(3):300-4.

69. Wadsworth ME, Butterworth SL, Hardy RJ, Kuh DJ, Richards M, Langenberg C, et al. The life course prospective design: an example of benefits and problems associated with study longevity. Soc Sci Med. 2003;57(11):2193-205.

70. De Stavola BL, dos Santos Silva I, McCormack V, Hardy RJ, Kuh DJ, Wadsworth ME. Childhood growth and breast cancer. Am J Epidemiol. 2004;159(7):671-82.

71. Berkey CS, Frazier AL, Gardner JD, Colditz GA. Adolescence and breast carcinoma risk. Cancer. 1999;85(11):2400-9.

72. Mitan LA. Menstrual dysfunction in anorexia nervosa. J Pediatr Adolesc Gynecol. 2004;17(2):81-5.

73. Xu H, Li PH, Barrow TM, Colicino E, Li C, Song R, et al. Obesity as an effect modifier of the association between menstrual abnormalities and hypertension in young adult women: Results from Project ELEFANT. PLoS One. 2018;13(11):e0207929.

74. Tauqeer Z, Gomez G, Stanford FC. Obesity in Women: Insights for the Clinician. J Womens Health (Larchmt). 2018;27(4):444-57.

75. Rich-Edwards JW, Goldman MB, Willett WC, Hunter DJ, Stampfer MJ, Colditz GA, et al. Adolescent body mass index and infertility caused by ovulatory disorder. Am J Obstet Gynecol. 1994;171(1):171-7.

76. Hartz AJ, Barboriak PN, Wong A, Katayama KP, Rimm AA. The association of obesity with infertility and related menstural abnormalities in women. Int J Obes. 1979;3(1):57-73.

77. Radimer KLBC. Breast cancer risks associated with obesity in: BA Stoll (Ed), Reducing Breast Cancer Risk in Women, Kluwer Academic, Dordrecht. 1995:145.

78. Frisch RE, Wyshak G, Albright NL, Albright TE, Schiff I, Witschi J, et al. Lower lifetime occurrence of breast cancer and cancers of the reproductive system among former college athletes. Am J Clin Nutr. 1987;45(1 Suppl):328-35.

79. Shawon MSR, Eriksson M, Li J. Body size in early life and risk of breast cancer. Breast Cancer Res. 2017;19(1):84.

80. Eriksson L, Czene K, Rosenberg L, Humphreys K, Hall P. The influence of mammographic density on breast tumor characteristics. Breast Cancer Res Treat. 2012;134(2):859-66.

81. Yochum L, Tamimi RM, Hankinson SE. Birthweight, early life body size and adult mammographic density: a review of epidemiologic studies. Cancer Causes Control. 2014;25(10):1247-59.

82. Rice MS, Bertrand KA, Lajous M, Tamimi RM, Torres-Mejia G, Biessy C, et al. Body size throughout the life course and mammographic density in Mexican women. Breast Cancer Res Treat. 2013;138(2):601-10.

83. Rice MS, Bertrand KA, VanderWeele TJ, Rosner BA, Liao X, Adami HO, et al. Mammographic density and breast cancer risk: a mediation analysis. Breast Cancer Res. 2016;18(1):94.

84. Bertrand KA, Baer HJ, Orav EJ, Klifa C, Shepherd JA, Van Horn L, et al. Body fatness during childhood and adolescence and breast density in young women: a prospective analysis. Breast Cancer Res. 2015;17:95.

85. Boyd N, Martin L, Chavez S, Gunasekara A, Salleh A, Melnichouk O, et al. Breast-tissue composition and other risk factors for breast cancer in young women: a cross-sectional study. Lancet Oncol. 2009;10(6):569-80.

86. Must A, Phillips SM, Naumova EN, Blum M, Harris S, Dawson-Hughes B, et al. Recall of early menstrual history and menarcheal body size: after 30 years, how well do women remember? Am J Epidemiol. 2002;155(7):672-9.

87. Freedman DS, Sherry B. The validity of BMI as an indicator of body fatness and risk among children. Pediatrics. 2009;124 Suppl 1:S23-34.

88. Alexeeff SE, Odo NU, Lipson JA, Achacoso N, Rothstein JH, Yaffe MJ, et al. Age at Menarche and Late Adolescent Adiposity Associated with Mammographic Density on Processed Digital Mammograms in 24,840 Women. Cancer epidemiology, biomarkers & prevention. 2017;26(9):1450-8.

89. Bardia A, Vachon CM, Olson JE, Vierkant RA, Wang AH, Hartmann LC, et al. Relative weight at age 12 and risk of postmenopausal breast cancer. Cancer epidemiology, biomarkers & prevention. 2008;17(2):374-8.

90. Baer HJ, Tworoger SS, Hankinson SE, Willett WC. Body fatness at young ages and risk of breast cancer throughout life. Am J Epidemiol. 2010;171(11):1183-94.

91. Must A, Willett WC, Dietz WH. Remote recall of childhood height, weight, and body build by elderly subjects. Am J Epidemiol. 1993;138(1):56-64.

92. Kuczmarski RJ, Ogden CL, Grummer-Strawn LM, Flegal KM, Guo SS, Wei R, et al. CDC growth charts: United States. Adv Data. 2000(314):1-27.

93. Graham SJ, Ness S, Hamilton BS, Bronskill MJ. Magnetic resonance properties of ex vivo breast tissue at 1.5 T. Magn Reson Med. 1997;38(4):669-77.

94. Graham SJ, Bronskill MJ, Byng JW, Yaffe MJ, Boyd NF. Quantitative correlation of breast tissue parameters using magnetic resonance and X-ray mammography. Br J Cancer. 1996;73(2):162-8.

95. Reiter EO, Fuldauer VG, Root AW. Secretion of the adrenal androgen, dehydroepiandrosterone sulfate, during normal infancy, childhood, and adolescence, in sick infants, and in children with endocrinologic abnormalities. J Pediatr. 1977;90(5):766-70.

96. Butler LM, Gold EB, Greendale GA, Crandall CJ, Modugno F, Oestreicher N, et al. Menstrual and reproductive factors in relation to mammographic density: the Study of Women's Health Across the Nation (SWAN). Breast Cancer Res Treat. 2008;112(1):165-74.

97. Dite GS, Gurrin LC, Byrnes GB, Stone J, Gunasekara A, McCredie MR, et al. Predictors of mammographic density: insights gained from a novel regression analysis of a twin study. Cancer epidemiology, biomarkers & prevention. 2008;17(12):3474-81.

98. Dorgan JF, Klifa C, Deshmukh S, Egleston BL, Shepherd JA, Kwiterovich PO, Jr., et al. Menstrual and reproductive characteristics and breast density in young women. Cancer Causes Control. 2013;24(11):1973-83.

99. Heng D, Gao F, Jong R, Fishell E, Yaffe M, Martin L, et al. Risk factors for breast cancer associated with mammographic features in Singaporean chinese women. Cancer epidemiology, biomarkers & prevention. 2004;13(11 Pt 1):1751-8.

100. Titus-Ernstoff L, Tosteson AN, Kasales C, Weiss J, Goodrich M, Hatch EE, et al. Breast cancer risk factors in relation to breast density (United States). Cancer Causes Control. 2006;17(10):1281-90.

101. Tehranifar P, Reynolds D, Flom J, Fulton L, Liao Y, Kudadjie-Gyamfi E, et al. Reproductive and menstrual factors and mammographic density in African American, Caribbean, and white women. Cancer Causes Control. 2011;22(4):599-610.

102. Novotny R, Daida Y, Morimoto Y, Shepherd J, Maskarinec G. Puberty, body fat, and breast density in girls of several ethnic groups. Am J Hum Biol. 2011;23(3):359-65.

103. Houghton LC, Jung S, Troisi R, LeBlanc ES, Snetselaar LG, Hylton NM, et al. Pubertal timing and breast density in young women: a prospective cohort study. Breast Cancer Research. 2019;21(1):122.

104. Lee JM, Appugliese D, Kaciroti N, Corwyn RF, Bradley RH, Lumeng JC. Weight status in young girls and the onset of puberty. Pediatrics. 2007;119(3):e624-30.

105. Davison KK, Susman EJ, Birch LL. Percent body fat at age 5 predicts earlier pubertal development among girls at age 9. Pediatrics. 2003;111(4 Pt 1):815-21.

106. Wang Y. Is obesity associated with early sexual maturation? A comparison of the association in American boys versus girls. Pediatrics. 2002;110(5):903-10.

107. Adair LS, Gordon-Larsen P. Maturational timing and overweight prevalence in US adolescent girls. Am J Public Health. 2001;91(4):642-4.

108. Kaplowitz PB, Slora EJ, Wasserman RC, Pedlow SE, Herman-Giddens ME. Earlier onset of puberty in girls: relation to increased body mass index and race. Pediatrics. 2001;108(2):347-53.

109. Zhai L, Liu J, Zhao J, Liu J, Bai Y, Jia L, et al. Association of Obesity with Onset of Puberty and Sex Hormones in Chinese Girls: A 4-Year Longitudinal Study. PLoS One. 2015;10(8):e0134656.

110. Leitao RB, Rodrigues LP, Neves L, Carvalho GS. Development of adiposity, obesity and age at menarche: an 8-year follow-up study in Portuguese schoolgirls. Int J Adolesc Med Health. 2013;25(1):55-63.

111. Tremblay L, Frigon JY. The interaction role of obesity and pubertal timing on the psychosocial adjustment of adolescent girls: longitudinal data. Int J Obes (Lond). 2005;29(10):1204-11.

112. Li W, Liu Q, Deng X, Chen Y, Liu S, Story M. Association between Obesity and Puberty Timing: A Systematic Review and Meta-Analysis. Int J Environ Res Public Health. 2017;14(10).

113. Barcellos Gemelli IF, Farias EDS, Souza OF. Age at Menarche and Its Association with Excess Weight and Body Fat Percentage in Girls in the Southwestern Region of the Brazilian Amazon. J Pediatr Adolesc Gynecol. 2016;29(5):482-8.

114. St George IM, Williams S, Silva PA. Body size and the menarche: the Dunedin Study. J Adolesc Health. 1994;15(7):573-6.

115. Bau AM, Ernert A, Schenk L, Wiegand S, Martus P, Gruters A, et al. Is there a further acceleration in the age at onset of menarche? A cross-sectional study in 1840 school children focusing on age and bodyweight at the onset of menarche. Eur J Endocrinol. 2009;160(1):107-13.

116. Gavela-Perez T, Garces C, Navarro-Sanchez P, Lopez Villanueva L, Soriano-Guillen L. Earlier menarcheal age in Spanish girls is related with an increase in body mass index between pre-pubertal school age and adolescence. Pediatr Obes. 2015;10(6):410-5.

117. Ramezani Tehrani F, Mirmiran P, Gholami R, Moslehi N, Azizi F. Factors influencing menarcheal age: results from the cohort of tehran lipid and glucose study. Int J Endocrinol Metab. 2014;12(3):e16130.

118. García Cuartero B, Gónzalez Vergaz A, Frías García E, Arana Cañete C, Díaz Martínez E, Tolmo MD. Assessment of the secular trend in puberty in boys and girls. An Pediatr (Barc). 2010;73(6):320-6.

119. Rosenfield RL, Lipton RB, Drum ML. Thelarche, pubarche, and menarche attainment in children with normal and elevated body mass index. Pediatrics. 2009;123(1):84-8.

120. Chen C, Zhang Y, Sun W, Chen Y, Jiang Y, Song Y, et al. Investigating the relationship between precocious puberty and obesity: a cross-sectional study in Shanghai, China. BMJ Open. 2017;7(4):e014004.

121. Nieuwenhuis D, Pujol-Gualdo N, Arnoldussen IAC, Kiliaan AJ. Adipokines: A gear shift in puberty. Obes Rev. 2020.

122. de Ridder CM, Thijssen JH, Bruning PF, Van den Brande JL, Zonderland ML, Erich WB. Body fat mass, body fat distribution, and pubertal development: a longitudinal study of physical and hormonal sexual maturation of girls. J Clin Endocrinol Metab. 1992;75(2):442-6.

123. Lassek W, Gaulin S. Brief communication: Menarche is related to fat distribution. American journal of physical anthropology. 2007;133:1147-51.

124. Loomba-Albrecht L, Styne D. Effect of puberty on body composition. Current opinion in endocrinology, diabetes, and obesity. 2009;16:10-5.

125. Alotaibi MF. Physiology of puberty in boys and girls and pathological disorders affecting its onset. J Adolesc. 2019;71:63-71.

126. Simonneaux V, Bahougne T. A Multi-Oscillatory Circadian System Times Female Reproduction. Front Endocrinol (Lausanne). 2015;6:157-.

127. Marques P, Skorupskaite K, George JT, Anderson RA. Physiology of GNRH and Gonadotropin Secretion. In: Feingold KR, Anawalt B, Boyce A, Chrousos G, Dungan K, Grossman A, et al., editors. Endotext. South Dartmouth (MA): MDText.com, Inc.; 2000.

128. Biro FM, Pinney SM, Huang B, Baker ER, Walt Chandler D, Dorn LD. Hormone changes in peripubertal girls. J Clin Endocrinol Metab. 2014;99(10):3829-35.

129. Aksglaede L, Sorensen K, Petersen JH, Skakkebaek NE, Juul A. Recent decline in age at breast development: the Copenhagen Puberty Study. Pediatrics. 2009;123(5):e932-9.

130. Cabrera SM, Bright GM, Frane JW, Blethen SL, Lee PA. Age of thelarche and menarche in contemporary US females: a cross-sectional analysis. J Pediatr Endocrinol Metab. 2014;27(1-2):47-51.

131. Tanner JM. Issues and advances in adolescent growth and development. J Adolesc Health Care. 1987;8(6):470-8.

132. Bay K, Andersson AM, Skakkebaek NE. Estradiol levels in prepubertal boys and girls--analytical challenges. Int J Androl. 2004;27(5):266-73.

133. McCartney CR, Blank SK, Prendergast KA, Chhabra S, Eagleson CA, Helm KD, et al. Obesity and sex steroid changes across puberty: evidence for marked hyperandrogenemia in pre- and early pubertal obese girls. J Clin Endocrinol Metab. 2007;92(2):430-6.

134. Boyd NF, Stone J, Martin LJ, Jong R, Fishell E, Yaffe M, et al. The association of breast mitogens with mammographic densities. Br J Cancer. 2002;87(8):876-82.

135. Yong M, Atkinson C, Newton KM, Aiello Bowles EJ, Stanczyk FZ, Westerlind KC, et al. Associations between endogenous sex hormone levels and mammographic and bone densities in premenopausal women. Cancer causes & control : CCC. 2009;20(7):1039-53.

136. Noh JJ, Maskarinec G, Pagano I, Cheung LW, Stanczyk FZ. Mammographic densities and circulating hormones: a cross-sectional study in premenopausal women. Breast. 2006;15(1):20-8.

137. Borugian MJ, Spinelli JJ, Gordon PB, Abanto Z, Brooks-Wilson A, Pollak MN, et al. Fasting insulin and endogenous hormones in relation to premenopausal breast density (Canada). Cancer Causes Control. 2014;25(3):385-94.

138. Walker K, Fletcher O, Johnson N, Coupland B, McCormack VA, Folkerd E, et al. Premenopausal Mammographic Density in Relation to Cyclic Variations in Endogenous Sex Hormone Levels, Prolactin, and Insulin-like Growth Factors. Cancer Research. 2009;69(16):6490.

139. Verheus M, Peeters PH, van Noord PA, van der Schouw YT, Grobbee DE, van Gils CH. No relationship between circulating levels of sex steroids and mammographic breast density: the Prospect-EPIC cohort. Breast Cancer Res. 2007;9(4):R53.

140. McCormack VA, Dowsett M, Folkerd E, Johnson N, Palles C, Coupland B, et al. Sex steroids, growth factors and mammographic density: a cross-sectional study of UK postmenopausal Caucasian and Afro-Caribbean women. Breast Cancer Research. 2009;11(3):R38.

141. Sprague BL, Trentham-Dietz A, Gangnon RE, Buist DS, Burnside ES, Bowles EJ, et al. Circulating sex hormones and mammographic breast density among postmenopausal women. Horm Cancer. 2011;2(1):62-72.

142. Woolcott CG, Courneya KS, Boyd NF, Yaffe MJ, McTiernan A, Brant R, et al. Association between sex hormones, glucose homeostasis, adipokines, and inflammatory markers and mammographic density among postmenopausal women. Breast Cancer Res Treat. 2013;139(1):255-65.

143. Greendale GA, Palla SL, Ursin G, Laughlin GA, Crandall C, Pike MC, et al. The association of endogenous sex steroids and sex steroid binding proteins with mammographic density: results from the Postmenopausal Estrogen/Progestin Interventions Mammographic Density Study. Am J Epidemiol. 2005;162(9):826-34.

144. Schoemaker MJ, Folkerd EJ, Jones ME, Rae M, Allen S, Ashworth A, et al. Combined effects of endogenous sex hormone levels and mammographic density on postmenopausal breast cancer risk: results from the Breakthrough Generations Study. Br J Cancer. 2014;110(7):1898-907.

145. Tamimi RM, Hankinson SE, Colditz GA, Byrne C. Endogenous sex hormone levels and mammographic density among postmenopausal women. Cancer epidemiology, biomarkers & prevention. 2005;14(11 Pt 1):2641-7.

146. Bremnes Y, Ursin G, Bjurstam N, Rinaldi S, Kaaks R, Gram IT. Endogenous sex hormones, prolactin and mammographic density in postmenopausal Norwegian women. Int J Cancer. 2007;121(11):2506-11.

147. Jung S, Egleston BL, Chandler DW, Van Horn L, Hylton NM, Klifa CC, et al. Adolescent endogenous sex hormones and breast density in early adulthood. Breast Cancer Res. 2015;17(1):77.

148. Guercio G, Rivarola MA, Chaler E, Maceiras M, Belgorosky A. Relationship between the growth hormone/insulin-like growth factor-I axis, insulin sensitivity, and adrenal androgens in normal prepubertal and pubertal girls. J Clin Endocrinol Metab. 2003;88(3):1389-93.

149. Ibanez L, Valls C, Ong K, Dunger DB, de Zegher F. Metformin therapy during puberty delays menarche, prolongs pubertal growth, and augments adult height: a randomized study in low-birth-weight girls with early-normal onset of puberty. J Clin Endocrinol Metab. 2006;91(6):2068-73.

150. Kleinberg DL, Ruan W. IGF-I, GH, and Sex Steroid Effects in Normal Mammary Gland Development. Journal of Mammary Gland Biology and Neoplasia. 2008;13(4):353-60.

151. Sternlicht MD. Key stages in mammary gland development: The cues that regulate ductal branching morphogenesis. Breast Cancer Research. 2005;8(1):201.

152. Ebeling P, Koivisto VA. Physiological importance of dehydroepiandrosterone. Lancet. 1994;343(8911):1479-81.

153. Ahmed ML, Ong KK, Dunger DB. Childhood obesity and the timing of puberty. Trends Endocrinol Metab. 2009;20(5):237-42.

154. Chen JH, Chen WP, Chan S, Yeh DC, Su MY, McLaren CE. Correlation of endogenous hormonal levels, fibroglandular tissue volume and percent density measured using 3D MRI during one menstrual cycle. Ann Oncol. 2013;24(9):2329-35.

155. Warren R, Skinner J, Sala E, Denton E, Dowsett M, Folkerd E, et al. Associations among mammographic density, circulating sex hormones, and polymorphisms in sex hormone metabolism genes in postmenopausal women. Cancer epidemiology, biomarkers & prevention. 2006;15(8):1502-8.

156. Greendale GA, Reboussin BA, Sie A, Singh HR, Olson LK, Gatewood O, et al. Effects of estrogen and estrogen-progestin on mammographic parenchymal density. Postmenopausal Estrogen/Progestin Interventions (PEPI) Investigators. Annals of internal medicine. 1999;130(4 Pt 1):262-9.

157. Rosner W, Hryb DJ, Kahn SM, Nakhla AM, Romas NA. Interactions of sex hormone-binding globulin with target cells. Mol Cell Endocrinol. 2010;316(1):79-85.

158. Kleinberg DL. Early mammary development: growth hormone and IGF-1. J Mammary Gland Biol Neoplasia. 1997;2(1):49-57.

159. Walden PD, Ruan W, Feldman M, Kleinberg DL. Evidence that the mammary fat pad mediates the action of growth hormone in mammary gland development. Endocrinology. 1998;139(2):659-62.

160. Mukhina S, Liu D, Guo K, Raccurt M, Borges-Bendris S, Mertani HC, et al. Autocrine Growth Hormone Prevents Lactogenic Differentiation of Mouse Mammary Epithelial Cells. Endocrinology. 2006;147(4):1819-29.

161. Mol JA, Henzen-Logmans SC, Hageman P, Misdorp W, Blankenstein MA, Rijnberk A. Expression of the gene encoding growth hormone in the human mammary gland. J Clin Endocrinol Metab. 1995;80(10):3094-6.

162. Raccurt M, Lobie PE, Moudilou E, Garcia-Caballero T, Frappart L, Morel G, et al. High stromal and epithelial human gh gene expression is associated with proliferative disorders of the mammary gland. J Endocrinol. 2002;175(2):307-18.

163. Bchini O, Andres AC, Schubaur B, Mehtali M, LeMeur M, Lathe R, et al. Precocious mammary gland development and milk protein synthesis in transgenic mice ubiquitously expressing human growth hormone. Endocrinology. 1991;128(1):539-46.

164. Nagasawa H, Noguchi Y, Mori T, Niki K, Namiki H. Suppression of normal and preneoplastic mammary growth and uterine adenomyosis with reduced growth hormone level

in SHN mice given monosodium glutamate neonatally. Eur J Cancer Clin Oncol. 1985;21(12):1547-51.

165. Mertani HC, Delehaye-Zervas MC, Martini JF, Postel-Vinay MC, Morel G. Localization of growth hormone receptor messenger RNA in human tissues. Endocrine. 1995;3(2):135-42.

166. Mertani HC, Garcia-Caballero T, Lambert A, Gerard F, Palayer C, Boutin JM, et al. Cellular expression of growth hormone and prolactin receptors in human breast disorders. Int J Cancer. 1998;79(2):202-11.

167. Kleinberg DL, Ruan W, Catanese V, Newman CB, Feldman M. Non-lactogenic effects of growth hormone on growth and insulin-like growth factor-I messenger ribonucleic acid of rat mammary gland. Endocrinology. 1990;126(6):3274-6.

168. Kleinberg DL, Feldman M, Ruan W. IGF-I: an essential factor in terminal end bud formation and ductal morphogenesis. J Mammary Gland Biol Neoplasia. 2000;5(1):7-17.

169. Couldrey C, Moitra J, Vinson C, Anver M, Nagashima K, Green J. Adipose tissue: a vital in vivo role in mammary gland development but not differentiation. Dev Dyn. 2002;223(4):459-68.

170. Richards RG, Klotz DM, Walker MP, Diaugustine RP. Mammary gland branching morphogenesis is diminished in mice with a deficiency of insulin-like growth factor-I (IGF-I), but not in mice with a liver-specific deletion of IGF-I. Endocrinology. 2004;145(7):3106-10.

171. Gallego MI, Binart N, Robinson GW, Okagaki R, Coschigano KT, Perry J, et al. Prolactin, growth hormone, and epidermal growth factor activate Stat5 in different compartments of mammary tissue and exert different and overlapping developmental effects. Dev Biol. 2001;229(1):163-75.

172. Marshman E, Streuli CH. Insulin-like growth factors and insulin-like growth factor binding proteins in mammary gland function. Breast Cancer Res. 2002;4(6):231-9.

173. Scacchi M, Pincelli AI, Cavagnini F. Growth hormone in obesity. Int J Obes Relat Metab Disord. 1999;23(3):260-71.

174. Bohlke K, Cramer DW, Trichopoulos D, Mantzoros CS. Insulin-like growth factor-I in relation to premenopausal ductal carcinoma in situ of the breast. Epidemiology. 1998;9(5):570-3.

175. Agurs-Collins T, Adams-Campbell LL, Kim KS, Cullen KJ. Insulin-like growth factor-1 and breast cancer risk in postmenopausal African-American women. Cancer Detect Prev. 2000;24(3):199-206.

176. Yu H, Shu XO, Li BD, Dai Q, Gao YT, Jin F, et al. Joint effect of insulin-like growth factors and sex steroids on breast cancer risk. Cancer epidemiology, biomarkers & prevention. 2003;12(10):1067-73.

177. Krajcik RA, Borofsky ND, Massardo S, Orentreich N. Insulin-like growth factor I (IGF-I), IGF-binding proteins, and breast cancer. Cancer epidemiology, biomarkers & prevention. 2002;11(12):1566-73.

178. Hankinson SE, Willett WC, Colditz GA, Hunter DJ, Michaud DS, Deroo B, et al. Circulating concentrations of insulin-like growth factor-I and risk of breast cancer. Lancet. 1998;351(9113):1393-6.

179. Toniolo P, Bruning PF, Akhmedkhanov A, Bonfrer JM, Koenig KL, Lukanova A, et al. Serum insulin-like growth factor-I and breast cancer. Int J Cancer. 2000;88(5):828-32.

180. Kaaks R, Lundin E, Rinaldi S, Manjer J, Biessy C, Soderberg S, et al. Prospective study of IGF-I, IGF-binding proteins, and breast cancer risk, in northern and southern Sweden. Cancer Causes Control. 2002;13(4):307-16.

181. Del Giudice ME, Fantus IG, Ezzat S, McKeown-Eyssen G, Page D, Goodwin PJ. Insulin and related factors in premenopausal breast cancer risk. Breast Cancer Res Treat. 1998;47(2):111-20.

182. Mulhall C, Hegele RA, Cao H, Tritchler D, Yaffe M, Boyd NF. Pituitary Growth Hormone and Growth Hormone–Releasing Hormone Receptor Genes and Associations with Mammographic Measures and Serum Growth Hormone. Cancer Epidemiology Biomarkers & Prevention. 2005;14(11):2648.

183. Byrne C, Colditz GA, Willett WC, Speizer FE, Pollak M, Hankinson SE. Plasma insulin-like growth factor (IGF) I, IGF-binding protein 3, and mammographic density. Cancer Res. 2000;60(14):3744-8.

184. Guo YP, Martin LJ, Hanna W, Banerjee D, Miller N, Fishell E, et al. Growth factors and stromal matrix proteins associated with mammographic densities. Cancer epidemiology, biomarkers & prevention. 2001;10(3):243-8.

185. Budak E, Fernandez Sanchez M, Bellver J, Cervero A, Simon C, Pellicer A. Interactions of the hormones leptin, ghrelin, adiponectin, resistin, and PYY3-36 with the reproductive system. Fertil Steril. 2006;85(6):1563-81.

186. Dobrzyn K, Smolinska N, Kiezun M, Szeszko K, Rytelewska E, Kisielewska K, et al. Adiponectin: A New Regulator of Female Reproductive System. Int J Endocrinol. 2018;2018:7965071.

187. Reinehr T, Roth CL. Is there a causal relationship between obesity and puberty? Lancet Child Adolesc Health. 2019;3(1):44-54.

188. Martin L. Implications of adiponectin in linking metabolism to testicular function. Endocrine. 2013;46.

189. Mathew H, Castracane VD, Mantzoros C. Adipose tissue and reproductive health. Metabolism. 2018;86:18-32.

190. Silva LF, VandeHaar MJ, Weber Nielsen MS, Smith GW. Evidence for a local effect of leptin in bovine mammary gland. J Dairy Sci. 2002;85(12):3277-86.

191. Silva LFP, Etchebarne BE, Weber Nielsen MS, Liesman JS, Kiupel M, VandeHaar MJ. Intramammary Infusion of Leptin Decreases Proliferation of Mammary Epithelial Cells in Prepubertal Heifers. Journal of Dairy Science. 2008;91(8):3034-44.

192. Hassink SG, Sheslow DV, de Lancey E, Opentanova I, Considine RV, Caro JF. Serum leptin in children with obesity: relationship to gender and development. Pediatrics. 1996;98(2 Pt 1):201-3.

193. Schernhammer ES, Tworoger SS, Eliassen AH, Missmer SA, Holly JM, Pollak MN, et al. Body shape throughout life and correlations with IGFs and GH. Endocr Relat Cancer. 2007;14(3):721-32.

194. Poole EM, Tworoger SS, Hankinson SE, Schernhammer ES, Pollak MN, Baer HJ. Body size in early life and adult levels of insulin-like growth factor 1 and insulin-like growth factor binding protein 3. Am J Epidemiol. 2011;174(6):642-51.

195. Diorio C, Pollak M, Byrne C, Mâsse B, Hébert-Croteau N, Yaffe M, et al. Insulin-like growth factor-I, IGF-binding protein-3, and mammographic breast density. Cancer epidemiology, biomarkers & prevention. 2005;14(5):1065-73.

196. Maskarinec G, Takata Y, Chen Z, Gram IT, Nagata C, Pagano I, et al. IGF-I and mammographic density in four geographic locations: a pooled analysis. Int J Cancer. 2007;121(8):1786-92.

197. Stuedal A, Ursin G, Veierød MB, Bremnes Y, Reseland JE, Drevon CA, et al. Plasma levels of leptin and mammographic density among postmenopausal women: a cross-sectional study. Breast Cancer Res. 2006;8(5):R55.

198. Glasow A, Kiess W, Anderegg U, Berthold A, Bottner A, Kratzsch J. Expression of leptin (Ob) and leptin receptor (Ob-R) in human fibroblasts: regulation of leptin secretion by insulin. J Clin Endocrinol Metab. 2001;86(9):4472-9.

199. Alowami S, Troup S, Al-Haddad S, Kirkpatrick I, Watson PH. Mammographic density is related to stroma and stromal proteoglycan expression. Breast Cancer Res. 2003;5(5):R129-35.

200. Das U. Das UN. Is obesity an inflammatory condition? Nutrition 17: 953-66. Nutrition (Burbank, Los Angeles County, Calif). 2001;17:953-66.

201. Sejrsen K, Huber JT, Tucker HA, Akers RM. Influence of nutrition of mammary development in pre- and postpubertal heifers. J Dairy Sci. 1982;65(5):793-800.

202. Comninos AN, Jayasena CN, Dhillo WS. The relationship between gut and adipose hormones, and reproduction. Human Reproduction Update. 2013;20(2):153-74.

203. Singh A, Choubey M, Bora P, Krishna A. Adiponectin and Chemerin: Contrary Adipokines in Regulating Reproduction and Metabolic Disorders. Reprod Sci. 2018;25(10):1462-73.

204. Tsatsanis C, Dermitzaki E, Avgoustinaki P, Malliaraki N, Mytaras V, Margioris AN. The impact of adipose tissue-derived factors on the hypothalamic-pituitary-gonadal (HPG) axis. Hormones (Athens). 2015;14(4):549-62.

205. Unsworth A, Anderson R, Britt K. Stromal fibroblasts and the immune microenvironment: partners in mammary gland biology and pathology? J Mammary Gland Biol Neoplasia. 2014;19(2):169-82.

206. Macias H, Hinck L. Mammary Gland Development. Wiley interdisciplinary reviews Developmental biology. 2012;1:533-57.

207. Kojima Y, Acar A, Eaton EN, Mellody KT, Scheel C, Ben-Porath I, et al. Autocrine TGF-beta and stromal cell-derived factor-1 (SDF-1) signaling drives the evolution of tumor-promoting mammary stromal myofibroblasts. Proc Natl Acad Sci U S A. 2010;107(46):20009-14.

208. Orimo A, Gupta PB, Sgroi DC, Arenzana-Seisdedos F, Delaunay T, Naeem R, et al. Stromal fibroblasts present in invasive human breast carcinomas promote tumor growth and angiogenesis through elevated SDF-1/CXCL12 secretion. Cell. 2005;121(3):335-48.

209. Niranjan B, Buluwela L, Yant J, Perusinghe N, Atherton A, Phippard D, et al. HGF/SF: a potent cytokine for mammary growth, morphogenesis and development. Development. 1995;121(9):2897-908.

210. Silberstein GB, Daniel CW. Reversible inhibition of mammary gland growth by transforming growth factor-beta. Science. 1987;237(4812):291-3.

211. Ingman WV, Robertson SA. Mammary Gland Development in Transforming Growth Factor Beta1 Null Mutant Mice: Systemic and Epithelial Effects1. Biology of Reproduction. 2008;79(4):711-7.

212. Ewan KB, Shyamala G, Ravani SA, Tang Y, Akhurst R, Wakefield L, et al. Latent transforming growth factor-beta activation in mammary gland: regulation by ovarian hormones affects ductal and alveolar proliferation. Am J Pathol. 2002;160(6):2081-93.

213. Fang WB, Mafuvadze B, Yao M, Zou A, Portsche M, Cheng N. TGF-beta Negatively Regulates CXCL1 Chemokine Expression in Mammary Fibroblasts through Enhancement of

Smad2/3 and Suppression of HGF/c-Met Signaling Mechanisms. PLoS One. 2015;10(8):e0135063.

214. Gao Y, Wang Y, Li Y, Xia X, Zhao S, Che Y, et al. TGF-beta1 promotes bovine mammary fibroblast proliferation through the ERK 1/2 signalling pathway. Cell Biol Int. 2016;40(7):750-60.

215. Huo CW, Chew G, Hill P, Huang D, Ingman W, Hodson L, et al. High mammographic density is associated with an increase in stromal collagen and immune cells within the mammary epithelium. Breast Cancer Res. 2015;17(1):79.

216. Shawky MS, Ricciardelli C, Lord M, Whitelock J, Ferro V, Britt K, et al. Proteoglycans: Potential Agents in Mammographic Density and the Associated Breast Cancer Risk. J Mammary Gland Biol Neoplasia. 2015;20(3-4):121-31.

217. Provenzano PP, Inman DR, Eliceiri KW, Knittel JG, Yan L, Rueden CT, et al. Collagen density promotes mammary tumor initiation and progression. BMC Med. 2008;6:11.

218. García-Mendoza MG, Inman DR, Ponik SM, Jeffery JJ, Sheerar DS, Van Doorn RR, et al. Neutrophils drive accelerated tumor progression in the collagen-dense mammary tumor microenvironment. Breast Cancer Research. 2016;18(1):49.

219. Esbona K, Inman D, Saha S, Jeffery J, Schedin P, Wilke L, et al. COX-2 modulates mammary tumor progression in response to collagen density. Breast Cancer Res. 2016;18(1):35.

220. Steude JS, Maskarinec G, Erber E, Verheus M, Hernandez BY, Killeen J, et al. Mammographic Density and Matrix Metalloproteinases in Breast Tissue. Cancer Microenvironment. 2010;3(1):57-65.

221. Jackson HW, Hojilla CV, Weiss A, Sanchez OH, Wood GA, Khokha R. Timp3 deficient mice show resistance to developing breast cancer. PLoS One. 2015;10(3):e0120107.

222. Huo CW, Waltham M, Khoo C, Fox SB, Hill P, Chen S, et al. Mammographically dense human breast tissue stimulates MCF10DCIS.com progression to invasive lesions and metastasis. Breast Cancer Res. 2016;18(1):106.

223. DeFilippis RA, Chang H, Dumont N, Rabban JT, Chen Y-Y, Fontenay GV, et al. CD36 Repression Activates a Multicellular Stromal Program Shared by High Mammographic Density and Tumor Tissues. Cancer Discovery. 2012;2(9):826.

224. Gregoire F, Smas C, Sul HS. Gregoire FM, Smas CM, Sul HSUnderstanding adipocyte differentiation. Physiol Rev 78:783-809. Physiological reviews. 1998;78:783-809.

225. Sfeir Z, Ibrahimi A, Amri E, Grimaldi P, Abumrad N. CD36 antisense expression in 3T3-F442A preadipocytes. Mol Cell Biochem. 1999;192(1-2):3-8.

226. Need EF, Atashgaran V, Ingman WV, Dasari P. Hormonal regulation of the immune microenvironment in the mammary gland. J Mammary Gland Biol Neoplasia. 2014;19(2):229-39.

227. Gouon-Evans V, Rothenberg M, Pollard J. Postnatal mammary gland development requires macrophages and eosinophils. Development (Cambridge, England). 2000;127:2269-82.

228. Sun X, Ingman WV. Cytokine networks that mediate epithelial cell-macrophage crosstalk in the mammary gland: implications for development and cancer. J Mammary Gland Biol Neoplasia. 2014;19(2):191-201.

229. Ingman WV, Wyckoff J, Gouon-Evans V, Condeelis J, Pollard JW. Macrophages promote collagen fibrillogenesis around terminal end buds of the developing mammary gland. Dev Dyn. 2006;235(12):3222-9.

230. Pixley FJ, Stanley ER. CSF-1 regulation of the wandering macrophage: complexity in action. Trends Cell Biol. 2004;14(11):628-38.

231. Yadav A, Saini V, Arora S. MCP-1: chemoattractant with a role beyond immunity: a review. Clin Chim Acta. 2010;411(21-22):1570-9.

232. Deshmane SL, Kremlev S, Amini S, Sawaya BE. Monocyte chemoattractant protein-1 (MCP-1): an overview. J Interferon Cytokine Res. 2009;29(6):313-26.

233. Sun X, Glynn DJ, Hodson LJ, Huo C, Britt K, Thompson EW, et al. CCL2-driven inflammation increases mammary gland stromal density and cancer susceptibility in a transgenic mouse model. Breast Cancer Res. 2017;19(1):4.

234. Chew GL, Huo CW, Huang D, Hill P, Cawson J, Frazer H, et al. Increased COX-2 expression in epithelial and stromal cells of high mammographic density tissues and in a xenograft model of mammographic density. Breast Cancer Res Treat. 2015;153(1):89-99.

235. Colbert DC, McGarry MP, O'Neill K, Lee NA, Lee JJ. Decreased size and survival of weanling mice in litters of IL-5-/ -mice are a consequence of the IL-5 deficiency in nursing dams. Contemp Top Lab Anim Sci. 2005;44(3):53-5.

236. Sferruzzi-Perri AN, Robertson SA, Dent LA. Interleukin-5 transgene expression and eosinophilia are associated with retarded mammary gland development in mice. Biol Reprod. 2003;69(1):224-33.

237. DeNichilo MO, Panagopoulos V, Rayner TE, Borowicz RA, Greenwood JE, Evdokiou A. Peroxidase enzymes regulate collagen extracellular matrix biosynthesis. Am J Pathol. 2015;185(5):1372-84.

238. Panagopoulos V, Leach DA, Zinonos I, Ponomarev V, Licari G, Liapis V, et al. Inflammatory peroxidases promote breast cancer progression in mice via regulation of the tumour microenvironment. Int J Oncol. 2017;50(4):1191-200.

239. Cichon MA, Radisky DC. Extracellular matrix as a contextual determinant of transforming growth factor-beta signaling in epithelial-mesenchymal transition and in cancer. Cell Adh Migr. 2014;8(6):588-94.

240. Fain JN, Tichansky DS, Madan AK. Transforming growth factor beta1 release by human adipose tissue is enhanced in obesity. Metabolism. 2005;54(11):1546-51.

241. Sun X, Robertson SA, Ingman WV. Regulation of epithelial cell turnover and macrophage phenotype by epithelial cell-derived transforming growth factor beta1 in the mammary gland. Cytokine. 2013;61(2):377-88.

242. Ingman WV, Robertson SA. Transforming growth factor-beta1 null mutation causes infertility in male mice associated with testosterone deficiency and sexual dysfunction. Endocrinology. 2007;148(8):4032-43.

243. Sun X, Gierach GL, Sandhu R, Williams T, Midkiff BR, Lissowska J, et al. Relationship of mammographic density and gene expression: analysis of normal breast tissue surrounding breast cancer. Clin Cancer Res. 2013;19(18):4972-82.

244. Yang WT, Lewis MT, Hess K, Wong H, Tsimelzon A, Karadag N, et al. Decreased TGFbeta signaling and increased COX2 expression in high risk women with increased mammographic breast density. Breast Cancer Res Treat. 2010;119(2):305-14.

245. Boyd NF, Dite GS, Stone J, Gunasekara A, English DR, McCredie MR, et al. Heritability of mammographic density, a risk factor for breast cancer. N Engl J Med. 2002;347(12):886-94.

246. Pankow JS, Vachon CM, Kuni CC, King RA, Arnett DK, Grabrick DM, et al. Genetic analysis of mammographic breast density in adult women: evidence of a gene effect. J Natl Cancer Inst. 1997;89(8):549-56.

247. Ursin G, Lillie EO, Lee E, Cockburn M, Schork NJ, Cozen W, et al. The relative importance of genetics and environment on mammographic density. Cancer epidemiology, biomarkers & prevention. 2009;18(1):102-12.

248. Stone J, Dite GS, Gunasekara A, English DR, McCredie MR, Giles GG, et al. The heritability of mammographically dense and nondense breast tissue. Cancer epidemiology, biomarkers & prevention. 2006;15(4):612-7.

249. Varghese JS, Thompson DJ, Michailidou K, Lindström S, Turnbull C, Brown J, et al. Mammographic breast density and breast cancer: evidence of a shared genetic basis. Cancer Res. 2012;72(6):1478-84.

250. Stone J, Thompson DJ, Dos Santos Silva I, Scott C, Tamimi RM, Lindstrom S, et al. Novel Associations between Common Breast Cancer Susceptibility Variants and Risk-Predicting Mammographic Density Measures. Cancer Res. 2015;75(12):2457-67.

251. Stone J, Folkerd E, Doody D, Schroen C, Treloar SA, Giles GG, et al. Familial correlations in postmenopausal serum concentrations of sex steroid hormones and other mitogens: a twins and sisters study. J Clin Endocrinol Metab. 2009;94(12):4793-800.

252. Hong Y, Pedersen NL, Brismar K, Hall K, de Faire U. Quantitative genetic analyses of insulin-like growth factor I (IGF-I), IGF-binding protein-1, and insulin levels in middle-aged and elderly twins. J Clin Endocrinol Metab. 1996;81(5):1791-7.

253. Odefrey F, Stone J, Gurrin LC, Byrnes GB, Apicella C, Dite GS, et al. Common genetic variants associated with breast cancer and mammographic density measures that predict disease. Cancer Res. 2010;70(4):1449-58.

254. Lee E, Van Den Berg D, Hsu C, Ursin G, Koh WP, Yuan JM, et al. Genetic variation in transforming growth factor beta 1 and mammographic density in Singapore Chinese women. Cancer Res. 2013;73(6):1876-82.

255. Lindström S, Thompson DJ, Paterson AD, Li J, Gierach GL, Scott C, et al. Genome-wide association study identifies multiple loci associated with both mammographic density and breast cancer risk. Nat Commun. 2014;5:5303.

256. Vachon CM, Scott CG, Fasching PA, Hall P, Tamimi RM, Li J, et al. Common breast cancer susceptibility variants in LSP1 and RAD51L1 are associated with mammographic density measures that predict breast cancer risk. Cancer epidemiology, biomarkers & prevention. 2012;21(7):1156-66.

257. Houghton LC, Knight JA, Wei Y, Romeo RD, Goldberg M, Andrulis IL, et al. Association of Prepubertal and Adolescent Androgen Concentrations With Timing of Breast Development and Family History of Breast Cancer. JAMA Netw Open. 2019;2(2):e190083-e.

258. Boyd NFHJ. Mammographic density of the breast: the authors reply. N Engl J Med 2003;348 (2) 174–5.

259. Wong EM, Southey MC, Fox SB, Brown MA, Dowty JG, Jenkins MA, et al. Constitutional methylation of the BRCA1 promoter is specifically associated with BRCA1 mutation-associated pathology in early-onset breast cancer. Cancer Prev Res (Phila). 2011;4(1):23-33.

260. Brennan K, Garcia-Closas M, Orr N, Fletcher O, Jones M, Ashworth A, et al. Intragenic ATM methylation in peripheral blood DNA as a biomarker of breast cancer risk. Cancer Res. 2012;72(9):2304-13.

261. Iwamoto T, Yamamoto N, Taguchi T, Tamaki Y, Noguchi S. BRCA1 promoter methylation in peripheral blood cells is associated with increased risk of breast cancer with BRCA1 promoter methylation. Breast Cancer Res Treat. 2011;129(1):69-77.

262. Severi G, Southey MC, English DR, Jung CH, Lonie A, McLean C, et al. Epigenome-wide methylation in DNA from peripheral blood as a marker of risk for breast cancer. Breast Cancer Res Treat. 2014;148(3):665-73.

263. van Veldhoven K, Polidoro S, Baglietto L, Severi G, Sacerdote C, Panico S, et al. Epigenome-wide association study reveals decreased average methylation levels years before breast cancer diagnosis. Clin Epigenetics. 2015;7(1):67.

264. Xu Z, Bolick SC, DeRoo LA, Weinberg CR, Sandler DP, Taylor JA. Epigenome-wide association study of breast cancer using prospectively collected sister study samples. J Natl Cancer Inst. 2013;105(10):694-700.

265. Heyn H, Carmona FJ, Gomez A, Ferreira HJ, Bell JT, Sayols S, et al. DNA methylation profiling in breast cancer discordant identical twins identifies DOK7 as novel epigenetic biomarker. Carcinogenesis. 2013;34(1):102-8.

266. Chen M, Wong EM, Nguyen TL, Dite GS, Stone J, Giles GG, et al. Associations between environmental breast cancer risk factors and DNA methylation-based risk-predicting measures. bioRxiv. 2018:446484.

267. Li S, Dugué PA, Baglietto L, Severi G, Wong EM, Nguyen TL, et al. Genome-wide association study of peripheral blood DNA methylation and conventional mammographic density measures. Int J Cancer. 2019;145(7):1768-73.

268. Li S, Wong EM, Bui M, Nguyen TL, Joo JE, Stone J, et al. Inference about causation between body mass index and DNA methylation in blood from a twin family study. Int J Obes (Lond). 2019;43(2):243-52.

269. Fenton SE, Reed C, Newbold RR. Perinatal environmental exposures affect mammary development, function, and cancer risk in adulthood. Annu Rev Pharmacol Toxicol. 2012;52:455-79.

270. Hilakivi-Clarke L, de Assis S, Warri A. Exposures to synthetic estrogens at different times during the life, and their effect on breast cancer risk. J Mammary Gland Biol Neoplasia. 2013;18(1):25-42.

271. Li S, Wong EM, Dugué P-A, McRae AF, Kim E, Joo J-HE, et al. Genome-wide average DNA methylation is determined in utero. International Journal of Epidemiology. 2018;47(3):908-16.

272. Jernstrom H, Loman N, Johannsson OT, Borg A, Olsson H. Impact of teenage oral contraceptive use in a population-based series of early-onset breast cancer cases who have undergone BRCA mutation testing. Eur J Cancer. 2005;41(15):2312-20.

273. Anderson TJ, Battersby S, King RJ, McPherson K, Going JJ. Oral contraceptive use influences resting breast proliferation. Hum Pathol. 1989;20(12):1139-44.

274. Binder AM, Corvalan C, Mericq V, Pereira A, Santos JL, Horvath S, et al. Faster ticking rate of the epigenetic clock is associated with faster pubertal development in girls. Epigenetics. 2018;13(1):85-94.

275. Saji S, Jensen EV, Nilsson S, Rylander T, Warner M, Gustafsson JÅ. Estrogen receptors α and β in the rodent mammary gland. Breast Cancer Research. 2000;2(1):S.11.

276. Cheng G, Weihua Z, Warner M, Gustafsson JA. Estrogen receptors ER alpha and ER beta in proliferation in the rodent mammary gland. Proc Natl Acad Sci U S A. 2004;101(11):3739-46.

277. Gomes-Rochette NF, Souza LS, Tommasi BO, Pedrosa DF, Eis SR, Fin ID, et al. Association of PvuII and XbaI polymorphisms on estrogen receptor alpha (ESR1) gene to changes into serum lipid profile of post-menopausal women: Effects of aging, body mass index and breast cancer incidence. PLoS One. 2017;12(2):e0169266.

278. Souza MA, Fonseca Ade M, Bagnoli VR, Barros N, Neves EM, Moraes SD, et al. The expression of the estrogen receptor in obese patients with high breast density (HBD). Gynecol Endocrinol. 2014;30(1):78-80.

279. Tchatchou S, Jung A, Hemminki K, Sutter C, Wappenschmidt B, Bugert P, et al. A variant affecting a putative miRNA target site in estrogen receptor (ESR) 1 is associated with breast cancer risk in premenopausal women. Carcinogenesis. 2009;30(1):59-64.

280. Binder AM, Stiemsma LT, Keller K, van Otterdijk SD, Mericq V, Pereira A, et al. Inverse association between estrogen receptor-α DNA methylation and breast composition in adolescent Chilean girls. Clin Epigenetics. 2018;10(1):122.

281. Russo J, Ao X, Grill C, Russo IH. Pattern of distribution of cells positive for estrogen receptor alpha and progesterone receptor in relation to proliferating cells in the mammary gland. Breast Cancer Res Treat. 1999;53(3):217-27.

282. Ewan KB, Oketch-Rabah HA, Ravani SA, Shyamala G, Moses HL, Barcellos-Hoff MH. Proliferation of estrogen receptor-alpha-positive mammary epithelial cells is restrained by transforming growth factor-beta1 in adult mice. Am J Pathol. 2005;167(2):409-17.

283. Band AM, Laiho M. Crosstalk of TGF-β and estrogen receptor signaling in breast cancer. J Mammary Gland Biol Neoplasia. 2011;16(2):109-15.

284. Sehl ME, Henry JE, Storniolo AM, Ganz PA, Horvath S. DNA methylation age is elevated in breast tissue of healthy women. Breast Cancer Res Treat. 2017;164(1):209-19.

285. Hofstatter EW, Horvath S, Dalela D, Gupta P, Chagpar AB, Wali VB, et al. Increased epigenetic age in normal breast tissue from luminal breast cancer patients. Clin Epigenetics. 2018;10(1):112.

286. Hochberg Z, Belsky J. Evo-devo of human adolescence: beyond disease models of early puberty. BMC Med. 2013;11:113.

287. Hochberg Z. Developmental plasticity in child growth and maturation. Front Endocrinol (Lausanne). 2011;2:41.

288. (NHMRC) NHaMRC Australian Code for the Care and Use of Animals for Scientific Purposes 2013(8).

289. Li G, Vega R, Nelms K, Gekakis N, Goodnow C, McNamara P, et al. A role for Alström syndrome protein, alms1, in kidney ciliogenesis and cellular quiescence. PLoS Genet. 2007;3(1):e8.

290. Wu LL, Russell DL, Wong SL, Chen M, Tsai TS, St John JC, et al. Mitochondrial dysfunction in oocytes of obese mothers: transmission to offspring and reversal by pharmacological endoplasmic reticulum stress inhibitors. Development. 2015;142(4):681-91.

291. Guy CT, Cardiff RD, Muller WJ. Induction of mammary tumors by expression of polyomavirus middle T oncogene: a transgenic mouse model for metastatic disease. Mol Cell Biol. 1992;12(3):954-61.

292. Allen E. The oestrous cycle in the mouse. American Journal of Anatomy. 1922;30(3):297-371.

293. Caligioni CS. Assessing reproductive status/stages in mice. Curr Protoc Neurosci. 2009;Appendix 4:Appendix 4I.

294. LaRocca J, Pietruska J, Hixon M. Akt1 is essential for postnatal mammary gland development, function, and the expression of Btn1a1. PLoS One. 2011;6(9):e24432.

295. Ibáñez CA, Vázquez-Martínez M, León-Contreras JC, Reyes-Castro LA, Rodríguez-González GL, Bautista CJ, et al. Different Statistical Approaches to Characterization of Adipocyte Size in Offspring of Obese Rats: Effects of Maternal or Offspring Exercise Intervention. Front Physiol. 2018;9:1571-.

296. Bardia A, Vachon CM, Olson JE, Vierkant RA, Wang AH, Hartmann LC, et al. Relative weight at age 12 and risk of postmenopausal breast cancer. Cancer Epidemiol Biomarkers Prev. 2008;17(2):374-8.

297. Engmann NJ, Golmakani MK, Miglioretti DL, Sprague BL, Kerlikowske K, Breast Cancer Surveillance C. Population-Attributable Risk Proportion of Clinical Risk Factors for Breast Cancer. JAMA oncology. 2017;3(9):1228-36.

298. Paine IS, Lewis MT. The Terminal End Bud: the Little Engine that Could. J Mammary Gland Biol Neoplasia. 2017;22(2):93-108.

299. Wang Y, Chaffee TS, LaRue RS, Huggins DN, Witschen PM, Ibrahim AM, et al. Tissue-resident macrophages promote extracellular matrix homeostasis in the mammary gland stroma of nulliparous mice. Elife. 2020;9.

300. Zhao Y, Tan YS, Aupperlee MD, Langohr IM, Kirk EL, Troester MA, et al. Pubertal high fat diet: effects on mammary cancer development. Breast Cancer Res. 2013;15(5):R100.

301. Landskroner-Eiger S, Park J, Israel D, Pollard JW, Scherer PE. Morphogenesis of the developing mammary gland: stage-dependent impact of adipocytes. Dev Biol. 2010;344(2):968-78.

302. Kandlikar SG, Perez-Raya I, Raghupathi PA, Gonzalez-Hernandez J-L, Dabydeen D, Medeiros L, et al. Infrared imaging technology for breast cancer detection – Current status, protocols and new directions. International Journal of Heat and Mass Transfer. 2017;108:2303-20.

303. Cecchini MG, Dominguez MG, Mocci S, Wetterwald A, Felix R, Fleisch H, et al. Role of colony stimulating factor-1 in the establishment and regulation of tissue macrophages during postnatal development of the mouse. Development. 1994;120(6):1357-72.

304. Gouon-Evans V, Lin EY, Pollard JW. Requirement of macrophages and eosinophils and their cytokines/chemokines for mammary gland development. Breast Cancer Res. 2002;4(4):155-64.

305. Surmi BK, Hasty AH. Macrophage infiltration into adipose tissue: initiation, propagation and remodeling. Future Lipidol. 2008;3(5):545-56.

306. Burhans MS, Hagman DK, Kuzma JN, Schmidt KA, Kratz M. Contribution of Adipose Tissue Inflammation to the Development of Type 2 Diabetes Mellitus. Compr Physiol. 2018;9(1):1-58.

307. Chawla A, Nguyen KD, Goh YP. Macrophage-mediated inflammation in metabolic disease. Nat Rev Immunol. 2011;11(11):738-49.

308. Cinti S, Mitchell G, Barbatelli G, Murano I, Ceresi E, Faloia E, et al. Adipocyte death defines macrophage localization and function in adipose tissue of obese mice and humans. J Lipid Res. 2005;46(11):2347-55.

309. Morange PE, Alessi MC, Verdier M, Casanova D, Magalon G, Juhan-Vague I. PAI-1 produced ex vivo by human adipose tissue is relevant to PAI-1 blood level. Arterioscler Thromb Vasc Biol. 1999;19(5):1361-5.

310. Cancello R, Henegar C, Viguerie N, Taleb S, Poitou C, Rouault C, et al. Reduction of macrophage infiltration and chemoattractant gene expression changes in white adipose tissue of morbidly obese subjects after surgery-induced weight loss. Diabetes. 2005;54(8):2277-86.

311. Bastelica D, Morange P, Berthet B, Borghi H, Lacroix O, Grino M, et al. Stromal cells are the main plasminogen activator inhibitor-1-producing cells in human fat: evidence of differences between visceral and subcutaneous deposits. Arterioscler Thromb Vasc Biol. 2002;22(1):173-8.

312. Alessi MC, Poggi M, Juhan-Vague I. Plasminogen activator inhibitor-1, adipose tissue and insulin resistance. Curr Opin Lipidol. 2007;18(3):240-5.

313. Steppan CM, Bailey ST, Bhat S, Brown EJ, Banerjee RR, Wright CM, et al. The hormone resistin links obesity to diabetes. Nature. 2001;409(6818):307-12.

314. Degawa-Yamauchi M, Bovenkerk JE, Juliar BE, Watson W, Kerr K, Jones R, et al. Serum resistin (FIZZ3) protein is increased in obese humans. J Clin Endocrinol Metab. 2003;88(11):5452-5.

315. Lee JH, Bullen JW, Jr., Stoyneva VL, Mantzoros CS. Circulating resistin in lean, obese, and insulin-resistant mouse models: lack of association with insulinemia and glycemia. Am J Physiol Endocrinol Metab. 2005;288(3):E625-32.

316. Collin GB, Cyr E, Bronson R, Marshall JD, Gifford EJ, Hicks W, et al. Alms1-disrupted mice recapitulate human Alström syndrome. Hum Mol Genet. 2005;14(16):2323-33.

317. Arsov T, Silva DG, O'Bryan MK, Sainsbury A, Lee NJ, Kennedy C, et al. Fat Aussie—A New Alström Syndrome Mouse Showing a Critical Role for ALMS1 in Obesity, Diabetes, and Spermatogenesis. Molecular Endocrinology. 2006;20(7):1610-22.

318. Olson LK, Tan Y, Zhao Y, Aupperlee MD, Haslam SZ. Pubertal exposure to high fat diet causes mouse strain-dependent alterations in mammary gland development and estrogen responsiveness. Int J Obes (Lond). 2010;34(9):1415-26.

319. Fata JE, Chaudhary V, Khokha R. Cellular turnover in the mammary gland is correlated with systemic levels of progesterone and not 17beta-estradiol during the estrous cycle. Biol Reprod. 2001;65(3):680-8.

320. Chua AC, Hodson LJ, Moldenhauer LM, Robertson SA, Ingman WV. Dual roles for macrophages in ovarian cycle-associated development and remodelling of the mammary gland epithelium. Development. 2010;137(24):4229-38.

321. Bjørndal B, Burri L, Staalesen V, Skorve J, Berge RK. Different adipose depots: their role in the development of metabolic syndrome and mitochondrial response to hypolipidemic agents. J Obes. 2011;2011:490650.

322. Frederich RC, Hamann A, Anderson S, Löllmann B, Lowell BB, Flier JS. Leptin levels reflect body lipid content in mice: evidence for diet-induced resistance to leptin action. Nat Med. 1995;1(12):1311-4.

323. Alessi MC, Peiretti F, Morange P, Henry M, Nalbone G, Juhan-Vague I. Production of plasminogen activator inhibitor 1 by human adipose tissue: possible link between visceral fat accumulation and vascular disease. Diabetes. 1997;46(5):860-7.

324. Sawdey MS, Loskutoff DJ. Regulation of murine type 1 plasminogen activator inhibitor gene expression in vivo. Tissue specificity and induction by lipopolysaccharide, tumor necrosis factor-alpha, and transforming growth factor-beta. J Clin Invest. 1991;88(4):1346-53.

325. Annecke K, Schmitt M, Euler U, Zerm M, Paepke D, Paepke S, et al. uPA and PAI-1 in breast cancer: review of their clinical utility and current validation in the prospective NNBC-3 trial. Adv Clin Chem. 2008;45:31-45.

326. Grøndahl-Hansen J, Christensen IJ, Rosenquist C, Brünner N, Mouridsen HT, Danø K, et al. High Levels of Urokinase-type Plasminogen Activator and Its Inhibitor PAI-1 in Cytosolic Extracts of Breast Carcinomas Are Associated with Poor Prognosis. Cancer Research. 1993;53(11):2513.

327. Holst-Hansen C, Johannessen B, Høyer-Hansen G, Rømer J, Ellis V, Brünner N. Urokinase-type plasminogen activation in three human breast cancer cell lines correlates with their in vitro invasiveness. Clin Exp Metastasis. 1996;14(3):297-307.

328. Koli K, Keski-Oja J. 1alpha,25-dihydroxyvitamin D3 and its analogues down-regulate cell invasion-associated proteases in cultured malignant cells. Cell Growth Differ. 2000;11(4):221-9.

329. Arita Y, Kihara S, Ouchi N, Takahashi M, Maeda K, Miyagawa J, et al. Paradoxical decrease of an adipose-specific protein, adiponectin, in obesity. Biochem Biophys Res Commun. 1999;257(1):79-83.

330. Yamamoto Y, Hirose H, Saito I, Tomita M, Taniyama M, Matsubara K, et al. Correlation of the adipocyte-derived protein adiponectin with insulin resistance index and serum high-density lipoprotein-cholesterol, independent of body mass index, in the Japanese population. Clin Sci (Lond). 2002;103(2):137-42.

331. Matsubara M, Maruoka S, Katayose S. Inverse relationship between plasma adiponectin and leptin concentrations in normal-weight and obese women. Eur J Endocrinol. 2002;147(2):173-80.

332. Miyoshi Y, Funahashi T, Kihara S, Taguchi T, Tamaki Y, Matsuzawa Y, et al. Association of serum adiponectin levels with breast cancer risk. Clin Cancer Res. 2003;9(15):5699-704.

333. Mantzoros C, Petridou E, Dessypris N, Chavelas C, Dalamaga M, Alexe DM, et al. Adiponectin and breast cancer risk. J Clin Endocrinol Metab. 2004;89(3):1102-7.

334. Tworoger SS, Eliassen AH, Kelesidis T, Colditz GA, Willett WC, Mantzoros CS, et al. Plasma Adiponectin Concentrations and Risk of Incident Breast Cancer. The Journal of Clinical Endocrinology & Metabolism. 2007;92(4):1510-6.

335. Robinson SD, Silberstein GB, Roberts AB, Flanders KC, Daniel CW. Regulated expression and growth inhibitory effects of transforming growth factor-beta isoforms in mouse mammary gland development. Development. 1991;113(3):867-78.

336. Ahima RS, Lazar MA. Adipokines and the peripheral and neural control of energy balance. Mol Endocrinol. 2008;22(5):1023-31.

337. Samad F, Yamamoto K, Pandey M, Loskutoff DJ. Elevated expression of transforming growth factor-beta in adipose tissue from obese mice. Mol Med. 1997;3(1):37-48.

338. Maffei M, Halaas J, Ravussin E, Pratley RE, Lee GH, Zhang Y, et al. Leptin levels in human and rodent: measurement of plasma leptin and ob RNA in obese and weight-reduced subjects. Nat Med. 1995;1(11):1155-61.

339. Ruan W, Kleinberg DL. Insulin-like growth factor I is essential for terminal end bud formation and ductal morphogenesis during mammary development. Endocrinology. 1999;140(11):5075-81.

340. Richert MM, Wood TL. The insulin-like growth factors (IGF) and IGF type I receptor during postnatal growth of the murine mammary gland: sites of messenger ribonucleic acid expression and potential functions. Endocrinology. 1999;140(1):454-61.

341. Hughes K, Watson CJ. The spectrum of STAT functions in mammary gland development. Jakstat. 2012;1(3):151-8.

342. Humphreys RC, Bierie B, Zhao L, Raz R, Levy D, Hennighausen L. Deletion of Stat3 blocks mammary gland involution and extends functional competence of the secretory epithelium in the absence of lactogenic stimuli. Endocrinology. 2002;143(9):3641-50.

343. Pensa S, Watson CJ, Poli V. Stat3 and the inflammation/acute phase response in involution and breast cancer. J Mammary Gland Biol Neoplasia. 2009;14(2):121-9.

344. Takeda K, Noguchi K, Shi W, Tanaka T, Matsumoto M, Yoshida N, et al. Targeted disruption of the mouse Stat3 gene leads to early embryonic lethality. Proc Natl Acad Sci U S A. 1997;94(8):3801-4.

345. Thorn SR, Giesy SL, Myers MG, Jr., Boisclair YR. Mammary ductal growth is impaired in mice lacking leptin-dependent signal transducer and activator of transcription 3 signaling. Endocrinology. 2010;151(8):3985-95.

346. Ye J, Gao Z, Yin J, He Q. Hypoxia is a potential risk factor for chronic inflammation and adiponectin reduction in adipose tissue of ob/ob and dietary obese mice. Am J Physiol Endocrinol Metab. 2007;293(4):E1118-28.

347. Seo JB, Moon HM, Noh MJ, Lee YS, Jeong HW, Yoo EJ, et al. Adipocyte determination- and differentiation-dependent factor 1/sterol regulatory element-binding protein 1c regulates mouse adiponectin expression. J Biol Chem. 2004;279(21):22108-17.

348. Favero G, Stacchiotti A, Castrezzati S, Bonomini F, Albanese M, Rezzani R, et al. Melatonin reduces obesity and restores adipokine patterns and metabolism in obese (ob/ob) mice. Nutr Res. 2015;35(10):891-900.

349. Lin SY, Yang CP, Wang YY, Hsiao CW, Chen WY, Liao SL, et al. Interleukin-4 Improves Metabolic Abnormalities in Leptin-Deficient and High-Fat Diet Mice. Int J Mol Sci. 2020;21(12).

350. Ji Y, Sun S, Xu A, Bhargava P, Yang L, Lam KS, et al. Activation of natural killer T cells promotes M2 Macrophage polarization in adipose tissue and improves systemic glucose tolerance via interleukin-4 (IL-4)/STAT6 protein signaling axis in obesity. J Biol Chem. 2012;287(17):13561-71.

351. Kubota T, Inoue M, Kubota N, Takamoto I, Mineyama T, Iwayama K, et al. Downregulation of macrophage Irs2 by hyperinsulinemia impairs IL-4-indeuced M2a-subtype macrophage activation in obesity. Nature Communications. 2018;9(1):4863.

352. Kim S, Jin Y, Choi Y, Park T. Resveratrol exerts anti-obesity effects via mechanisms involving down-regulation of adipogenic and inflammatory processes in mice. Biochem Pharmacol. 2011;81(11):1343-51.

353. Mauer J, Chaurasia B, Goldau J, Vogt MC, Ruud J, Nguyen KD, et al. Signaling by IL-6 promotes alternative activation of macrophages to limit endotoxemia and obesity-associated resistance to insulin. Nat Immunol. 2014;15(5):423-30.

354. Wallenius V, Wallenius K, Ahrén B, Rudling M, Carlsten H, Dickson SL, et al. Interleukin-6-deficient mice develop mature-onset obesity. Nat Med. 2002;8(1):75-9.

355. Matthews VB, Allen TL, Risis S, Chan MH, Henstridge DC, Watson N, et al. Interleukin-6-deficient mice develop hepatic inflammation and systemic insulin resistance. Diabetologia. 2010;53(11):2431-41.

356. Franco C, Bengtsson BA, Johannsson G. The GH/IGF-1 Axis in Obesity: Physiological and Pathological Aspects. Metab Syndr Relat Disord. 2006;4(1):51-6.

357. Rasmussen MH, Frystyk J, Andersen T, Breum L, Christiansen JS, Hilsted J. The impact of obesity, fat distribution, and energy restriction on insulin-like growth factor-1 (IGF-1), IGF-binding protein-3, insulin, and growth hormone. Metabolism. 1994;43(3):315-9.

358. De Pergola G, Zamboni M, Pannacciulli N, Turcato E, Giorgino F, Armellini F, et al. Divergent effects of short-term, very-low-calorie diet on insulin-like growth factor-I and insulin-like growth factor binding protein-3 serum concentrations in premenopausal women with obesity. Obes Res. 1998;6(6):408-15.

359. Kunitomi M, Wada J, Takahashi K, Tsuchiyama Y, Mimura Y, Hida K, et al. Relationship between reduced serum IGF-I levels and accumulation of visceral fat in Japanese men. Int J Obes Relat Metab Disord. 2002;26(3):361-9.

360. Mårin P, Kvist H, Lindstedt G, Sjöström L, Björntorp P. Low concentrations of insulin-like growth factor-I in abdominal obesity. Int J Obes Relat Metab Disord. 1993;17(2):83-9.

361. Rasmussen MH, Hvidberg A, Juul A, Main KM, Gotfredsen A, Skakkebaek NE, et al. Massive weight loss restores 24-hour growth hormone release profiles and serum insulin-like growth factor-I levels in obese subjects. J Clin Endocrinol Metab. 1995;80(4):1407-15.

362. Chan PC, Hsiao FC, Chang HM, Wabitsch M, Hsieh PS. Importance of adipocyte cyclooxygenase-2 and prostaglandin E2-prostaglandin E receptor 3 signaling in the development of obesity-induced adipose tissue inflammation and insulin resistance. Faseb j. 2016;30(6):2282-97.

363. Wang W, Yang J, Qi W, Yang H, Wang C, Tan B, et al. Lipidomic profiling of high-fat diet-induced obesity in mice: Importance of cytochrome P450-derived fatty acid epoxides. Obesity (Silver Spring). 2017;25(1):132-40.

364. Zhang X, Luo Y, Wang C, Ding X, Yang X, Wu D, et al. Adipose mTORC1 Suppresses Prostaglandin Signaling and Beige Adipogenesis via the CRTC2-COX-2 Pathway. Cell Rep. 2018;24(12):3180-93.

365. Banhos Danneskiold-Samsøe N, Sonne SB, Larsen JM, Hansen AN, Fjære E, Isidor MS, et al. Overexpression of cyclooxygenase-2 in adipocytes reduces fat accumulation in inguinal white adipose tissue and hepatic steatosis in high-fat fed mice. Sci Rep. 2019;9(1):8979.

366. Clouthier DE, Comerford SA, Hammer RE. Hepatic fibrosis, glomerulosclerosis, and a lipodystrophy-like syndrome in PEPCK-TGF-beta1 transgenic mice. J Clin Invest. 1997;100(11):2697-713.

367. Derynck R MK. The TGF- family. Cold Spring Harbor, NY: Cold Spring Harbor Laboratory Press. 2007.

368. Zamani N, Brown CW. Emerging roles for the transforming growth factor-{beta} superfamily in regulating adiposity and energy expenditure. Endocr Rev. 2011;32(3):387-403.

369. Choy L, Skillington J, Derynck R. Roles of autocrine TGF-beta receptor and Smad signaling in adipocyte differentiation. J Cell Biol. 2000;149(3):667-82.

370. Qiu TH, Chandramouli GV, Hunter KW, Alkharouf NW, Green JE, Liu ET. Global expression profiling identifies signatures of tumor virulence in MMTV-PyMT-transgenic mice: correlation to human disease. Cancer Res. 2004;64(17):5973-81.

371. Lim E, Wu D, Pal B, Bouras T, Asselin-Labat M-L, Vaillant F, et al. Transcriptome analyses of mouse and human mammary cell subpopulations reveal multiple conserved genes and pathways. Breast Cancer Research. 2010;12(2):R21.

372. Lin EY, Jones JG, Li P, Zhu L, Whitney KD, Muller WJ, et al. Progression to malignancy in the polyoma middle T oncoprotein mouse breast cancer model provides a reliable model for human diseases. Am J Pathol. 2003;163(5):2113-26.

373. Toft DJ, Cryns VL. Minireview: Basal-like breast cancer: from molecular profiles to targeted therapies. Mol Endocrinol. 2011;25(2):199-211.

374. Davie SA, Maglione JE, Manner CK, Young D, Cardiff RD, MacLeod CL, et al. Effects of FVB/NJ and C57Bl/6J strain backgrounds on mammary tumor phenotype in inducible nitric oxide synthase deficient mice. Transgenic Res. 2007;16(2):193-201.

375. Miyoshi Y, Funahashi T, Tanaka S, Taguchi T, Tamaki Y, Shimomura I, et al. High expression of leptin receptor mRNA in breast cancer tissue predicts poor prognosis for patients with high, but not low, serum leptin levels. Int J Cancer. 2006;118(6):1414-9.

376. Wu MH, Chou YC, Chou WY, Hsu GC, Chu CH, Yu CP, et al. Circulating levels of leptin, adiposity and breast cancer risk. Br J Cancer. 2009;100(4):578-82.

377. Guo S, Liu M, Wang G, Torroella-Kouri M, Gonzalez-Perez RR. Oncogenic role and therapeutic target of leptin signaling in breast cancer and cancer stem cells. Biochim Biophys Acta. 2012;1825(2):207-22.

378. Khabaz MN, Abdelrahman A, Butt N, Damnhory L, Elshal M, Aldahlawi AM, et al. Immunohistochemical staining of leptin is associated with grade, stage, lymph node involvement, recurrence, and hormone receptor phenotypes in breast cancer. BMC Womens Health. 2017;17(1):105.

379. Cleary MP, Juneja SC, Phillips FC, Hu X, Grande JP, Maihle NJ. Leptin receptor-deficient MMTV-TGF-alpha/Lepr(db)Lepr(db) female mice do not develop oncogene-induced mammary tumors. Exp Biol Med (Maywood). 2004;229(2):182-93.

380. Cleary MP, Phillips FC, Getzin SC, Jacobson TL, Jacobson MK, Christensen TA, et al. Genetically obese MMTV-TGF-alpha/Lep(ob)Lep(ob) female mice do not develop mammary tumors. Breast Cancer Res Treat. 2003;77(3):205-15.

381. Watson CJ, Miller WR. Elevated levels of members of the STAT family of transcription factors in breast carcinoma nuclear extracts. Br J Cancer. 1995;71(4):840-4.

382. Gritsko T, Williams A, Turkson J, Kaneko S, Bowman T, Huang M, et al. Persistent activation of stat3 signaling induces survivin gene expression and confers resistance to apoptosis in human breast cancer cells. Clin Cancer Res. 2006;12(1):11-9.

383. Ranger JJ, Levy DE, Shahalizadeh S, Hallett M, Muller WJ. Identification of a Stat3-dependent transcription regulatory network involved in metastatic progression. Cancer Res. 2009;69(17):6823-30.

384. Jones LM, Broz ML, Ranger JJ, Ozcelik J, Ahn R, Zuo D, et al. STAT3 Establishes an Immunosuppressive Microenvironment during the Early Stages of Breast Carcinogenesis to Promote Tumor Growth and Metastasis. Cancer Res. 2016;76(6):1416-28.

385. Baumann H, Morella KK, White DW, Dembski M, Bailon PS, Kim H, et al. The full-length leptin receptor has signaling capabilities of interleukin 6-type cytokine receptors. Proc Natl Acad Sci U S A. 1996;93(16):8374-8.

386. Bendinelli P, Maroni P, Pecori Giraldi F, Piccoletti R. Leptin activates Stat3, Stat1 and AP-1 in mouse adipose tissue. Mol Cell Endocrinol. 2000;168(1-2):11-20.

387. Tanabe K, Okuya S, Tanizawa Y, Matsutani A, Oka Y. Leptin induces proliferation of pancreatic beta cell line MIN6 through activation of mitogen-activated protein kinase. Biochem Biophys Res Commun. 1997;241(3):765-8.

388. Hu X, Juneja SC, Maihle NJ, Cleary MP. Leptin--a growth factor in normal and malignant breast cells and for normal mammary gland development. J Natl Cancer Inst. 2002;94(22):1704-11.

389. Nash MA, Lenzi R, Edwards CL, Kavanagh JJ, Kudelka AP, Verschraegen CF, et al. Differential expression of cytokine transcripts in human epithelial ovarian carcinoma by solid tumour specimens, peritoneal exudate cells containing tumour, tumour-infiltrating lymphocyte (TIL)-derived T cell lines and established tumour cell lines. Clin Exp Immunol. 1998;112(2):172-80.

390. Prokopchuk O, Liu Y, Henne-Bruns D, Kornmann M. Interleukin-4 enhances proliferation of human pancreatic cancer cells: evidence for autocrine and paracrine actions. Br J Cancer. 2005;92(5):921-8.

391. Todaro M, Alea MP, Di Stefano AB, Cammareri P, Vermeulen L, Iovino F, et al. Colon cancer stem cells dictate tumor growth and resist cell death by production of interleukin-4. Cell Stem Cell. 2007;1(4):389-402.

392. Todaro M, Lombardo Y, Francipane MG, Alea MP, Cammareri P, Iovino F, et al. Apoptosis resistance in epithelial tumors is mediated by tumor-cell-derived interleukin-4. Cell Death Differ. 2008;15(4):762-72.

393. Olver S, Apte S, Baz A, Kienzle N. The duplicitous effects of interleukin 4 on tumour immunity: how can the same cytokine improve or impair control of tumour growth? Tissue Antigens. 2007;69(4):293-8.

394. Li Z, Jiang J, Wang Z, Zhang J, Xiao M, Wang C, et al. Endogenous interleukin-4 promotes tumor development by increasing tumor cell resistance to apoptosis. Cancer Res. 2008;68(21):8687-94.

395. Gocheva V, Wang HW, Gadea BB, Shree T, Hunter KE, Garfall AL, et al. IL-4 induces cathepsin protease activity in tumor-associated macrophages to promote cancer growth and invasion. Genes Dev. 2010;24(3):241-55.

396. Jakowlew SB. Transforming growth factor-beta in cancer and metastasis. Cancer Metastasis Rev. 2006;25(3):435-57.

397. Haque S, Morris JC. Transforming growth factor-β: A therapeutic target for cancer. Hum Vaccin Immunother. 2017;13(8):1741-50.

398. Pardali K, Moustakas A. Actions of TGF-beta as tumor suppressor and pro-metastatic factor in human cancer. Biochim Biophys Acta. 2007;1775(1):21-62.

399. Sun X, Bernhardt SM, Glynn DJ, Hodson LJ, Woolford L, Evdokiou A, et al. Attenuated TGFB signalling in macrophages decreases susceptibility to DMBA-induced mammary cancer in mice. Breast Cancer Res. 2021;23(1):39.

400. Obeid E, Nanda R, Fu YX, Olopade OI. The role of tumor-associated macrophages in breast cancer progression (review). Int J Oncol. 2013;43(1):5-12.

401. Collaborative Group on Hormonal Factors in Breast Cancer. Menarche, menopause, and breast cancer risk: individual participant meta-analysis, including 118 964 women with breast cancer from 117 epidemiological studies. Lancet Oncol. 2012;13(11):1141-51.

402. Kamikawa A, Ichii O, Yamaji D, Imao T, Suzuki C, Okamatsu-Ogura Y, et al. Diet-induced obesity disrupts ductal development in the mammary glands of nonpregnant mice. Dev Dyn. 2009;238(5):1092-9.

403. Hilakivi-Clarke L, Clarke R, Onojafe I, Raygada M, Cho E, Lippman M. A maternal diet high in n - 6 polyunsaturated fats alters mammary gland development, puberty onset, and breast cancer risk among female rat offspring. Proc Natl Acad Sci U S A. 1997;94(17):9372-7.

404. Hilakivi-Clarke L, Cho E, Cabanes A, DeAssis S, Olivo S, Helferich W, et al. Dietary modulation of pregnancy estrogen levels and breast cancer risk among female rat offspring. Clin Cancer Res. 2002;8(11):3601-10.

405. Hilakivi-Clarke L, Stoica A, Raygada M, Martin MB. Consumption of a high-fat diet alters estrogen receptor content, protein kinase C activity, and mammary gland morphology in virgin and pregnant mice and female offspring. Cancer Res. 1998;58(4):654-60.

406. Welsch CW. Relationship between dietary fat and experimental mammary tumorigenesis: a review and critique. Cancer Res. 1992;52(7 Suppl):2040s-8s.

407. Zheng Q, Dunlap SM, Zhu J, Downs-Kelly E, Rich J, Hursting SD, et al. Leptin deficiency suppresses MMTV-Wnt-1 mammary tumor growth in obese mice and abrogates tumor initiating cell survival. Endocr Relat Cancer. 2011;18(4):491-503.

408. Yakar S, Nunez NP, Pennisi P, Brodt P, Sun H, Fallavollita L, et al. Increased tumor growth in mice with diet-induced obesity: impact of ovarian hormones. Endocrinology. 2006;147(12):5826-34.

409. Hanahan D, Weinberg RA. The hallmarks of cancer. Cell. 2000;100(1):57-70.

410. Li X, Placencio V, Iturregui JM, Uwamariya C, Sharif-Afshar AR, Koyama T, et al. Prostate tumor progression is mediated by a paracrine TGF-beta/Wnt3a signaling axis. Oncogene. 2008;27(56):7118-30.

411. Provenzano PP, Inman DR, Eliceiri KW, Keely PJ. Matrix density-induced mechanoregulation of breast cell phenotype, signaling and gene expression through a FAK-ERK linkage. Oncogene. 2009;28(49):4326-43.

412. Trimboli AJ, Cantemir-Stone CZ, Li F, Wallace JA, Merchant A, Creasap N, et al. Pten in stromal fibroblasts suppresses mammary epithelial tumours. Nature. 2009;461(7267):1084-91.

413. Juliano RL, Haskill S. Signal transduction from the extracellular matrix. J Cell Biol. 1993;120(3):577-85.

414. Taipale J, Keski-Oja J. Growth factors in the extracellular matrix. Faseb j. 1997;11(1):51-9.

415. Lochter A, Bissell MJ. Involvement of extracellular matrix constituents in breast cancer. Semin Cancer Biol. 1995;6(3):165-73.

416. Li X, Zhang M, Pan X, Xu Z, Sun M. "Three Hits" Hypothesis for Developmental Origins of Health and Diseases in View of Cardiovascular Abnormalities. Birth Defects Res. 2017;109(10):744-57.

417. Lee PN, Forey BA, Coombs KJ. Systematic review with meta-analysis of the epidemiological evidence in the 1900s relating smoking to lung cancer. BMC Cancer. 2012;12:385.

418. Walboomers JM, Jacobs MV, Manos MM, Bosch FX, Kummer JA, Shah KV, et al. Human papillomavirus is a necessary cause of invasive cervical cancer worldwide. J Pathol. 1999;189(1):12-9.

419. Breast Cancer Risk and Prevention. The American Cancer Society www.cancer.org/cancer/breast-cancer/risk-and-prevention.html. .

420. Colditz GA, Bohlke K. Priorities for the primary prevention of breast cancer. CA Cancer J Clin. 2014;64(3):186-94.

421. Sprague BL, Trentham-Dietz A, Egan KM, Titus-Ernstoff L, Hampton JM, Newcomb PA. Proportion of invasive breast cancer attributable to risk factors modifiable after menopause. Am J Epidemiol. 2008;168(4):404-11.

422. Katz TA. Potential Mechanisms underlying the Protective Effect of Pregnancy against Breast Cancer: A Focus on the IGF Pathway. Front Oncol. 2016;6:228.

423. MacMahon B, Trichopoulos D, Brown J, Andersen AP, Aoki K, Cole P, et al. Age at menarche, probability of ovulation and breast cancer risk. Int J Cancer. 1982;29(1):13-6.

424. Mathews TJ, Hamilton BE. Mean Age of Mothers is on the Rise: United States, 2000-2014. NCHS Data Brief. 2016(232):1-8.

425. Boyd NF, Rommens JM, Vogt K, Lee V, Hopper JL, Yaffe MJ, et al. Mammographic breast density as an intermediate phenotype for breast cancer. Lancet Oncol. 2005;6(10):798-808.

426. Brisson J, Brisson B, Coté G, Maunsell E, Bérubé S, Robert J. Tamoxifen and mammographic breast densities. Cancer epidemiology, biomarkers & prevention. 2000;9(9):911-5.

427. Greendale GA, Reboussin BA, Slone S, Wasilauskas C, Pike MC, Ursin G. Postmenopausal hormone therapy and change in mammographic density. J Natl Cancer Inst. 2003;95(1):30-7.

428. Freedman M, San Martin J, O'Gorman J, Eckert S, Lippman ME, Lo SC, et al. Digitized mammography: a clinical trial of postmenopausal women randomly assigned to receive raloxifene, estrogen, or placebo. J Natl Cancer Inst. 2001;93(1):51-6.

429. Colditz GA, Bohlke K, Berkey CS. Breast cancer risk accumulation starts early: prevention must also. Breast Cancer Res Treat. 2014;145(3):567-79.

430. Pike MC, Krailo MD, Henderson BE, Casagrande JT, Hoel DG. 'Hormonal' risk factors, 'breast tissue age' and the age-incidence of breast cancer. Nature. 1983;303(5920):767-70.

431. Colditz GA, Frazier AL. Models of breast cancer show that risk is set by events of early life: prevention efforts must shift focus. Cancer epidemiology, biomarkers & prevention. 1995;4(5):567-71.

432. Tseng M, Olufade TO, Evers KA, Byrne C. Adolescent lifestyle factors and adult breast density in U.S. Chinese immigrant women. Nutr Cancer. 2011;63(3):342-9.

433. Dorgan JF, Liu L, Klifa C, Hylton N, Shepherd JA, Stanczyk FZ, et al. Adolescent diet and subsequent serum hormones, breast density, and bone mineral density in young women: results of the Dietary Intervention Study in Children follow-up study. Cancer epidemiology, biomarkers & prevention. 2010;19(6):1545-56.

434. Haars G, van Gils CH, Elias SG, Lokate M, van Noord PA, Peeters PH. The influence of a period of caloric restriction due to the Dutch famine on breast density. Int J Cancer. 2010;126(9):2211-5.

435. Hanson MA, Gluckman PD. Early developmental conditioning of later health and disease: physiology or pathophysiology? Physiol Rev. 2014;94(4):1027-76.

436. Beckett PR, Jahoor F, Copeland KC. The efficiency of dietary protein utilization is increased during puberty. J Clin Endocrinol Metab. 1997;82(8):2445-9.

437. Mauras N. Combined recombinant human growth hormone and recombinant human insulin-like growth factor I: lack of synergy on whole body protein anabolism in normally fed subjects. J Clin Endocrinol Metab. 1995;80(9):2633-7.

438. Ling PR, Gollaher C, Colon E, Istfan N, Bistrian BR. IGF-I alters energy expenditure and protein metabolism during parenteral feeding in rats. Am J Clin Nutr. 1995;61(1):116-20.

439. Ahima RS, Prabakaran D, Mantzoros C, Qu D, Lowell B, Maratos-Flier E, et al. Role of leptin in the neuroendocrine response to fasting. Nature. 1996;382(6588):250-2.

440. Kolaczynski JW, Considine RV, Ohannesian J, Marco C, Opentanova I, Nyce MR, et al. Responses of leptin to short-term fasting and refeeding in humans: a link with ketogenesis but not ketones themselves. Diabetes. 1996;45(11):1511-5.

441. Soliman AT, Yasin M, Kassem A. Leptin in pediatrics: A hormone from adipocyte that wheels several functions in children. Indian J Endocrinol Metab. 2012;16(Suppl 3):S577-87.

442. Castellano JM, Navarro VM, Fernández-Fernández R, Nogueiras R, Tovar S, Roa J, et al. Changes in hypothalamic KiSS-1 system and restoration of pubertal activation of the reproductive axis by kisspeptin in undernutrition. Endocrinology. 2005;146(9):3917-25.

443. Root AW, Powers PS. Anorexia nervosa presenting as growth retardation in adolescents. J Adolesc Health Care. 1983;4(1):25-30.

444. Danziger Y, Mukamel M, Zeharia A, Dinari G, Mimouni M. Stunting of growth in anorexia nervosa during the prepubertal and pubertal period. Isr J Med Sci. 1994;30(8):581-4.

445. Siegel JH, Hardoff D, Golden NH, Shenker IR. Medical complications in male adolescents with anorexia nervosa. J Adolesc Health. 1995;16(6):448-53.

446. Modan-Moses D, Yaroslavsky A, Kochavi B, Toledano A, Segev S, Balawi F, et al. Linear growth and final height characteristics in adolescent females with anorexia nervosa. PLoS One. 2012;7(9):e45504.

447. Miller KK. Endocrine Dysregulation in Anorexia Nervosa Update. The Journal of Clinical Endocrinology & Metabolism. 2011;96(10):2939-49.

448. Modan-Moses D, Stein D, Pariente C, Yaroslavsky A, Ram A, Faigin M, et al. Modulation of Adiponectin and Leptin during Refeeding of Female Anorexia Nervosa Patients. The Journal of Clinical Endocrinology & Metabolism. 2007;92(5):1843-7.

449. Ginsburg E, Vonderhaar B. Whole organ culture of the mouse mammary gland. Methods in Mammary Gland Biology and Breast Cancer Research. Kluwer Academic Plenum Publishers, New York. 2000.